vol. 4, no. 1
jan. 1958

THE SOVIET JOURNAL OF
ATOMIC ENERGY

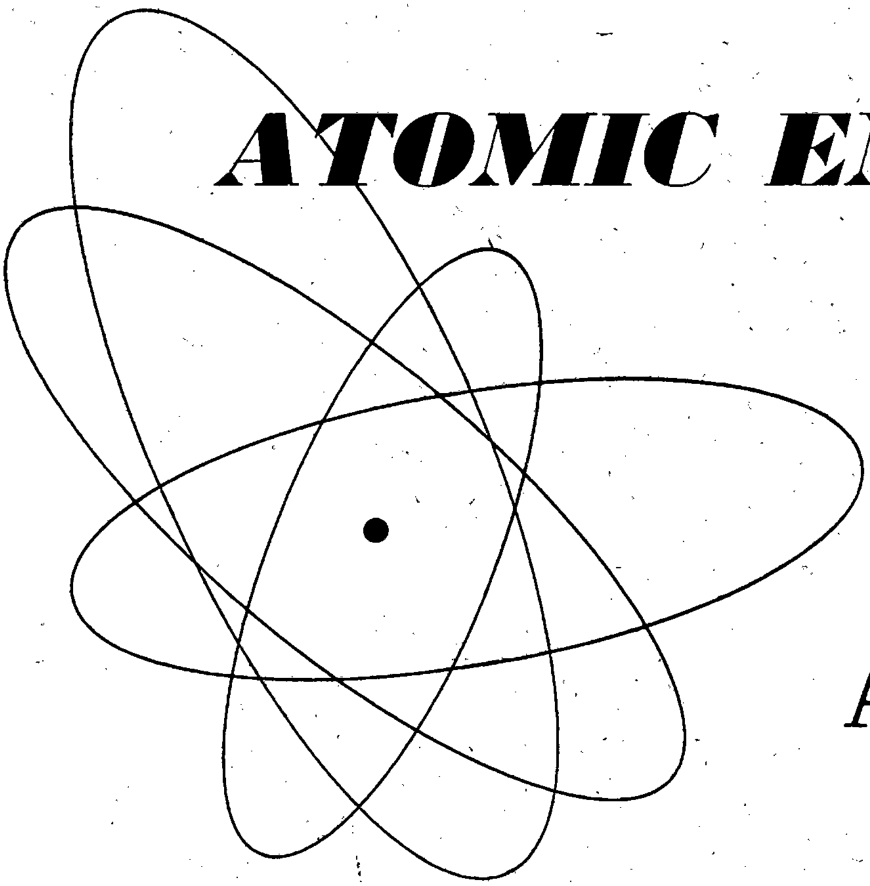

Атомная
энергия

TRANSLATED FROM RUSSIAN

CONSULTANTS BUREAU, INC.

NUCLEAR REACTIONS IN LIGHT NUCLEI
IN ENGLISH TRANSLATION

Supplement No. 5, 1957 Soviet Journal of Atomic Energy

Ten papers describing in detail (with diagrams of all apparatus), important experiments by the Academy of Sciences, USSR, 1951–1955. Mainly concerned with measurements of the total and differential cross sections and product angular distributions in interactions involving isotopes of light elements, many of which are of interest in connection with thermonuclear fusion reactions. Makes detailed comparisons of all available experimental data; discusses errors and means of avoiding them; refers extensively to Soviet and non-Soviet literature.

CONTENTS: Determination of the total cross sections for the $D(d,n)He^3$ reaction in the energy range 20–220 kev; Investigation of the D-D reaction in the deuteron-energy range 0.20–1.75 Mev; The D-D reaction in the deuteron-energy range 100–1000 kev; Measurements of the yields and effective cross sections of the $D(t,n)He^4$ and $D(d,p)T$ reactions using thick targets of heavy ice; Measurement of the effective cross section for the $D(t,n)He^4$ reaction in the deuteron-energy range 40–730 kev; Total effective cross section of tritium for neutrons with energies of 2.5 and 14 Mev; Measurement of the effective cross section for the Li^6 (n,d) reaction for 2.5 Mev neutrons; Total effective cross sections for Li^6 and Li^7 for neutrons with energies of 2.5 and 14 Mev; Effective cross section for the $Be^9(n,d)He^6$ reaction; Specific stopping power of 150–1100 Mev in nickel. English translation, 71 pages, $15.00

*For subscribers to our translation of the 1957 Soviet Journal of Atomic Energy only $10.00

* * *

ACOUSTICS AND ULTRASONICS
RUSSIAN-ENGLISH GLOSSARY

10,000 Russian terms. Covers acoustics, ultrasonics electro-acoustics, with emphasis on the rapidly growing field of ultrasonics. Terms selected from thousands of pages of the most recent issues of Soviet physics and engineering journals, especially the Journal of Acoustics, the Journal of Technical Physics, and Radio-Engineering, as well as from Russian acoustics texts. Russian equivalents are also provided for terms selected from the following: IRE Standards; the International Dictionary of Physics and Electronics; the Russian translation of L. Bergman's "Ultrasonics Theory". 23 page index of Russian-English equivalents for names commonly found in acoustics and ultrasonics literature. 193 pages, only $10.00

This is the latest in a series of 8 specialized glossaries being published preliminary to publication, in 1959, of our Russian-English Physics Dictionary, which will be comprehensive, authoritative, permanently bound. *Pre-publication subscribers to the Dictionary* also receive each of the 8 glossaries upon publication **all for only $50.00**

Write for free catalogs fully describing the Dictionary and 8 glossaries, as well as our current Russian-English translation-publishing program.

Consultants Bureau's translation by *bilingual scientists.* Clear reproduction by multilith process from IBM "cold type", (except glossaries, which are varityped), including all diagrammatic and tabular material; books staple bound in durable paper covers.

CONSULTANTS BUREAU, INC.
227 W. 17th St., NEW YORK 11, N. Y.

vol. 4, no. 1
jan. 1958

THE SOVIET JOURNAL OF
ATOMIC ENERGY

ATOMNAIA ENERGIIA

A publication of the Academy of Sciences of the USSR

Year and issue of first translation:
volume 1, number 1, january 1956

TRANSLATED FROM RUSSIAN

Annual Subscription	*$75.00*
Single Issue	*20.00*

CONSULTANTS BUREAU, INC.
227 W. 17th St., NEW YORK 11, N. Y.

Printed in the United States

γ-RAY SPECTRA FROM THE RADIATION CAPTURE OF NEUTRONS FOR EVEN-EVEN RADIATING NUCLEI WITH ROTATIONAL LEVELS

L. V. Groshev, A. M. Demidov, V. N. Lutsenko
and V. I. Pelekhov

Using a magnetic Compton spectrometer, we measured the spectra of the γ-rays arising from the capture of thermal neutrons by nuclei of gadolinium, erbium, hafnium, dysprosium and tantalum in the energy range 0.3-9 Mev. We determined the energies and the intensities of the γ-lines. For the first three elements, the radiating nuclei are the even-even nuclei ${}_{64}Gd^{156}_{92}$, ${}_{64}Gd^{158}_{94}$, ${}_{68}Er^{168}_{100}$ and ${}_{72}Hf^{178}_{106}$, which have rotational structural levels close to the ground state. The peculiarity of the spectra of these nuclei is the presence of a group of closely placed intense γ-lines with energies of ~ 1 Mev. These lines are absent in the case of even-odd (for example, ${}_{66}Dy^{165}_{99}$) and odd-odd radiating nuclei (for example, ${}_{73}Ta^{182}_{109}$). The peculiarities of the γ-ray spectra noted are due to the structure of the lower nuclear levels.

The present work is a continuation of previous investigations by the authors on the spectra of γ-rays, arising during the capture of neutrons by atomic nuclei. The measurements were carried out with a magnetic Compton spectrometer in the energy range 0.3-9 Mev on the RFT reactor of the Academy of Sciences of the USSR. The experimental conditions and method of measurement and processing of data obtained were described previously [1].

In the spectrum of γ-rays from the radiation capture of neutrons by the nuclei of a heavy element which does not lie close to the magic numbers, the main part of the γ-transitions from a spectrum which is not resolvable by our apparatus [1]. In measuring the spectra of these elements, we observed that in a case where the radiating nucleus was even-even and had a system of rotational levels close to the ground state ($90 \leq N \leq 112$), the γ-ray spectrum had a sharply expressed peculiarity. This lay in the fact that on the background of the continuous spectrum, there was a group of closely placed intense lines with energies of ~ 1 Mev. In the case of even - odd and odd-odd nuclei, this peculiarity was not present.

It is regrettable that even-even nuclei with rotational levels are formed in the (n, γ) reaction only in an extremely limited number of cases. We were able to measure the γ-ray spectra for only four such nuclei, namely ${}_{64}Gd^{156}_{92}$, ${}_{64}Gd^{158}_{94}$, ${}_{68}Er^{168}_{100}$ and ${}_{72}Hf^{178}_{106}$. For comparison we obtained spectra for even-odd (${}_{66}Dy^{165}_{99}$) and odd - odd (${}_{73}Ta^{182}_{109}$) radiating nuclei. Below we present and discuss the results we obtained.

Gadolinium

The spectrum of the γ-rays, emitted during the absorption of thermal neutrons by gadolinium, was measured both for the natural mixture of isotopes and for the isotopes Gd^{155} and Gd^{157}. In the first case the sample irradiated consisted of 1.8 g of gadolinium oxide, deposited on five discs of thin aluminum foil, 60 mm in diameter. The discs were placed at a distance of 2.5 cm from each other inside a graphite container, which was placed in a channel in the thermal column of the reactor. The samples of separated isotopes consisted respectively of 30 and 50 mg of the oxides of Gd^{155} and Gd^{157}.

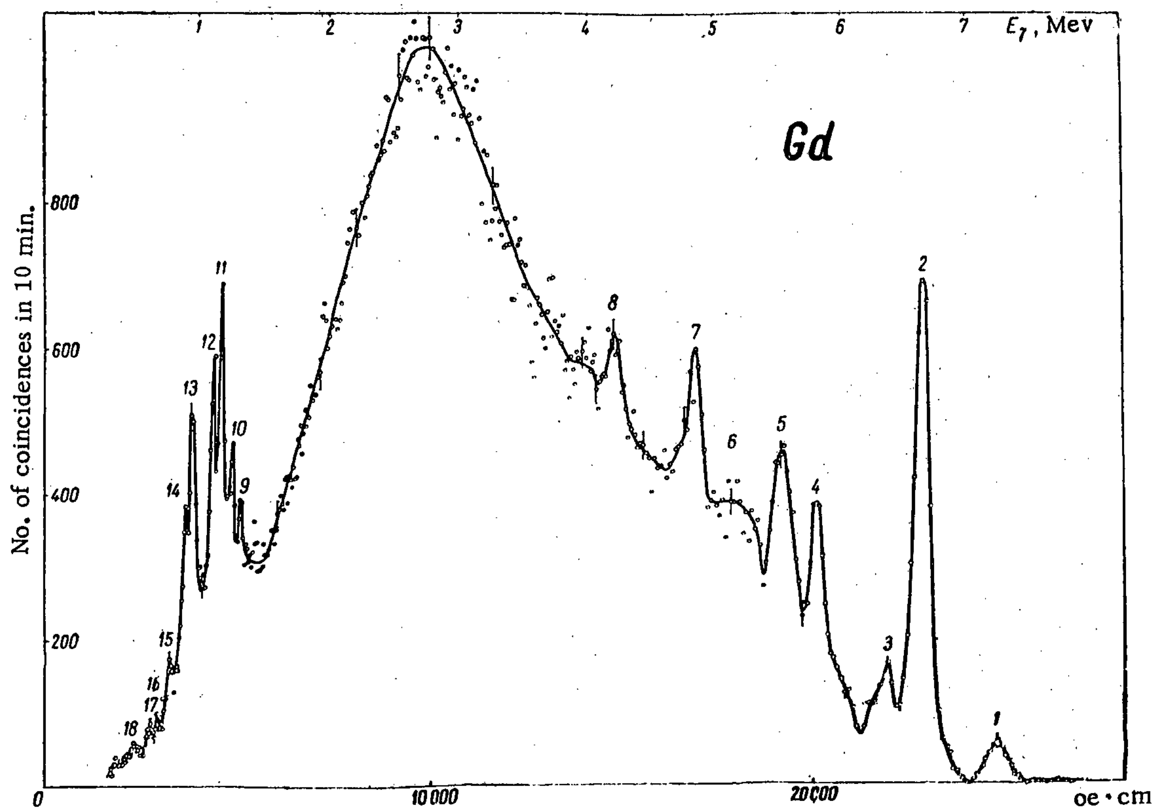

Fig. 1. Experimental γ-ray spectrum of Gd_2O_3.

TABLE 1

Some Data on Gadolinium Isotopes

Isotope (target)	Content in natural mixture, %	Isotopic absorption cross section, barns	Contribution to total thermal neutron absorption cross section,* %	Content in sample enriched in Gd^{157}, %	Content in sample enriched in Gd^{155}, %	Neutron binding energy in product-nucleus, Mev	
						measured [2]	calc.**
Gd^{152}	0.20	<125***	0.0006	None	<0.1	—	6.8
Gd^{154}	2.15	—	—	None	0.5	6.37±0.056	6.5
Gd^{155}	14.8	70 000±2 000	23.5	0.6	97.3	8.46±0.056	7.9
Gd^{156}	20.6	—	—	1.7	1.7	6.33±0.056	6.2
Gd^{157}	15.7	160 000±6 000	57	91.4	0.5	7.87±0.056	7.6
Gd^{158}	24.8	4±2***	0.002	5.2	<0.1	—	5.8
Gd^{160}	21.8	1.5±2***	0.00007	1.1	<0.1	—	5.6

* $\sigma_a = (44\,000 + 2000)$ barns.
** Calculated by Weizsäcker's formula [3].
*** Activation cross section.

In Table 1 we give the isotopic composition of the irradiated samples, the effective absorption cross sections and the neutron binding energies for the isotopes of gadolinium.*

---

* The experimental determination of the binding energies, given in this and all later tables, were kindly reported to us by Dr. Johnson (University of Minnesota, USA) before their publication, for which the authors are very grateful to Dr. Johnson.

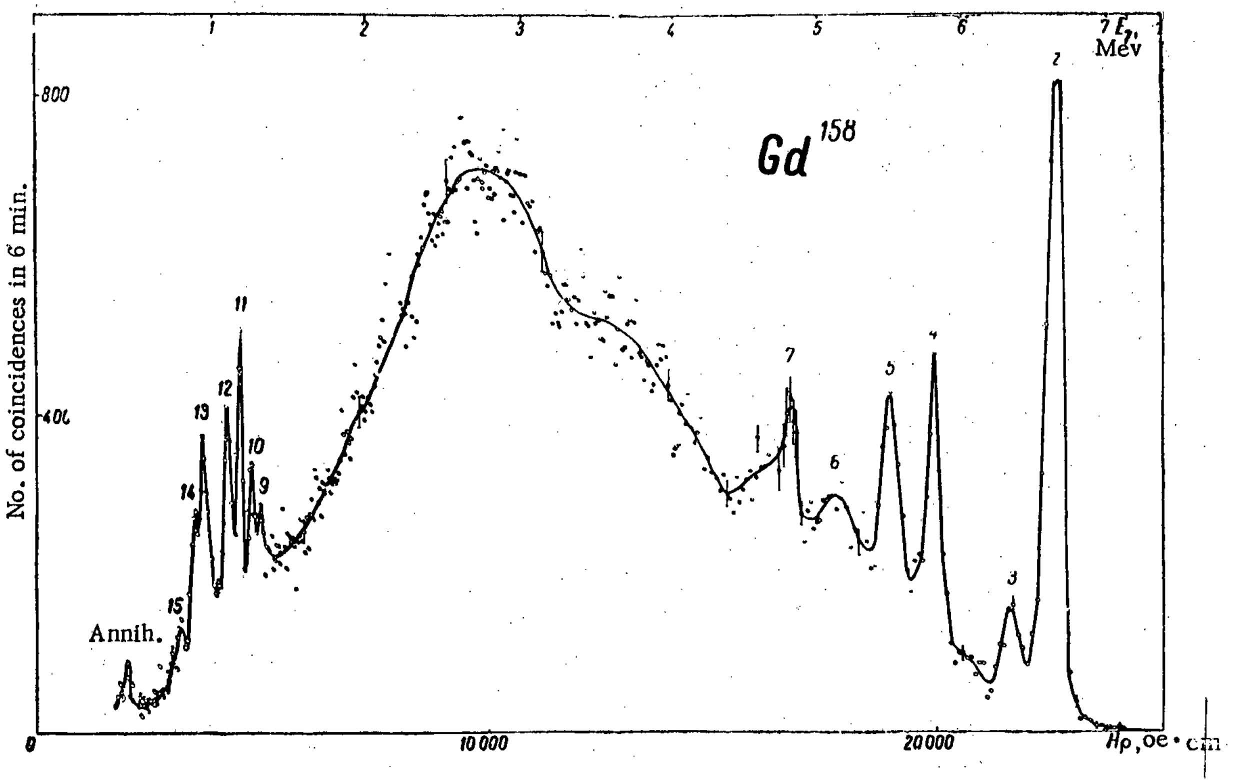

Fig. 2. Experimental γ-ray spectrum of $Gd_2^{158}O_3$.

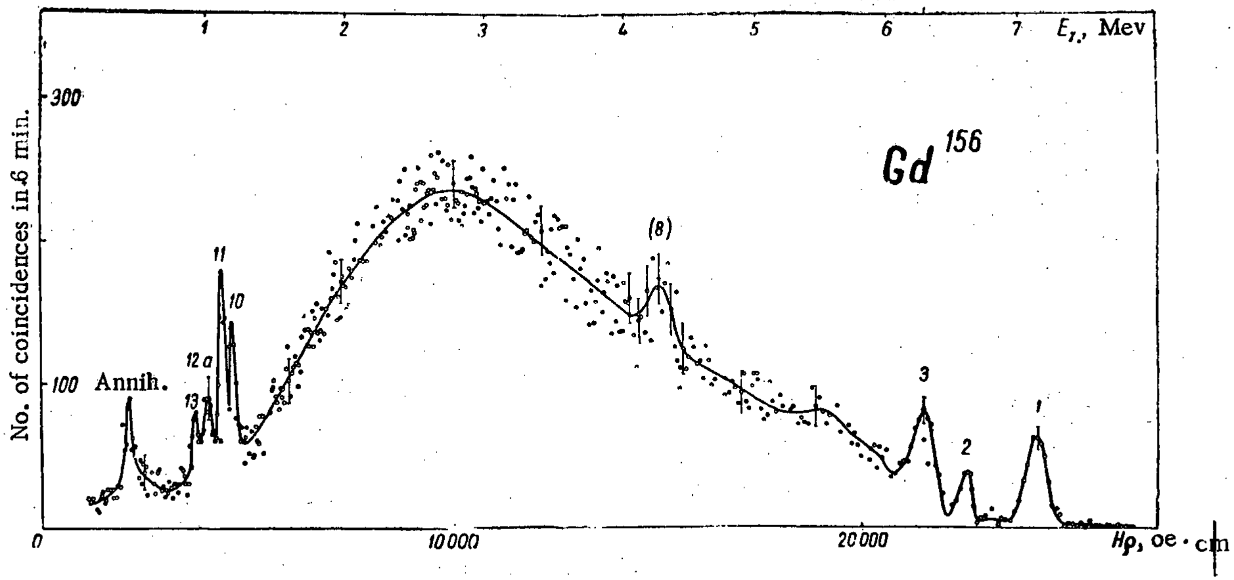

Fig. 3. Experimental γ-ray spectrum of $Gd_2^{156}O_3$.

The total cross section for the capture of thermal neutrons by gadolinium, equal to (44,000 ± 2000) barns, and the data in Table 1 indicate that in the case of natural gadolinium the spectrum should consist mainly of γ-rays from Gd^{158} (~ 60%) and Gd^{156} (~ 25%). For the samples of separated isotopes, the γ-rays must almost entirely belong to the isotopes Gd^{156} and Gd^{158}, respectively.

The experimental γ-ray spectra obtained with samples of Gd_2O_3, $Gd_2^{157}O_3$ and $Gd_2^{155}O_3$ are given in Figures 1, 2 and 3. Along the abscissas at the bottom of the diagrams are plotted the values of $H\rho$ in oe·cm and above, the energy of the γ-rays in Mev. Along the ordinate are plotted the numbers of coincidences in a given time interval. They were obtained after subtracting the background, determined by the number of coincidences for a sample surrounded with boron, and the introduction of a correction for the presence of electrons from pairs, formed by the γ-rays in the radiator, together with Compton electrons.

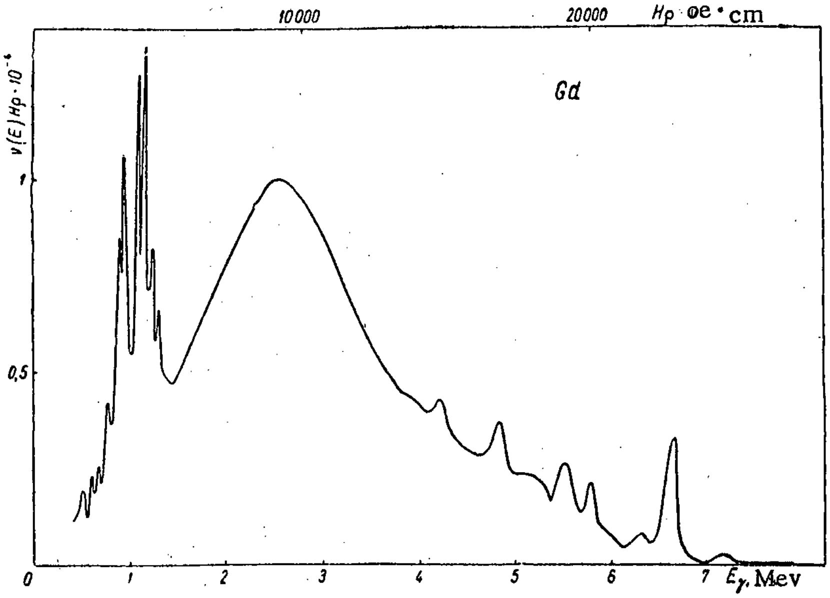

Fig. 4. Corrected γ-ray spectrum of Gd_2O_3.

Usually we measured the spectrum for the sample investigated with a lead block in front of it to absorb the γ-rays coming from the active zone of the reactor. Under these conditions, due to the absorption of thermal neutrons by the lead, lines appeared in the spectrum with energies of 6.72 and 7.38 Mev, which made it difficult to obtain a reliable spectrum in this energy region. Therefore, for energies above 6.4 Mev, the measurements were carried out after substituting a bismuth block for the lead block. The results obtained in this way are also plotted in Figures 1, 2 and 3 for $E_\gamma > 6.4$ Mev.

A corrected γ-ray spectrum for a sample of Gd_2O_3 is shown in Figure 4. On it, the γ-ray energy in Mev and the value of $H\rho$ in oe·cm is plotted along the abscissa. The value of $\nu(E)H\rho \cdot 10^{-4}$ [1] is given along the ordinate, where the value $\nu(E)$ equals the number of γ-quanta emitted per neutron capture for a unit interval of γ-ray energy (1 Mev).

The energies and intensities of the γ-lines in spectra obtained in the present work and also by other authors are given in Table 2. The intensities of the lines are expressed in the numbers of γ-quanta per 100 neutron captures. They were determined by normalization of the emitted energy to the neutron binding energy. The γ-lines given in Table 2 for natural gadolinium and the isotopes Gd^{156} and Gd^{158} are responsible for 11, 9 and 12% respectively, of the total energy radiated by these nuclei.

Comparison of the spectra given shows that the lines 2-7* in the spectrum of the natural mixture of isotopes belong to the isotope Gd^{158}. To the isotope Gd^{156} evidently belongs line 1, which is absent in the spectrum of Gd^{158}, and probably line 8. Actually, in the Gd^{156} spectrum, the latter lies practically within the limits of stat-

TABLE 2

Energies and Intensities of Gadolinium γ-rays

Results of this work							Results of other work							
							Kinsey and Bartholomew [4]		Skliarevskii, et al. [5]			Groshev et. al[6]	Church, Goldhaber [7]	Fenstermacher et al. [8]*
designation of γ-lines	Isotopes irradiated													
	Gd (natural mixture of isotopes)		Gd^{158}		Gd^{156}									
	E_γ Mev	I**	E_γ Mev	I**	E_γ Mev	I**	E_γ Mev	I**	E_γ Mev	I**	Isotope irradiated	E_γ Mev	E_γ Mev	E_γ Mev
							7.78±0.05	0.03						
1	7.33±0.03	0.17	—	—	7.33±0.03	1	7.36±0.05	0.03						
2	6.74±0.01	2.1	6.74±0.01	3,7	6.74±0.03	0.4	6.73±0.03	0.5						
3	6.44±0.03	0.5	6.44±0.03	0,4	6.44±0.035	1.3	6.41±0.04	0.2						
4	5.86±0.02	0.6	5.88±0.03	1,8	—	—	5.87±0.04	0.2						
5	5.63±0.03	0.8	5.62±0.03	1,3	—	—	5.61±0.04	0.3						
6***	~5.2	—	~5.2	—	—	—								
7	4.93±0.02	0.8	4.92±0.04	0,8	—	—								
8	4.30±0.04	0.5	—	—	~4.3	—								
9	1.32±0.02	2	1.33±0.02	2	—	—								
10	1.26±0.02	4	1.26±0.02	3	1.24±0.02	9								
11	1,180±0.015	10	1.185±0.015	9	1.17±0.02	15								1.16±0.04
12	1.12±0.02	8	1.110±0.015	8	—	—								
12a	—	—	—	—	1.06±0.02	6								
13	0.96±0.02	11	0.96±0.02	13	(0.96±0.02)	7								0.95±0.03
14	0.91±0.02	8	0.900±0.015	8										
15	0.78±0.02	3	0.78±0.02	5										
16	(0.69±0.02)	1												
17	(0.64±0.02)	2												0.65±0.02
18	0.55±0.02	3												
									0.196	34****	Gd^{156}	0.196	0.1987	0.20±0.01
									0.183	29****	Gd^{158}	0.179	0.1817	
									0.087	50****	Gd^{156}	0.088	0.0888	
									0.079	53****	Gd^{158}	0.079	0.0791	

---

*Investigation of γ-rays emitted during the capture of resonance neutrons.

**Intensity in quanta per 100 neutron captures.

***Unresolved group lines.

****Intensity of transition taking into account conversion.

istical error, which must be quite large here (the low statistical accuracy of measurement for the Gd^{155} spectrum was due to the fact that a small amount of material was used). Line 3 is found in the spectra of both isotopes. We cannot exclude the possibility that line 2 in the Gd^{156} spectrum may be explained by the presence of small traces of the isotope Gd^{157} in the sample of Gd^{155}.

A group of intense peaks with energies of ~ 1 Mev were found in the spectra of both Gd^{156} and Gd^{158}. Due to the greater neutron absorption in Gd^{157}, all the clearly separated peaks in the spectrum of the natural mixture of isotopes (peaks 9-15) were shown in the spectrum of Gd^{158}. The energies of the lines 10, 11 and 13, found in the spectrum of Gd^{156}, within the limits of error, agreed with the energies of the corresponding lines in the Gd^{158} spectrum. The line 12a in the Gd^{156} spectrum was not separated in the spectrum of the natural mixture of isotopes due to its low intensity. We were not able to assign the low intensity lines 16-18 to a definite isotope.

We did not detect the line with an energy of 7.78 Mev and an intensity of 0.03 quanta, found by Kinsey and Bartholomew [4]. If this line was present in our spectrum, its intensity was less than 0.02 quanta per 100 captures. The energies of the γ-rays we found agree well with the data of Kinsey and Bartholomew. However, there is a discrepancy in the intensities. The reason for this discrepancy was not clear to us. In our measurements, the intensities of the γ-rays may be high due to neglecting the conversion of γ-rays and also the presence of γ-rays with energies less than 0.03 Mev. In the case of gadolinium, the increase due to this should not exceed 8%.

Erbium

The sample irradiated was 30 g of erbium oxide with the natural isotopic composition.

In Table 3 we give data on the stable isotopes of erbium and the neutron binding energies for the product-nuclei. The total thermal neutron absorption cross section for the natural mixtures of erbium isotopes equals (166 ± 16) barns. The contribution to it from the separate isotopes is practically unknown. At out request, V. V. Skliarevskii measured the spectrum of the γ-rays from the capture of thermal neutrons by erbium in the low energy range using a scintillation spectrometer. It was shown that in the radiating isotope of erbium, there was a system of rotational levels, characteristic of an even-even nucleus with a number of neutrons between 90 and 112. Thus the probability of a transition from the first to the second excited states, allowing for internal

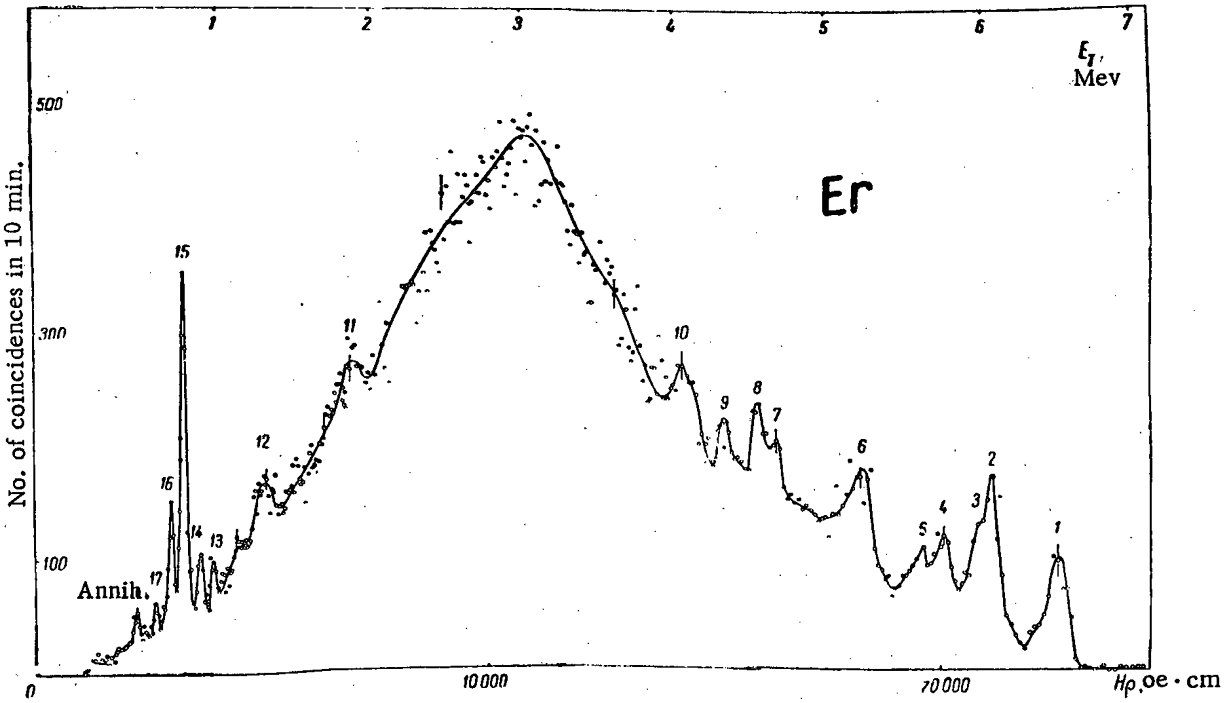

Fig. 5. Experimental γ-ray spectrum of Er_2O_3.

---

*Line 7 in the γ-ray spectrum of Gd^{158} was obtained after subtraction of the line with energy 4.95 Mev, emitted by C^{13} which is formed by the absorption of neutrons by the graphite container.

TABLE 3

Some Data on Erbium Isotopes

Isotope (target)	Content in the natural mixture,%	Isotopic absorption cross section, barns	Contribution to the total thermal absorption cross section, %	Neutron binding energy in the product-nucleus, Mev	
				measured [2]	calculated **
Er^{162}	0.136				6.9
Er^{164}	1.56				6.6
Er^{166}	33.4			6.46±0.056	6.3
Er^{167}	22.9			7.76±0.056	7.5
Er^{168}	27.1	2.0±0.4***	0.3		5.9
Er^{170}	14.9	9±2***	0.8		5.6

---

* $\sigma_a = (166 \pm 16)$ barns.

**Calculated by Weizsäcker's formula [3].

***Activation cross section.

TABLE 4

Energies and Intensities of Erbium γ-rays

Results of this work			Results of other work				
			Skliarevskii, et al. [5]		Dzhelepov et al, [11]	Fenstermacher et al. [11]	
designation of γ-lines	E_γ Mev	I**	E_γ Mev	I**	E_γ Mev	E_γ Mev	I**
1	6.680±0.015	0.9					
2	6.202±0.015	1.3					
3	6.07±0.03	0.5					
4	5.88±0.03	0.6					
5	5.73±0.04	0.4					
6	5.34±0.03	1					
7	4.77±0.035	0.6					
8	4.66±0.03	1					
9	4.42±0.045	0.6					
*10****	~4.1						
*11****	~1.9						
*12****	~1.3						
13	1.01±0.02	3					
14	0.94±0.02	5					
15	0.828±0.01	36				0.82±0.02	
16	0.736±0.015	10				0.73±0.02	
17	0.64±0.02	4					
						0.28±0.01	5
			0.185	82****		0.188±0.01	~50
			0.082	85****	0.0798		

---

*Investigation of γ-rays from resonance capture of neutrons.

**Intensity in quanta per 100 neutron captures.

***Unresolved group of lines.

****Intensity taking into account conversion.

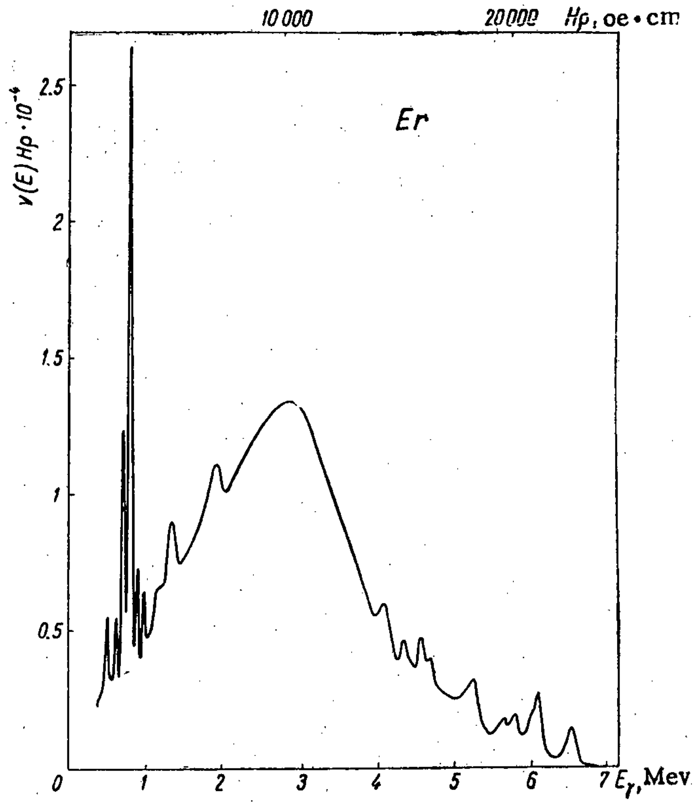

Fig. 6. Corrected γ-ray spectrum of Er_2O_3.

conversions, amounted to ~ 80 γ-quanta per 100 neutron captures. In the capture of neutrons by erbium, it is possible to form only a single even-even isotope, namely Er^{168}. From this we concluded that the main contribution to the absorption of neutrons by erbium was from the single odd isotope Er^{167}. Therefore, the main part of the erbium γ-ray spectrum must be ascribed to Er^{168}.

The experimental and corrected γ-ray spectra of erbium are shown in Figures 5 and 6. The energies of the erbium γ-ray spectrum are given in Table 4. There, we give the results of measurements by other authors for the low energy range. The intensities of the lines in numbers of γ-quanta per 100 neutron captures given in the table were obtained by normalization using the following formula [1]:

$$\int_{0.3}^{E_{max}} E_\gamma \nu(E_\gamma)\, dE_\gamma = (7.76 \cdot 0.8 + 6.3 \cdot 0.2) \text{ Mev}$$

where 7.76 Mev is the neutron binding energy of Er^{168} and 6.3 Mev is the average binding energy taken for the rest of the isotopes. The erbium γ-lines, given in Table 4, are responsible for about 10% of the energy radiated by the sample.

Hafnium

In the measurements with hafnium, 85 g of hafnium oxide HfO_2 was used as the radiation sample. Data on the isotopes of hafnium are given in Table 5. The total thermal neutron absorption cross section for hafnium equals (115 ± 15) barns. The data given in the table indicates that the γ-radiation accompanying the absorption of thermal neutrons by the natural mixture of hafnium isotopes would mainly belong to Hf^{178} (~ 70 %) and partly to Hf^{179} (~ 20%). The rest of the isotopes would make a comparatively small contribution.

TABLE 5

Some Data on Hafnium Isotopes

Isotope (target)	Content in the natural mixture, %	Isotopic absorption cross section, barns	Contribution to the total thermal neutron absorption cross section, % *	Neutron binding energy in the product-nucleus, Mev	
				measured	calculated **
Hf^{174}	0.18	1500±1000	2,4		
Hf^{176}	5,2	15±15	0.7	6.70±0.09 [10] 6,28±0.056 [2]	6.4
Hf^{177}	18.4	380±30	65.4	7.55±0.056 [2]	7.9
Hf^{178}	27.1	75±10	19	6,52±0.12 [10]	
Hf^{179}	13.8	65±15	8,3	6.18±0.056 [2]	
Hf^{180}	35.4	13±15	4,2	7.32±0.056 [2]	5.4

---

* σ_a = (115 ± 15) barns.

**Calculated by Weizsäcker's formula [3].

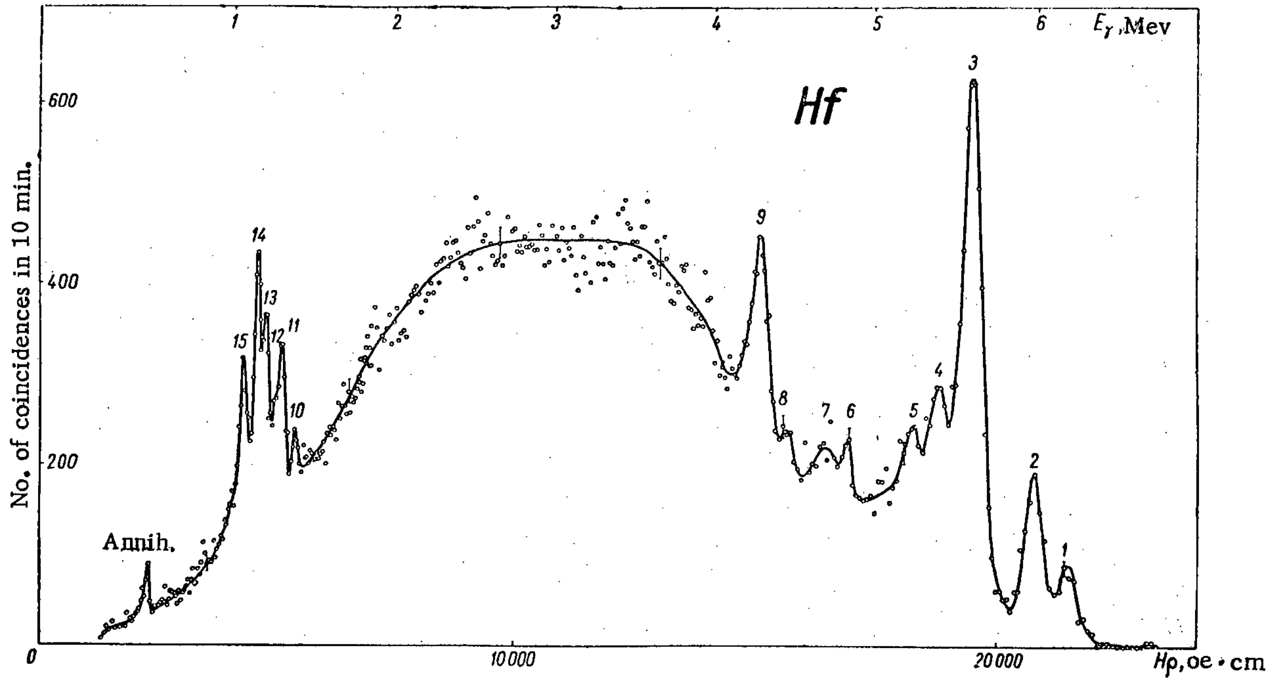

Fig. 7. Experimental γ-ray spectrum of HfO_2.

The experimental and corrected γ-ray spectra of HfO_2 are shown in Figures 7 and 8.

The energies and intensities of the γ-lines of the HfO_2 spectrum obtained in this work are given in Table 6. There we also give the results of measurements by other authors in the low energy region. The γ-lines given in Table 6 are responsible for about 12% of the energy radiated by the hafnium nuclei during their capture of thermal neutrons.

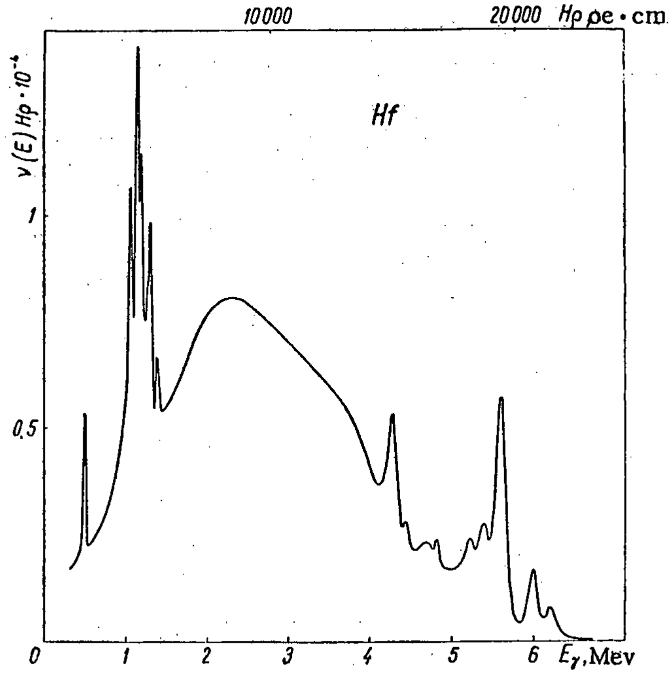

Fig. 8. Corrected γ-ray spectrum of HfO_2.

Dysprosium

The irradiated sample was 1.8 g of Dy_2O_3, deposited as a thin layer on three discs of thin aluminum foil. Data on the isotopes of dysprosium are given in Table 7. The total absorption cross section of the natural mixture of dysprosium isotopes equals (1100 ± 150) barns. Comparison of this with the activation cross section of Dy^{164} shows that the capture of neutrons by Dy^{164} amounts to approximately 70% and, consequently, the greater part of the γ-rays belong to Dy^{165}. The thermal neutron absorption cross sections of the other dysprosium isotopes were unknown to us.

The neutron binding energy of the Dy^{165} nucleus has not been measured experimentally as yet. In the last column of Table 7 we give the binding energy calculated by Weizsäcker's formula [3]. For Dy^{165} it equals 5.8 Mev. We also used this value in determining the γ-line intensities in γ-quanta per 100 neutron captures.

The experimental and corrected γ-ray spectra of dysprosium are given in Figures 9 and 10. The energies and intensities of the dysprosium γ-lines are given in Table 8. The γ-rays given account for 17% of the energy emitted by the nucleus, i. e., somewhat more than in the case of an even-even nucleus.

Tantalum

The sample was 425 g of metallic tantalum. The experimental and corrected γ-ray spectra of tantalum are given in Figures 11 and 12. The energies and intensities of the γ-lines are given in Table 9. They agree well with the results of Bartholomew and Kinsey [17], except for the intensity of the γ-line with an energy of 6.04 Mev. The reason for the discrepancy in this case was not clear to us. As in the work of Bartholomew and Kinsey, the half-width of the peak at an energy of 6.04 Mev which we obtained exceeds the standard value. Though we, too, resolved this peak into two components (lines 1 and 2), in Table 9 we give the total intensity of these lines, since the ratio of their intensities could not be determined sufficiently reliably.

TABLE 6

Energies and Intensities of Hafnium γ-rays

Results of this work			Results of other work					
			Skliarevskii et al. [5]		Sharf-Goldhaber et al. [12]	Heydenberg, Temmer [13]	Sunyar [14]	Bockelman et al. [15]*
designation of γ-lines	E_γ Mev	I**	E_γ Mev	I**	E_γ Mev	E_γ Mev	E_γ Mev	E_γ Mev
1	6.39 ±0.04	0.5						
2	6.14 ±0.02	1						
3	5.730±0.012	3.6						
4	5.49 ±0.03	1.2						
5	5.34 ±0.03	1						
6	4.92 ±0.03	0.5						
7	4.80 ±0.045	0.4						
8	4.54 ±0.04	0.2						
9	4.385±0.015	1.6						
10	1.415±0.015	1.2						
11	1.339±0.015	5						
12	1.30 ±0.02	3						
13	1.220±0.015	7						
14	1.180±0.015	9						
15	1.090±0.015	6						
					0.501			
					0.4436			
					0.3324			0.33±0.01
			0.213	66***	0.216			0.22±0.01
			0.092	71***	0.0933	0.090	0.093	0.090±0.005
					0.0576			

---

*Investigation of γ-rays from resonance absorption of neutrons.

**Intensity in quanta per 100 neutron captures.

***Intensity taking into account conversion.

TABLE 7

Some Data on Dysprosium Isotopes

Isotope (target)	Content in natural mixture %	Isotopic absorption cross section, barns	Contribution to total thermal neutron absorption cross section*, %	Neutron binding energy in product-nucleus, Mev	
				measured [2]	calculated ***
Dy^{156}	0.0524	—	—	—	7.0
Dy^{158}	0.0902	—	—	—	6.6
Dy^{160}	2.294	—	—	6.41±0.056	6.4
Dy^{161}	18.88	—	—	8.17±0.056	7.7
Dy^{162}	25.53	—	—	6.27±0.056	6.0
Dy^{163}	24.97	—	—	7.63±0.056	7.4
Dy^{164}	28.18	510±20. $T_{1/2}=1.3$ min.** 2100±300. $T_{1/2}=2.4$ hrs. **	67	—	5.8

---

*$\sigma_a = (1100 \pm 150)$ barns.

**Activation cross section.

***Calculated by Weizsäcker's formula [3].

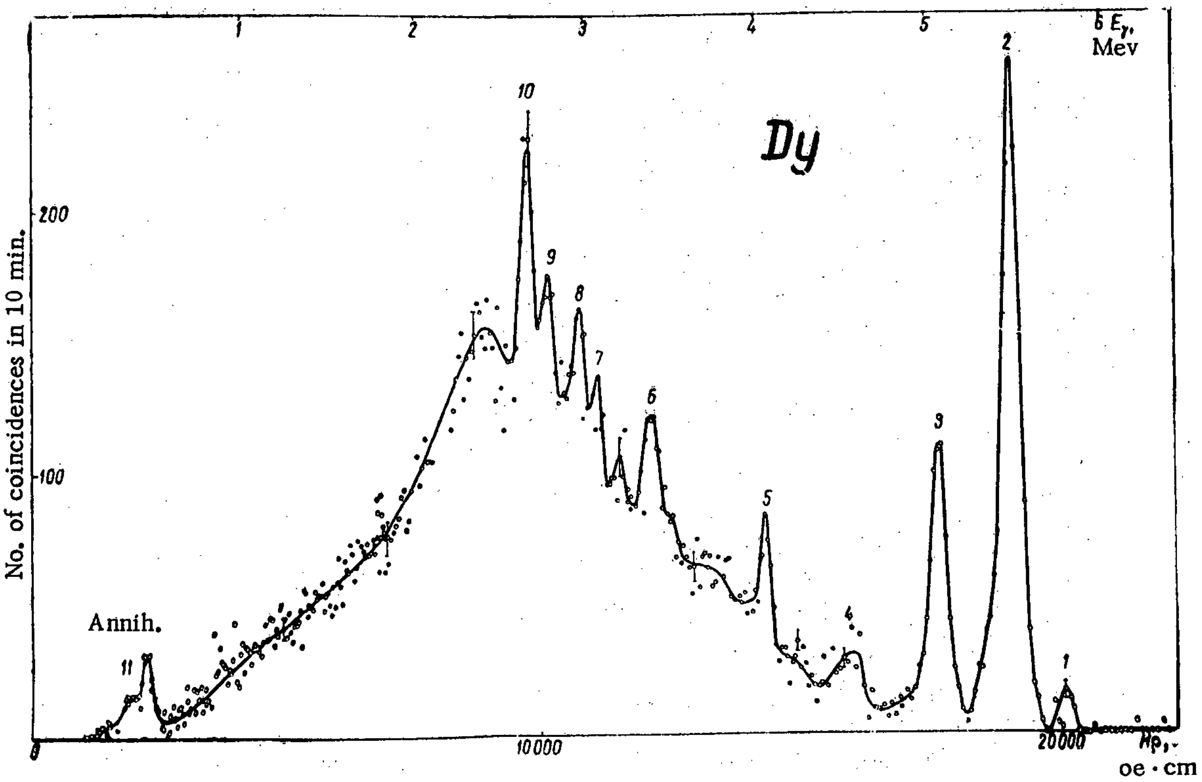

Fig. 9. Experimental γ-ray spectrum of Dy_2O_3.

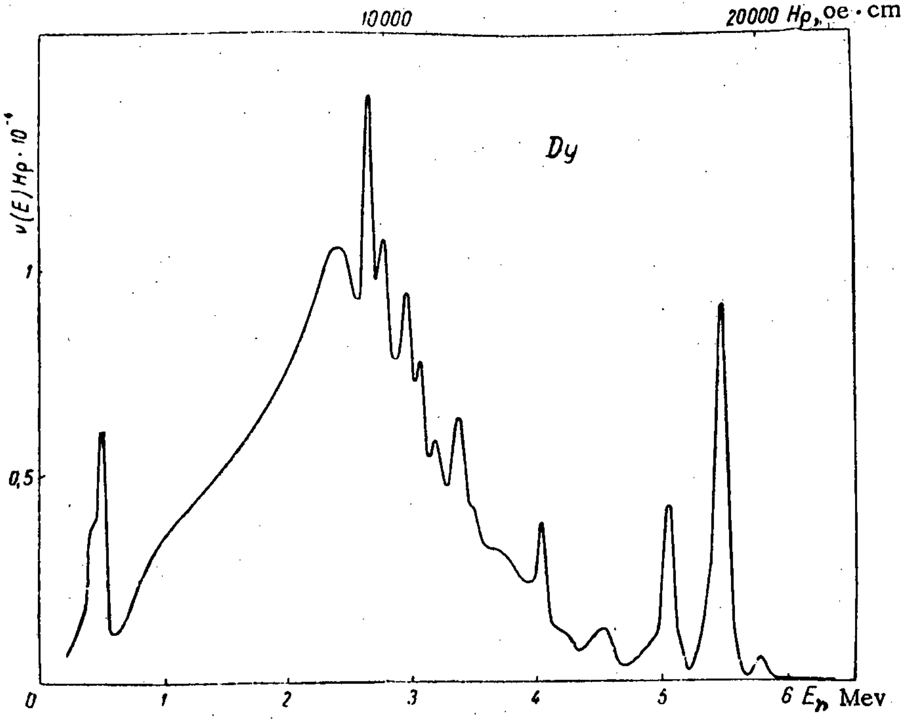

Fig. 10. Corrected γ-ray spectrum of Dy_2O_3.

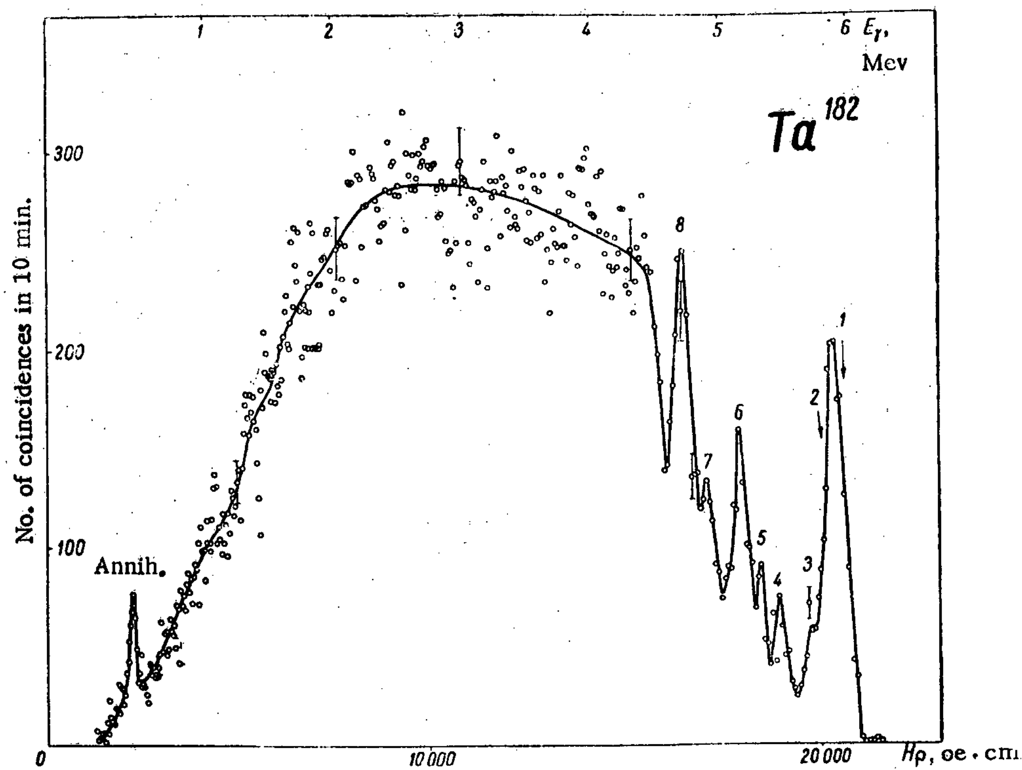

Fig. 11. Experimental γ-ray spectrum of Ta^{182}.

TABLE 8

Energies and Intensities of dysoprosium γ-rays

Results of this work			Results of other work		
			Skliarevskii et al. [5]		Gibdon, Meuhlhause [16]
designation of γ-lines	E_γ Mev	I*	E_γ Mev	I*	E_γ Mev
1	5.87 ±0.02	0.26			
2	5.580±0.015	5.9			
3	5.15 ±0.02	2.7			
4	4.65 ±0.04	0.5			
5	4.10 ±0.025	1.2			
6	3.48 ±0.03	1.6			
7	3.14 ±0.03	1.3			
8	3.04 ±0.03	1.9			
9	2.86 ±0.03	2.1			
10	2.74 ±0.025	3.9			
11	0.42 ±0.02	4			
			0.180	21**	0.188
			0.104	49**	0.108
			0.078	16**	0.080

Tantalum has one stable isotope Ta^{181}. The neutron binding energy in the Ta^{182} nucleus formed equals 6.03 ± 0.15 Mev [18]. Line 1 probably corresponds to a transition between the initial and the ground states. Almost nothing is known about the excited levels of Ta^{182}.

DISCUSSION OF RESULTS

From the spectra given above it is obvious that in the case of heavy nuclei that are not situated near to the magic numbers, the main part of the γ-transitions forms the unresolvable part of the spectrum, due to the closeness of the levels in these nuclei. On both sides of the continuous spectrum, a series of peaks separates out. The peaks in the high energy region correspond to γ-transitions from the initial state, produced by the capture of a neutron, to lower nuclear levels. In contrast to light nuclei, here the separate lines, as a rule, have a low intensity: ~ 1 quantum per 100 neutron captures. The lines situated on the initial part of the continuous spectrum correspond to transitions between the lower levels.

---

*Intensity in quanta per 100 neutron captures.

**Intensity taking into account conversion.

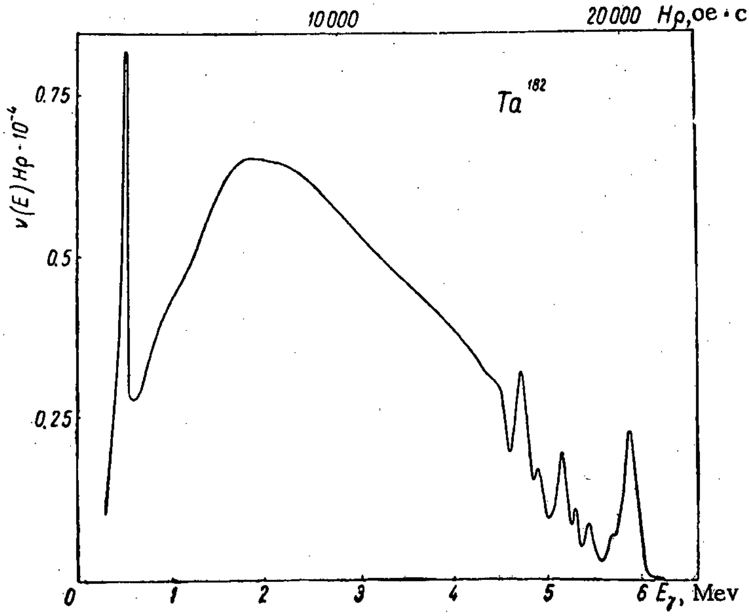

Fig. 12. Corrected γ-ray spectrum of Ta^{182}.

TABLE 9

Energies and Intensities of Tantalum γ-Rays

Results of this work			Results of other work			
			Bartholomew and Kinsey [17]		Skliarevskii et al. [5]	
designation of γ-lines	E_γ Mev	I*	B_γ Mev	I*	E_γ Mev	I*
1	6.04±0.02	1.8	6.07±0.03	0.7		
2	5.94±0.03					
3	5.80±0.03	0.3	5.78±0.05	0.3		
4	5.54±0.03	0.4	5.57±0.03	0.3		
5	5.36±0.03	0.3	5.38±0.03	0.3		
6	5.24±0.03	0.8	5.21±0.03	0.5		
7	4.99±0.03	0.4	5.05±0.03	0.5		
8	4.83±0.03	1.2	4.84±0.03	1		
					0.272	70
					0.170	22
					0.133	30
					0.107	15.2

---

*Intensity in quanta per 100 neutron captures.

From the spectra of Gd^{156}, Gd^{158} and Hf^{178}, it is very clear that in these cases in the low energy region (~ 1 Mev) there are groups of closely placed intense lines. Their total intensity is about 50 quanta per 100 neutron captures. Apparently, a similar picture is found in the case of erbium. However, the latter example is less convincing as here the distribution of the thermal neutron absorption between the isotopes has not been unequivocally established.

The lower states of all the even-even nuclei mentioned have the characteristics 0^+, 2^+, 4^+ and energies of 0, ~ 80 and ~ 300 kev. Transitions between these levels always have high intensity. With our apparatus we were unable to measure γ-rays of such low energies; however, they were readily observed by the luminescence method [5].

To return to the even-even radiating nuclei which interest us, it is notable that for the intense lines lying in the region of ~ 1 Mev, the difference in their energies, in many cases, agrees quite well with the spacing between the levels of the rotation bands of the ground state (Table 10 for Gd^{158} and Gd^{156}). From this we can conclude that the group of intense lines with energies of about 1 Mev correspond to transitions into the ground state and the rotation levels closest to it.* In its turn, this forces one to admit that in these nuclei there must exist a small number of heavily populated levels in the region of 1 Mev. From this, however, it does not follow that the nucleus is obliged to have a low density of levels in this energy region. A small number of levels with a high capacity may also appear in the presence of

---

*The high intensity of the γ-transitions considered also indicates that these γ-lines correspond to transitions between lower nuclear levels.

TABLE 10

Energy Differences of the γ-Lines of the Radiating Isotopes Gd^{158} and Gd^{156}

Gd^{158}				Gd^{156}			
designation of γ-line,	energy of γ-line, kev	difference in energy of γ-lines*, kev	level spacing, kev	designation of γ-line,	energy of γ-line, kev	difference in energy of γ-lines*, kev	level spacing, kev
9 *10*	1320 1260	60±20	80 (Ground state – second excited)	*10* *11*	1240 1170	70±30	89 (Ground state – second excited)
10 *11*	1260 1180	80±20		*11* *12a*	1170 1060	110±30	
11 *12*	1180 1120	60±20		*12a* *13*	1060 960	100±30	
9 *12*	1320 1120	200±20	180 (First excited – second excited)	*10* *12a*	1240 1060	180±30	198 (First excited – second excited)
12 *13*	1120 960	160±20		*11* *13*	1170 960	210±30	

---

*The differences in energy of the γ-lines were determined from the positions of the tops of the corresponding peaks.

a high level density if they belong to bands of collective excitation. In this case we would observe an agglomeration of transitions into the ground states of the bands of collective excitation at energies of ~ 1 Mev, if the probability of transition between the levels of this band and the levels of the bands with equal or close projections of total angular moment (K) on the axis of symmetry of the nucleus, was much greater than the probability of a transition to the level of the first rotational band (K = 0). Apparently, transitions from the ground state bands to levels of the first rotational band also result in the appearance of intense peaks in the region of ~ 1 Mev in our spectra.

In particular, such a picture was observed in the scheme of γ-transitions for the $_{74}W^{182}_{108}$ nucleus (Fig. 13 taken from paper [19]), which also belongs to the category of nuclei considered and has been thoroughly examined in investigating the β-decay of Ta^{182}. Alaga et al., [20], in considering this scheme, came to the conclusion that in this nucleus there were bands of collective excitation at energies of ~ 1 Mev. Apparently, there is a similar picture in the case of the even-even radiating nuclei Gd^{156}, Gd^{158}, Er^{168} and Hf^{178} which we investigated.

To confirm this picture it is necessary to perform measurements on the γ-ray spectra in the region of 0-2 Mev with considerably greater accuracy than was possible with our apparatus. Such measurements would make it clear whether there were present in these nuclei the comparatively intense γ-rays, which may be assigned to transitions in higher bands of collective excitation.

As Figures 9 and 11 show, in even-odd and odd-odd radiating nuclei, lying in the same range of values of N, groups of intense lines in the energy region of ~ 1 Mev are completely absent. This is due to the fact that in even-odd and particularly in odd - odd nuclei, even at excitation energies of ~ 0.3-0.5 Mev there is a high density of levels, belonging to the different configurations. Under these conditions, during the radiation of the nucleus the most strongly populated are the lowest of its levels, between which the transitions are such that they cannot be recorded by the apparatus we used.

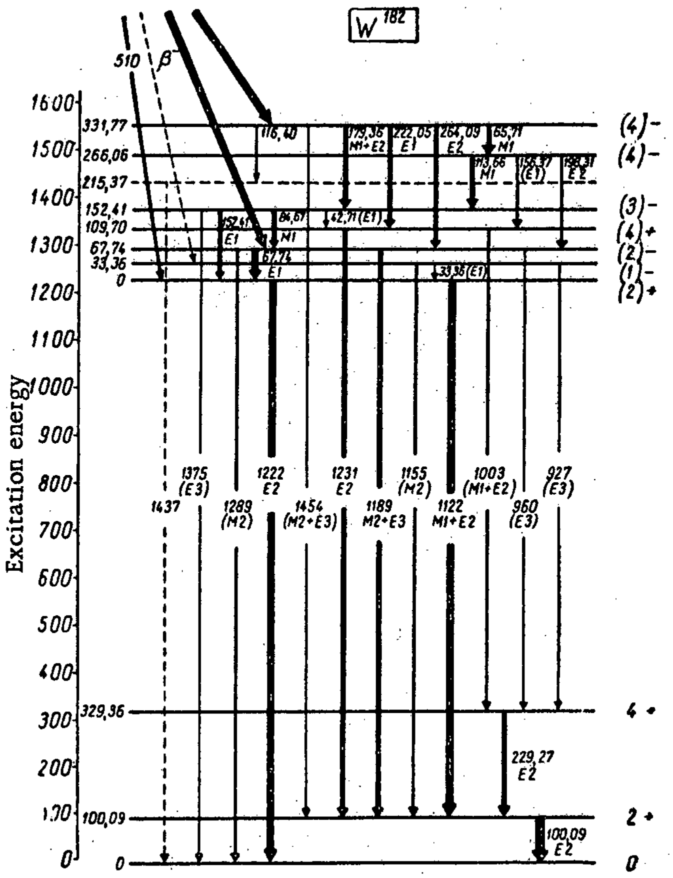

Fig. 13. Scheme of γ-transitions of the W^{182} nucleus.

TABLE 11

Characteristics of the Initial States of Gd^{156}, Gd^{158} and Hf^{178}

Target-nucleus		Radiating product-nucleus	
	spin and evenness of ground state		spin and evenness of initial state
Gd^{155}	3/2 - [21]	Gd^{156}	1-; 2-
Gd^{157}	3/2 - [21]	Gd^{158}	1-; 2-
Hf^{177}	7/2 - [22]	Hf^{178}	3-; 4-

We should nota a series of circumstances concerning high energy transitions from the initial state, produced by the capture of a neutron. In Table 11 we give the moments and the evenness for the ground states of the irradiated nuclei and the initial states of the radiating nuclei. As has already been shown, the final nuclei in all cases have a system of rotation levels with characteristics 0^+, 2^+, 4^+, close to the ground state. Therefore, in Gd^{156}, Gd^{158} and Hf^{178} E1-transitions are able to go to several of these levels. However, according to our measurements, intensity of such transitions is insignificantly small. Thus for Gd^{158} it does not exceed 0.02 quanta per 100 neutron captures and in the case of Hf^{178} the limit of the value is 0.01. This can be explained by the following circumstances. A number of authors (see for example [23]) have shown that the coupling energy

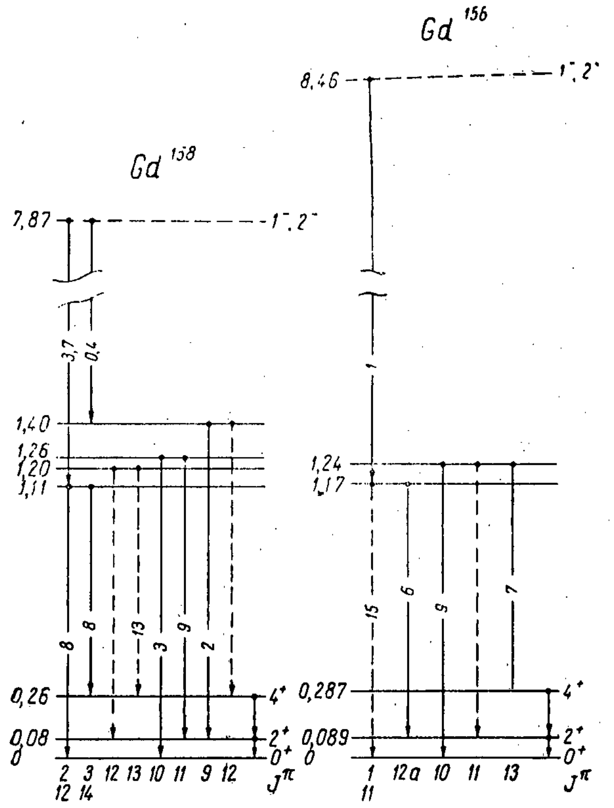

Fig. 14. Scheme of γ-transitions of the Gd^{158} and Gd^{156} nuclei.

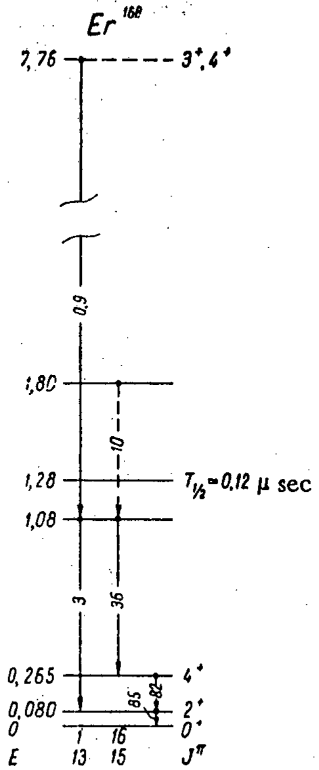

Fig. 15. Scheme of γ-transitions of the Er^{168} nucleus.

of the nucleons is greater the greater their orbital spin moments l. Consequently, we may assume that the even-even nuclei in the ground states have final neutrons with high values of l (for Gd^{156}, Gd^{158} and Hf^{178}, in all probability, $l = 3$ [24]). Therefore, the E1-transitions considered will be associated with large changes in l for a neutron, which can considerably reduce their probability.

For the even-even nuclei we investigated, almost nothing is known on the excited states, besides the levels of the lower rotational band. Therefore, it is impossible to construct reliable schemes of γ-transitions for them. However, using the interpretation of the group of intense lines given above, we can suggest the schemes of γ-transitions for the nuclei Gd^{158} and Gd^{156}, given in Figure 14. They are naturally not unequivocal and can only illustrate the character of the transitions in the even-even nuclei considered.

After this article had been written, a report [25] appeared on the results of investigation of the decay $Tm^{168} \xrightarrow{\text{K-capture}} Er^{168}$. γ-Rays were observed with energies 0.0804; 0,0999; 0.185; 0.199; 0.247; 0.448; 0.720 and 0.810 Mev. In the work it was assumed that in Er^{168} there were excited levels with energies of 0,080; 0.265; 1.080; 1.28 Mev (metastable level with $T_{1/2} = 0.12\,\mu$ sec) and 1.80 Mev. Several of the γ-lines measured by us fit well into this scheme of levels (Fig. 15).

We should note that in the study of different β-decaying substances, in a number of cases schemes of levels were obtained for even-even nuclei, reminiscent of the schemes in Figures 14 and 15. This is so, for example, in the case of ${}_{62}Sm^{152}$, ${}_{64}Gd^{154}$ and ${}_{94}Pu^{238}$ [26].

Received August 31, 1957

LITERATURE CITED

[1] L. V. Groshev, B. P. Ad'iasevich and A. M. Demidov, "Physical Investigations," Report of Soviet Delegation at the International Conference on Peaceful Uses of Atomic Energy (Acad. Sci. USSR Press, 1955) p. 252; Acad. Sci. USSR Session on the Peaceful Uses of Atomic Energy (Meeting of Phys.-math. Div.) (Acad. Sci. USSR Press, 1955)p. 270.

[2] W. H. Johnson, private communication.

[3] E. Fermi, Nuclear Physics [Russian translation] (IL, 1951) p. 16.

[4] B. B. Kinsey and G. A. Bartholomew, Can. J. Phys. 31, 1051 (1953).

[5] V. V. Skliarevskii, E. P. Stepanov and B. A. Obiniakov, J. Atomic Energy (USSR) 4, 1, 22 (1958) [present issue, translation page 19.]

[6] L. V. Groshev, A. M. Demidov and V. A. Naidenov, Izv. AN SSSR (in press).

[7] E. L. Church and M. Goldhaber, Phys. Rev. 95, 626A (1954).

[8] C. A. Fenstermacher, T. E. Springer and H. L. Schultz, Bull. Am. Phys. Soc., Ser. II 2, 218 (1957).

[9] B. S. Dzhelepov, B. K. Preobrazhenskii and K. Ia. Gromov, Izv. AN SSSR (in press).

[10] R. Tobin and J. McElhinney, Bull. Am. Phys. Soc., Ser. II 1, 340 (1956).

[11] C. A. Fenstermacher, R. L. Hickok and H. L. Schultz, Bull. Am. Phys. Soc., Ser. II 2, 41 (1957).

[12] J. W. Mihelich, G. Scharf-Goldhaber and M. McKeown, Phys. Rev. 94, 794A (1954).

[13] N. P. Heyderburg and G. M. Temmer, Phys. Rev. 100, 150 (1955).

[14] A. W. Sunyar, Phys. Rev. 95, 626A (1954).

[15] C. K. Bockelman, C. A. Fenstermacher and J. E. Draper, Bull. Am. Phys. Soc., Ser. II 2, 41 (1957).

[16] C. T. Hibdon and C. O. Muehlhause, Phys. Rev. 88, 943 (1952).

[17] G. A. Bartoholomew and B. B. Kinsey, Can. J. Phys. 31, 1025 (1953).

[18] J. A. Harvey, Phys. Rev. 81, 353 (1951).

[19] J. J. Murray, F. Boehm, P. Marmier and J. W. M. DuMond, Phys. Rev. 97, 1007 (1955).

[20] G. Alaga, K. Alder, A. Bohr and B. Mottelson, Kong. Danske. Vidensk. Selsk., Mat.-fis. Medd. 29, No. 9 (1955).

[21] W. Low, Phys. Rev. 103, 1309 (1956); D. R. Speck, Phys. Rev. 101, 1725 (1956).

[22] D. R. Speck and F. A. Jenkins, Phys. Rev. 101, 1831 (1956).

[23] J. M. Blatt and V. F. Weisskopf, Theoretical Nuclear Physics [Russian translation] (IL, 1954) p. 598.

[24] M. G. Mayer and J. H. Jensen, Elementary Theory of Nuclear Shell Structure (1955) p. 74.

[25] K. P. Jacob and J. W. Michelich, Bull. Am. Phys. Soc., Ser. II 2, 260 (1957).

[26] B. S. Dzhelepov and L. K. Peker, Decay Schemes of Radioactive Isotopes [in Russian] (Izd. AN SSSR, Moscow-Leningrad, 1957).

INVESTIGATION OF THE γ-RAYS ACCOMPANYING THERMAL-NEUTRON CAPTURE BY CERTAIN RARE-EARTH NUCLEI

V. V. Skliarevskii, E. P. Stepanov and B. A. Obiniakov

Using a scintillation spectrometer measurements have been made of the spectra of γ-rays accompanying thermal-neutron capture in a number of nuclei.

A number of intense lines have been found below 300 kev in the γ-ray spectra for thermal-neutron capture in europium, gadolinium, dysprosium, holmium, erbium, thulium, hafnium and tantalum. Lines corresponding to $4^+ \rightarrow 2^+$ and $2^+ \rightarrow 0^+$ transitions between rotational levels of Er^{168} and Hf^{178} were found in the erbium and hafnium spectra. The intensity of these transitions corresponds to 0.5-0.8 photons per capture event.

Using a scintillation spectrometer with a NaI(Tl) crystal (3.0 cm in diameter, 1.2 cm thick) measurements have been made of the γ-rays accompanying thermal-neutron capture in europium, gadolinium, dysprosium, holmium, erbium, thulium, and tantalum, in the energy region below 300 kev. A diagram of the experimental arrangement is shown in Figure 1. The work was carried out using the neutron beam from the RFT reactor of the Academy of Sciences, USSR. The pulse heights were measured in a 30-channel analyzer. The energy discrimination of the spectrometer was 15 percent for the 320 kev γ-rays from Cr^{51} and 20 percent for the 102 kev γ-rays from Gd^{153}.

To determine the intensities of the capture γ-rays (the number of photons per capture event) a comparison was made of the areas of the photo-peaks for the γ-rays being studied and the 480-kev γ-rays formed in the $B^{10}(n,\alpha)Li^7$ reaction in a boron target. The yield for these γ-rays was taken as 0.93 . This method of determining the intensities of capture γ-rays was first used in [1].

As is apparent from Figures 2-4, the photo-peaks which appear in the spectra are found in a rather continuous distribution; part of the effect is due to the background (amounting to 5-30 percent of this distribution, depending on the target) but the main contribution is that of pulses produced by the harder capture γ-rays from the target.

Because of this continuous distribution it is difficult to determine the areas of the photo-peaks. Thus, additional measurements of the spectra were carried out in which lead or tin filters were placed between the target and the crystal; these filters absorbed a known fraction of the γ-rays being measured and the areas of the photo-peaks were then determined from the differences in the spectra measured with and without the filter. Since the filters have virtually no effect on the background, the differences in these spectra are completely determined by the radiation being studied.

In some cases the measurements in which the absorbers were used made it possible to establish the presence of γ-ray peaks which remained unnoticed when the simple spectra were taken. This effect is illustrated in the europium spectrum (Fig. 5).

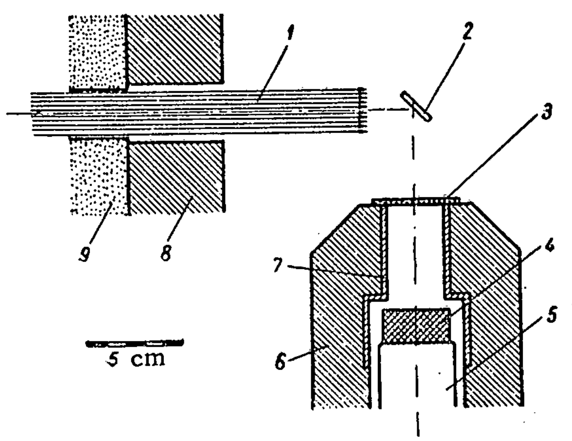

Fig. 1. Diagram of the experiment. 1) Neutron beam; 2) target; 3) boron absorber; 4) crystal; 5) type "C" photomultiplier; 6) lead shield; 7) absorber (0.3 mm of tantalum plus 0.5 mm of tin plus 0.2 mm of copper) for attenuating the x-ray, K-radiation from lead; 8) collimator; 9) boron collimator.

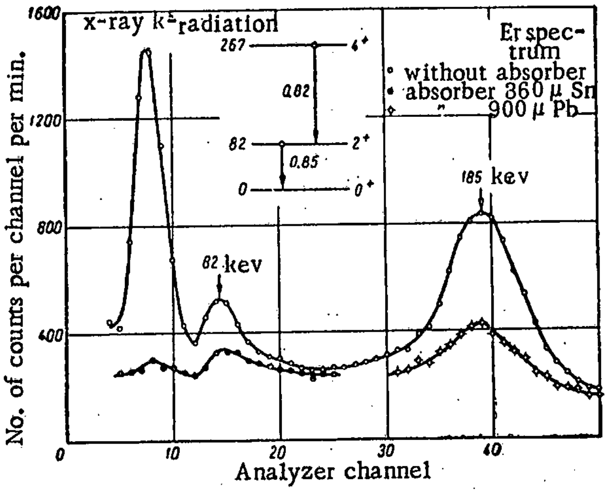

Fig. 2. Erbium spectrum. The proposed level scheme for Er^{168} is shown. Figures near the arrows on the level scheme indicate the intensity of the transition.

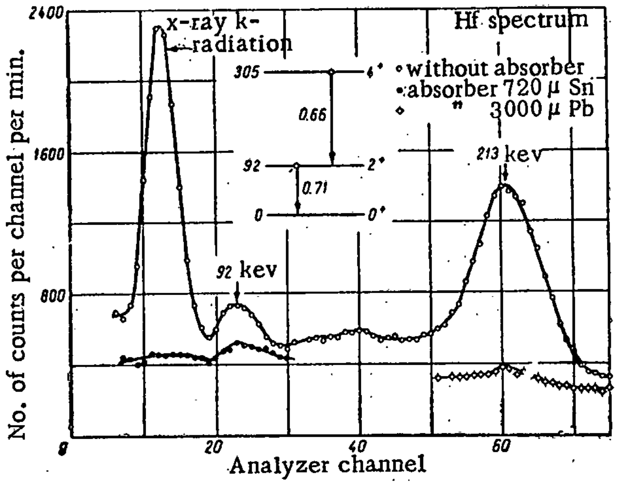

Fig. 3. Hafnium spectrum. The proposed level scheme for Hf^{178} is shown.

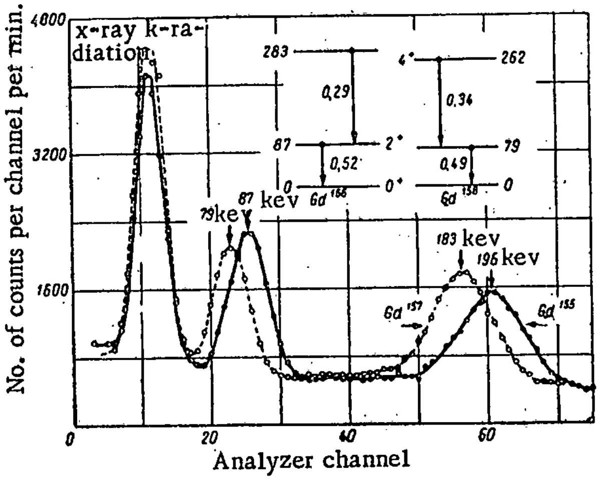

Fig. 4. Gadolinium spectrum. The solid line corresponds to the γ-rays emitted by the Gd^{155} target, the dotted line corresponds to the Gd^{157} target. The level schemes proposed for the isotopes Gd^{156} and Gd^{158} formed in neutron capture are shown. The figures near the arrows on the level diagram indicate the intensity of the transition.

The dependence of spectrometer efficiency on γ-ray energy was computed in the usual way [2]. The ratio of the number of pulses at the photopeak to the total number of pulses produced by the γ-rays, which is required for these calculations, was measured using a number of sources of monochromatic γ-rays with energies of 102 kev (Gd^{153}), 145 kev (Ce^{141}), 320 kev (Cr^{51}), 480 kev (the $B^{10}(n, \alpha)Li^7$ reaction) and 662 kev (Cs^{137}).

The targets were powders of the oxides, pressed into aluminum containers 20 mm in diameter and 0.3 mm thick. The background spectrum was measured with an empty aluminum container.

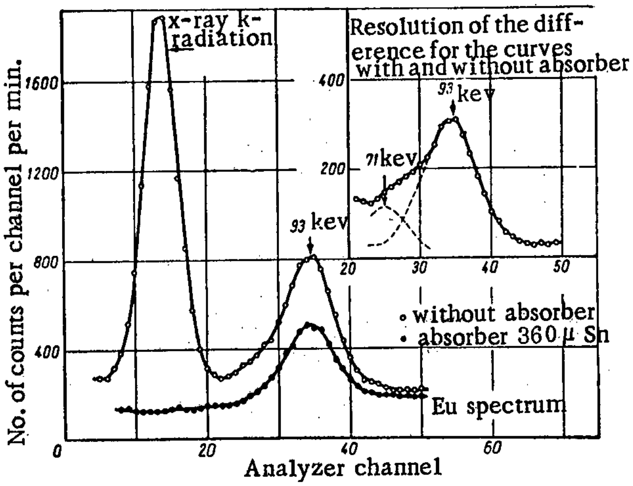

Fig. 5. Europium spectrum. On the 93-kev line is shown the unresolved line at 71 kev which can be separated graphically as shown in the insert.

As a rough check on the purity of the targets each target was used in a measurement of the total thermal-neutron cross section using the transmission method with a boron target as a detector; the γ-rays from this target were measured with the scintillation spectrometer. The results of these measurements indicated that the materials being investigated had no significant contamination.

Results of the Measurements

Erbium. The way in which each isotope contributes to the capture cross section in erbium is known. In the spectrum obtained in the present work (Fig. 2) the γ-ray lines at 82 and 185 kev are particularly pronounced. The energy ratio for these lines is in good agreement with the energy ratio for rotational levels of an even-even nucleus. The corresponding energy-level scheme is shown in Figure 2. The high intensity of these lines (the number of photons per capture event), computed from the total neutron capture cross section in erbium, indicates that the main contribution to the thermal-neutron capture cross section in a natural mixture of erbium isotopes is due to Er^{167} – the only erbium isotope which can form an even-even nucleus in neutron capture. The first rotational level is known from experiments on γ-rays in Coulomb excitation [3]. The value of 79 kev for the first level obtained in this work is in good agreement with the present value. The present results for the second level are in agreement with those of [4] in which 188-kev γ-rays were found with an intensity of approximately 0.5.

Hafnium. The main contribution to the thermal-neutron capture cross section in hafnium is due to Hf^{177}. In the capture neutron γ-ray spectrum for hafnium (Fig. 3) the line at 92 kev corresponds to a transition from the first rotational level in Hf^{178}, known from Coulomb excitation experiments [3]. The 213-kev line corresponds to a transition from the second rotational level in Hf^{178} to the first; however, a significant contribution may also be due to the 215-kev γ-rays emitted in the isomeric transition in Hf^{179} with a half-life of 20 sec. The contribution of the isomeric transition was determined by measuring the spectrum from the hafnium target immediately after the neutron beam was cut off and was found to be 20 percent of the total intensity of the 213-kev line.

These data confirm the results of [5] in which lines at 90, 220 and 330 kev were found in the γ-ray spectrum accompanying capture of resonance neutrons.

Gadolinium. In References [6] and [7], in which studies were made of the spectra of internal conversion electrons for γ-rays accompanying thermal-neutron capture in gadolinium, it was established that there are 79 and 180 kev γ-rays corresponding to the $Gd^{157}(n, \gamma)\, Gd^{158}$ reaction and 89 and 196-kev γ-rays corresponding to the $Gd^{155}(n, \gamma)\, Gd^{156}$ reaction.

The measurements of the yields of these γ-rays was carried out in different isotopes in the present case. In the Gd^{155} target the content of the isotope being studied was 97.3 percent while in the Gd^{157} target this figure was 91.4 percent. The spectra for these targets are shown in Figure 4.

In erbium and hafnium we carried out measurements of the $\gamma - \gamma$-coincidences which indicated that the γ-rays corresponding to the proposed transition $4^+ \rightarrow 2^+$ and $2^+ \rightarrow 0^+$ in the even-even nuclei Er^{168} and Hf^{178} are actually emitted in cascade fashion.

A general feature of capture γ-rays emitted by even-even isotopes of erbium, hafnium and gadolinium is the high intensity of the $4^+ \rightarrow 2^+$ and $2^+ \rightarrow 0^+$ transitions; it follows that a considerable fraction of the transitions from the higher levels go to the 4^+ level.

Isotope emitting the γ-ray	Energy of the γ-ray, kev	Intensity of the γ-ray (number of photons per neutron capture event),* ν_γ	Multipolarity of the transition	α_K	α_L	Intensity of the transition $\nu = \nu_\gamma(1 + \alpha_K + \alpha_L)$
Er^{168}	82	0.18	E2	1.6	2.1	0.85
	185	0.64	E2	0.20	0.084	0.82
Hf^{178}	92	0.19	E2	1.0	1.7	0.71
	213	0.55	E2	0.13	0.07	0.66
Gd^{158}	79	0.104	E2	2.0	2.05	0.53
	183	0.22	E2	0.22	0.09	0.29
Gd^{156}	87	0.137	E2	1.37	1.25	0.50
	196	0.277	E2	0.17	0.054	0.34
Dy^{165}	78	0.028	M1	4.1	0.68	0.16
	104	0.018	E3	3.4	22.6	0.49**
	180	0.16	E2	0.22	0.1	0.21
Eu^{152}	72	0.044				
	90	0.20				
Ho^{168}	121	0.20				
	142	0.31				
Ta^{182}	107	0.152				
	133	0.30				
	170	0.22				
	272	0.7				
Tu^{170}	150	0.073				

---

* ν_γ for Er^{168} is computed for a total neutron capture cross section in erbium σ = 166 barns. In all the other cases the isotope cross sections are used [11].

** This value of the intensity for the isomeric transition with a half-life of 1.3 min actually represents a fraction of the cross section for the production of $Dy^{165\,m}$ in the total neutron capture cross section for Dy^{164}. In Reference [12] a value of 0.7 was obtained for this fraction.

In the neutron capture γ-ray spectrum of dysprosium there are lines corresponding to the well-known transition between the lowest levels of Dy^{165} [8]. A number of rather intense lines appearing in the capture γ-ray spectrum of europium, holmium, thulium and tantalum correspond to transitions between the lower levels of the odd-odd nuclei Eu^{152}, Ho^{168}, Tu^{170} and Ta^{182}. The presently-available data are still insufficient for establishing the scheme for the lowest levels in these nuclei.

The energies and intensities of the γ-rays are given in the table.

The accuracy in the determination of the energies and yields of the γ-rays is 2-3 percent and 20-30 percent, respectively. In view of the high values of the conversion coefficients, the accuracy in the determination of which is small, the total intensities of transitions with energies greater than 100 kev are obtained with an accuracy of approximately 40 percent. The conversion coefficients for the K- and L-shells were taken from the tables in [9] and [10].

The authors are indebted to Academician I. V. Kurchatov for his interest in the work and to Professor L. V. Groshev, V. M. Strutinskii and D. P. Grechukhin for a number of valuable comments and Professor I. A. Zaozerskii for kindly furnishing the rare-earth samples.

We wish to express our gratitude to G. P. Mel'nikov for providing reliable operation of the electronic apparatus.

Received August 8, 1957

LITERATURE CITED

[1] I. V. Estulin, L. F. Kalinkin and A. S. Melioranskii, J. Exptl.-Theoret. Phys. (USSR) 31, 886 (1956). *

[2] K. Liden, and N. Starfelt, Ark. f. Fys. 7, 428 (1954).

[3] N. P. Heydenburg and G. M. Temmer, Phys. Rev. 100, 150 (1955).

[4] C. A. Fenstermacher, R. L. Hickok and H. L. Schultz, Bull. Am. Phys. Soc., Ser. II 2, 41 (1957).

[5] C. K. Bockelman, C. A. Fenstermacher and J. E. Draper, Bull. Am. Phys. Soc. Ser. II 2, 41 (1957).

[6] E. L. Church and M. Goldhaber, Phys. Rev. 95, 626 (1954).

[7] L. V. Groshev, A. M. Demidov and V. A. Naidenov, Report to the Seventh All-Union Conference on Nuclear Spectroscopy (Leningrad, 1957).

[8] B. S. Dzhelepov and L. K. Peker, Decay Schemes for Radioactive Isotopes, ** (Izd. AN SSSR, Leningrad, 1957).

[9] L. A. Sliv and I. M. Band, Tables of Internal Conversion Coefficients for Gamma Radiation, Part I, ** (Izd. AN SSSR, Moscow-Leningrad, 1956).

[10] G. F. Dranitsyna, Internal Conversion Coefficients for L_I-, L_{II}- L_{III} - Subshells (Izd. AN SSSR, Moscow-Leningrad, 1957).

[11] D. J. Hughes, Pile Neutron Research *** (IL, 1954).

[12] G. Weber, Z. f. Naturforschung 9a, 115 (1954).

---

* See English translation.

** In Russian.

*** Russian translation.

NUCLEAR INFORMATION OBTAINABLE FROM LOW ENERGY NEUTRON SPECTROSCOPY

D. J. Hughes

(Brookhaven National Laboratory, Upton, L. I., New York)

The results of measurements of thermal-neutron cross sections, level distributions in the resonance region, $\overline{\Gamma_n^0}/D$ ratios, and determinations of the effective nuclear radius from potential scattering of slow neutrons are considered.

A discrepancy in the results of measurements of the thermal-neutron fission cross section in U^{235} is noted. The distribution of levels exhibits a deficiency in small spacings as compared with a random distribution, i. e., there seems to be a "repulsion" of levels. The dependence of $\overline{\Gamma_n^0}/D$ on atomic number A is nonmonotonic, in accordance with the complex-potential model of the nucleus; however there is a considerable discrepancy between the experimental data and theory for atomic numbers in the neighborhood of 100. The effective radius determined from potential scattering of slow neutrons indicates a nonmonotonic dependence on A, in agreement with the model of a semi-transparent nucleus with smeared-out edges.

*

In discussing nuclear information obtained from neutron experiments I feel somewhat squeezed in two directions. On one hand, in view of the papers of Bethe, Wheeler, Wigner, and others, it would be presumptuous of me to talk about the nuclear theory that has been developed on the basis of the experimental cross sections. On the other hand it wouldn't be quite right to talk about the experimental techniques, considering the many reports on these that we are to hear. What I do wish to talk about, therefore, is this narrow region into which I am squeezed — the treatment of the experimental data as it passes out of the realm of measurement to become the basis for nuclear theory. I am glad to be thus limited, for I can concentrate on what seems to me an important matter, that is, how to make the nuclear data good enough so that it can be legitimately and safely used by theoreticians.

The material of this conference divides rather neatly into two parts, low energy and high energy, but in a sense other than energy there is a marked difference between these two categories. The high energy work is quite difficult, I think, compared to the low energy work; as a result there are a lot more data available in the latter region. If you will merely glance at the abstracts you will notice that most of those concerning low energy deal with a lot of numbers, such as parameters of various isotopes, and so on, whereas many of the high energy papers discuss the developing experimental techniques.

In the low energy field we are in a spot where many instruments are running steadily, turning out data night and day. In fact, one of the papers this afternoon, by Malkonian, will deal with the problem of what we will do with all this data pouring out of thousand-channel analyzers all over the world. Now the point that I want to emphasize strongly is that, faced with this great accumulation of our own data, we do have a certain

---

*Report to the International Conference on the Interaction of Neutrons with Nuclei held at Columbia University in September, 1957. (A report on the conference is given on page 125 of this issue.

responsibility. In his introductory talk, President Kirk considered the social responsibility of scientists, and now I want to add another that we experimentalists have — to see that the numbers we turn over to the theoreticians are good. Bethe has shown that the problem of dealing with these numbers in nuclear and reaction theory is extremely great even if the theoreticians can trust them completely. But if the theoretician must in addition decide whether the numbers are good or not, and how to correct them if not, the task is almost impossible.

So in the time I have available, let me consider a few cases for which we do have quite a lot of information but where we have to be very careful, probably more careful than we have been in the past, in producing valid sets of data for use in constructing and testing nuclear models. I shall begin by mentioning very briefly some thermal neutron cross sections, at the low energy end of the resonance region, just to remind you that there still are such things that require careful work. Then I'll talk a bit about the question of the level spacing distribution, which was already considered briefly by Bethe, followed by the strength function, and finally the question of potential scattering and its relation to the nuclear radius.

Thermal Cross Sections

On the thermal cross sections, which I'm putting in here primarily to remind us that we're not through with these supposedly well-known standards, let us look at one of the most outstanding thermal cross sections that have given difficulty, the cross section of boron. Some ten years ago, everyone believed that the thermal cross section of boron was 703 barns, and when some measurements indicated that perhaps it was about 730, these were thought to be unbelievable. But as most of you know, the thermal cross section of boron has now crept up to 755, and we are not absolutely sure it has stopped. We think it has stopped at 755, but I would not bet on it with very high odds. I am sure that you are thinking that it is a very simple thing to measure and we certainly should know it well. My own feeling is that the present value will not change much, but it certainly has required much careful recent work to establish it.

The other thermal cross section that has been the subject of much work is that of U^{235}, primarily its fission cross section. True, you can hardly think of a cross section more fundamental to the whole atomic energy business than the fission cross section of U^{235}. A few years ago we all believed that the fission cross section of U^{235} was 550 barns, the total absorption 650, and capture was 100. Well, since that time, the fission cross section has crawled up from 550 to 582 ± 10 barns, and it looks as if it's going to break 600 soon. So again you say it is easy, it is just a relatively straight-forward, simple measurement, and we have lots of velocity selectors. But it has gone up during these years, and it's the sort of thing, in a way, of which physicists throughout the world should be a little ashamed and not rest until things are better stabilized. Stability certainly hasn't been attained at present; several careful measurements recently have given values of 555, 579, and 606 barns, each accurate to about one percent. On my recent rip to Europe, I discussed this discrepancy at every laboratory I visited, and I hope that I got some measurements started in various countries throughout the world. Perhaps a year from now we can say that this cross section has stopped changing, just the way that we now feel that boron has stopped.

Level Spacing Distribution

With this brief reminder that there still is work to be done on the fundamental standard cross sections, I will go ahead to something that is of more recent interest and has more direct relationship to nuclear structure. This is the matter of the spacing distribution of individual levels in a nuclide, and again it is a good example of the necessity of great care in treatment of experimental details. It was noticed a year or so ago that levels in U^{238} occurred with surprising regularity, and for a short time it seemed that the neutron resonances occurred every 18 volts, almost without exception. This result at least stimulated further work and it soon turned out the levels were hardly that regular. Whether they were completely random or not was not clear from the available data, however.

Recently, there has been increasing evidence that there is a deficiency of small spacings, the "level repulsion" effect. I would like to review briefly some results that J. A. Harvey and I have obtained during the last few months. A moment's reflection will make you realize that there are many reasons why the observed distribution of level spacings is not correct. Of course, when levels are very close together they cannot be resolved and some small spacings will be missed. However, in correcting for this effect it is necessary to study the question of possible correlation between the spacing of two levels and the size of the levels, given by their neutron widths Γ_n^0.

We all know that the $\overline{\Gamma_n^0}/D$ ratio is something that doesn't vary widely from nuclide to nuclide, but this ratio applies to the average Γ_n^0 and the average spacing D. But what if there is a correlation between the individual D's, that is local spacing, S, and the individual Γ_n^0 ? In fact, a literal interpretation of the usual derivation of the $\overline{\Gamma_n^0}/D$ ratio would lead one to suspect a local correlation. If this is true, levels close together will be small, hence the loss of small spacings would be more serious than it would be for no correlation. Thus even before the correction to the experimental spacings can be begun, it is necessary to investigate a possible Γ_n^0 and D correlation on a local scale.

We have investigated this matter reasonably carefully, with the results shown in Figure 1. Here we have plotted, for a number of zero-spin target nuclides, the number of cases in which we find particular ratios of Γ_n^0/S to the average, or $\overline{\Gamma_n^0}/D$. If Γ_n^0/S is a local phenomena, all these points should be clustered about unity, but in contrast a continuous distribution is seen. The theoretical curve is based on a Porter-Thomas distribution of Γ_n^0, a distribution of spacings that I will show you in a minute or two, and an assumption of no correlation between individual Γ_n^0 and S. Since it looks as if this agreement is reasonably good, we can conclude that width-to-spacing is not a local correlation.

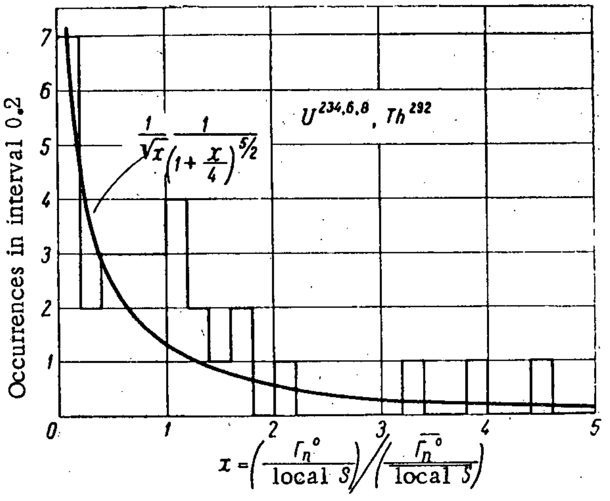

Fig. 1. Experimental ratios of the "local" Γ_n^0/S to the average value for zero-spin nuclides, together with a computed curve based on the assumption of no local correlation.

It is then possible to go ahead and investigate the observed spacing distributions. Figure 2 is the distribution for the zero spin target nuclides U^{234}, U^{236}, U^{238} and Th^{232}, for which there is no difficulty of the presence of two spin states. The triangles are the experimental points, and the correction increases the number of small spacings. This correction is an extremely complicated one to make. We're quite sure we have made it correctly, and are also quite sure we can't explain it to anybody. However, as soon as we decide how to explain it, we are going to publish this work. In Figure 2 the results are compared with an exponential curve, corresponding to a random distribution, and the disagreement is not really very great. There does seem to be deficiency of small spacings, however. In Figure 3, the same data are shown compared with a distribution that is simply a convenient algebraic expression, $4xe^{-2x}$. It is seen that here the correction is smaller than in Figure 2, and the corrected results definitely show a repulsion effect, agreeing reasonably well with the curve.

Since there are only a few available even-even nuclei, the statistics are poor in Figures 2 and 3. But, having a reasonable distribution established, we can now look at the case of two spin states combined, the non-zero spin target nuclides, where we have much more data. Figure 4 shows the case of odd nuclei in which there are the two spin states. Here the statistical error is smaller, but the distributions do not differ as much from exponential as for the zero-spin cases. This is simply because two nonrandom distributions, one for each spin state, produce a distribution more nearly random when combined. Here the experimental results are shown with the theoretical curve based on the expression shown in Figure 4. Also shown in Figure 4 by the solid line is an expression suggested by Wigner at the Oak Ridge conference in the fall of 1956. Actually the points agree reasonably well with either curve and definitely show a repulsion effect.

We are looking forward very much to hearing what Wigner will have to say later in this conference on the theoretical side of the level spacing distribution. Experimentally we believe quite firmly now in the repulsion effect, a deficiency of small level spacings relative to a random distribution

Strength Function, $\overline{\Gamma_n^0}/D$

Here again is an example that shows how careful we must be in presenting the experimental data. The experimental points from a number of laboratories are shown in Figure 5. They show the wavelike characteristics

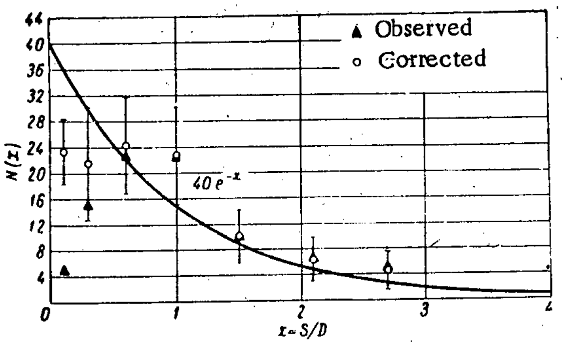

Fig. 2. Comparison of the observed and corrected level spacing distributions for zero-spin nuclides, with a random distribution (the exponential curve).

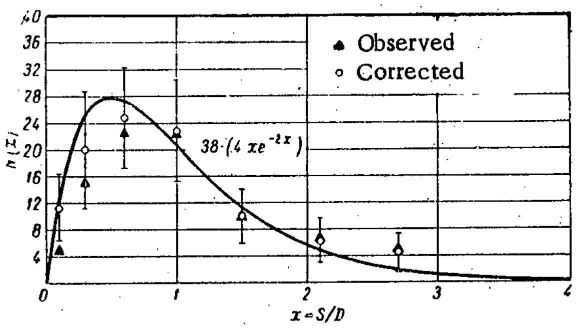

Fig. 3. Comparison of the observed and corrected level spacing distributions for zero-spin nuclides with a distribution showing repulsion at small spacings.

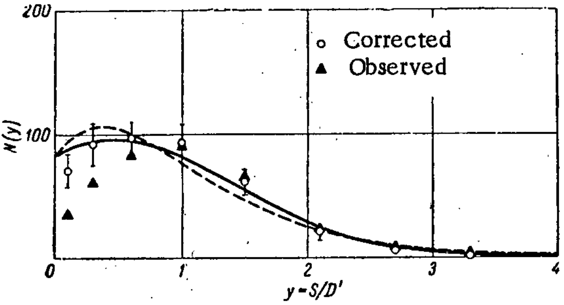

Fig. 4. Comparison of the observed and corrected level spacing distributions for nuclides of non-zero spin with curves representing the combination of both spin states. The dashed curve is based on the curve of Figure 3 for a single spin state and the solid curve on the Wigner distribution.

expected from the cloudy crystal ball model, but the disagreement at certain atomic weights is quite large, particularly around atomic weight 100, where the experimental points are low by about a factor of 5. The theoretical curves in Figure 5 are based on a diffuse-edge nucleus of parameters shown, but without the effect of the aspherical nuclear shape. Some recent calculations of Chase and Willets, to be presented later at this conference, improve the agreement above A = 120.

There will be other papers on the experimental side of this question later in the conference, and also several theoretical papers. The question that naturally occurs, in the light of all this activity, is how far is it profitable to push this kind of comparison. Certainly the experimental points can be improved, but it's not easy, and the question is how many years of our lives should we spend improving experimental data, that is, how much will be learned about nuclear structure by adjusting the parameters of the theory to get better and better agreement. I think that is mainly a question for the theoreticians to answer, however.

Potential Scattering and the Nuclear Radius

My last example of the kind of work that requires great care to get answers that mean anything, concerns the matter of potential scattering and the nuclear radius. Here there are important points on both the experimental and the theoretical sides. There are rather fundamental theoretical questions concerning the nature of the potential scattering. What is the real meaning of the statement that potential scattering is the value of the cross section that occurs between resonances? Obviously, the scattering will be affected by the nearby resonances, but the question is how many resonances are nearby. Must you subtract the effect of five or ten resonances on either side of the point in question, or several thousand ? Again, if the analysis of performed at a second point, say a kilovolt away from the first, will the same result be obtained ? Thus the very question of what meaning is there to the term potential scattering is an important one.

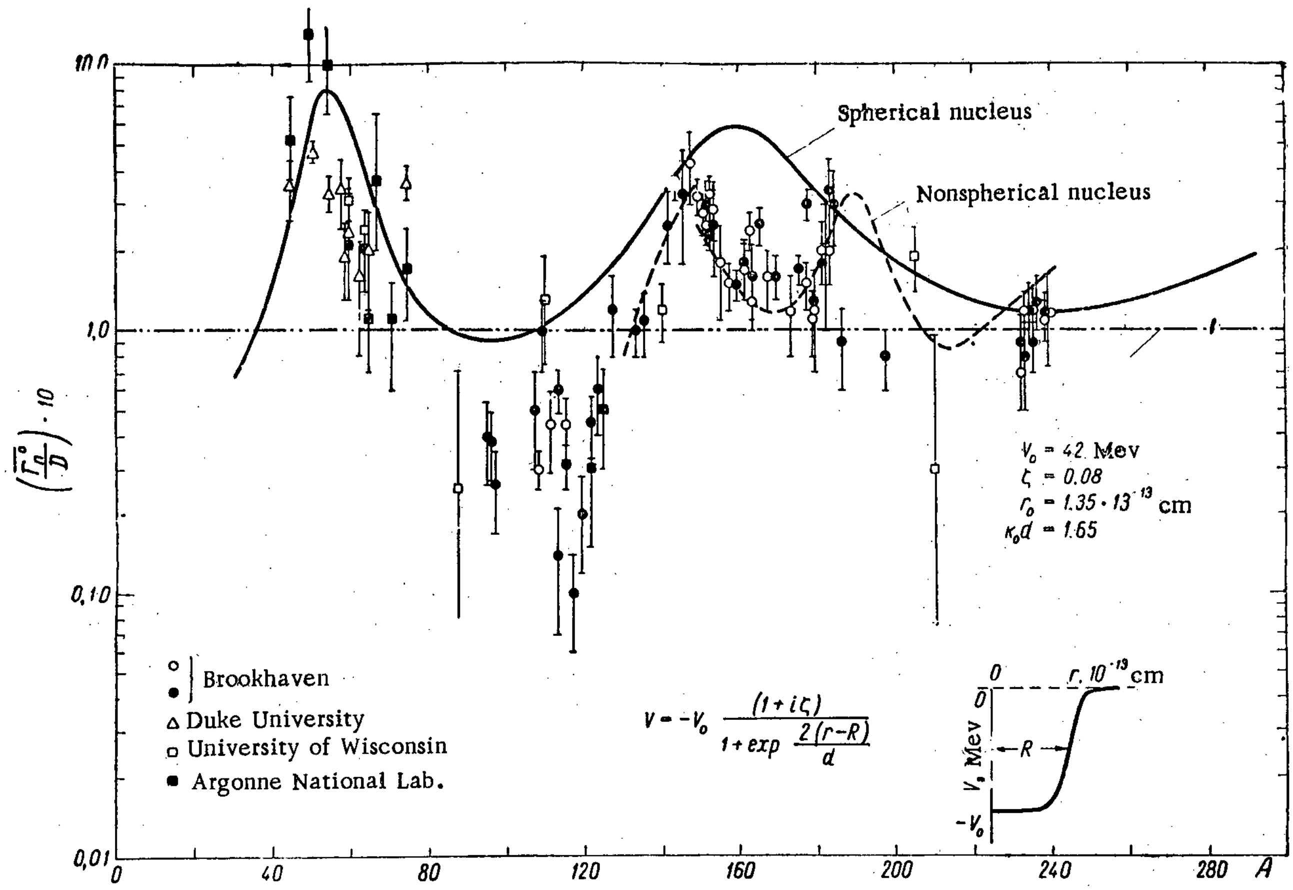

Fig. 5. Experimental values of the $\overline{\Gamma_n^0}/D$ ratio, or strength function, and the optical model values for spherical and nonspherical nuclei.

On the experimental side, the related question is one of the correct procedure for obtaining the potential scattering. If we simply look at the cross section at low energy, we shall get very misleading results. For a long time it was thought that the potential scattering of U^{238}, for example, was about 8 barns, because if capture is subtracted from the total cross section at low energy, what is left is a rather flat cross section with a value of about 8 barns. If this value is substituted into the expression $\sigma_{pot} = 4\pi R^2$, a small R is obtained, which definitely disagrees with other data.

The results of a much more correct method is shown in Figure 6, the open circles of which show the total cross section of U^{238} in the region 20 to 80 ev. It is possible to correct the cross section at any point for the effect of the resonances, primarily the resonance-potential interference. It can be done quite accurately because the parameters of the levels are well known. When the correction is made the closed circles represent the cross section with resonances removed. The resulting cross section is now very flat with energy at a value of 10.7 barns, much higher than the 8 barns obtained from the cross section near zero energy. Also, the potential scattering cross sections do seem to have a definite meaning, for the same result is obtained at one kev neutron energy. Thus the potential scattering as obtained by removing a small number of resonances is constant for energy changes for a kev or so.

Now the interesting question of the relationship of this potential scattering to nuclear structure can be considered. In Figure 7 are shown theoretical curves and recent results obtained at Brookhaven, by methods to be described

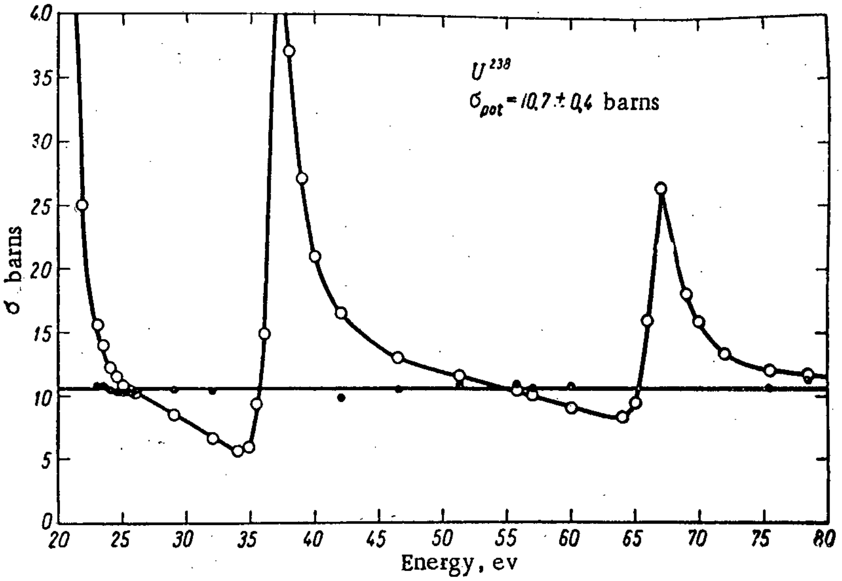

Fig. 6. The total cross section of U^{238} as observed (open circles) and after correction for the effect of resonances (closed circles). The corrected curve is the potential scattering.

in more detail by Seth later at this conference. The smooth curve labelled $r_0A^{1/3}$ is based on an $r_0 = 1.35 \times 10^{-13}$ cm and gives the distance to the half-way point of the potential, as shown in the inset. The cloudy crystal ball model with the constants listed (assuming a spherical shape) gives the curve that oscillates about the smooth line. This curve gives R', where $4\pi (R')^2$ is the potential scattering of slow neutrons. The experimental points seem to verify the predictions of the cloudy crystal ball, except in the region of highly deformed nuclei, A about 140 to 240. These results are similar to Figure 5 for the strength function, where the verification of the model was reasonably good. Again, as for Figure 5, the agreement is made much better when the aspherical shape is included, as given by Chase and Willets' calculation, to be reported later in this conference.

However, these results can be used for another purpose in addition to verifying the optical model, that is, to obtain a value for R. Here we definitely need help from the theoreticians in the interpretation. The points oscillate about the smooth line, which is based on an r_0 of $1.35 \cdot 10^{-13}$ cm. The dependence on the model actually is not very great, so we can think of these results as determinations of R, hence r_0. In order words, the results give an r_0 of 1.35, and we must consider to what extent that answer is dependent on the constants of the model. In Figure 5, the position of the maxima is determined by KR, where K is the wave number of the neutron in the nucleus and R is the nuclear radius. Stated in another way, the position of the maxima is determined by the well depth V, times the radius squared. Similarly, the angular distribution of neutron or proton scattering is determined by this same quantity, VR^2. R is not obtained separately from the V.

However, in the potential scattering work we get R without knowledge of V. The reason is that the places where the theoretical curve crosses the $r_0A^{1/3}$ line are determined by VR^2, but VR^2 is obtained from the strength function results of Figure 5. In other words, the points at which the nucleus acts like a black nucleus ($R' = R$) are fixed by the strength function results, so that tells us how to obtain R from the results of Figure 7. For instance, the strength function results show that at A near 110 the cross section is $4\pi R^2$, and we thus get a value of R, which leads to $r_0 = 1.35 \cdot 10^{-13}$ cm. Now this, of course, gives the radius of the potential well felt by the neutrons, not the matter distribution. Around A = 180, it is difficult to use the results to get an accurate value of r_0 because of the large effect of the aspherical nuclear shape. However, as already pointed out, this region is useful to verify the computed effect of the aspherical shape on the potential scattering. However, at lower A, near 120 where nuclei are spherical, the combination of this work together with the strength function results can be used to get a good value of the radius of the potential.

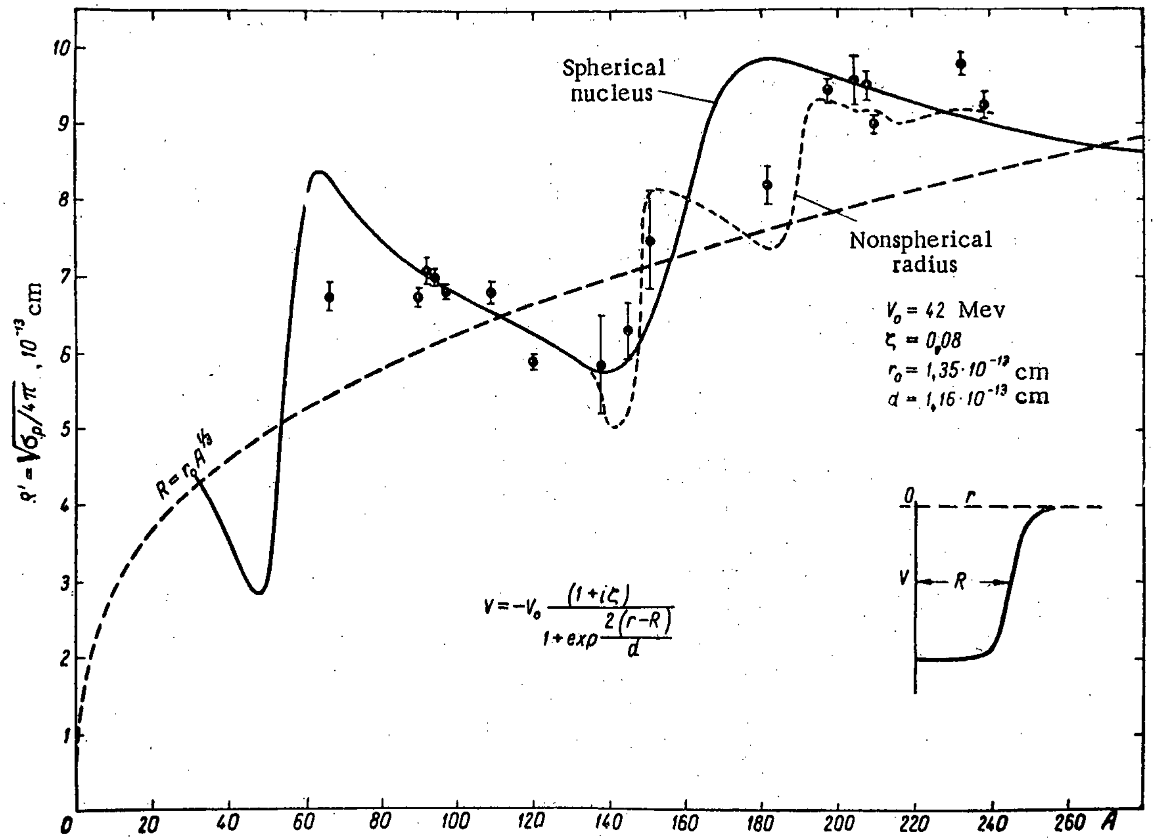

Fig. 7. Measured values of the effective radius R', compared with the optical model calculations for spherical and nonspherical nuclei. A curve for the nuclear radius R is also shown.

The topics considered here are only a few examples of matters where really hard work and careful attention to details is very important. The work is certainly not finished; in spite of all the thousand-channel analysers there still remains much to be done. Actually, some phases have hardly started ; here in my opinion the two outstanding ones are the study of capture gamma rays as a function of neutron energy, and the whole host of effects as function of level spin. As so few spins have been determined, the whole field of the dependence of radiation widths, fission width, etc., on spin remains to be investigated.

Received December 12, 1957

INVESTIGATION OF THE STRUCTURAL CHANGES TAKING PLACE IN A URANIUM-MOLYBDENUM ALLOY UNDER THE ACTION OF NEUTRON IRRADIATION

S. T. Konobeevskii, N. F. Pravdiuk, K. P. Dubrovin, B. M. Levitskii,
L. D. Panteleev and V. M. Golianov

An alloy of uranium with 9 wt.% molybdenum was subjected to neutron irratiation, after which the electrical resistivity was measured and the structure studied by x-ray and microposcopic analysis. Preliminary heat treatment allowed specimens to be obtained with an $\alpha + \gamma'$ eutectoid structure having various grain sizes. It was established that the rate of diffusion leading to homogenization under the action of irradiation in annealed specimens is inversely proportional to the square of the grain size (the period of the lamellar eutectoid). In a homogeneous specimen (γ-phase) irradiation causes a change in properties and structure which rapidly (in 2-4 hours) attains a limiting value, which is explained as being due to radiation annealing. Disordering was found in the γ'-phase, with a transition to the cubic lattice which took place under the influence of irradiation during the first hours of exposure.

All these phenomena are satisfactorily accounted for on the basis of the theory previously developed [2], although the magnitudes of the thermal-spike region and of the energy liberated in it, equal respectively to $2.5 \cdot 10^{-17}$ cc and approximately 2 Mev, are less than were determined in [2].

An alloy of uranium with 9% molybdenum can exist in two states at room temperature. On the not-too-slow cooling of this alloy from temperatures above 600° C, the high-temperature γ-phase is retained in it, taking the form of a homogeneous solid solution of molybdenum in uranium. The homogeneous state appears to be metastable at low temperatures. Annealing the alloy in the temperature range 350-550° C causes decomposition of the solid solution into a eutectoid mixture of lamellae of α-uranium and the intermetallic compound γ'. As has been shown, the compound γ' is an ordered solid solution whose composition corresponds to the formula U_2Mo. The reverse transformation of eutectoid into γ-phase takes place on heating in the temperature range 590-610° C.

In previous work [1] it was shown that while specimens of the homogeneous alloy retain their phase composition on irradiation, specimens of the heterogeneous alloy show partial or complete homogenization after irradiation. Such a transformation from one state to another was revealed by a sharp change in the electrical resistivity, temperature coefficient of electrical resistivity, density and hardness of the heterogeneous alloy after its irradiation and was definitely confirmed by x-ray structural analysis.

A theoretical explanation of the observed phenomenon was given in [2], in which it was shown that the transformation of the heterogeneous state into the homogeneous during irradiation can be regarded as the result of unusual diffusion caused by intermingling of the atoms of the alloy in microvolumes of the specimen due to slowing down of the fission products. The concentration of molybdenum at any point of the specimen (x) must vary during irradiation in accordance with the following relationship:

$$C=C_{\text{av}}\left[1+\sum_{n=1}^{n=\infty}\frac{\lambda}{\pi na}\sin\frac{\pi na}{\lambda}\cos\frac{2\pi nx}{\lambda}e^{-\frac{4\pi 2n^2}{\lambda^2}Dt}\right], \tag{1}$$

where a is the width of the lamellae of the γ-phase; λ is the period of alternation of the lamellae (the total width of the lamellae); t is the irradiation time; D is the diffusion coefficient. The value of D can also be found theoretically from the expression for "thermal spikes":*

$$D=1{,}16\cdot 10^{-18}\left(\frac{E}{T}\right)^{5/3}W, \tag{2}$$

where E is the energy (in kev) expended by the fission products in mixing the atoms of the alloy in the microvolume; T is the minimum temperature (in °K) at which the intermingling of the atoms in the microvolume of the alloys can be observed; W is the specific heat (in watts) evolved by 1 g of alloy during irradiation.

The theoretical value of the diffusion coefficient (2) can be compared with the value (1) obtained from a study of the rate of homogenization of the alloy. From this a parameter E/T is found. It follows from (1) that the homogenization time must be proportional to the square of the period of the eutectoid (the thickness of the double layer $\alpha+\gamma'$), which in [2] was provisionally taken as equal to 1 μ. For this value of λ a value was obtained for E/T of about 9 kev/°C and for E (taking the lowest temperature of homogenization T as equal to 2000°C) of about 18 Mev. This estimate, judging from the present work, was too high.

In [3] a study was made of the action of irradiation on alloys of uranium with 9, 10.5 and 12 weight % molybdenum and with 10 weight % niobium. The authors arrived at the conclusion that in all these alloys irradiation gives rise to a transformation of the heterogeneous structure to the homogeneous one and gave an explanation which had the same basis as that presented above.

In the present work, designed to verify the theoretical relationship between the rate of diffusion and the period of the eutectoid structure, a study was made of the transformation of the heterogeneous structure of the uranium alloy containing 9 weight % molybdenum into the homogeneous structure in relation to the size of the eutectoid lamellae and also to the amount of irradiation. Varying degrees of dispersion of the eutectoid were obtained by annealing specimens of the alloy at various temperatures.

Material

The alloy of uranium with 9 weight % molybdenum was prepared by melting under vacuum in an induction furnace (chemical analysis of the alloy gave 9.05 weight % molbydenum). Ingots of the alloy were reduced by hot and cold rolling to a thickness of 0.1 mm. From such thin sheets specimens were cut for measuring the electrical resistivity. The same specimens were subsequently used for the x-ray investigations.

Heat Treatment

All the specimens were given a homogenizing anneal for 3 hours at 1000°C. Annealing was carried out in a quartz tube in a vacuum of $1\text{-}5\cdot 10^{-6}$ mm Hg. After the 3-hour anneal the quartz tube containing the specimens was cooled in air. Some of the specimens after such heat treatment were used to study the effect of irradiation on the properties of the alloy in the γ-solid-solution state. The remainder of the specimens were used for obtaining eutectoid structures of various lamellar sizes by annealing at temperatures from 550 to 400°C (Table 1).

Annealing was carried out in evacuated quartz capsules (the vacuum before sealing off was 10^{-6} mm Hg). After annealing, the specimens in the capsules were cooled in air. The period of holding at each temperature was determined from the C-curves (Fig. 1) previously obtained for this alloy. Curve I corresponds to the beginning of decomposition of the γ-phase and Curve II to the end. The extent of transformation of the γ-phase was determined by measuring the electrical resistivity (R) and the temperature coefficient of electrical resistivity

---

*This terminology does not agree completely with that in the English literature, in which "thermal spikes" differ from "displacement spikes" postulated by Brinkman.

(α) of each specimen after annealing. Such a check showed that all the specimens were completely transformed into the heterogeneous state with the exception of specimen No. 5, which had been annealed at 400° C for 700 hours. Judging by the values of R and α for the annealed specimen No. 5, it was concluded that decomposition in it had proceeded to the extent of approximately 84 percent.

TABLE 1

Characteristics of the Specimens of Uranium – 9 weight % Molybdenum Alloy Studied

Specimen No.	Condition	Heat treatment		Mean period of eutectoid, microns	Remarks
		temp., °C	time, hrs.		
1	Quenched (homogeneous)	1000	3	–	–
2	Annealed (eutectoid)	550	1000	1.0	–
3	" "	500	100	0.3	–
4	" "	450	100	0.16	–
5	" "	400	700	0.1	Decomposed 84%

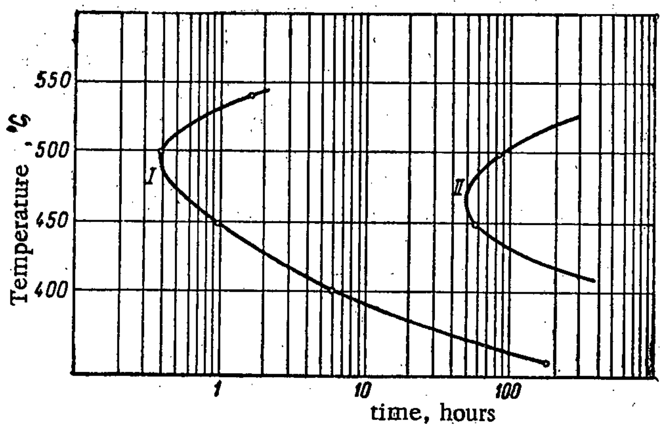

Fig. 1. C-curves for uranium – 9 weight % molybdenum alloy.

Irradiation

Irradiation was carried out in the RFT reactor in a neutron flux of $2 \cdot 10^{13}$ neutrons/cm^2·sec. Before irradiation the specimens were firmly gripped between the two halves of a magnesium cone, which were then pressed into the conical aperture of an aluminum container. The container was hermetically sealed with a lid and placed at the bottom of an aluminum tube, surrounded by water in the reactor, the temperature of which did not exceed 50°C. Calculation and an experiment carried out previously on the direct measurement of the temperature of an alloy specimen during irradiation made it possible to assume that the temperature of the specimens did not exceed 100°C during irradiation. After irradiation, which lasted from 1 hour to 35 days, the container was removed from the reactor and opened remotely. Before measurements were begun, the specimens were allowed to give off radiation for a month.

Measurement of the Electrical Properties

The transition of the heterogeneous structure to the homogeneous on irradiation was followed by measuring the electrical resistivity of alloy specimens of dimensions $0.1 \cdot 2 \cdot 50$ mm. In view of the comparatively small radioactivity of the specimens after irradiation, all measurements were carried out after local protection on a potentiometric instrument of the type UPI 3/3. Before and after irradiation the specimens were placed in the same holder, in which the potential knife-edges made contact with the specimen in the same places. Duplicate measurements showed that the maximum scatter did not exceed ± 0.1%. During the measurements the holder with the specimen in it was thermostatically controlled in a bath filled with carbon tetrachloride. The temperature of the bath was measured with a mercury thermometer to an accuracy of 0.1°C. The electrical resistivity of each specimen was determined at two temperatures (at approximately 20° and 70°C) and from the results obtained the temperature coefficient of electrical resistivity was calculated. The relationship between the variation in electrical properties of the alloy and its structure can be seen from the graph (Fig. 2). The electrical resistivity of a heterogeneous alloy increased with rise in temperature. Its temperature coefficient of electrical resistivity in the range 20-100° C was $1.15 \cdot 10^{-3}$ per degree.

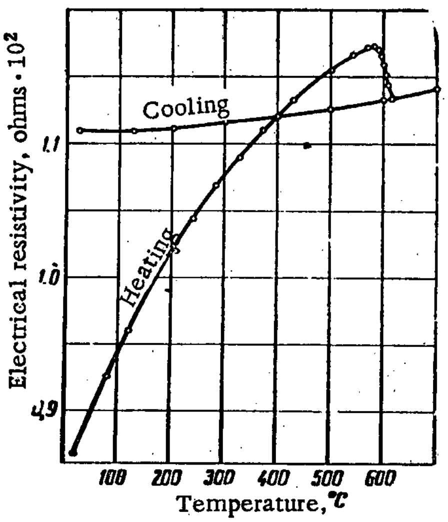

Fig. 2. Change in electrical resistivity of a heterogeneous specimen on heating and cooling.

The heterogeneous alloy transforms to the homogeneous state at temperatures of 590-610° C. During this transition the electrical resistivity of the alloy decreases by approximately 4%. Cooling the alloy at a rate of 3°C per minute does not lead to the reverse transition to the heterogeneous state, and the γ-phase is retained down to room temperature. As can be seen from the graph, the temperature coefficient of the homogeneous alloy in the range 20-100°C is almost zero, and its electrical resistivity at normal temperature is approximately 28% greater than the resistivity of the heterogeneous alloy.

Figure 3 shows a typical microstructure of the eutectoid consisting of alternate lamellae of α- and γ'-phase. The degree of dispersion of the eutectoid or the size of the lamellae depends on the annealing temperature.

Figure 4 shows the relationship between the total width of the lamellae of the $\alpha + \gamma'$-phases (the period of alternation) and the annealing temperature. As can be seen from the graph, this value is equal to approximately 0.1μ if the specimens were annealed at 400°C and of the order of 1μ for specimens annealed at 550° C. Such small quantities were measured with an accuracy of $\pm\ 0.05\,\mu$ with the electron microscope at a magnification of 17,000.

Curves showing the relationship between the electrical resistivity of the alloy specimens and the amount of irradiation are given in Figure 5. Curve 1 is drawn for the homogeneous specimen No. 1 and Curves 2-5 for specimens Nos. 2-5, which were annealed before irradiation at temperatures of 550, 500, 450 and 400° C, respectively (see Table 1).

As can be seen from Figure 5, the change in electrical resistivity of any alloy takes place in two stages. At the beginning of irradiation, during approximately the first 2 hours, a sharp increase in electrical resistivity takes place in all the alloys. During further irradiation the increase in resistivity of the homogeneous specimen rapidly falls off and reaches saturation after approximately 4 hours irradiation. The electrical resistivity of heterogeneous specimens, after a similar sharp rise, increases gradually during further irradiation. The maximum increase in resistivity for the homogeneous specimen was equal to approximately 4.5%, while for heterogeneous specimens it was about 7% at this stage. We may note that in this first stage the change in electrical resistivity of heterogeneous specimens does not depend on the degree of dispersion of the eutectoid and is approximately the same for all specimens.

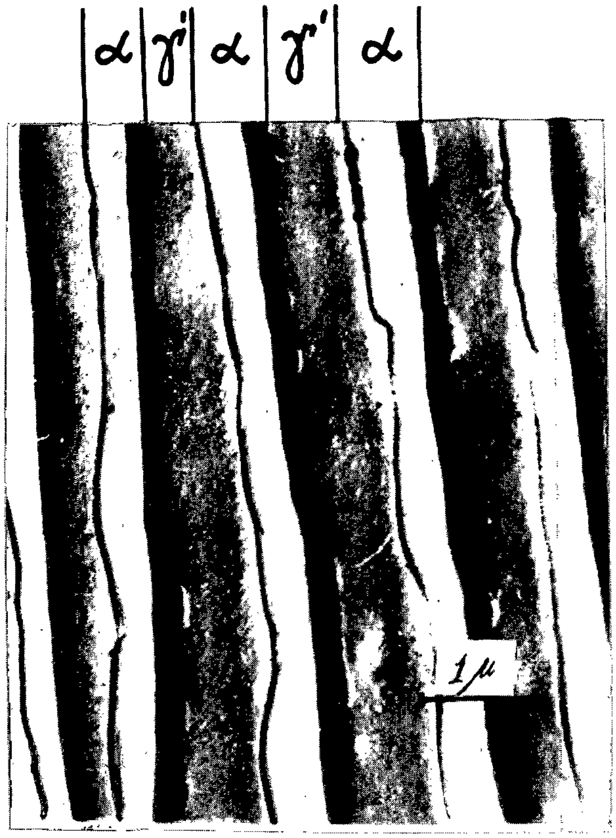

Fig. 3. Microstructure of uranium — 9 weight % molybdenum alloy after heating at 550° C for 1000 hours (x 17,000).

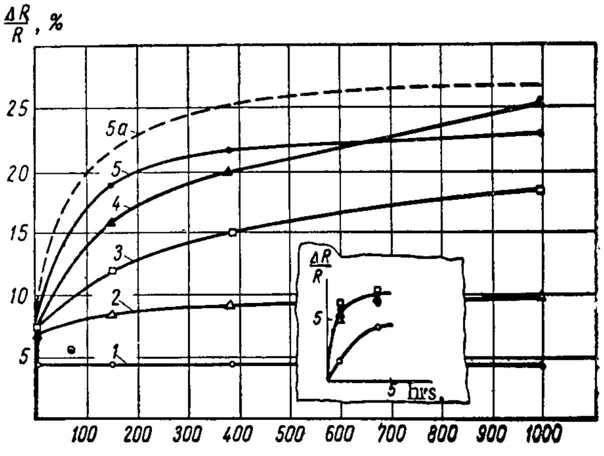

Fig. 5. Dependence of electrical resistivity of specimens of uranium — 9 weight % molybdenum alloy on time of holding during irradiation in a flux of $2 \cdot 10^{13}$ neutrons/cm^2 · sec.

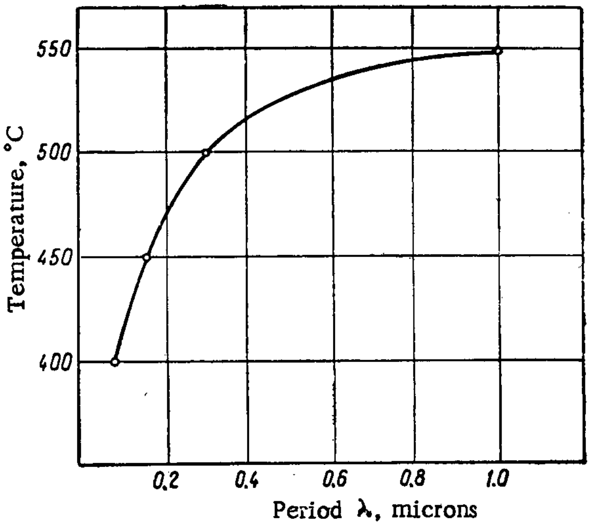

Fig. 4. Width of lamellae of the $\alpha + \gamma'$-phases in relation to the annealing temperature.

The second stage is characterized by the fact that the electrical resistivity of the homogeneous specimen remains constant, while that of the heterogeneous specimens increases, the rate of increase depending to a considerable extent on the degree of dispersion of the eutectoid. From the curves presented it can be seen that the higher the annealing temperature of the specimens, and consequently the greater the size of the lamellae in the eutectoid, the more slowly the electrical resistivity of the alloy specimens increases. It may be assumed that such a change in the electrical resistivity depends on the transformation of the heterogeneous structure to the homogeneous during irradiation. This conclusion is confirmed by the curves showing the change in the temperature coefficient of electrical resistivity of the heterogeneous specimens during irradiation, which are presented in Figure 6. On increasing the amount of irradiation the temperature coefficient of resistivity of all the heterogeneous specimens decreases, approximating to zero. The temperature coefficient of resistivity of the specimen annealed to 400°C and having a finely dispersed eutectoid decreased to zero after irradiation for 400 hours, which corresponds to practically complete homogeneity.

Specimen No. 4 approaches the homogeneous state only after holding for 1000 hours. As can be seen from the curves in Figures 5 and 6, specimen No. 2, the structure of which consists of a coarse ($\alpha + \gamma'$) eutectoid, is transformed into the homogeneous condition very slowly during irradiation.

Figure 5 shows that the increase in electrical resistivity of specimen No. 4 after irradiation for 1000 hours is greater than that of specimen No. 5. This can be explained by the fact that specimen No. 5, as has already been noted, did not attain complete heterogeneity during annealing at 400°C.

The broken line 5a in Figure 5 shows the assumed course of the curve for specimen No. 5 if this specimen had been completely heterogeneous before irradiation.

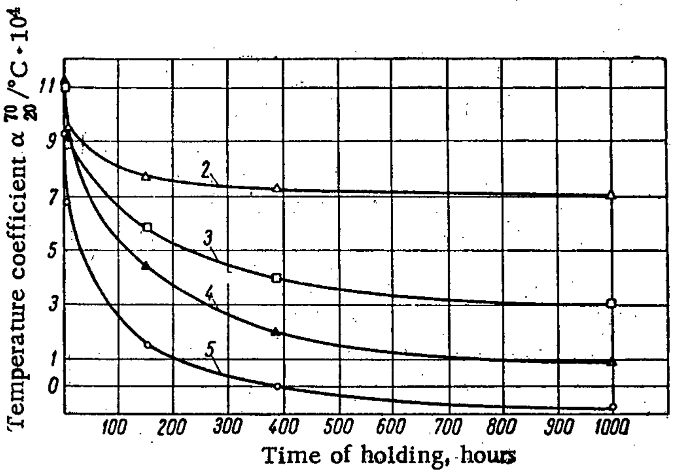

Fig. 6. Change in the temperature coefficient of electrical resistivity of heterogeneous specimens in relation to the time of holding during irradiation in a flux of $2 \cdot 10^{13}$ neutrons per $cm^2 \cdot sec$.

During irradiation of the alloy there takes place on the one hand a change in the concentration of molybdenum in the α- and γ'- lamellae and on the other a change in the relative amounts of the α- and γ-phases. It is difficult to estimate the separate effects of these factors on the electrical resistivity of the alloy. However for our purposes this is not necessary, since all the specimens are similar to one another in the initial state and remain so throughout the whole process of homogenization, differing only in the period of the structure and consequently in the time required to attain corresponding states.

Hence if we draw a horizontal straight line on Figure 5 it will cut the curves showing the change of electrical resistivity in points whose abscissae will correspond to the irradiation times necessary for the attainment of identical (corresponding) states. As can be seen from Expression (1), this time must be inversely proportional to the square of the period of alternation λ. We will draw two horizontal straight lines: one through the point corresponding to $\Delta R/R = 9\%$ and the second through the point corresponding to $\Delta R/R = 15\%$. The times sought are equal to 6, 20, 50 and 280 hours respectively for specimens No. 5, 4, 3 and 2 ($\Delta R/R = 9\%$) and 38, 125 and 385 hours for specimens No. 5, 4 and 3 ($\Delta R/R = 15\%$). The first times bear the following relation to one another 1 : 3.33 : 8.35 : 46.7, that is they are related as the squares of the numbers 1 : 1.82 : 2.89 : 6.83. The relationship for the second three times of irradiation is 1 : 3.29 : 10.1 or as the squares of the numbers 1 : 1.82 : 3.19. As can be seen from Figure 4, the values of λ for specimens No. 5, 4, 3 and 2 are in the ratio 0.8 : 1.6 : 3 : 10. Thus the experimental results on the whole confirm well the theory put forward that the amount of irradiation is inversely proportional to the square of the period of alternation of the eutectoid lamellae in the heterogeneous alloy.

Theoretical Discussion

As was shown in [2], the coefficient of radiation diffusion can be expressed as

$$D = \frac{Nv}{24} (\Delta z)^2, \tag{3}$$

where N is the number of acts of fission in unit volume: v is the volume of a thermal spike, and $(\Delta z)^2$ is the mean square of the linear dimensions of a thermal spike, which with a correction for the superposition of thermal spikes can be expressed as

$$\frac{2}{3}r^2 = 0.257v^{2/3},$$

from which, having substituted for N,

$$N = 3.1 \cdot 10^{10}\rho W,$$

where W is the specific thermal emission expressed in w/g, we obtain

$$D = 0.0332 \cdot 10^{10}\rho v^{5/3} W.$$

Having substituted for the density ρ its value for a homogeneous alloy $\rho = 17.4$ we finally obtain

$$D = 0.577 \cdot 10^{10} v^{5/3} W. \qquad (4)$$

The experimental value of D can be found from the equation

$$\frac{4\pi^2}{\lambda^2} Dt = \ln 11.2.$$

This formula is obtained from the requirement of tenfold diminution in the first harmonic of decay in the Fourier series for the concentration of molybdenum in the eutectoid consisting of alternate lamellae of uranium and the intermetallic compound U_2Mo.

Finally we obtain for v

$$v^{5/3} = 0.20 \cdot 10^{-11} \frac{\lambda^2}{t}; \quad W = 5.3 \text{ watts}.$$

Expressing λ in microns and t in hours, we have

$$v = 11.2 \cdot 10^{-15} \left(\frac{\lambda^2}{t}\right)^{3/5}.$$

From this, using data given in [2], it is also possible to obtain

$$\frac{E}{T} = 0.471 \left(\frac{\lambda^2}{t}\right)^{3/5},$$

where E is expressed in Mev and λ in microns. Using experimental data from this paper we can obtain values of v and E/T x 2000 (Table 2).

Let us return now to the variation in electrical resistivity of the homogeneous specimen No. 1 during irradiation. The observed increase in electrical resistivity of the γ-phase can also be explained by the existence of thermal spikes. The volume of metal constituting a thermal spike is similar to an annealed zone in which previously existing defects in the crystal lattice have partially disappeared. The state of the metal after such a thermal spike is characterized by a certain completely determined concentration of defects which define the properties. As long as all the metal has not passed through the thermal-spike condition, defects will accumulate in it and will lead to a corresponding increase in the electrical resistivity. However, as soon as the whole volume of the specimen has passed through the thermal-spike condition, further irradiation can give rise to no new changes of state, and from that moment the electrical resistivity of the specimen will not vary.

In this particular case no attention is paid to the effect of the accumulation of fission fragments (as impurities) on the change of properties of the alloy in view of the fact that their concentration, as calculation shows, should not exceed $10^{-2}\%$..

On the basis of these assumptions it is easy to determine the volume of a thermal spike from the rate of change of a property of the homogeneous specimen, that is by another method which does not depend on previous calculation — from the rate of diffusion of the heterogenized alloy.

TABLE 2

Values of v and E/T x 2000

Specimen No.	λ, micron	$t_{0.1}$ hr	$v \cdot 10^{17}$, cc	E/T x 2000, Mev
5 (annealed at 400°C)	0.1	250	2.58	2.16
4 (annealed at 450°C)	0.16	840	2.18	1.90
		Mean	2.38	2.08

TABLE 3

Mean Value of the Volume of the Thermal-Spike Region

	Volume of region, cc	Radius of spherical cavity, cm
From diffusion data	$2.38 \cdot 10^{-17}$	$1.78 \cdot 10^{-6}$
From annealing data for the homogeneous phase	$6.28 \cdot 10^{-17}$	$2.46 \cdot 10^{-6}$

The rate of increase of volume (V) which has passed through the thermal-spike state, $\frac{dV}{dt}$, is proportional to the volume of the thermal spike v and the number of fissions (per sec) in the specimen N and also to the volume (1 − V) which has not passed through the thermal-spike state. Thus

$$\frac{dV}{dt} = (1 - V)Nv.$$

Integrating this equation, we find

$$V = 1 - e^{-Nvt}.$$

With Nvt = 1, approximately 63% of the total volume of the specimen passes through the thermal-spike condition. The maximum increase in the electrical resistivity of the homogeneous specimen on irradiation (see Fig. 5) is equal to 4.5 %. If it is assumed that the electrical resistivity increases in proportion to the volume of metal which has passed through the thermal-spike condition, then after time $1/(Nv) = \tau$ the electrical resistivity of the homogeneous specimen should increase by $4.5 \cdot 0.63 = 2.8\%$. From the curve showing the change of electrical resistivity of the homogeneous specimen on irradiation, it is possible to determine directly the time τ and, knowing N, to calculate the volume of a thermal spike.

If it is assumed that on each act of fission 200 Mev is liberated, then the number of fissions N expressed in terms of the specific heat evolution W (in watts per 1 g of alloy) is:

$$N = 3.1 \cdot 10^{10} W\rho = 2.95 \cdot 10^{12},$$

where ρ is the density of the alloy, equal to 17.4 g/cc, and W = 5.3 w/g. From Figure 5 it can be seen that the electrical resistivity of the homogeneous alloy increases by 2.8% after 1.5 hours. From this it follows that

$$v = \frac{1}{N\tau} = 6.28 \cdot 10^{-17}\ \text{см}^3.$$

The volume of a thermal spike as calculated from diffusion data and that calculated from the increase in electrical resistivity in the homogeneous γ-phase differ somewhat (Table 3), but they appear to be of the same order. The somewhat larger volume of the thermal-spike region in the second case is easy to understand, since complete atomic relaxation clearly requires a lower temperature than that required for the complete intermingling of the atoms essential for the appearance of radiation diffusion.

It can readily be seen that if this temperature is assumed to be 800-900°C instead of 2000°C as was taken above for complete intermingling, then the energy expended in a thermal spike and for the case of annealing in the homogeneous phase is of the same order as that in [2], i. e., about 2 Mev. Thus the sum total of these data shows conclusively enough that in the thermal-spike region the expenditure of energy is of the order of 1-2% of the total energy of fission.

X-Ray Data

An x-ray investigation by the method described in [4] fully confirms the conclusions reached above on the basis of electrical-resistivity measurements of irradiated specimens.

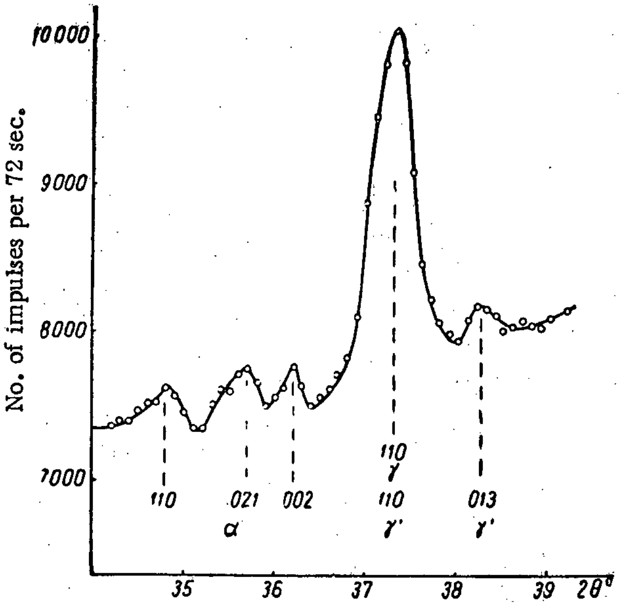

Fig. 7. X-radiogram of a heterogeneous specimen of uranium — 9 weight % molybdenum alloy after irradiation for 1000 hours in a flux of $2 \cdot 10^{13}$ neutrons/cm^2 sec.

In Figures 7-13 are presented the x-radiograms of the specimens investigated, drawn through points at every 6'. On the ordinate are plotted the mean values (of three measurements) of the number of impulses of the counter for a period of 72 seconds, while on the abscissa are the double Bragg angles read off from the spectrometer scale. Figure 7 gives the initial reading of the radioactive specimen; the remaining figures give, for convenience of comparison, the structure lines after deduction of the radioactive background. (Indices of the lines are shown on the diagrams.) The accuracy of determination of the position of the lines is about 0.02°, which for the range of Bragg angles considered corresponds to a possible error $\Delta d/d =$ $= 0.001$.

The results of measuring the x-radiograms are given in Table 4. From the x-ray data the following conclusions may be drawn:

1. Quenching the uranium — 9 weight % molybdenum alloy from 1000°C gives the pure γ-phase with a parameter a = 3.408 kX. The half width of the (110) line is equal to 0.14° (Fig. 8).

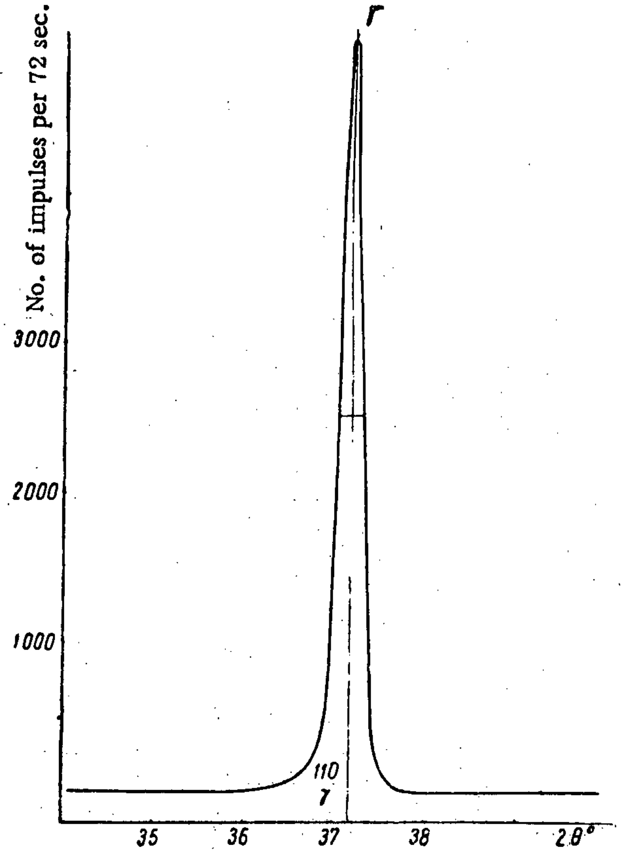

Fig. 8. X-radiogram of the homogeneous specimen before irradiation (quenched from 1000°C). Γ is the position of the (110) γ maximum for the homogeneous specimen.

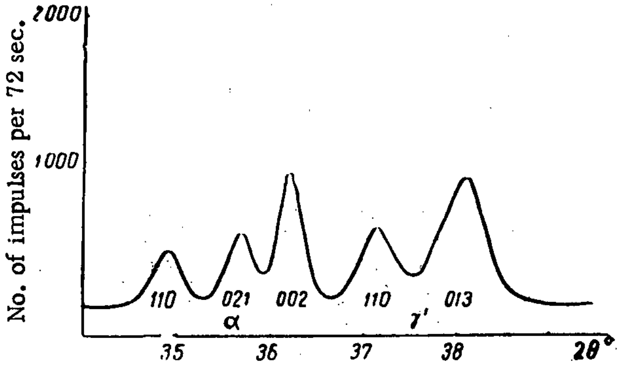

Fig. 9. X-radiogram of a heterogeneous specimen before irradiation (annealed at 450°C for 100 hrs).

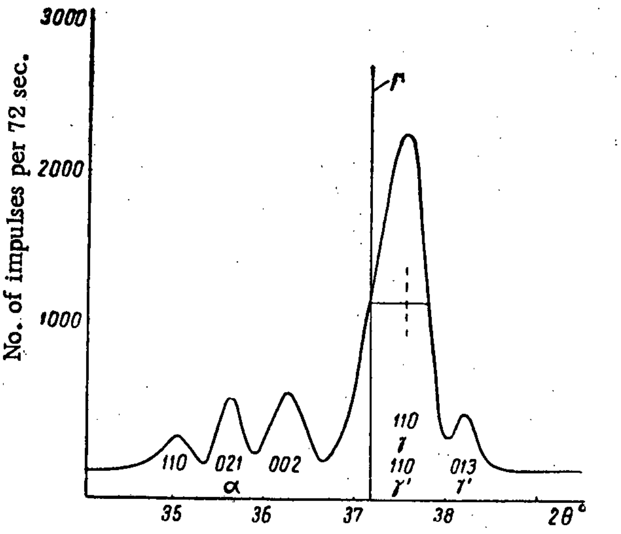

Fig. 10. X-radiogram of heterogeneous specimen No. 2 after irradiation. Γ is the position of the (110) γ line for the homogeneous specimen.

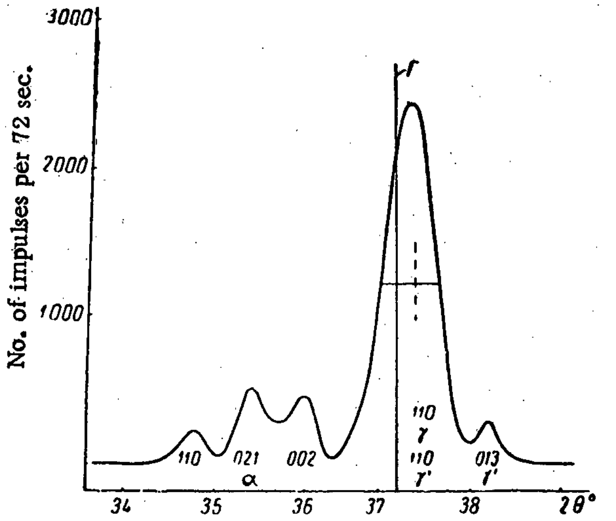

Fig. 11. X-radiogram of heterogeneous specimen No. 3 after irradiation. Γ is the position of maximum of the (110)γ line for the homogeneous specimen.

2. Annealing at 450°C for 1000 hours leads to a heterogeneous structure consisting of the α-phase, characterized on the x-radiogram by the triplet (110—021—002), and the γ'-doublet (110—013). The ratio of the areas of the triplet and the γ'-doublet equals 0.87 (Fig. 9).

3. Irradiating a heterogeneous specimen for 1000 hours leads to varying results, depending on the temperature of the preceding heterogenizing anneal and consequently on the grain size or period of the lamellar (α + γ') eutectoid.

4. In specimen No. 2, which has the largest eutectoid period in the initial state, only an insignificant decrease in the amount of α-phase is observed after irradiation for 1000 hours (Fig. 10 and Table 4). At the same time the amount of γ'-phase decreased markedly and a new $(110)\gamma$ line appeared, occupying a position corresponding approximately to the center of gravity of the (110—013) doublet of the γ'-phase. The new $(110)\gamma$ line is asymmetric with an asymmetry index of 1.85. The half width of the $(110)\gamma$ line is 0.33°, i. e., it is considerably greater than the half width of the corresponding line of the γ-phase in an alloy normally treated and quenched from 1000°C (0.14°).

5. In specimen No. 3 the amount of α-phase decreased. The ratio $\frac{I_\alpha + I_{\gamma'}}{I_\alpha + I_{\gamma'} + I_\gamma}$ is in this case equal to 0.35, compared with 0.45 for the previous case. The deviation $\Delta\theta$ in the position of the line from the "normal" position for the 9% solid solution also decreased. The asymmetry index and the half width of the line decreased too.

6. The changes proceed in the same direction on the x-radiograms of specimens No. 4 and 5. In specimen No. 5 we observe the almost complete disappearance of the α-phase and the second component of the $(110-013)\gamma'$ doublet; the position of the $(110)\gamma$ line coincides almost exactly with the position of this line on the x-radiogram of the quenched 9% specimen (Fig. 13). The line has the normal width and symmetry.

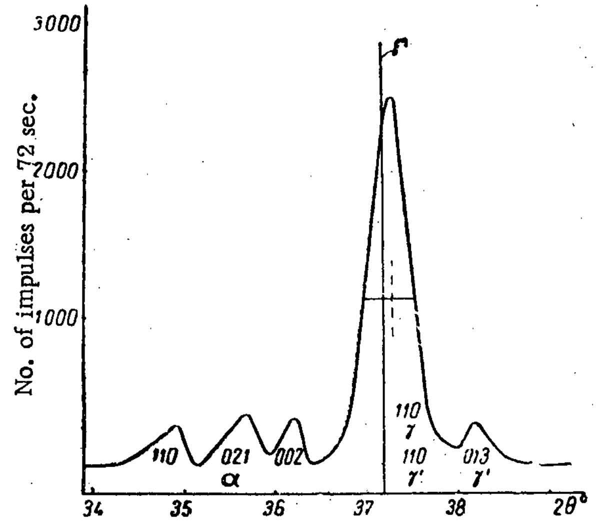

Fig. 12. X-radiogram of heterogeneous specimen No. 4 after irradiation. Γ is the position of the maximum of the (110) γ line for the homogeneous specimen.

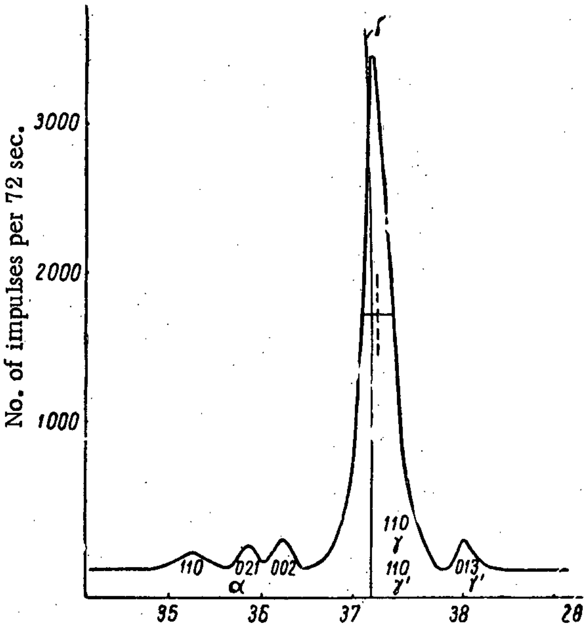

Fig. 13. X-radiogram of heterogeneous specimen No. 5 after irradiation. Γ is the position of the maximum of the $(110)\gamma$ line for the homogeneous specimen.

The partial weakening of the α-phase lines in specimens No. 2, 3 and 4 and their almost complete disappearance in specimen No. 5 correspond exactly to the "recovery" of the electrical resistivity in these specimens, which varies with the different degrees of dispersion of the $(\alpha + \gamma')$ eutectoid.

Special interest attaches to the fact that, in agreement with the x-ray data, the appearance of the cubic γ-phase precedes homogenization. It may be assumed from this that the γ-phase is formed in the first place at the expense of the direct transformation of the tetragonal phase to the cubic phase under the influence of irradiation. First of all the lattice parameter of the γ-phase formed in the limiting case in the absence of appreciable diffusion (specimen No. 2) corresponds almost exactly to the parameter of the solid solution with a composition corresponding to the stoichiometric ratio for the γ'-phase (the compound U_2Mo). Since the tetragonal character of the γ'-phase lattice is only a consequence of the ordered arrangement, it is natural to assume that irradiation first causes disordering in the γ'-phase (the compound U_2Mo has a layer structure) and that this gives rise to the transformation of the lattice from tetragonal to cubic.

TABLE 4

Data from Measurement on the X-Radiograms of Irradiated Specimens

Specimen number	Initial state	I_α * relative	$\frac{I_\alpha+I_{\gamma'}}{I_\alpha+I_{\gamma'}+I_\gamma}$ **	Position of (110) γ line		Half-width of (110) γ	Index of asymmetry of (110) γ
				$\theta°$	$\Delta\theta°$	$B_{1/2}°$	
2	Annealed 1000 hr at 550°C	800	0.45	18.80	0.20	0.33	1.85
3	Annealed 100 hr at 500°C	645	0.35	18.71	0.11	0.31	1.50
4	Annealed 100 hr at 450°C	440	0.25	18.66	0.06	0.27	1.25
5	Annealed 700 hr at 400°C	160	0.10	18.62	0.02	0.18	1.10
1	Quenched from 1000°C	0	0	18.60	0	0.14	1.00

Further change consists in slower diffusion, leading to a reduction in the molybdenum content in the γ-phase and to an increase in the amount of γ-phase at the expense of the disappearing α-phase. The variation in the γ-phase parameter for specimens with different initial dispersions of the eutectoid confirms this conclusion, already reached above from observations of the intensity of the α-phase lines. All this agrees entirely with the conclusions reached on the basis of the electrical-resistivity measurements. Of course it would be desirable to verify these conclusions by observing on an x-ray photograph the changes in a single specimen subjected to varying amounts of irradiation, though this is difficult to carry out in practice. It appears to us that the series of specimens differing in the rate at which diffusion takes place in them also gives a very clear picture of the subsequent stages of the transformation and consequently corresponds to the progress of the radiation homogenization process with time.

The rapid disordering of the γ'-phase is the result of the action of thermal spikes, which mix up the atoms of the ordered compound and transform it into a disordered solid solution. This process must be completed in a time comparable with that required for the whole volume occupied by the ordered phase to pass through the thermal-spike state.

We have seen above that in the initial state of irradiation a rather sharp rise in electrical resistivity occurs both in the homogeneous (quenched) state and in the heterogeneous (annealed) state. Moreover, it is found that the initial jump in the electrical resistivity for the heterogeneous specimens is approximately 1.5 times greater than that for the homogeneous specimen and is practically identical for the various heterogeneous specimens. In the light of the x-ray data presented here it is obvious that the additional increase in the electrical resistivity of the heterogeneous specimens is connected with the disordering of the γ'-phase which occurs in all the heterogeneous specimens. This disordering proceeds simultaneously with the accumulation of primary defects caused

---

*I_α is the area of the α-phase triplet (110—021—002). For a specimen annealed at 450°C and not irradiated, I_α = 980 conventional units.

**I_γ is the area of the γ-phase (110) line; $I_{\gamma'}$-phase (110) and (013) lines.

by acts of fission. Consequently there is a certain limit to the accumulation of defects at which the creation of defects is balanced by radiation annealing. Under the conditions of our experiment both processes — disordering and accumulation of defects — come to an end after 2-4 hours, after which there follows a further slow change in the ratio of the amounts of the α- and γ-phases, due to radiation diffusion and depending mainly on the length of the diffusion path.

SUMMARY

The sum total of the data relating to the electrical resistivity and structure of the uranium-molybdenum alloy indicates the part played by thermal spikes, i. e., regions of great retardation of fission fragments, in the change of properties of fissile material under the action of neutron irradiation. It has been established that: 1) thermal spikes are the cause of radiation annealing which leads to rapid saturation of the properties of the γ-phase under conditions of irradiation; 2) in compounds of the ordered-solid-solution type, such as the γ'-phase, thermal spikes cause rapid disordering; 3) the intermingling of the atoms in the region of a thermal spike is the cause of the interdiffusion of uranium and molybdenum atoms which produces homogenization of the initially heterogeneous structure.

The theoretically predicted relationship between the diffusion rate and the square of the period of the heterogeneous structure has been fully confirmed. It appears possible to deduce the values of the fundamental parameters of a thermal spike — the volume of the spike and the energy dissipated in it — from independent experiments, one relating to the homogeneous state and the other to the heterogeneous state. A number of unsolved problems still remain in connection with the role of thermal spikes in rhombic α-uranium, where, as is well known, spontaneous "growth" phenomena occur and where the saturation of properties which takes place in the cubic γ-phase apparently is not observed.

Further experimental and theoretical studies are required to solve these problems.

LITERATURE CITED

[1] S. T. Konobeevskii, N. F. Pravdiuk and V. I. Kutaitsev, Investigations in the Fields of Geology, Chemistry and Metallurgy (Report by the Soviet Delegation to the International Conference on the Peaceful Uses of Atomic Energy) [in Russian] (Izd. AN SSSR, 1955), p. 263.

[2] S. T. Konobeevskii, J. Atomic Energy (USSR) No. 2, 63 (1956).*

[3] M. L. Bleiberg, L. J. Jones and B. Lustman, J. Appl. Phys. 27, 11, 1270 (1956).

[4] N. F. Pravdiuk, Investigations in the Fields of Geology, Chemistry and Metallurgy (Report by the Soviet Delegation to the International Conference on the Peaceful Uses of Atomic Energy) [in Russian] (Izd. AN SSSR, 1955), p. 165.

---

*Original Russian pagination. See C. B. Translation.

SPECIAL FINE-GRAINED EMULSION FOR NUCLEAR RESEARCH

N. A. Perfilov, N. P. Novikova and E. I. Prokof'eva

A method has been found for manufacturing special high-uniformity fine-grained emulsions with a most probable size of 0.04-0.08μ for the microcrystals . A method of potentiometric control of the emulsification process is presented which provides good reproducibility of the emulsions. Depending on the purpose of the research, using this method it is possible to fabricate special fine-grained emulsions for detection of charged particles with any sensitivity — from fragments up to relativistic particles — with track densities of 60 grains/100μ of particle range.

INTRODUCTION

As the dimensions of the microcrystals in a nuclear emulsion are reduced a considerable improvement in the resolving power of the emulsion in detection of charged particles of different types and energy becomes possible. The charged particle encounters a microcrystal of the emulsion and in interacting transfers part of its energy to the electrons. A certain number of electrons from the bound state may be transferred to the conduction level and create conditions for the formation of an exposure center at the microcrystal. The higher the specific energy loss of the particle the higher will be the probability for formation of a development center, all other conditions being equal.

In the interaction of a fast particle with the electrons a certain number of electrons may receive energy sufficient to cause them to move beyond the boundaries of the microcrystal and allow development in a neighboring crystal. The smaller the dimensions of the microcrystal the more important will be this effect in forming the track of the charged particle. The effective use of S-electrons with small energies leads to improved resolving power in fine-grained emulsions. In addition to the improved resolving power, fine-grained emulsions make it possible to measure with high accuracy the angles between particle tracks in nuclear disintegrations and multiple scattering of a single particle. With a reduction in the dimensions of the microcrystals of the emulsion the change in the nature of the background due to x-rays and γ-rays makes the scanning of the emulsion easier.

In general, emulsions for nuclear research have a most probable diameter (ranging from 0.2-0.3 μ) for the undeveloped crystals. In 1949 we were able to obtain emulsions with a most probable diameter lying between 0.04 and 0.08 μ for the silver-bromide microcrystals, that is, a grain dimension approximately 5 times smaller than usual. In the course of the last several years development work has been carried out on improving the synthesis of the emulsions and increasing their sensitivity. The present paper is devoted to a report of the results which have been obtained.

Principles of Fabricating the Special Fine-Grained Emulsion

In investigating the effect of the proportions of potassium bromide and silver nitrate on the size of the microcrystals in the photographic emulsion and its sensitivity in detecting fast charged particles by a method in which three solutions were used [1], an interesting fact was observed [2]. If the synthesis of the photographic emulsion is carried out with a small excess of silver nitrate (beyond the equivalent amount of potassium bromide) maintaining the indicated proportion throughout emulsification, up to the time at which cooling takes place, a photographic emulsion which is very fine-grained and uniform in crystal size is obtained; this emulsion can detect charged particles.

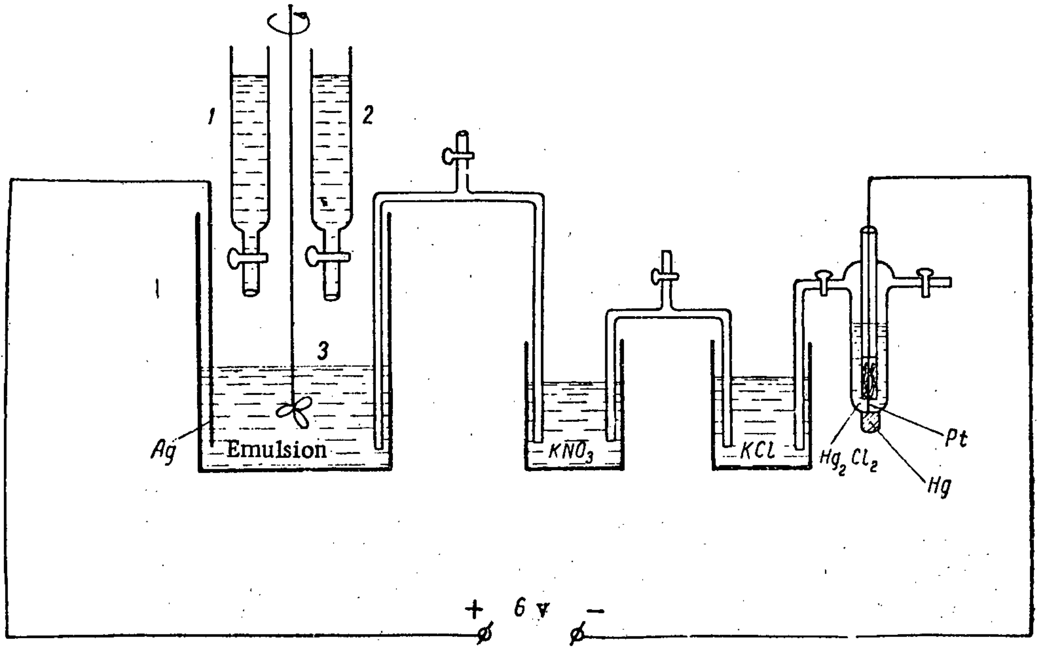

Fig. 1. Potentiometer circuit.

The most important stage in the fabrication of the photoemulsion is the emulsification process; the proper method is determined by the type of emulsion. To monitor the emulsification process we have used a potentiometric method [3] which allows continuous high-accuracy control of the proportion between the numbers of bromine ions and silver ions in the emulsion. In Figure 1 is shown a diagram of the potentiometer circuit. In the tank marked 3, containing a gelatin solution, there is a silver electrode and electrolytic cells with calomel elements. The circuit is connected to a PPTV-1 potentiometer and a 6-volt source. Above the tank there are two burettes containing a 60 percent solution of silver nitrate 1 and a 40 percent solution of potassium bromide with various additives 2. During emulsification the solutions are continuously dripped from burettes 1 and 2 into the tank 3 where they are mixed with the gelatin by a mechanical stirrer. The emulsification time is determined by the amount of obtained emulsion. For 100 ml of liquid emulsion this quantity is approximately 18 minutes. During emulsification a continuous measurement is made of the potential (with respect to the calomel element) of the emulsion being formed. By regulating the rate at which the solutions are introduced the potential can be changed positively or negatively. Using the known relation for the potential of the saturated solution of silver bromide the emulsification can be carried out under conditions of equivalence or with an excess of bromine ions or silver ions. This method of preparation makes it possible to obtain emulsions with standard characteristics.

Sensitivity in Detection of Charged Particles

To classify them in terms of sensitivity to charged particles, photoemulsions can be divided into three types, differing only in the contents of a small number of additives and the method of sensitization.

Type 1. Low-sensitivity emulsions "P-9, fragment" are capable of detecting particles with high specific ionization losses: multiply charged fragment ions, α-particles with energies from 20 to 30 Mev, and protons with energies from 1-2 Mev.

Because of the fine-grains in emulsions of this type it is possible to distinguish visually between fragment tracks and tracks produced by α-particles and protons. For illustration, in Figure 2 are shown microphotographs of tracks produced by fragments of uranium fission and tracks of α-particles from natural radioactive uranium (a);

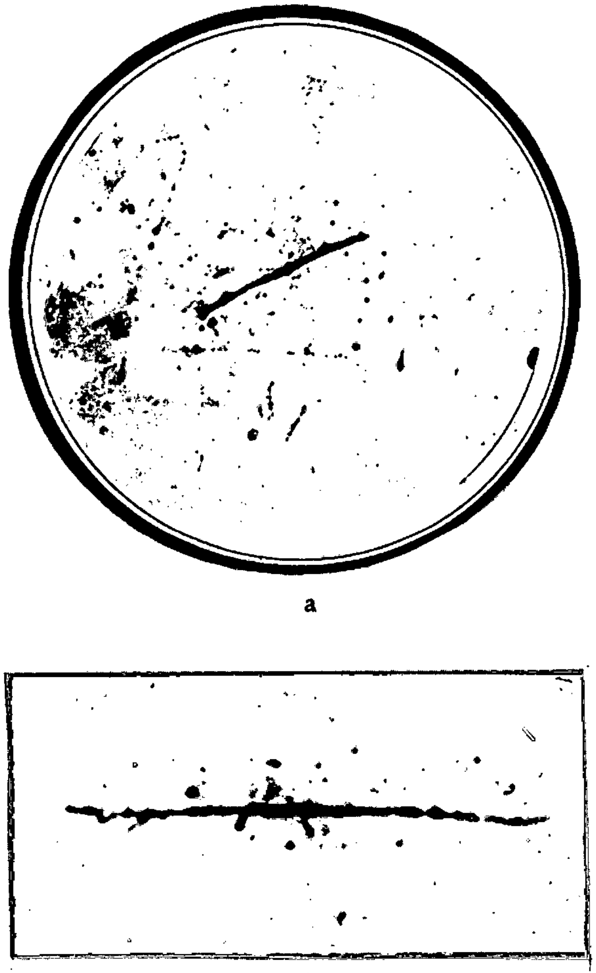

Fig. 2. a)Microphotograph of tracks of fission fragments and α-particles in "P-9, fragment" emulsion (x 1000); b) microphotograph of tracks of fragments flying apart in opposite directions (x 2500).

in addition there are microphotographs of tracks produced by fragments flying apart in opposite directions (b). In Figure 3 are shown the results obtained by photometry of tracks of light fragments and heavy fragments in uranium fission. A photometer makes it possible to determine the point at which the fission occurs (by using the break in darkening density). It should be noted that a trained observer can determine this point without the help of a photometer. Plates fabricated from "P-9, fragment" emulsion have been used for a long time in studying fission processes associated with slow neutrons. They are also suitable for the detection of multiply charged ions (fragments) against a background of a large number of α-particles when the oxidation method is used [4].

Type II. The sensitivity of "P-9, sensitive" emulsions is such as to allow detection of protons with energies of approximately 50 Mev. In contrast with the "P-9, fragment" emulsion they are subjected to a second development, before which the sensitizer is introduced. Films made from "P-9, sensitive" emulsions are used in studying nuclear reactions involving protons with energies of 600 Mev. To observe a significant number of tracks per unit surface we are limited to that sensitivity for which the primary protons do not register; thus tracks due to these latter particles do not complicate the scanning. Under these conditions the products of the nuclear reaction (α-particles of virtually all energies, which may appear at a given primary-proton energy and protons with energies up to 50 Mev) can be observed; it is also possible to measure their energy. In Figure 4 are shown microphotographs of meson tracks produced in $\pi - \mu$-decay (a) detected in emulsions of this type and tracks produced by nitrogen ions with energies of approximately 60 Mev (b). To show the resolving power, in Figure 5 are shown curves of the darkening density as a function of range* for various charged particles in this emulsion.

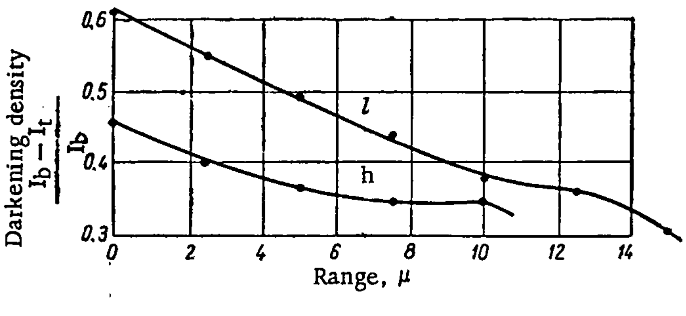

Fig. 3. Photometry of tracks of light (l) and heavy (h) fragments in uranium fission. I_b) photomultiplier current in measuring the background near the track; I_t) photomultiplier current in the measurement of given particle track.

---

*For the last 50 μ of range.

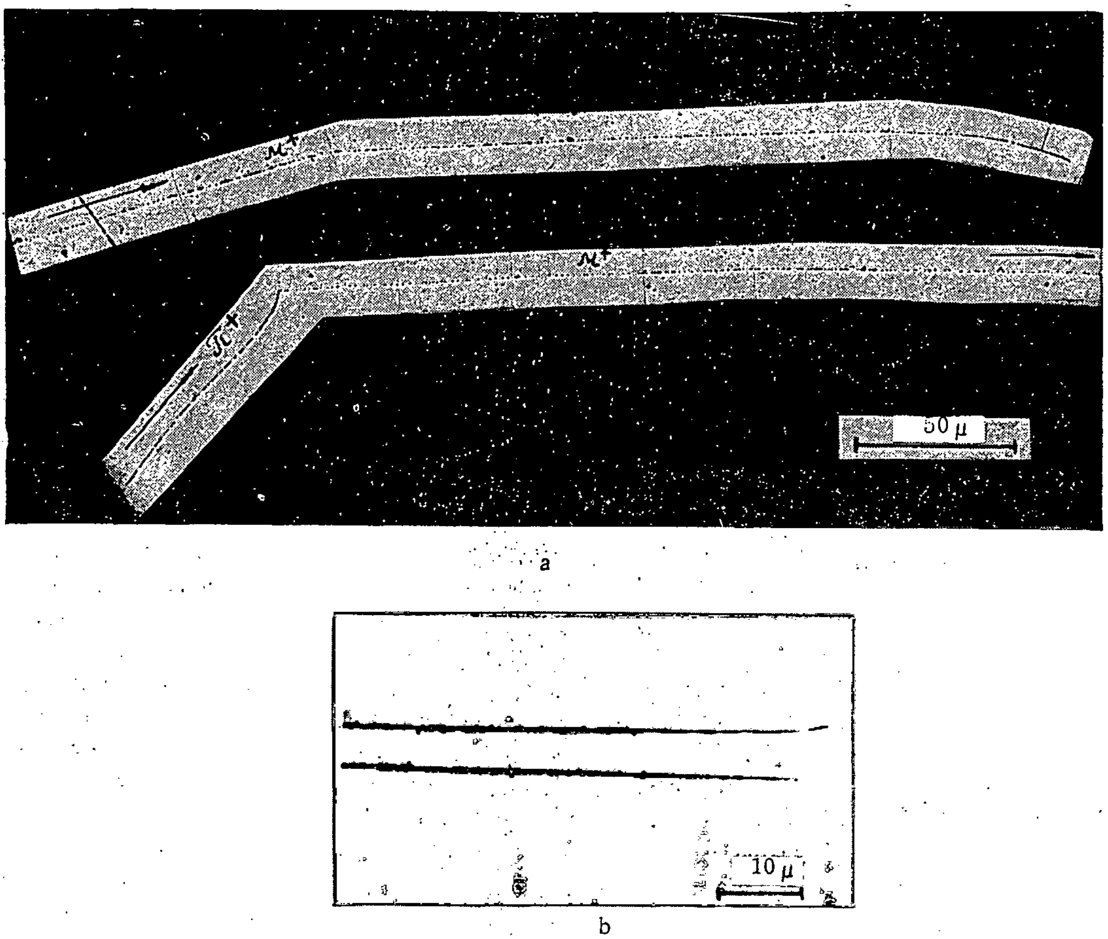

Fig. 4. a) Microphotograph of meson tracks from $\pi - \mu$-decay in "P-9, sensitive" emulsion; b) microphotograph of tracks of nitrogen ions with energies of approximately 60 Mev in a "P-9,sensitive" emulsion.

In "P-9, fragment" emulsions and "P-9, sensitive" emulsions the concentration by weight of the crystals in a dry layer is (84 ± 1)% with respect to the weight of gelatin. The shrinkage factor is 2.5 ± 0.1. The stopping power of a dry photo layer is about the same as the stopping power of a C-2 Ilford emulsion. In Figure 6 is shown a particle size distribution for the microcrystals in a P-9 emulsion. The most probable dimensions for the microcrystals are approximately 0.08, 0.06 and 0.04 μ.

Because of the small dimensions of the microcrystals the plate is transparent to the long-wave part of the visible spectrum. In Figure 7 are shown values of the attenuation coefficient* for emulsions with crystal dimensions of 0.08 and 0.06 μ as a function of the light wave length. It follows from Curves I and II that to attenuate radiation at a wave length of 800 mμ by a factor of $\underline{e}$ a layer of thickness of approximately 25-100μ is required. In principle the small attentuation for the long-wave part of the visible spectrum yields the possibility of observing particle tracks in the layer without fixing. A microphotograph of α-particle tracks (Fig. 8) was obtained in a plate with an emulsion thickness of 100 μ, developed after exposure to α-particles without subsequent dissolving and removal of silver bromide from the layer. Better results are obtained with smaller microcrystals of silver bromide; however, as the dimensions of the crystals are reduced the sensitivity to charged particles characterized by small specific ionizing losses is also reduced.

---

* The measurements of the attenuation coefficient were made by P. M. Valov.

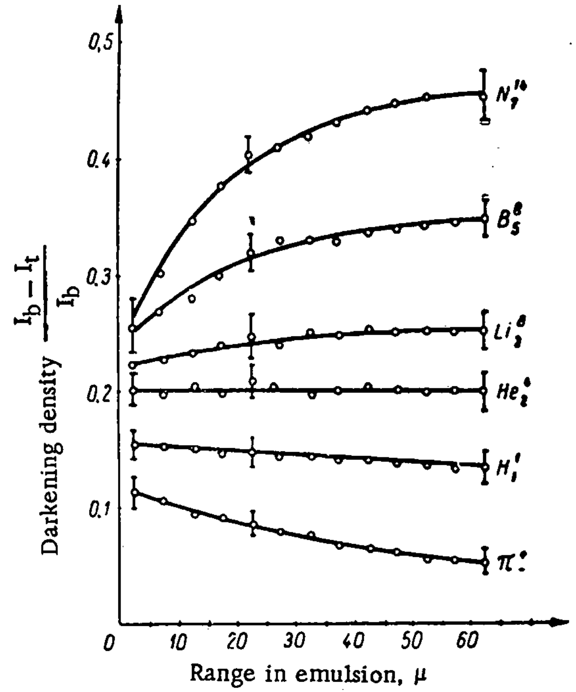

Fig. 5. Darkening density as a function of range of various charged particles.

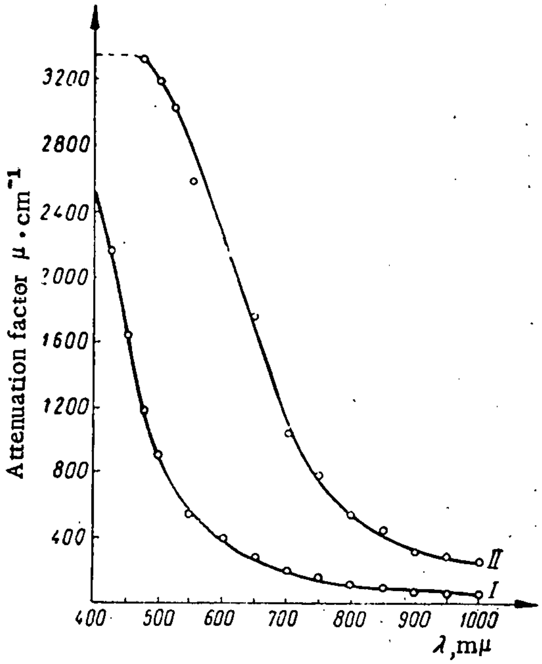

Fig. 7. The attentuation coefficient for emulsions with the following crystal sizes: I) 0.08 μ; II) 0.06 μ.

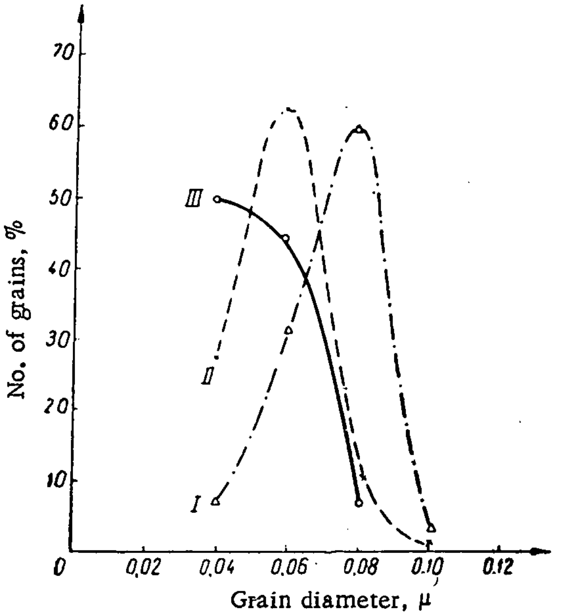

Fig. 6. Curve showing the size distribution of silver bromide microcrystals in P-9 emulsion. I, II, III are curves for emulsions with the same ratio of silver bromide and gelatin but with different amounts of potassium iodide added.

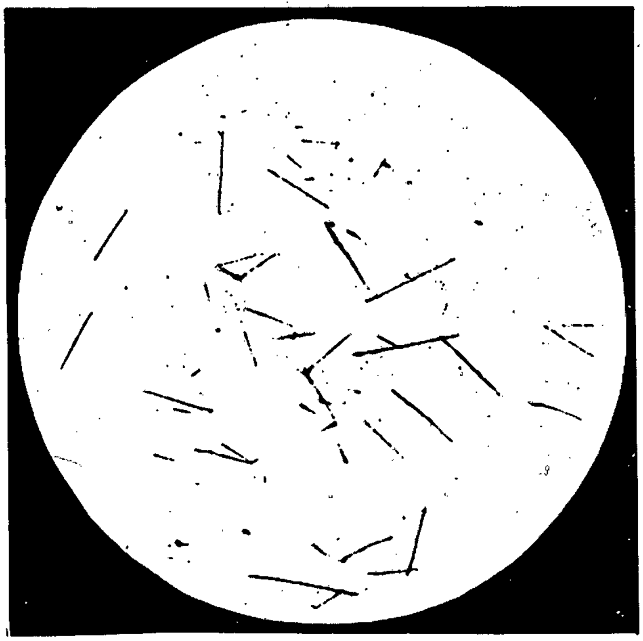

Fig. 8. Microphotograph of α-particle tracks in an unfixed layer (x 650).

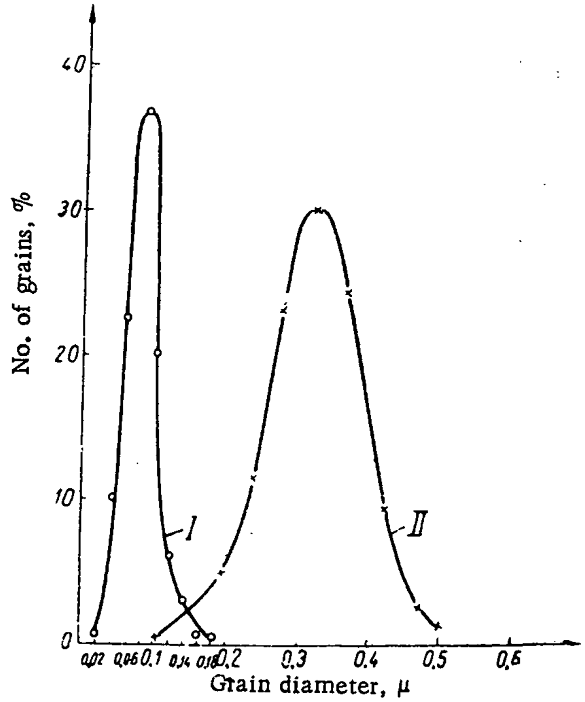

Fig. 9. Size distribution curves for silver bromide microcrystals: I) PR emulsion; II) G-5 emulsion.

We have already reported data on P-8 emulsions [2], [3]. The P-8 emulsion differs from the P-9 emulsion only in the somewhat larger gelatin content (the silver bromide content in a dry layer of P-8 emulsion is 73 percent). The deformation factor in the P-8 emulsion is smaller by a factor of 2.

Type III. These emulsions (PR "relativistic") detect minimum ionization charged particles. In Figure 9 is shown a distribution curve for undeveloped microcrystals in a PR emulsion and, for comparison purposes, a distribution curve for the microcrystals in the G-5 Ilford emulsion. The PR emulsion records relativistic electrons with a mean track density of 60 grains per 100 μ of particle range. The number of grains in the last 100 μ of the electron range is approximately 90 per 100 μ. In the last 10 μ of the range the track of the electron appears in the form of a continuous chain of grains.

In 1954, Demers [5] was successful in obtaining an emulsion which recorded relativistic particles and which had a microcrystal size of approximately 0.08μ. However, the density of developed grains in the particle tracks was only 15 grains per 100 μ of particle range. Apparently the smaller sensitivity of the Demers

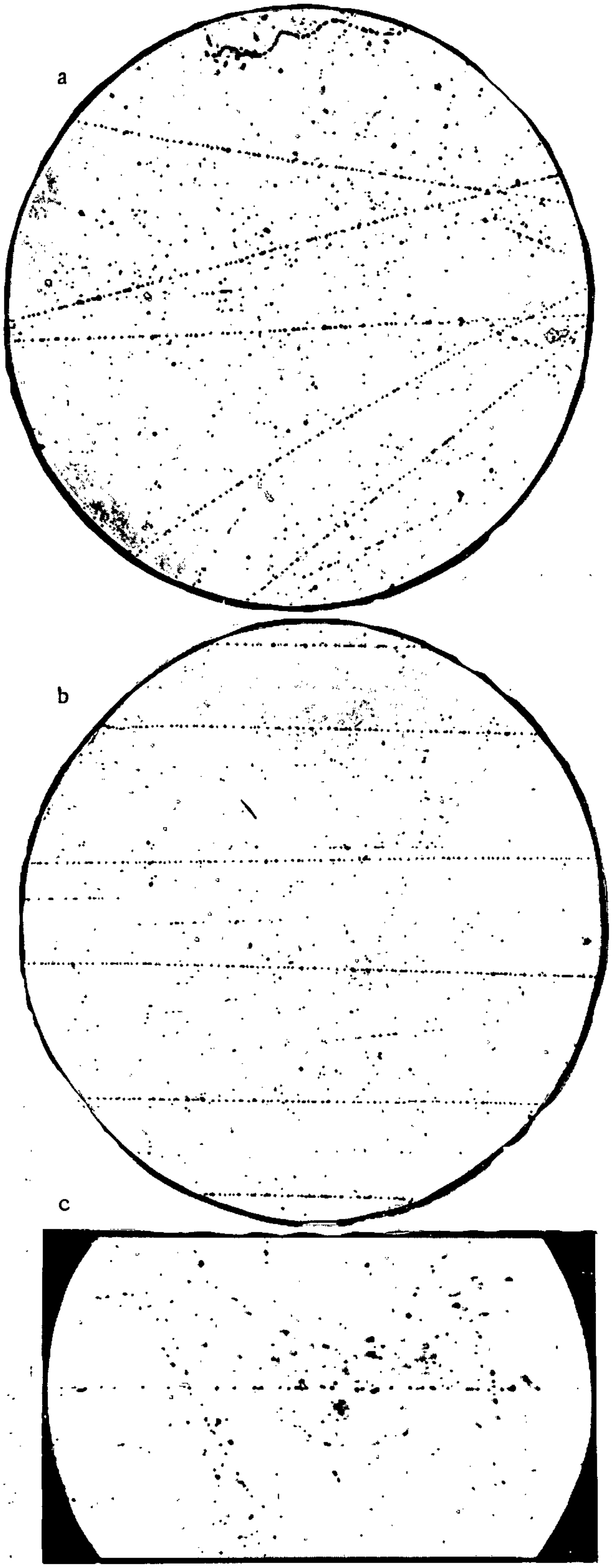

Fig. 10. a) Microphotographs of tracks of relativistic electrons recorded in PR emulsion (x 570); b) microphotograph of tracks of 300-Mev mesons in PR emulsion (x 570); c) microphotograph of tracks of a relativistic electron recorded in G-5 emulsion (x 570).

emulsion is due to the fact that the synthesis of the emulsion is carried out with an excess of potassium bromide. In addition, the sensitization process for the PR emulsion is different from that used by Demers.

In low-sensitivity nuclear emulsions the sensitivity is usually determined by the maximum energy of the particles, the tracks of which can still be distinguished against the background of fog. The sensitivity of emulsions which detect minimum ionization relativistic particles is more conveniently expressed in terms of the number of grains which are capable of being developed after passage of the relativistic particle. From a comparison of available relativistic emulsions [Kodak NT-4, Ilford G-5, NIKFI-R *, and the present PR emulsion (cf Table)] it follows that the most sensitive emulsion is the Kodak NT-4 whereas the least sensitive is the PR emulsion. However, in spite of the lower sensitivity, the visibility of relativistic tracks is better in emulsions with larger grains because of the higher density of developed grains in the particle track.

Emulsion	Mean dimensions of undeveloped microcrystals, μ	Number of developed grains per 100 μ of particle range	Yield of developed grains
Kodak NT-4	0.4	45	0.25
Ilford G-5	0.27	36	0.13
NIKFI-R	0.28	~ 40	0.15
PR	0.08	60	0.07

The mean of developed grain size in tracks of relativistic particles obtained in PR emulsion is approximately 0.3 μ. In G-5 emulsion, upon development the dimension of the crystals increase by a factor of 1.5-2. In the PR emulsion, in which the undeveloped microcrystals are 0.08 μ, the dimensions of the crystal are increased by approximately a factor of 4. Apparently in fine-grained emulsions several grains tend to be developed together rather than individually. An idea of the uniformity of grain dimensions in PR emulsion can be obtained from the microphotograph of the tracks (Fig. 10).

Change of Sensitivity of Special Fine-Grained Emulsions in Storage and Regression of the Latent Image

When Type I photo emulsions are stored there is no change in characteristics, at least for a period of a year. The sensitivity of Type II plates does not change in a period of 6-8 months. The storage properties of Type III plates have not been investigated in detail. Tests completed at the present time indicate that the sensitivity after sensitization remains unchanged for a period of 20 days. The question of the change of properties of this emulsion in time requires additional investigation. There are also some incomplete data on regression in fine-grained emulsions. In a Type I plate the regression is very marked. The tracks of α-particles from polonium vanish after two weeks.

The development centers in Type II plates are considerably more stable. The latent image is not subject to the deteriorating effect of oxidizers and the capacity for development remains unchanged for a month for α-particles from polonium and approximately 2 weeks for electrons with energies of tens of kev. The regression of tracks of relativistic particles in PR emulsion has not been investigated.

Received May 21, 1957

LITERATURE CITED

[1] B. H. Carrol, J. Chem. Educ. 8, 2341 (1931); T. T. Baker, Photographic Emulsion Technique (Boston, 1941); P. Demers, Can. J. Res. A 25, No. 4, 223 (1947).

---

* The data on Kodak NT-4 and Ilford G-5 emulsions is taken from [6]; for the NIKFI-R emulsion the data are taken from a calculation of the number of developed grains in the tracks of relativistic mesons.

[2] N. A. Perfilov, N. I. Gerling and E. I. Prokof'eva, Trudy RIAN 7, 1 (1956).

[3] N. A. Perfilov, E. I. Prokof'eva and N. R. Novikova, Ibid.

[4] N. A. Perfilov, J. Exptl.-Theoret.Phys. (USSR) 16, 285 (1946).

[5] P. Demers, Can. J. Phys. No. 8, 538 (1954).

[6] Physics of Cosmic Rays, [Russian translation] (IL, 1956), Vol. 2, p. 146.

DETERMINATION OF THE COMPOSITIONS AND INSTABILITY CONSTANTS OF SOME OXALATE COMPLEXES OF Pu^{+3} BY AN ION EXCHANGE METHOD

A. D. Gel'man, N. N. Matorina and A. I. Moskvin

The complex formation of Pu^{+3} ions in oxalate solutions over the pH range 1.4-3.0 was studied by an ion exchange method. It was established that in this pH range the complex ions $[Pu(C_2O_4)_2]^-$ and $[Pu(HC_2O_4)_4]^-$ are formed and that their instability constants are $K_{H'} = 7.1 \cdot 10^{-10}$ and $K_{H''} = 1.1 \cdot 10^{-11}$, respectively. The value of the instability constant of the complex ion $[Pu(C_2O_4)_2]^-$ agrees satisfactorily with the instability constant of the corresponding complex ion, obtained by a solution method.

By studying complex oxalate ions of Pu^{+3} using the solution method, we determined the composition and the instability constants of the complex ions formed at pH ≈ 8 [1].

In this report we give the results of investigating oxalate complex ions of Pu^{+3} in the pH range 1.4-3.0 by an ion exchange method. This method has been used by many investigators [2]-[12] for determining the compositions and instability constants of various complex compounds. However, it allows only the determination of the ratio Me/addendum in the inner sphere of the complex ion. This ratio does not always give a correct coordination number as in the inner sphere of the complex ion, together with the molecules or ions of the complex-forming agent, there may also be molecules of water, whose number cannot be determined directly by studying ion-exchange equilibria.

However, the presence of an H_2O molecule or a change in the number of moles of H_2O in the inner sphere of the complex ion does not affect the value of the instability constant. Therefore, this method may also be used both to determine the instability constant and to establish the composition of the complex ions.

In this work we studied the distribution of trivalent plutonium between solution and adsorbent, as described in papers [6]-[8], to determine the compositions and instability constants of complex oxalate compounds of Pu^{+3}. We obtained the distribution coefficients of Pu^{+3} between unimolar solutions of NH_4Cl and an adsorbent relative to the pH of the solution investigated. For this purpose we prepared a series of 1M NH_4Cl solutions with various pH values (from 1.6-3.5), containing Pu^{+3} in indicator amounts (50,000 to 100,000 dis/min in 1 ml of solution);* NH_4Cl was added to keep the ionic strength of the solution constant ($\mu \approx 1$); the pH of the solutions was adjusted with 1M HCl solution. To 25 ml of solution with a definite pH was added 0.5 g of adsorbent, cation exchange resin KU-2 [13], previously saturated with NH_4^+ ions. The solution was shaken with the adsorbent for 3 hours in an atmosphere of nitrogen at a temperature of 20 ± 1°C. This time was quite sufficient to establish equilibrium in the cationite — solution system. For solutions containing weighable amounts of Pu^{+3}, it was shown by spectrophotometric analysis for Pu^{+4} that during the time of the experiment there was no oxidation $Pu^{+3} \rightarrow Pu^{+4}$. The concentration of trivalent plutonium, both in the initial solutions and in the equilibrium solutions, was determined radiometrically. From the data obtained we calculated the distribution coefficient of Pu^{+3} between the liquid and solid phases. The results of the experiments are given in Table 1.

---

*A solution of Pu^{+3} chloride was prepared by reduction of Pu^{+4} with hydrazine ($N_2H_4 \cdot HCl$).

TABLE 1

Distribution Coefficients of Pu^{+3} in 1 M NH_4Cl Solution at Various pH Values

Equilibrium pH value of the 1 M NH_4Cl solution	Pu^{+3} concentration in the equilibrium solution, % of original $C_{Pu^{+3}}$	Amount of adsorbed Pu^{+3}, % of original $q_{Pu^{+3}}$	Distribution coefficient $A = \frac{C_{Pu^{+3}}}{q_{Pu^{+3}}}$
1.63	28.4	71.6	0.40
2.00	28.6	71.4	0.40
2.29	28.5	71.5	0.40
2.40	27.8	72.2	0.39
2.95	29.0	71.0	0.41
3.18	30.6	69.4	0.44
3.34	27.4	72.6	0.38
3.48	29.1	70.9	0.41

The distribution coefficient A did not change over the pH range investigated. This meant that for the Pu^{+3} concentrations used the adsorbent took up an extremely small amount of material, i. e., $q_{Pu^{+3}} << G_\infty$ (G_∞ is the capacity of the cationite).

From the ion-exchange equation [14]

$$\frac{q_{Pu^{+3}}^{1/3}}{G_\infty - q_{Pu^{+3}}} = K \frac{C_{Pu^{+3}}^{1/3}}{C_{NH_4^+}}$$

it follows that

$$\frac{q_{Pu^{+3}}^{1/3}}{C_{Pu^{+3}}^{1/3}} = \frac{K \cdot G_\infty}{C_{NH_4^+}},$$

where K is the ion-exchange equilibrium constant. As $C_{NH_4^+}$ = const, then $\frac{q_{Pu^{+3}}}{C_{Pu^{+3}}}$ = const. In the pH range 1.4-3.0, the capacity of the cationite KU-2, which has the strongly acid SO_3H^- group, should not change. The constancy of the distribution coefficient also indicates that Pu^{+3} is not hydrolyzed in the given pH range.

In a similar way we studied the distribution of Pu^{+3} between 1 M NH_4Cl solution and the adsorbent in the presence of oxalate. The concentration of $H_2C_2O_4$ in all the experiments equalled 0.005 mole/liter. Data from these experiments is shown in Figure 1.

On decreasing the pH of the solution, the adsorption of Pu^{+3} by the cationite strongly increased, due to decomposition of the complex oxalate ions on increasing the concentration of hydrogen ions. At pH < 1.4 the complex oxalate ions were practically completely dissociated and, on the other hand, at pH > 3.0 almost all the Pu^{+3} was present in the form of complex ions.

Under the given conditions, both the ions $C_2O_4^{-2}$ and $HC_2O_4^-$ may participate in complex formation. To calculate the concentrations of these ions it is necessary to know the dissociation constants of oxalic acid at the corresponding ionic strengths of the solution. These values were obtained by potentiometric titration of a 0.005 M solution of $H_2C_2O_4$ in 1 M NH_4Cl ($\mu \approx 1$). For the titration we used a 0.1 M KOH solution. The values of the dissociation constant of $H_2C_2O_4$, determined in this way, were $K_1 = 1.4 \cdot 10^{-2}$ and $K_2 = 1.5 \cdot 10^{-4}$, respectively. Using the equation for the dissociation of oxalic acid to the first and the second stages and the values found for K_1 and K_2, it is possible to determine the concentrations of $C_2O_4^{-2}$ and $HC_2O_4^-$ ions at any pH value of the solution. The formation processes of Pu^{+3} complex ions in the pH range investigated may be expressed by the following equations:

$$Pu^{+3} + nHC_2O_4^- \rightleftarrows [Pu(C_2O_4)_n]^{3-2n} + nH^+, \tag{1}$$

$$Pu^{+3} + mH_2C_2O_4 \rightleftarrows [Pu(HC_2O_4)_m]^{3-m} + mH^+. \tag{2}$$

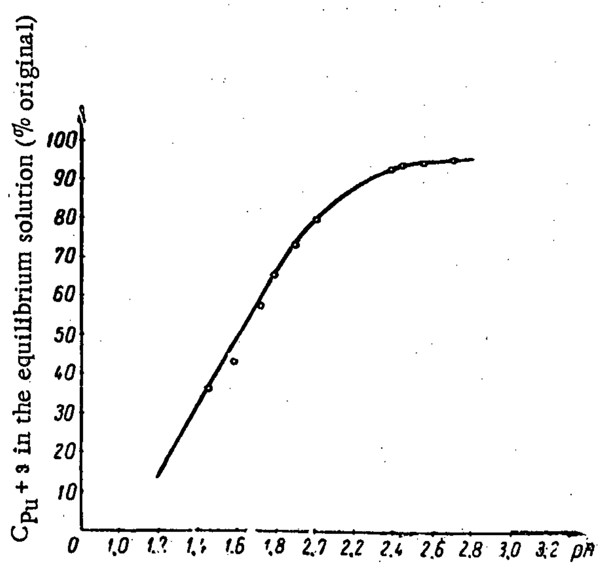

Fig. 1. Distribution of Pu^{+3} between 1 M NH_4Cl solution and a cationite relative to the pH in the presence of $H_2C_2O_4$.

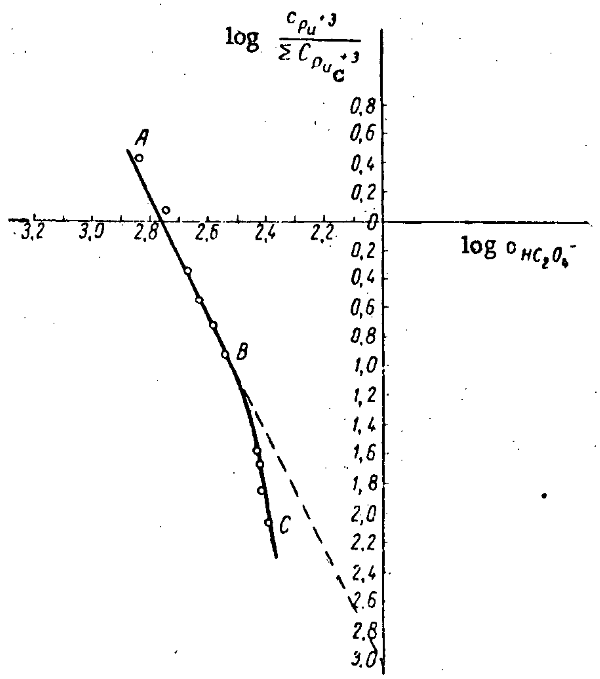

Fig. 2. Relation between the distribution of Pu^{+3} in a solution-cationite system and the concentration of $HC_2O_4^-$ ions in the solution. $C_{Pu_C^{+3}}$ is the concentration of Pu^{+3} in the complex.

The equilibrium constants of these reactions respectively equal:

$$K_a' = \frac{a_{Pu^{+3}} \cdot a^n_{HC_2O_4^-}}{a_{[Pu(C_2O_4)n]^{3-2n}} \cdot a^n_{H^+}} = \frac{c_{Pu^{+3}} \cdot c^n_{HC_2O_4^-}}{c_{[Pu(C_2O_4)n]^{3-2n}} \cdot c^n_{H^+}} \cdot \frac{\gamma_{Pu^{+3}} \cdot \gamma^n_{HC_2O_4^-}}{\gamma_{[Pu(C_2O_4)n]^{3-2n}} \cdot \gamma^n_{H^+}}; \tag{3}$$

$$K^a = \frac{a_{Pu^{+3}} \cdot a^m_{H_2C_2O_4}}{a_{[Pu(HC_2O_4)m]^{3-m}} \cdot a^m_{H^+}} = \frac{c_{Pu^{+3}} \cdot c^m_{H_2C_2O_4}}{c_{[Pu(HC_2O_4)m]^{3-m}} \cdot c^m_{H^+}} \cdot \frac{\gamma_{Pu^{+3}} \cdot \gamma^m_{H_2C_2O_4}}{\gamma_{[Pu(HC_2O_4)m]^{3-m}} \cdot \gamma^m_{H^+}}, \tag{4}$$

where a is the activity, c the concentration and γ the activity coefficient of the corresponding ions. The constants K'_a and K''_a are related to the overall instability constants of the complex ions

$$k_i' = \frac{c_{Pu^{+3}} \cdot c^n_{C_2O_4^{-2}} \cdot \gamma_{Pu^{+3}} \cdot \gamma^n_{C_2O_4^{-2}}}{c_{[Pu(C_2O_4)n]^{3-2n}} \cdot \gamma_{[Pu(C_2O_4)n]^{3-2n}}}, \tag{5}$$

$$k_i'' = \frac{c''_{Pu^{+3}} \cdot c^m_{HC_2O_4^-} \cdot \gamma_{Pu^{+3}} \cdot \gamma^m_{HC_2O_4^-}}{c_{[Pu\,(HC_2O_4)m]^{3-m}} \cdot \gamma_{[Pu\,(HC_2O_4)m]^{3-m}}} \qquad (6)$$

by the relation $k_i = K_a \cdot K_D^j$, where K_D is the dissociation constant of the acid for the corresponding dissociation stage and j is the number of coordinated anions of the complex-forming acid, associated with 1 atom of plutonium.

Under our conditions (μ = const) the ratio of the activity coefficients is constant; therefore we may write:

$$K_i' = \frac{c_{Pu^{+3}} \cdot c^n_{C_2O_4^{-2}}}{c_{[Pu\,(C_2O_4)_n]^{3-2n}}}, \qquad (7)$$

$$K_i'' = \frac{c_{Pu^{+3}} \cdot c^m_{HC_2O_4^-}}{c_{[Pu\,(HC_2O_4)m]^{3-m}}}, \qquad (8)$$

where $K'_i = \frac{k'_i}{B'}$ and $K''_i = \frac{k''_i}{B''}$ (B' and B" are the ratios of the activity coefficients). Taking logarithms of Equations (7) and (8) we obtain

$$\log K_i' = \log \frac{c_{Pu^{+3}}}{c_{[Pu\,(C_2O_4)n]^{3-2n}}} + n \log c_{C_2O_4^{-2}}, \qquad (9)$$

$$\log K_i'' = \log \frac{c_{Pu^{+3}}}{c_{[Pu\,(HC_2O_4)m]^{3-m}}} + m \log c_{HC_2O_4^-}. \qquad (10)$$

The concentration of plutonium ions in the equilibrium solution is equal to the total of the concentration of complex ions and the concentration of free Pu^{+3} ions:

$$C_{Pu^{+3}} = c_{Pu^+} + c_{[Pu\,(C_2O_4)n]^{3-2n}} + c_{[Pu\,(HC_2O_4)m]^{3-m}}. \qquad (11)$$

From Equations (7), (8) and (11) it follows that

$$\frac{C_{Pu^{+3}}}{c_{Pu^{+3}}} = 1 + \frac{c^n_{C_2O_4^{-2}}}{K_i'} + \frac{c^m_{HC_2O_4^-}}{K_i''}. \qquad (12)$$

To determine the composition of complex oxalate ions of Pu^{+3} we plotted a logarithmic curve (Fig. 2). The points of Section AB lie on a line whose slope equals 4. Consequently, we may assume that in the pH range 1.4-1.9 the complex ion with the composition $[Pu(CH_2O_4)_4]^-$ is predominantly formed. At higher values of pH a mixture of two or more complex ions of trivalent plutonium are formed.

In Table 2 we give values of the instability constant K''_i of the complex $[Pu(HC_2O_4)_4]^-$, calculated by Equation (8). Since in all cases the starting concentration $C_{Pu^{+3}} << C_{H_2C_2O_4}$, then the change in the concentration of $H_2C_2O_4$ due to complex formation was disregarded. The value of the instability constant did not change over the pH range 1.4 to 1.9, confirming that the complex ion $[Pu(HC_2O_4)_4]^-$ was present in solution.

The average value of the instability constant of the complex ion $[Pu(HC_2O_4)_4]^-$ was then used to calculate its concentration in solution and to determine the total concentration of other complex ions formed at pH from 1.7 to 3.0. Thus the concentration of Pu^{+3} ions was determined by the equation

$$C_{Pu^{+3}} = A \cdot q_{Pu^{+3}}, \qquad (13)$$

and the ion $[Pu(HC_2O_4)_4]^-$ by Equation (8).

According to Equations (8) and (11)

$$N = C_{Pu^{+3}} - c_{Pu^{+3}} - \frac{c_{Pu^{+3}} \cdot c^{m}_{HC_2O_4^-}}{K''_i}, \tag{14}$$

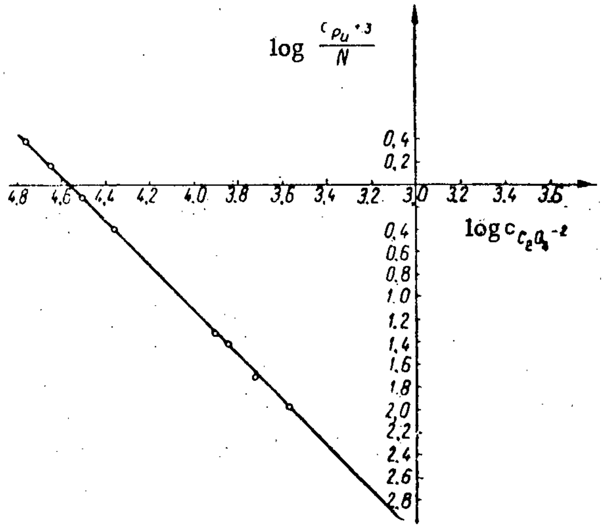

Fig. 3. Relation between the distribution of Pu^{+3} in a solution-cationite system and the concentration of $C_2O_4^{-2}$ ions in the solution.

TABLE 2

Instability Constants of Complex Oxalate Ions of Pu^{+3}

Equilibrium pH value of the solution	Concentration of $C_2O_4^{-2}$ ion in the equilibrium solution, mole/liter	Concentration of $HC_2O_4^-$ ion in the equilibrium solution, mole/liter	Concentration of free Pu^{+3} ions, %	Conc. of the complex ion $(Pu(C_2O_4)_2]$ in solution, %		Conc. of the complex ion $(Pu(HC_2O_4)_4]$ in solution, %		$K'_i \cdot 10^{10}$	$K''_i \cdot 10^{11}$
				from exptl. data	from average value of K'_i	from exptl. data	from the average value of K''_i		
1.47	$6.45 \cdot 10^{-6}$	$1.46 \cdot 10^{-3}$	25.7	—	—	10.1	10.2	—	1.15
1.55	$8.80 \cdot 10^{-6}$	$1.61 \cdot 10^{-3}$	24.4	—	—	14.6	14.4	—	1.12
1.60	$1.07 \cdot 10^{-5}$	$1.79 \cdot 10^{-3}$	23.0	—	—	19.6	20.7	—	1.20
1 73	$1.72 \cdot 10^{-5}$	$2.13 \cdot 10^{-3}$	17.3	6.8	7.21	32.7	31.2	7.5	1.09
1.80	$2.22 \cdot 10^{-5}$	$2.34 \cdot 10^{-3}$	14.2	12.8	9.86	—	37.4	5.5	—
1.90	$3.11 \cdot 10^{-5}$	$2.61 \cdot 10^{-3}$	11.1	16.1	15.1	—	45.1	6.7	—
2.00	$4.35 \cdot 10^{-5}$	$2.89 \cdot 10^{-3}$	8.4	19.2	22.4	—	51.4	8.3	—
2.35	$1.24 \cdot 10^{-4}$	$3.69 \cdot 10^{-3}$	2.4	52.7	52.1	—	38.9	7.0	—
2.40	$1.43 \cdot 10^{-4}$	$3.80 \cdot 10^{-3}$	2.0	56.4	57.6	—	36.6	7.2	—
2.50	$1.86 \cdot 10^{-4}$	$3.92 \cdot 10^{-3}$	1.3	68.6	63.3	—	26.9	6.6	—
2.65	$2.72 \cdot 10^{-4}$	$4.06 \cdot 10^{-3}$	0.8	78.2	83.4	—	19.0	7.6 average $7.1 \cdot 10^{-10}$	average 1.14×10^{-11}

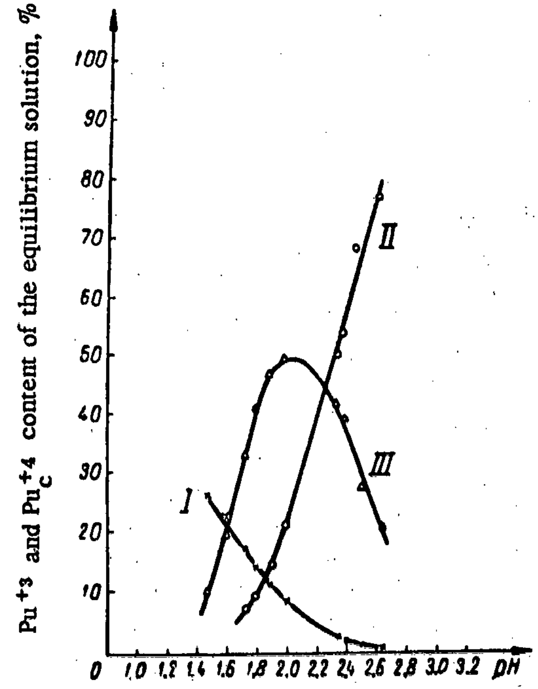

Fig. 4. Effect of solution pH on the concentration of Pu^{+3} ions. I) Pu^{+3}; II) $[Pu(C_2O_4)_2]^-$; III) $[Pu(HC_2O_4)_4]^-$.

where N expresses the total concentration of other complex ions in the solution. A graph of the relation between log $\frac{c_{Pu^{+3}}}{N}$ and the logarithm of the equilibrium concentration of $C_2O_4^{-2}$ ion in the pH range from 1.7 to 2.7 is shown in Figure 3. All the points obtained fall on a line with a slope equal to 2. Thus at pH > 1.7, a mixture of the two complex ions $[Pu(C_2O_4)_2]^-$ and $[Pu(HC_2O_4)_4]^-$ is formed. The value of the instability constant of the complex ion $[Pu(C_2O_4)_2]^-$ in this pH range was calculated by Equation (14), where

$$N = \frac{c_{Pu^{+3}} \cdot c^2_{C_2O_4^{-2}}}{K_i'}.$$

The results of calculating the instability constants and concentrations of the complex ions and also the data used in the calculation are summarized in Table 2. The relation between the concentration of these ions and the pH of the solution is shown in Figure 4.

As Table 2 shows, the instability constant of the complex ion $[Pu(C_2O_4)_2]^-$ has a constant value over the whole pH range. Consequently, in a solution at pH > 1.7, a mixture of the complex ions $[Pu(C_2O_4)_2]^-$ and $[Pu(HC_2O_4)_4]^-$ is formed, having $K'_i = 7.1 \cdot 10^{-10}$ and $K''_i = 1.1 \cdot 10^{-11}$, respectively.

The constants K'_i and K''_i correspond to complete decomposition of the complex ions by the equations:

$$[Pu(C_2O_4)_2]^- \rightleftarrows Pu^{+3} + 2C_2O_4^{-2}, \qquad (15)$$

$$[Pu(HC_2O_4)_4]^- \rightleftarrows Pu^{+3} + 4HC_2O_4^-. \qquad (16)$$

If there are two or more complex ions with unknown values of K_i present in the solution at the same time, then using Equations (11) and (12), obtained for several experimental points of the curve (see Fig. 1), we can always obtain a system of equations where the number of unknowns equals the number of equations. By solving such a system, we obtain all values of $\underline{n}$, $\underline{m}$ and K_i'. Such a problem may always be solved readily by the method of least squares [15]. We should note that the value of K_i for the complex ion $[Pu(C_2O_4)_2]^-$, found by the ion-exchange method, agrees quite satisfactorily with the value of this constant, obtained by a solution method [1]. The corresponding instability constants equal $4.9 \cdot 10^{-10}$ (from solution data) and $7.1 \cdot 10^{-10}$ (ion-exchange method). Some of the deviation in the values given may be explained by the different ionic strengths of the solutions, used for determining the instability constant by these two methods.

The complex ions with a large number of oxalate groups, which we found previously at pH ≈ 8, were not found in this case as all the experiments were carried out in the pH range 1.4-3.0. As Figure 1 shows, the method we chose does not allow investigations at higher pH values. This problem may be solved by using an anionite.

Received August 15, 1957

LITERATURE CITED

[1] A. D. Gel'man, N. N. Matorina and A. I. Moskvin, J. Atomic Energy (USSR) 3, 10, 308 (1957).*

[2] G. A. Kniazev, V. V. Fomin and O. I. Zakharov-Nartsissov, J. Inorg. Chem. (USSR) 1, 2, 342 (1956).

---

* Original Russian pagination. See C. B. Translation.

[3] V. V. Fomin and V. V. Sin'kovskii, J. Inorg. Chem. (USSR) 1, 10, 2316. (1956).

[4] V. V. Fomin, L. N. Fedotova, V. V. Sin'kovskii and M. A. Andreeva, J. Phys. Chem.(USSR) 29, 2052(1955).

[5] S. Froneus, Acta Chem. Scand. 5, 859 (1951).

[6] J. Schubert, J. Phys. Coll. Chem. 52, 340 (1948).

[7] J. Schubert, E. R. Russel and L. S. Mayer, J. Biol. Chem. 185, 387 (1940).

[8] S. Iu. Elovich, and N. N. Matorina, J. Phys. Chem. (USSR) 30, 383 (1956).

[9] L. I. Tikhonova and M. M. Seniavin, J. Inorg. Chem. (USSR) 2, 1, 74 (1957).

[10] V. I. Paramonova and B. V. Kolychev, J. Inorg. Chem. (USSR) 1, 8, 1896 (1956).

[11] V. I. Paramonova and A. S. Voevodskii, J. Inorg. Chem.(USSR) 1, 8, 1905 (1956).

[12] I. A. Korshunov. L. P. Pochinailo and V. M. Tikhomirova, J. Inorg. Chem. (USSR) 2, 1, 68. (1957).

[13] E. B. Trostianskaia, N. P. Losev and A. S. Tevlina, Prog. Chem. (USSR) 26, 1, 69 (1955).

[14] B. P. Nikol'skii and V. I. Paramonova, Prog. Chem.(USSR) 8, 1535 (1939).

[15] K. B. Iatsimirskii, J. Phys. Chem.(USSR) 25, 475 (1956).

POLAROGRAPHIC INVESTIGATION OF COMPLEX PLUTONIUM OXALATES

V. V. Fomin, S. P. Vorob'ev and M. A. Andreeva

The composition and stability of complex ions of tri- and tetravalent plutonium in oxalate solutions were investigated polarographically.

The complexes $Pu(C_2O_4)_4^{-4}$ (preponderant amount) and $Pu(C_2O_4)_4^{-5}$ were formed in solutions of potassium oxalate with pH 3.5-6. Under these conditions, Pu^{+4} gave a well expressed reverse reaction wave, suitable for the quantitative polarographic determination of plutonium. The oxidation-reduction potential of this reaction in 1 M potassium oxalate was equal to 0.205 v (relative to a saturated calomel electrode at a temperature of 25° C). Two Pu^{+4} complexes were simultaneously present in solutions at pH 6-8.

From data on the solubility of $Pu(C_2O_4)_3$, we determined the instability constants of the complex oxalate ions $Pu(C_2O_4)_3^{-3}$ and $Pu(C_2O_4)_4^{-5}$, and from the polarographic data those for $Pu(C_2O_4)_4^{-4}$ ions:

$$K_{Pu(C_2O_4)_4^{-5}} = 2.4 \cdot 10^{-12}. \quad K_{Pu(C_2O_4)_3^{-3}} = 2.2 \cdot 10^{-11}. \quad K_{Pu(C_2O_4)_4^{-4}} = 33 \cdot 10^{-28}.$$

The reports on the existence of oxalate complexes of trivalent plutonium are contradictory [1]. By spectrophotometry and solubility determination, W. Reas [2] established the existence of the Pu^{+4} ions $PuC_2O_4^{+}$, $Pu(C_2O_4)_2$, $Pu(C_2O_4)_3^{-2}$ and found the corresponding stability constants; he also showed the existence of $Pu(C_2O_4)_4^{-4}$ ions. There are references [1] to unpublished polarographic investigations of oxalate complexes of Pu^{+4}, but the results are not given.

The authors of this article investigated polarographically the complex ion formation of tri- and tetravalent plutonium with oxalate ion at concentrations of the latter from 10^{-3} to 1.2 M. The work was carried out on a V-301 polarograph, which automatically recorded the curves of current strength against voltage. A dropping mercury electrode acted as the cathode; the anode was a saturated calomel electrode (sce). 0.01% of gelatin was added to the solution to suppress the maxima. The experiments were carried out at 25 ± 0.1°C. Purified argon was passed for 20 minutes through the solution in the electrolyzer to remove dissolved oxygen. The argon was freed from oxygen by passing through a tube containing copper filings heated to 700°C, two bottles with a solution of divalent chromium, a bottle with water and an empty flask to trap splashes. The polarogram of the background (potassium oxalate), after the passage of argon, contained no waves up to the liberation of hydrogen. The correction for the resistance of the system (electrolyzer, intermediate bridge, calomel electrode and leads) was found, as usual, by determining the value of the half-wave potential under the same conditions, but with a different plutonium concentration in the solution, using a ratio of 1 : 16.

Potassium oxalate was used as the complex forming salt as its solubility is considerably greater than that of the sodium or ammonium salts; this made it possible to investigate the complex plutonium oxalates over a wider range of oxalate ion concentrations.

Solutions of potassium oxalate and oxalic acid were mixed together to investigate the effect of pH of the medium on complex formation. Before taking quantitative measurements, we proved the reversibility of the electrode reaction $Pu^{+4} \rightleftharpoons Pu^{+3}$ in an oxalic acid solution. In addition, we compared the half-wave potentials for continuous recording of curves and for plotting separate points (the electrode was maintained for 3 minutes at each value of the applied emf for plotting the curves by points). Waves from the same solutions continuously recorded and plotted as separate points, did not differ greatly in half-wave potentials or in wave height. The half-wave potential obtained by plotting points was 0.004-0.005 v more negative than the half-wave potential from continuous recording, with a measurement error of ± 0.002 v. This, apparently, is explained by the fact that the equilibrium at the electrode surface is not established immediately between the oxidized and reduced forms of plutonium ions. The concentration of the oxalate ions was calculated by the equation

$$\Sigma C_2O_4 = [C_2O_4''] + [HC_2O_4'] + [H_2C_2O_4] \tag{1}$$

(where ΣC_2O_4 is the analytical oxalate concentration) using the known concentration of hydrogen ions and the ionization constant of oxalic acid ($K_1 = 5.9 \cdot 10^{-2}$; $K_2 = 6.4 \cdot 10^{-5}$) [3]. The relation of the ionization constant of oxalic acid and the constant of the complex ions to the ionic strength of the solution was not considered. The usual methods for the polarographic investigation of complex formation were used [4]-[7].

Experimental Results and Discussion

We first plotted polarograms of the solutions, containing tetravalent plutonium and oxalate ions at different concentrations and with various solution pHs. The values of the half-wave potentials and wave heights are given in Table 1 and one of the polarograms is shown in Figure 1.

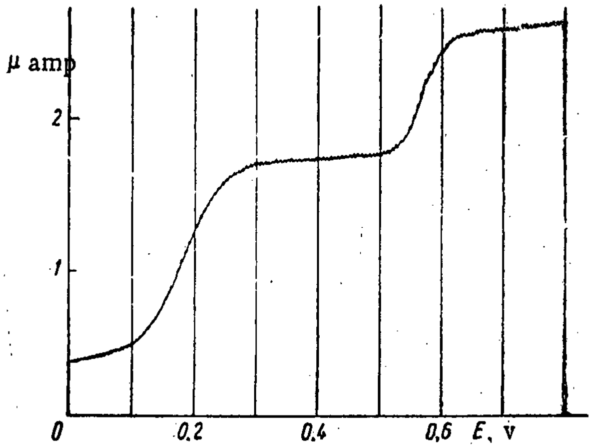

Fig. 1. Polarogram of Pu^{+4} in an oxalic acid solution at pH = 7.89.

TABLE 1

The Effect of Concentration of C_2O_4'' Ions and pH of the Medium on the Complex Formation of Pu^{+4} and Pu^{+3} (Total Oxalate Concentration – 1 N, Concentration of Pu^{+4} – $6.5 \cdot 10^{-5}$ M)

Conc. $[C_2O_4'']$ g-equiv/liter	Wave height, μ amps	Half-wave potential	pH of solution
1.000	1.60	—0.193	7.89
1.000	1.83	—0.192	7.04
0.997	1.94	—0.194	6.70
0.985	2.25	—0.193	6.03
0.918	2.29	—0.193	5.25
0.423	2.23	—0.195	4.06
0.098	2.24	—0.194	3.58
0.028	2.30	—0.178	2.97*
—	2.11	—0.144	2.25
—	The wave was displaced considerably towards positive potentials.		1.50

---

*Precipitation of oxalic acid was observed in the last samples.

A considerable displacement of the half-wave potential towards more negative values in comparison with the oxidation-reduction potential of Pu^{+4} and Pu^{+3} in a noncomplex-forming medium [8] indicated the presence of stable plutonium complexes in the solution. It was established that only one clearly expressed wave appeared on the polarogram at solution pHs of 3.5-6. Regardless of the sharp change in the concentration of oxalate ions in this pH range, the half-wave potential remained the same (Table 1). This indicates that the coordination numbers of Pu^{+4} and Pu^{+3} are equal. Two waves appear at pH 7.89. According to our hypothesis, two complexes exist in oxalic acid solutions at pH 6-8 and an equilibrium is slowly established between them, as with other elements [9]. The experiments carried out showed that at a pH close to

8 (Table 2) the ratio of the various complex ions changed considerably with time. A second wave appeared at more negative values of the half-wave potential. A third wave with a half-wave potential of about − 0.30 v appeared when CO_3'' ions were present in the alkaline medium (due to absorption of carbon dioxide from the air and this was confirmed by experiments with K_2CO_3 added).

TABLE 2

The Height of the Pu^{+4} Wave with $E_{1/2} = -0.205$ v the 1st and 9th Day After Preparing the Solutions

$K_2C_2O_4$ concentration M	pH of the solutions	Wave height the 1st day μamps	Wave height the 9th day μamps
0.10	8.08	3.42	2.22
0.23	8.50	3.38	2.36
0.49	8.63	3.34	2.71
0.75	8.68	3.46	2.61
1.01	8.72	3.37	2.93
1.14	8.72	3.38	3.01

TABLE 3

The Relation of Current Strength to Pu^{+4} Concentration in a Normal Potassium Oxalate Solution at pH 5.5

Wave height μamps	Half-wave potential, v	Pu^{+4} concentration, M
17.86	−0.195	$8 \cdot 10^{-4}$
9.40	−0.193	$4 \cdot 10^{-4}$
4.97	−0.197	$2 \cdot 10^{-4}$
2.63	−0.193	$1 \cdot 10^{-4}$
1.94	−0.194	$5 \cdot 10^{-5}$
0.72	−0.198	$2.5 \cdot 10^{-5}$
0.44	−0.197	$1.25 \cdot 10^{-5}$
0.24	−0.197	$6.25 \cdot 10^{-6}$

The reversibility of the reduction of the Pu^{+4} complex ion may be proved by the basic polarographic wave equation

$$E = E_{1/2} - \frac{0.059}{a} \log \frac{i}{i_d - i} . \qquad (2)$$

The various values of E and the corresponding magnitudes of $\frac{i}{i_d - i}$ of the wave were carefully measured on the polarogram of Pu^{+4} in a 1 M potassium oxalate solution at pH 5.5. Using them we plotted a graph of E as a function of $\log \frac{i}{i_d - i}$ (Fig. 2). The experimental points lay on a straight line, whose slope was equal to 0.063 v, which agrees well with the theoretical value for a = 1 and indicated that the reduction of Pu^{+4} complex ion at a mercury electrode proceeded with the participation of one electron, i. e., to Pu^{+3}.

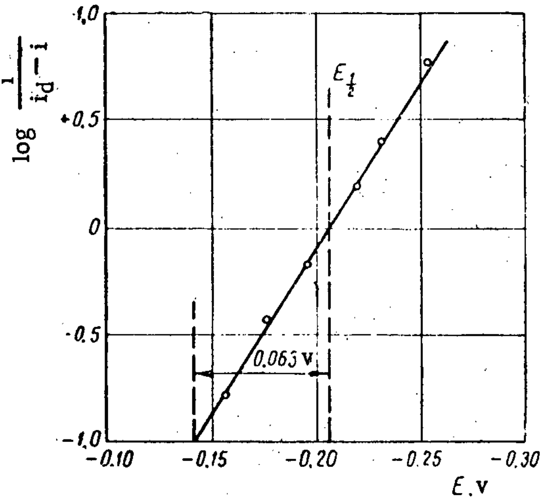

Fig. 2. Testing the reversibility of the reaction $Pu^{+4} \rightleftarrows Pu^{+3}$ in a 1 M solution of $K_2C_2O_4$ at pH 5.5

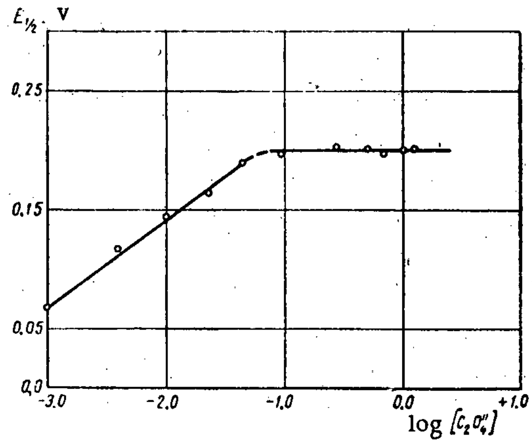

Fig. 3. The relation of the half-wave potential of Pu^{+4} reduction to the logarithm of the potassium oxalate concentration.

Experiments showed that at a pH of the oxalic acid solutions of 3.5-6, the current strength during the reduction was a linear function of the Pu^{+4} concentration (Table 3 and Fig. 3).

TABLE 4

Displacement of the Half-Wave Potential of Pu^{+4} Reduction in Relation to Potassium Oxalate Concentration; pH = 5.5

$K_2C_2O_4$ concentration M	Log of $K_2C_2O_4$ concentration	Half-wave potential, v	$\frac{K_{ox}}{K_{red}}$
$1 \cdot 10^{-3}$	−3.00	−0.069	$2.27 \cdot 10^{-17}$
$4 \cdot 10^{-3}$	−2.40	−0.118	$1.36 \cdot 10^{-17}$
$1 \cdot 10^{-2}$	−2.00	−0.141	$1.36 \cdot 10^{-17}$
$2.2 \cdot 10^{-2}$	−1.66	−0.164	$1.22 \cdot 10^{-17}$
$4.6 \cdot 10^{-2}$	−1.34	−0.188	$1.00 \cdot 10^{-17}$
$9.4 \cdot 10^{-2}$	−1.03	−0.197	$1.47 \cdot 10^{-17}$
$3 \cdot 10^{-1}$	−0.52	−0.201	$4.10 \cdot 10^{-17}$
$5 \cdot 10^{-1}$	−0.30	−0.200	$7.95 \cdot 10^{-17}$
$7 \cdot 10^{-1}$	−0.16	−0.198	$1.13 \cdot 10^{-16}$
1.00	−0.00	−0.199	$1.42 \cdot 10^{-16}$
1.20	+0.08	−0.201	$1.53 \cdot 10^{-16}$

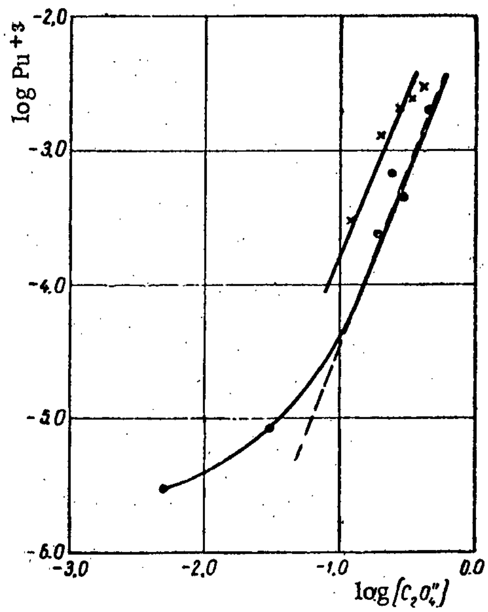

Fig. 4. Graph of the relation of the Pu^{+3} oxalate concentration to the logarithm of the oxalate ion concentration. ●●●●) according to data in Table 5; xx) according to data in Table 6.

Considering the reversibility of the reaction examined, the good reproducibility of the wave and the small value and constancy of the half-wave potential, this electrode reaction may be used under chosen conditions for the quantitative polarographic determination of plutonium. Using the equation for the half-wave potential

$$E_{1/2}=E^0-\frac{0,059}{a}\log\frac{D_{ox}}{D_{red.}}-\frac{0,059}{a}(p-q)\log Cx, \qquad (3)$$

one can determine the formal oxidation-reduction potential of Pu^{+4}/Pu^{+3} in a 1 M $K_2C_2O_4$ solution, if $\frac{D_{ox}}{D_{red}}$ is taken as ≈ 1. As shown by Figure 2, the half-wave potential of Pu^{+4} reduction in a 1 M potassium oxalate solution, relative to a sce at 25° C, was equal to − 0.205 v.

Determination of the Instability Constants of Oxalate Complexes of Tri- and Tetravalent Plutonium

Using the equation

$$E^0_c-E^0_s=\frac{0.059}{a}\log\frac{K_{ox}}{K_{red}}-\frac{0.059}{a}(p-q)\log Cx, \qquad (4)$$

where $E^0_c = (E_{1/2})_c$ is the potential of a system containing $K_2C_2O_4$ and Pu^{+4}; $E^0_s = (E_{1/2})_s$ is the potential of a noncomplex-forming system containing Pu^{+4}, the ratio of the instability constants K_{ox} and K_{red} may be found.

As $(E_{1/2})_s$ is a constant value, then Equation (4) is also a linear equation and therefore the difference in the coordination numbers p and q may be determined by the tangent of the slope of the line:

$$\Delta E_{1/2}=K-y\log Cx,$$

where

$$\Delta E_{1/2} = (E_{1/2})_c - (E_{1/2})_s; \quad K = \frac{0.059}{a} \log \frac{K_{ox}}{K_{red.}};$$
$$y = \frac{0.059}{a}(p - q) = \tan \alpha.$$

The values of the half-wave potentials were found from polarograms, plotted for different concentrations of potassium oxalate and a solution pH of 5.5 (Table 4).

In the range of potassium oxalate concentrations $10^{-3} - 1 \cdot 10^{-1}$ M, the difference in the coordination numbers was equal to 1. It follows from the data in Table 4 that in this region the ratio of the instability constants is equal to $1.5 \cdot 10^{-17}$.

The coordination numbers p and q equal each other in the range of potassium oxalate concentrations of $1 \cdot 10^{-1}$ - 1.2 M. In this case the ratio of the instability constants is equal to $1.4 \cdot 10^{-16}$. The increase in the difference in the number of coordinated groups with a decrease in the concentration of $C_2O_4^{''}$ ions may be explained only by a decrease in the coordination number for the complex Pu^{+3} compounds and the instability constant of the complex ion with the lower number of coordinated groups is approximately 10 times greater than the instability constant of the ion with the greater number of C_2O_4 groups.

Experiments carried out showed that if a precipitate of Pu^{+3} oxalate is introduced into a potassium oxalate solution, it rapidly dissolves on stirring. The polarogram of such a solution shows only a cathode wave and, consequently, the Pu^{+3} is oxidized to Pu^{+4}. If dissolved oxygen is first removed from the oxalic acid solution, and then the oxalate of trivalent plutonium is added, the polarogram of this solution shows an anode wave with a half-wave potential of −0.197 v. Apparently, Pu^{+3} forms complexes in oxalic acid solutions, but they are very rapidly oxidized by atmospheric oxygen. Our experiments also showed that even without dissolved oxygen in the oxalic acid solutions, the Pu^{+3} is slowly oxidized, though this may be explained by an effect of the α-radiation.

In order to find the instability constant of the Pu^{+3} complex, the solubility of the oxalate at various potassium oxalate concentrations was determined. Trivalent plutonium, prepared by reduction with hydrogen in the presence of platinized platinum [5], was added as a solution of the chloride to potassium oxalate solution in a sufficient amount to precipitate plutonium oxalate.

It was assumed that in the precipitation, an equilibrium was rapidly established between the precipitate and the solution. Polarograms were plotted immediately after the addition of the plutonium solution, then the pH of the solutions were determined. The Pu^{+3} concentration was found from the polarograms as the ratio of the diffusion coefficients of the oxalate complexes of Pu^{+4} and Pu^{+3}, found by measuring diffusion currents for equal Pu^{+4} and Pu^{+3} concentrations, which was equal to

$$\frac{D_{Pu^{+3}}}{D_{Pu^{+4}}} = \frac{i_{Pu^{+3}}}{i_{Pu^{+4}}} = 1.055.$$

Expressing the complex formation reaction in the form

$$[Pu_2(C_2O_4)_3 \cdot 9H_2O]_{sld} \rightleftarrows [2Pu(C_2O_4)_x^{3-2x}]_{sol} +$$
$$+ [(3 - 2x)\,C_2O_4^{''}]_{sol} + 9H_2O,$$

we find the equilibrium constant of this reaction

$$K = K_x^2 = [Pu(C_2O_4)_x^{3-2x}]^2 [C_2O_4^{''}]^{3-2x},$$
$$x = 0,\ 1,\ 2,\ 3,\ 4,\ \ldots$$

The solubility was determined by the concentration of complex ions in the solution

$$S = \sum [\mathrm{Pu}\,(C_2O_4)_x^{3-2x}] = \sum \frac{K_x}{[C_2O_4'']^{3/2-x}} .$$

In this case

$$\frac{d\ln S}{d\ln [C_2O_4'']} = \frac{d\ln S}{\frac{d\,[C_2O_4'']}{[C_2O_4'']}} = [C_2O_4]\cdot\frac{d\ln S}{d\,[C_2O_4'']} =$$

$$= [C_2O_4'']\cdot\frac{1}{\sum\frac{K_x}{[C_2O_4'']^{3/2-x}}}\cdot\sum\frac{-\left(\frac{3}{2}-x\right)\cdot K_x}{[C_2O_4'']^{3/2-x+1}} =$$

$$= \frac{1}{\sum\frac{K_x}{[C_2O_4'']^{3/2-x}}}\cdot\sum\frac{-\left(\frac{3}{2}-x\right)K_x}{[C_2O_4'']^{3/2-x}} =$$

$$= \frac{1}{\sum\frac{K_x}{[C_2O_4'']^{3/2-x}}}\cdot\left\{\sum\frac{-\frac{3}{2}\cdot K_x}{[C_2O_4'']^{3/2-x}} +\right.$$

$$\left.+\sum\frac{x\cdot K_x}{[C_2O_4'']^{3/2-x}}\right\} = -\frac{3}{2}+\frac{\sum x\,[\mathrm{Pu}\,(C_2O_4)_x^{3-2x}]}{\sum [\mathrm{Pu}\,(C_2O_4)_x^{3-2x}]},$$

since

$$\frac{K_x}{[C_2O_4]^{3/2-x}} = [\mathrm{Pu}\,(C_2O_4)_x^{3-2x}].$$

For the linear part of the solubility curve, which indicates the existence of one complex in the solution,

$$\frac{d\ln S}{d\ln [C_2O_4'']} = -\frac{3}{2}+x.$$

It follows from the experimental solubility curve (Fig. 4) that

$$\frac{d\ln S}{d\ln [C_2O_4'']} = \frac{62.5}{23.5} = 2{,}6.$$

Then x = 4.1, i. e., the coordination number found from the solubility curve for Pu^{+3} equals 4.

At potassium oxalate concentrations equal to $1\cdot 10^{-1} - 1.2$ M, the coordination numbers for Pu^{+4} and Pu^{+3} were equal, i. e., p = q = 4. At potassium oxalate concentrations less than $1\cdot 10^{-1}$ M only the number of coordinated groups for Pu^{+3} in the oxalate solution changed, which as shown above, equalled 3.

The instability constant of the Pu^{+3} complex was calculated by the formula

$$K_i^2 = \frac{L_p\,[C_2O_4'']^{2q-r}}{[\mathrm{Pu}\,(C_2O_4)_q]^2},$$

where _r_ is the number of oxalate groups in a simple Pu^{+3} oxalate; L_p is the solubility product for a simple Pu^{+3} oxalate.

TABLE 5

The Relation of the Solubility of Trivalent Plutonium Oxalate to the Concentration of Potassium Oxalate and the Value of the Instability Constant at q = 4.

Added $K_2C_2O_4$ M	Solution pH	Conc. C_2O_4'' M	Conc. Pu^{+3} M	Instability constant
0.17	2.7	0.005	$3.43\cdot10^{-6}$	—
0.37	3.2	0.034	$9.00\cdot10^{-6}$	$2.5\cdot10^{-12}$
0.50	3.9	0.168	$2.58\cdot10^{-4}$	$4.7\cdot10^{-12}$
0.60	3.8	0.176	$7.74\cdot10^{-4}$	$5.5\cdot10^{-12}$
0.78	3.9	0.263	$5.06\cdot10^{-4}$	$7.3\cdot10^{-12}$
0.87	4.2	0.435	$2.39\cdot10^{-3}$	$5.4\cdot10^{-12}$

TABLE 6

The Relation of Pu^{+3} Oxalate Solubility to a Different Potassium Oxalate Concentration (ionic strength of solution $\mu = 3$) and the Value of the Instability Constant at q = 4.

Added $K_2C_2O_4$ M	Solution pH	Conc. C_2O_4'' M	Conc. Pu^{+3} M	Instability constant
0.35	3.9	0.117	$0.32\cdot10^{-3}$	$1.5\cdot10^{\ 12}$
0.58	4.0	0.215	$1.40\cdot10^{-3}$	$1.6\cdot10^{\ 12}$
0.70	4.0	0.264	$1.80\cdot10^{-3}$	$2.1\cdot10^{-12}$
0.83	4.1	0.363	$2.70\cdot10^{-3}$	$3.1\ 10^{-12}$
0.95	4.1	0.420	$3.20\cdot10^{-3}$	$3.7\ 10^{-12}$

Reas and Konnik (see paper [1]) calculated the solubility product

$$K=\frac{[Pu^{+3}]^2\,[H_2C_2O_4]^3}{[H^+]^6}=2\cdot10^{-10}$$

and found that it remained approximately constant when the hydrogen ion concentration was changed from 0.22 to 3.7 M. Using the dissociation constants given above for oxalic acid, we find that

$$[Pu^{+3}]^2\,[C_2O_4'']=L_p=1.1\cdot10^{-26}.$$

Using this value for the solubility product, we calculated the instability constant of the ion $Pu(C_2O_4)_4^{-5}$, given in Table 5. The actual value of the constant depended on the accuracy with which the solubility product had been determined.* Similar experiments were carried out with a constant ionic strength in the solutions, which was maintained by adding potassium chloride (complex formation of Pu^{+3} with chlorine ion was disregarded in the presence of oxalate). Furthermore, the oxalate ion concentration was chosen in such a way that one form of complex ion would predominate in the solution (corresponding to the linear part in Fig. 4). However, even in this case, there was some increase in the constant, apparently caused by a higher solubility value at low oxalate ion concentrations, due to the presence of a complex with three coordinated groups.

The value of the ratio of instability constants of Pu^{+4} and Pu^{+3} oxalate complexes, equal to $1.4\cdot10^{-16}$, was given above. Knowing the instability constant for $Pu(C_2O_4)_4^{-5}$, we may determine the instability constant for the complex ion $Pu(C_2O_4)^{-4}_4$: $K_{Pu(C_2O_4)_4^{-4}}=2,4\times\times10^{-12}\cdot1,4\cdot10^{-16}=3,3\cdot10^{-28}$, if we assume that $K_{Pu(C_2O_4)_4^{-5}}=2,4\cdot10^{-12}$ (the average value of data in Table 6). The instability constant of the ion $Pu(C_2O_4)_3^{-3}$ equals $2.2\cdot10^{-11}$.

Received August 29, 1957

LITERATURE CITED

[1] G. Seaborg and J. Katz, The Actinides (Foreign Lit. Press, 1955).

[2] W. H. Reas, The Transuranium Elements (McGraw-Hill, 1949). 4, 14B, I, 423.

---

*Remark added during correction. In the article by A. D. Gel'man et al., (see page 55), L_p was taken as equal to $162\cdot10^{-25}$; therefore the constant K_i^2 was approximately 15 times greater than the one given in our work.

[3] Beilsteins, Handbuch der Organischen Chemie 2, 477 (1942).

[4] I. M. Kolthoff and D. D. Lingane, Polarography,(Foreign Lit. Press, 1945).

[5] J. Heyrovsky and D. Ilkovic, Coll. Czech. Chem. Commun. 7, 198 (1935).

[6] M. Stackelberg and H. Freyhold, Z. Elektrochem. 46, 120 (1940).

[7] J. J. Lingane, Chem. Rev. 29, 1 (1941).

[8] K. A. Kraus, The Transuranium Elements,(McGraw-Hill, 1949) 4, 14B, 1, 241.

[9] R. Brdicka, Coll. Czech. Chem. Commun. 2, 489, 545 (1930); 3, 396 (1931).

RADIOACTIVE DANGERS FROM CONTINUOUS ATOMIC BOMB TESTING

O. I. Leipunskii

The present article is a study of the hazards from the global radioactive fallout of continuous atomic bomb tests of 11 megaton TNT equivalent per year. The Sr^{90} concentration in the bones is calculated, as well as the number of incidences of leukemia (blood cancer) and the number of cases of genetic damage. Calculations show that at the end of the century the Sr^{90} concentration in vertebrae may be greater than the offician maximum allowable concentration for a large segment of the population, and that each year of continued testing increases by 44,000 the number of people in the world burdened with hereditary disease and increases the incidence of leukemia by 29,000 cases.

1. Criteria of Danger

We shall consider the action of radioactive fallout from high-energy explosions, this fallout being carried by air streams in the atmosphere and precipitating over the whole earth, so that atomic explosions affect the whole population of the earth (we shall not consider the local fallout in the region of the explosion).

The radiation dose from radioactive fallout is not large. Thus the biological problems which arise in this connection belong to the least investigated field of radiation medicine, namely the field of small chronic effects.

This problem is important because any harm that is done affects all of humanity without exception, threatening to change the hygienic conditions under which mankind evolved.

A quantitative evaluation of the possible damage is necessary for practical conclusions. This evaluation is complicated by the fact that the necessary data from the different fields of biology, biophysics, geophysics, etc., are at present incomplete, often inexact, and sometimes even contradictory. As did a previous work on the subject by the present author [3], this article attempts a quantitative approach to the problem of radioactive fallout hazards, based on the available data.

An evaluation of the hazards of atomic explosions depends strongly on whether radiative effects have or have not a threshold. If a threshold exists, the radiation below the biological threshold causes no harmful effects. If there is no threshold, then even small doses have some action.

The concept of the maximum allowable dose has been developed on the basis of peaceful work with radioactive substances. According to practice which is officially recognized in all countries, radiation of the order of the allowable norm may be generated without a health hazard. The concept of an allowable limit does in fact indicate that a threshold is assumed, and the allowable limit itself is taken to correspond to the effective threshold of the biological effects of radioactivity.

When radioactive substances are used in practice the organism is not irradiated uniformly, particularly when a radioactive isotope enters the organism, so that it has been required that the radiation be no greater than the allowable norm not only in the organism as a whole, but also in the particular organ, called the critical organ, in which the radiation is greatest. For instance, if Sr^{90} enters the organism, one may practically say that only the bones in which the strontium is assimilated are subject to radiation, and that the radiation to the rest of the organism is negligible.

Therefore the radiation dose due to strontium need be calculated only for the bones, and the bones (the skeleton) are the critical organ. The critical organ may be small compared to the whole organ (for instance, if radioactive iodine enters the system, the critical organ is the thyroid gland, whose weight is about 20 g). Nevertheless, the dose to the critical organ, rather than the mean dose to the whole organism, is the official measure of the radiation hazard.

Looked at in this way, the question of the danger of atomic explosions reduces to a determination of the radiation dose to a critical organ, followed by a comparison of this dose with the offician allowable norm. If the dose to the critical organ due to radioactive fallout from explosions is greater than the maximum allowable dose, then atomic armament tests are inadmissible from the point of view of official criteria for the health and safety of the population.

Since we are talking of world-wide effects of atomic explosions, it is clear that this dose should not be greater than the maximum allowable, not only when averaged over all of mankind, but also in separate groups of the population. In principle, not a single person should be subjected to radiation above the norm. This requirement necessitates an investigation not only of the mean global radiation, but also the statistical deviations from this mean.

One one-hundredth of one percent of the population is 250,000 persons. If, therefore, with a low mean dose there is a probability of 0.01% that a fluctuation occurs in which the dose is a certain value above the mean, this fluctuation will affect a large number of persons, namely several hundreds of thousands.

An evaluation of radiation hazards based on the allowable norm, or essentially based on the concept of a threshold to the action of radiation, is convenient in practice, although it is approximate and hardly corresponds to the physiological action of radiation. The available data show that in many cases it is doubtful that there exists a threshold.

With respect to genetic effects (mutations) it may be considered established [1], that there is no threshold and that ionizing radiation will have effects in arbitrary doses. It is quite probable that a similar statement is true with respect to leukemia. *

In the absence of a threshold, the evaluation of the hazards of atomic explosions involves just the determination of the number of illnesses caused by the radiation dose from the products of an atomic explosion. This necessitates knowing the relation between the number of illnesses and the dose. For most effects of radiation, this relationship is not known. Data exists only for mutations and leukemia. In both of these cases it is assumed that the probability of harmful effects is directly proportional to the radiation dose to the gonads (for mutations) or to the bones (for leukemia). Further, there do exist evaluations of the proportionality constant.

By comparing the number of illnesses due to an explosion with the number of the same kind of illnesses caused in other ways, one may judge how serious are the effects of atomic explosions when compared with other factors causing similar illnesses. This does not, however, refute the fact that even the smallest explosion is known to cause a certain number of hereditary and somatic diseases, and leads to serious injury to a definite number of individuals.

The calculations presented below are based both on the assumption of a threshold (taking account of the existing allowable radiation limit), and on the concept of nonthreshold effects.

---

*Leukemia is a serious illness of the blood, consisting of the unlimited multiplication of imperfect leucocytes, and is always fatal. It is supposed that this disease is caused by mutations in the cells of bone marrow [2]. Genetic victims (mutants) are persons with illnesses due to damage to elements of the reproductive cells from which the organism has developed. A characteristic property of such illnesses is their hereditary transmission from parents to descendants. There exist about 500 illnesses of this type [1], such as hemophilia, dwarfism, infantile idiocy, etc. From two to four percent of all births are burdened with genetic diseases, and ten to twenty-five percent of these come from mutations caused by the natural radioactive background.

The calculations based on the allowable radiation norm considers (see Section 3) irradiation of the skeleton by Sr^{90}, since when long-lifetime fragments enter the organism, the critical organ is the skeleton, and the active isotope is Sr^{90}. (One need consider only long-lifetime fragments, since the precipitation of the fragments from the stratosphere takes years and all short-lifetime fragments, decay before they reach the earth.) Of the two long-lifetime fragments, namely Sr^{90} and Cs^{137}, one need consider only Sr^{90} in calculating the maximum allowable dose to the critical organ. This is because this isotope is collected in the bones, and is eliminated from the organism one hundred and fifty times more slowly than is Cs^{137}, which enters the soft tissues. Its concentration in the organism is therefore correspondingly greater than that of Cs^{137}, whose action we may thus neglect. When dealing with nonthreshold effects, one must account for Cs^{137} in calculating the gonad radiation dose and the occurrence of mutations [3].

In calculating the dangers from the nonthreshold point of view, we shall deal with (see Section 4) the number of leukemia cases due to bone irradiation by Sr^{90}, C^{14}, and Cs^{137} (external radiation), and the number of mutant births due to gonad radiation by Cs^{137} and C^{14}.

We give here the quantitative criteria for danger in the case of threshold (a) and nonthreshold (b) effects:

a) The allowable radiation of a critical organ in nonindustrial personnel is considered to be 5 mr/day, or 1.8 r/year. This quantity is lower by a factor of ten than that for persons working in atomic industries (50 mr/day, or 18 r/year), and is ten times greater than the natural background (0.5 mr/day, or 0.18 r/year). Whether there is any basis for the allowable dose is not clear. The norm for persons who work under conditions of radiation would seem to be too high, as is indicated by the five year lower life expectancy for medical radiologists (according to British statistics). The simple division by ten of the norm for atomic industries, which leads to the norm for the population as a whole, is quite arbitrary.

Thus the officially accepted allowable norm of 5 mr/day or 1.8 r/year cannot be considered to have sufficient basis or to have been sufficiently analyzed and reconsidered. A natural norm is the natural background of 0.18 r/year. Increments above the natural background which are no greater than those of natural fluctuations (for instance, up to 0.3 mr/year as in some brick and concrete houses) are in all probability allowable.

b) As more accuracy is being attained in methods for recognizing the effects of radiation, data are being collected which throw doubt on the concept of threshold effects. One of the important effects of small radiation doses, namely harm to the genes and the occurrence of mutations, can take place even in a single act of ionization in the gene, and is therefore not a threshold effect. We may assume that there is likewise no threshold for occurrence of leukemia.

The probabilities for mutation and occurrence of leukemia are proportional to the dose. The proportionality constants are the following:

for leukemia [2]

$$2 \cdot 10^{-6} \frac{\text{cases}}{\text{year} \cdot \text{roentgen} \cdot \text{person}},$$

for mutations [3]

$$4 \cdot 10^{-4} \frac{\text{mutants}}{\text{r} \cdot \text{person}}^{*}.$$

In addition to clearly defined diseases (leukemia, genetic illnesses, etc.) chronic radiation in small doses may have a depressive effect on the organism, as in systematic nonobservance of hygienic rules. This may not cause any definite disease, but may affect life expectancy, productivity, resistance to infections, etc. The absence of any data which could be quantitatively dealt with restricts our calculations to only the two above-mentioned effects of radiation. Thus the quantitative results on the effects of atomic explosions will be somewhat too low.

---

*According to other data this proportionality constant is several times greater [1, 3].

2. A Calculation of the Amount of Strontium which is Precipitated on the Earth by Continuous Testing

a) The amount of strontium in the stratosphere. In high-energy bursts, fission fragments enter the stratosphere. According to Libby [4], the mean time the fragments spend in the stratosphere is ten years. The fragments gradually leave the stratosphere, entering the troposphere (in all probability by turbulent diffusion), from which they come to earth in the precipitation. The amount of strontium in the stratosphere is determined by the rate at which it enters it, the rate of its radioactive decay, and the precipitation rate, so that we may write

$$\begin{aligned}\frac{dQ}{dt} &= n - \frac{Q}{T_\text{p}} - \frac{Q}{T_\text{d}} = \\ &= n - Q\left(\frac{1}{T_\text{p}} + \frac{1}{T_\text{d}}\right) = n - \frac{Q}{T_\text{ep}},\end{aligned} \tag{1}$$

where Q is the amount of strontium in the stratosphere,* n is the amount of strontium entering the stratosphere daily, T_p is the time constant for the precipitation of strontium from the stratosphere (T_p = 10 years); T_d is the half-life of strontium (T_d = 40 years);

$$T_{ep} = \frac{T_p \cdot T_d}{T_p + T_d} = \frac{400}{50} = 8 \text{ years};$$

$$Q = nT_\text{ep}\left(1 - e^{-t/T_\text{ep}}\right). \tag{2}$$

The equilibrium value of Q is

$$Q_0 = nT_{ep} \tag{3}$$

(in eight years Q is 0.67 of its equilibrium value, and in sixteen years it is 0.87 of this value).

b) The amount of strontium on the earth N is given by the equation

$$\frac{dN}{dt} = \frac{Q}{T_\text{p}} - \frac{N}{T_\text{d}} = \frac{nT_\text{ep}\left(1 - e^{-t/T_\text{ep}}\right)}{T_\text{p}} - \frac{N}{T_\text{d}}, \tag{4}$$

$$\begin{aligned}N = \frac{nT_\text{ep}T_\text{d}}{T_\text{p}}\Bigg(1 &- \frac{T_\text{d}}{T_\text{d} - T_\text{ep}}\, e^{-t/T_\text{d}} + \\ &+ \frac{T_\text{ep}}{T_\text{d} - T_\text{ep}}\, e^{-t/T_\text{ep}}\Bigg)\end{aligned} \tag{4a}$$

from which we find that

$$\left.\begin{array}{ll} t \to \infty & N = N_\infty = \dfrac{nT_\text{ep}T_\text{d}}{T_\text{p}} = \dfrac{n \cdot 8 \cdot 40}{10} = 32\,n; \\ t = 20 \text{ yrs} & N = N_\infty \cdot 0.24 = 7{,}7n; \\ t = 48 \text{ yrs} & N = N_\infty \cdot 0.62 = 20n. \end{array}\right\} \tag{5}$$

---

*Here, as in the author's previous article [3], the amount of radioisotope is expressed in units of megatons (Mt), by which we mean the amount of isotope contained in the fission product of a burst whose energy is 1 Mt TNT equivalent.

Let us evaluate n on the assumption that the powerful bursts that have taken place since 1952 have occurred uniformly in time. From the data presented by Kulp and co-workers [4], at the end of 1955 (that is, after four years) there was about 3.2 μC/km^2, which corresponds to precipitation from 10 Mt.

Setting N = 10 Mt and t = 4 years into Equation (4), we obtain

$$n = \frac{N}{0.88} = \frac{10}{0.88} = 11 \text{ Mt/yr.}$$

The amount of precipitates on the earth corresponding to continuous uniform testing at the rate of 11 Mt/yr is given in Table 1.

TABLE 1

	t, years	n, Mt
At the beginning of 1952	0	0
At the end of 1955	4	10
At the end of 1972	~ 20	84
At the end of 2000	~ 48	218
Equilibrium value	∞	352

3. An Evaluation of the Dangers from the Point of View of Official Norms

Official norms require that the dose to the critical organ be not greater than 1.8 r/year. In the present case the critical organ is the skeleton (or more exactly, certain definite bones of the skeleton; see below).

Thus an evaluation of the danger reduces to determining the dose rate from Sr^{90} to the bones and comparing it with the allowable norm.

There are two ways to calculate the strontium dose to the bones. The first is based on the idea that the strontium-calcium ratio in the bones is given by this ratio in the soil with discrimination factors taken into account. These discrimination factors come into play as the strontium and calcium move on their biological path from the soil to plants, from plants to food, from food to blood, and from blood to the bones.

Since strontium is not entirely equivalent to calcium in its chemical properties, the strontium-calcium ratio decreases in each of the above-mentioned transitions.

Thus

$$\left(\frac{\text{Sr}}{\text{Ca}}\right)_{\text{bone}} = \left(\frac{\text{Sr}}{\text{Ca}}\right)_{\text{soil}} \cdot k_1 k_2 k_3 k_4,$$

where k_1 is the discrimination factor in the transition from soil to plants ($k_1 = 0.7$); k_2 is the discrimination factor in the transition from plants to food (milk) ($k_2 = 0.125$); k_3 is the discrimination factor in the transition from food to blood ($k_3 = 0.4$); k_4 is the discrimination factor in the transition from blood to bone ($k_4 = 0.33$) [4].

The direct use of discrimination factors is complicated because they are not well known and because of their great variation (in particular in the case of k_1 and k_2), as well as because of the variation in the concentration of calcium and precipitated Sr^{90} in the soil, the difficulty in accounting for the use of food from different locations with different calcium concentrations in the soil, the nonuniform distribution of strontium through the various parts of the skeleton, individual variations, etc. We shall therefore perform the calculation in a different way, using more direct measurements of the strontium concentration in bones, as presented by Kulp and co-workers [4], to determine the strontium in the bones (see Equation (8)). These data refer to the end of 1955, when the precipitation on the whole earth corresponded to 10 Mt (see Table 1).

Kulp and co-workers [4] give values for the Sr^{90} concentration at various locations and for various age groups, and present world-wide averages.

In choosing Kulp's value for a (the Sr^{90} concentration in $\mu\mu C/g$ Ca)* one should bear in mind the following facts:

a) The world-wide average cannot be used without taking into the account the distribution.

The distribution in values of a reflects the superposition of all the factors listed above in their natural combination (the distribution in the k coefficients, in homogeneity and precipitation, the distribution in the Sr^{90} and calcium concentration in the soil, various diets, individual susceptibilities, the spread in the concentration in the various bones of the skeleton, etc.).

It was mentioned above that values of a which occur 0.01 percent of the time will give the Sr^{90} concentration in hundreds of thousands of people. Therefore one must use not the mean values of a, but the largest values which occur in a small but definite fraction of the population in the statistical distribution of a values. The statistical sample in Kulp's work is not great, referring only to several hundred samples (taken over all age groups and many locations on the earth), and therefore values of a which occur with a probability of 0.1 or 0.01 percent cannot be calculated. At a given place, the spread in the a values is not great (about 50 percent).

In North America, there occurs a measurable number of cases (1.8 percent) in which the a values are ten times greater than the mean (Fig. 3 of [4]). Values of a five or more times as great as the mean occur 5.4 percent of the time, and those three or more times as great as the mean occur 11.4 percent of the time.

The distribution of a values (on the above-mentioned Fig. 3) is not gaussian, being asymmetric with a large number of large deviations. Such a wide distribution is not obtained if samples are taken only from a restricted area. This would seem to be a reflection of the world-wide statistical distribution in the strontium precipitation, the calcium content of the soil, variations in diet, and perhaps several other factors (such as individual susceptibility, etc.).

One cannot say whether or not this statistical distribution can be used for the population of young children, all of the calcium in whose organism contains some Sr^{90}. In any case, it is a fact that a significant part of the population (about 1.8 percent according to Kulp's Fig. 3) has a Sr^{90} concentration of 1.1 s. u. (with a mean value of 0.11 s. u.).

In children the highest concentration is found in the ribs (for instance in Houston, Texas), the figures for children up to four years being 2 to 2.5 s. u. (whereas the mean in Houston is 1.07 s. u.), and those for children between four and nine being 1.6 to 1.2 s. u. (with a mean of 1.08 s. u.).

b) Kulp and co-workers [4] note the nonuniformity in the strontium distribution in different bones of the skeleton (see Table 1 of [4]). In particular, they find that the Sr^{90} concentration in ribs is twice as great as the mean over the whole skeleton, and that the concentration in the spine is four times as great. In Table 2 (column 1) we give the mean values over the whole skeleton as obtained from Table 2 of [4] (0.11 s. u. for all ages, 0.3 s. u. for ages 0-4, 0.4 s. u. for ages 0-4 in the United States). Therefore in the ribs and vertebrae the quantities will be two and four times as great.

Columns 2 and 3 give the a values for ribs and vertebrae. They are obtained by multiplying the values in Column 1 by two and by four, in agreement with Kulp's Table 1. The calculated values are given in parentheses.

If we are to proceed on the basis of a critical organ, which is officially accepted as valid, we must consider not the skeleton as a whole to be the critical organ, but the vertebrae. We shall then use the figures we have obtained for the vertebrae by means of the coefficients of Kulp's Table 1. These figures are those in the last column of Table 2. As can be seen, the a value for the end of 1955 may be chosen as 4.4 s. u., which occurs in 1.8 percent of the cases investigated in North America.

---

* A Sr^{90} concentration of 1 $\mu\mu C/g$ Ca is called a "sunshine" or "strontium unit," which we shall henceforth abbreviate s. u.

TABLE 2

Values of a (Sr^{90} concentration in s. u.) the Fourth Year After the Start of Powerful Explosions (end of 1955)

	Average over skeleton	Ribs	Vertebrae
World-wide mean for all ages	0.11	(0.22)	(0.44)
For 1.8 percent of the cases in North America	1.1	(2.2)	(4.4)
World-wide mean for children up to 4 years of age	0.3	(0.6)	(1.2)
U. S. A. mean for children up to 4 years of age	0.4	(0.8)	(1.6)
Highest value in Houston	(1)	2.0	(4.0)

The question of the reliability of the data presented by Kulp in his Table 1 has yet to be answered. It is possible that the nonuniformity he notes in the strontium distribution may be of a kinetic origin, and that it may become more homogeneous as time goes on. The authors note that in the interval from 3 hours to 125 days the distribution pattern does not alter. Since the homogenization of the strontium concentration takes place not by means of diffusion in the bones, but through the blood, it would seem that it should take a time of the order of the biological elimination time of Sr^{90}. If this is true, the process of homogenization is equivalent to elimination of strontium, and will be accounted for as eliminated from the part of the skeleton being considered in Equation (6), which gives the amount of strontium in the bone.

We shall use the following notation.

Amount of Sr^{90} on the earth	N, Mt
Concentration of Sr^{90} in the soil (s is the concentration of strontium in the soil in the precipitation of 1 Mt)	sN
Concentration of Sr^{90} in food	$b = sNk_1k_2$ (s. u.)
The amount of calcium in the food entering the organism yearly	$c \frac{\text{Ca}}{\text{year}}$
The food-bone discrimination factor	k_3k_4
The strontium concentration in the bones	a(t), s. u.
The amount of calcium in the skeleton	M(t), g
The strontium content in the skeleton of an adult	$M_\infty = 1000$ g
The yearly intake of Sr^{90} by the bone	$m = bck_3k_4$ (s. u.)
The amount of strontium in the bone	$q(t) = a(t)\,M(t)$, $\mu\mu C$
The effective time constant for strontium elimination from the bone	$T_{eb} = \frac{T_d \cdot T_b}{T_d + T_b} = 11.3$ years (T_b is the time constant for the elimination of Sr^{90} from the organism, equal to 15.3 years [5])

In order to calculate the amount of Sr^{90} in the bone, let us consider the equation

$$\begin{gathered}\frac{dq}{dt} = m - \frac{q}{T_{\text{eb}}}, \\ m = sNk_1k_2ck_3k_4 = \nu N(t) = \\ = \nu N_\infty\left(1 - \frac{40}{32}e^{-t/40} + \frac{8}{32}e^{-t/8}\right),\end{gathered} \tag{6}$$

where $\nu = sk_1k_2k_3k_4c$ ($\mu\mu C$/yr-Mt).

Integrating (6) with the initial condition q = 0 (at t = 0), we obtain

$$q = \nu N_\infty T_{\text{eb}} \cdot F(t) = q_\infty F(t), \tag{7}$$

where $q_\infty = \nu N_\infty T_{\text{eb}}$ is the limiting value of the equilibrium concentration of the radioisotope in the organism, and

$$\begin{gathered}F(t) = 1 - \frac{T_1^2 e^{-t/T_{\text{d}}}}{(T_{\text{p}} - T_{\text{ep}})(T_{\text{d}} - T_{\text{eb}})} + \\ + \frac{T_{\text{ep}}^2 e^{-t/T_{\text{ep}}}}{(T_{\text{d}} - T_{\text{ep}})(T_{\text{ep}} - T_{\text{eb}})} - \\ - e^{-t/T_{\text{eb}}}\left[1 - \frac{T_{\text{d}}^2}{(T_{\text{d}} - T_{\text{ep}})(T_{\text{d}} - T_{\text{eb}})} + \right. \\ \left. + \frac{T_{\text{ep}}^2}{(T_{\text{d}} - T_{\text{ep}})(T_{\text{ep}} - T_{\text{eb}})} T_{\text{eb}}\right].\end{gathered} \tag{7'}$$

The radioisotope concentration in the critical organ is

$$a(t) = \frac{q(t)}{M} = \frac{\nu N_\infty T_{\text{eb}} F(t)}{M} \quad \mu\mu\,C/g. \tag{8}$$

The dose rate P in the critical organ can be calculated from the formula

$$P(t) = \frac{a(t) \cdot 1.8}{a_{\text{D}}} \ \text{r/yr} \tag{9}$$

where a_D is the concentration which gives a dose of 1.8 r/yr.

The dose in the critical organ is

$$D = \int_0^t P(t)\,dt = \frac{1.8\text{r}}{Ma_{\text{D}}} \int_0^t q(t)\,dt, \tag{10}$$

where

$$\begin{gathered}\int_0^t q(t)\,dt = \nu N_\infty T_{\text{eb}}\left[t - \frac{T_{\text{d}}^3\left(1 - e^{-t/T_{\text{d}}}\right)}{(T_{\text{d}} - T_{\text{ep}})(T_{\text{d}} - T_{\text{eb}})} + \right. \\ \left. + \frac{T_{\text{ep}}^3\left(1 - e^{t/T_{\text{ep}}}\right)}{(T_{\text{d}} - T_{\text{ep}})(T_{\text{d}} - T_{\text{eb}})} - T_{\text{eb}}\left(1 - e^{-t/T_{\text{eb}}}\right)\right] \times \\ \times \left[1 - \frac{T_{\text{d}}^2}{(T_{\text{d}} - T_{\text{ep}})(T_{\text{d}} - T_{\text{eb}})} + \right. \\ \left. + \frac{T_{\text{d}}^2}{(T_{\text{d}} - T_{\text{ep}})(T_{\text{ep}} - T_{\text{ed}})}\right].\end{gathered} \tag{11}$$

Let us find the concentration a(t) by using the above formulas.

In order to avoid uncertainties related to the large distribution in the numerical values of the coefficients $\underline{s}$, k_1, k_2, k_3 and k_4 which enter into ν (Equations (6) and (8)) let us use experimental data [4] on the strontium concentration in bones after the fourth year ($t = t_0$) to determine the product $\nu N_{\infty} T_{eb}$ (8); we have

$$a(t_0) = \frac{q(t_0)}{M(t_0)} = \frac{\nu N_{\infty} T_{eb} F(t_0)}{M(t_0)}, \tag{12}$$

where $a(t_0)$ is a known quantity (see Table 2). From this we arrive at

$$\nu N_{\infty} T_{eb} = \frac{a(t_0) M(t_0)}{F(t_0)}. \tag{13}$$

The Sr^{90} concentration at time $\underline{t}$ is

$$a(t) = \frac{q(t)}{M(t)} = a(t_0) \frac{M(t_0)}{M(t)} \cdot \frac{F(t)}{F(t_0)}. \tag{14}$$

The equilibrium concentration (as $t \rightarrow \infty$) is

$$a_{(\infty)} = \frac{q(\infty)}{c(\infty)} = \frac{a(t_0)}{F(t_0)} \cdot \frac{M(t_0)}{M(t)}; \quad [F(\infty) = 1]. \tag{15}$$

Inserting numerical values into (7') we obtain

$$F(t_0) = F(4 \text{ yrs}) = 0.0023. \tag{16*}$$

Therefore, according to (14)

$$\begin{aligned} a(t) &= a(4 \text{ yrs}) \frac{M(4 \text{ yrs})}{M(t)} \cdot \frac{F(t)}{F(4 \text{ yrs})} = \\ &= a(4 \text{ yrs}) \frac{1}{4} \frac{F(t)}{F(4 \text{ yrs})} = 109 a(4 \text{ yrs}) F(t), \end{aligned} \tag{17}$$

$$\begin{aligned} a(\infty) &= a(4 \text{ yrs}) \frac{M(4 \text{ yrs})}{M(\infty)} \cdot \frac{1}{F(4 \text{ yrs})} = \\ &= \frac{435}{4} \cdot a(4 \text{ yrs}) = 109 a(4 \text{ yrs}). \end{aligned} \tag{17'}$$

In Equation (17) we have set $\frac{1}{F(4 \text{ years})} = 435$ and $\frac{M(4 \text{ years})}{M(\infty)} = \frac{1}{4}$ (this latter being the ratio of the weight of a four year old child to that of an adult).

Table 3 gives the strontium concentrations in the vertebrae for various times (for the generation born in 1952) and the equilibrium concentration for a burst rate of 11 Mt/yr, as calculated by (17) and (17').

---

* This method for determining the constants in (8), although it is simple, has the disadvantage that they are found from their values at the time t_0 which is small compared with the time to which Equation (8) is applied; as more data is accumulated, this disadvantage can be overcome.

Table 3 gives the results for two cases. The first of these is Case A (columns 6 and 7), in which it is assumed that the original Sr^{90} concentration in the bones at the end of 1955 (the value of a(4 years) in Equation (17)) is the world-wide average, namely 1.2 s. u. (Table 2, line 3). In Case B (columns 8 and 9) the initial Sr^{90} concentration is greater, that is, equal to 4.4 s. u. (Table 2, line 2).

The dose rate (columns 7 and 9) is calculated assuming that it is allowable when $a = 100$ s. u. (1.8 r/yr).*

It is seen from Table 3 that continued testing of long duration at a rate of 11 Mt/yr is not permissible from the point of view of the existing official hygienic norm, since it will subject a large part of the population to a dose close to the allowable limit in the critical organ (vertebrae) in 1972 (Case B) or in the year 2000 (Case A).

4. A Calculation of the Dangers Without Assuming a Threshold (Number of Genetic Victims and Leukemia Cases)

As was shown in Section 1, the accepted practice of using maximum allowable limits is essentially a reflection of the concept of a threshold in the biological action of radiation, and this cannot be admitted as correct.

In many cases the nonthreshold point of view corresponds more nearly to reality. We shall evaluate the dangers from this point of view only for genetic defects and leukemia, since only such hazards can at present be quantitatively evaluated.

TABLE 3

Sr^{90} Concentration in Vertebrae

1	2	3	4	5	Sr^{90} concentration and dose rate to vertebrae			
Year	t, the time from start of 1952 (years)	$F(t)$	$\frac{F(t)}{F(4\ yrs)}$	$\frac{a(t)}{a(4\ yrs)}$	Case A		Case B	
					6	7	8	9
					$a(t)$ c. e.	dose rate, in % of allowable	$a(t)$	dose rate, in % allowable
1952	0	0	0	0	0	0	0	0
1956	4	0.0023	1	1	1.2	1.2	4.4	4.4
1972	20	0.123	53	13.4	16	16	59	59
2000	48	0.494	215	53.7	64	64	240	240
21 st century	∞	1	435	109	120	120	475	475

The author has already [3] calculated the number of genetic defects and the number of leukemia cases due to the radioactive products of a single 10 Mt burst.

It was found that in a population of 2.5 billion persons, such a burst will lead to no less than 40,000 mutations and 26,000 leukemia cases, or 4,000 mutations and 2,600 leukemia cases per megaton. It is clear that the total number of mutations due to continuous testing is obtained by summing the number of mutations from the separate bursts.

Thus each year of continuous testing will increase the total number of genetic mutants by 44,000 persons, and the number of leukemia cases by 29,000 persons.

It should be noted that the total number of illnesses per burst calculated in the previous article [3] takes place over the long decay time of the radioactive isotopes.

The appearance of some genetic cases may occur only after a long time also because some of the mutations are recessive, and a hereditary symptom resulting from a recessive mutation may occur only after many generations. Dominant mutations and leukemia cases will occur even in the first generation.

---

* The natural background is 0.18 r/yr, which corresponds to an Sr^{90} content of 10 s. u.

SUMMARY

1. Continued testing of nuclear armaments at a rate of about 11 Mt/yr will cause the dose to the critical organ (vertebra) at the end of the 20th century to be close to the official maximum allowable dose or higher. Large segments of the population will be subjected to this dose.

2. Each year of continued testing will cause the eventual occurrence of 44,000 genetic defects and 29,000 cases of leukemia.

Received November 21, 1957

LITERATURE CITED

[1] N. P. Dubinin, Radiation Genetics and Heredity [in Russian] (in press).

[2] E. B. Lewis, Science 125, 965 (1957).

[3] O. I. Leipunskii, "Radioactive Dangers of pure hydrogen and ordinary atomic bomb explosions," J. Atomic Energy (USSR) 3, 12, 530 (1957).*

[4] J. L. Kulp, W. R. Eckelmann, and A. K. Schulert, Science 125, 219 (1957).

[5] J. Radiol. et Electrol. 36, 10, bis (1955).

---

*Original Russian pagination. See C. B. Translation.

LETTERS TO THE EDITOR

AXIAL STABILITY AND LOCALIZATION OF BUNCHES IN A QUASI-NEUTRAL PLASMA, ACCELERATED BY ELECTROMAGNETIC FIELDS

G. A. Askar'ian

In connection with a recent proposal by Veksler [1], [2] concerning a method of coherent acceleration of plasma bunches it is of interest to consider the axial stability of bunches in a quasi-neutral plasma in a waveguide through which a radiation flux is propagating. This problem has been treated in detail in Ref. [3]; however, the model assumed there — a perfectly shielding bunch — does not allow examination of the behavior of the bunch at frequencies close to the plasma-resonance frequency and other regions of frequency and plasma parameters. For this reason the present author has carried out a more comprehensive analysis of the problem. By considering the bunch in terms of an oscillating model it is possible to describe more completely its behavior in electric fields; moreover, the force expressions which are employed make it possible to consider the specific characteristics of a plasma such as the anisotropy which arises in an external magnetic field, etc.

For simplicity it will be assumed that the radius of the bunch a, its displacement from the axis r, and the radius of the waveguide R meet the requirement $a \ll r \ll R$ and that the bunch moves at relatively slow velocities, i. e., we shall be interested in the stability of the bunch at the beginning of acceleration and under conditions of small deviations although these may exceed the dimensions of the bunch.

According to the oscillator model the displacement of the electron cloud with respect to the ion "matrix" in a quasi-homogeneous field E_{ext} is described by the equation

$$\ddot{x} + \omega_0^2 x - \gamma \dddot{x} = \frac{e}{m} E_{\text{ext}}$$

where e and m are the charge and mass of electron, ω_0 is the resonance frequency, which depends on the electron concentration in the plasma n_e and the shape of the bunch ($\omega_0^2 = \frac{4\pi}{3} \cdot \frac{e^2}{m} n_e$ for a quasi-spherical bunch), γ is a coefficient which characterizes the energy dissipation of the electron cloud (for example, neglecting the effect of the walls of the waveguide on the radiation of the bunch, as is valid for large waveguides and small internal plasma losses, $\gamma = \frac{2}{3}\frac{e}{m}\frac{Q}{c^3}$, where c is the velocity of light and Q is the effective oscillating charge of the electron cloud).

Consequently the projection of the electric dipole moment of the bunch in a given direction is related to the component of the electric field in the given direction by the relation

$$P_l = \alpha_l E_{0l} \sin(\omega t + \varphi_{P,l}),$$

where α_l is the dynamic polarizability factor, E_{0l} is the field amplitude in the region of the bunch and $\varphi_{P,l}$ is the phase shift between the projections of the field vector and the polarization vector. For example, in a wide waveguide

$$\alpha_l = \frac{eQ}{m}\left\{(\omega_0^2 - \omega^2)^2 + \left(\frac{2}{3}\frac{e}{m} Q \frac{\omega^3}{c^3}\right)^2\right\}^{-1/2}$$

and

$$\cos\varphi_{P,l}=\frac{\alpha_l m}{eQ}(\omega_0^2-\omega^2).$$

The relation between the projected magnetic moment of the bunch and an external sinusoidal magnetic field is given correspondingly in the form $M_l = \beta_l H_{0l} \sin(\omega t + \varphi_{M,l})$, where β_l and $\varphi_{M,l}$, just as α_l and $\varphi_{P,l}$ are functions of the parameters of the plasma, waves, and external field (cf. for example, Ref. [4]). In particular, if the plasma bunch completely screens the magnetic field of the wave, we will assume $\varphi_{M,l} = 0$ and $\beta_l = -\frac{\alpha_0}{2}$, where $\alpha_0 = a^3$ is the quasi-static polarization factor for an absolutely conducting sphere of radius a.

We calculate the forces acting on the bunch as a whole, tending to displace it from the axis of the wave guide. Taking the time average of the force acting on the alternating electric and magnetic dipoles, in an alternating electromagnetic field we have

$$(\overline{F}_P)_{\text{av}}=\nabla(\overline{P}\overline{E})_{\text{av}} \quad (\overline{F}_M)_{\text{av}}=\nabla(\overline{M}\overline{H})_{\text{av}}.$$

The fields of axially symmetric running E_0-waves and H_0-waves (cf. for example, Ref. [5]) close to the axis has the following form in "common" notation (the left-hand components in the curly brackets pertain to the electric wave):

$$\{E_z;\ H_z\}=\{E_a;\ H_a\}\cdot\left(1-\frac{\varkappa^2r^2}{4}\right)\sin(\omega t-hz),$$

$$\{E_r;\ H_r\}=\{E_a;\ -H_a\}\frac{hr}{2}\cos(\omega t-hz),$$

$$\{H_\varphi;\ E_\varphi\}=\{E_a;\ -H_a\}\frac{kr}{2}\cos(\omega t-hz),$$

where κ and h are the transverse and longitudinal wave numbers, $k^2 = h^2 + \kappa^2$, $\kappa = \frac{\mu}{R}$ (μ is the root of the corresponding Bessel function).

The radial components of the forces acting on a bunch displaced from the axis due to the E_0-field are:

$$(F_P)_{\text{av}}=\left(P_z\frac{\partial E_z}{\partial r}+P_r\frac{\partial E_r}{\partial r}\right)_{\text{av}}=\frac{\alpha}{8}E_a^2r(-2\varkappa^2+h^2)\cos\varphi_P$$

and

$$(F_{\text{M}})_{\text{av}}=\left(M_\varphi\frac{\partial H_\varphi}{\partial r}\right)_{\text{av}}=\frac{\beta}{8}E_a^2k^2r\cos\varphi_{\text{M}},$$

Hence the following expression may be taken as the stability criterion for the bunch:

$$\alpha(k^2-3\varkappa^2)\cos\varphi_P+\beta k^2\cos\varphi_{\text{M}}<0.$$

For example, for a bunch in a dense plasma $\left(\alpha\approx\alpha_0;\ \beta\approx-\frac{\alpha_0}{2};\ \cos\varphi_P=\cos\varphi_M=1\right)$ stability obtains when $k^2 < 6\kappa^2$. In wide waveguides ($\kappa \to 0$, quasi-uniform alternating electric field) the stability criterion for a bunch in a plasma which does not shield the magnetic field of the wave ($\beta \approx 0$), obtains when $\omega > \omega_0$.

If a strong longitudinal magnetic field is applied we can neglect the transverse polarizability and conductivity of the bunch; consequently, the main radial forces, which act on the alternating longitudinal dipole moment will be the Lorentz force due to the magnetic field and the force due to the inhomogeneous (in the z-direction) radial electric field. Thus $(F_P)_{av} = -\frac{\alpha}{4} E_a^2 \varkappa^2 r \cos\varphi_P$, i.e., a rotational force acts on the displaced bunch if $\cos\varphi_P > 0$ (frequencies below resonance).

The change in stability associated with the position of the bunch as a whole when a constant magnetic field is applied is not only of practical but also of phenomenological interest since there is some uncertainty as to the inhibiting effect on the transverse excursions of the bunch due to the application of a longitudinal field, etc.

Going over to the H_0-wave we may note that extremely high field amplitudes can be achieved in this case since the electric field does not cause emission from the walls of the waveguide.

In the absence of an external magnetic field the radial components of the averaged forces acting on the bunch due to the H_0 field are:

$$(F_P)_{av} = \left(P_\varphi \frac{\partial E_\varphi}{\partial r}\right)_{av} = \frac{\alpha}{8} H_a^2 k^2 r \cos\varphi_P,$$

$$(F_M)_{av} = \left(M_r \frac{\partial H_r}{\partial r} + M_z \frac{\partial H_z}{\partial r}\right)_{cp} =$$

$$= \frac{\beta}{8} H_a^2 r\ (h^2 - 2\varkappa^2) \cos\varphi_M.$$

The condition for axial stability is $\alpha k^2 \cos\varphi_P + \beta(h^2 - 2\kappa^2)\cos\varphi_M < 0$ for a wide waveguide ($\kappa \to 0$) and coincides with the condition for stability in the E_0-wave. If a strong longitudinal magnetic field is applied the radial forces virtually disappear (in the approximation being considered here) as far as the displaced bunch is concerned because of effects associated with transverse conductivity and the transverse polarizability of the plasma.

The results presented above indicate that there are good possibilities for controlling the axial stability over wide limits.

In addition to the axial stability of accelerated bunches being studied, it is of interest to estimate the magnitude of the pondermotive forces which act on the surface of the bunch in the electromagnetic field and which determine the initial deformation of the bunch.

We consider first the electric deformation of the surface of the bunch, taking account of the oscillatory properties of the plasma. When the electron cloud of the bunch is displaced with respect to the ion matrix by an amount $\underline{x}$, an uncompensated charge with a surface density given by the following expression appears at the surface:

$$\sigma = n_e e x \cos\Theta_E \quad \text{for} \quad x \ll a),$$

where Θ_E is the angle between the normal to the surface of the bunch and the direction of the external electric field. The effective electric field which acts on these polarized charges is equal to half the sum of the vectors of the fields at both sides of the bunch boundaries. Using the expressions for the potential exterior field

$$\Phi_1 = \left(-E_{ext}\ r + \frac{Qx}{r^2}\right)\cos\Theta_E \qquad (r \gg a)$$

and the potential interior field

$$\Phi_2 = \left(-E_{ext} + \frac{Qx}{a^3}\right) r \cos\Theta_E \qquad (r \ll a),$$

we obtain the following expressions for the radial and "meridian" components of the field:

$$E_r = \frac{1}{2}(E_{1r}+E_{2r})\big|_{r\to a} = \left(E_{\text{ext}} + \frac{1}{2}\frac{Qx}{a^3}\right)\cos\Theta_E$$

$$E_\Theta = \left(-E_{\text{ext}} + \frac{Qx}{a^3}\right)\sin\Theta_E.$$

Thus the time average of the surface density of the forces which act on the polarization charges when $E_{\text{ext}} = E_0 \sin \omega t$ and $x(t) = (\alpha/Q) E_0 \sin(\omega t + \varphi_p)$ are as follows:

$$(f_r)_{\text{av}} = \frac{3\alpha}{8\pi a^3} E_0^2 \left\{\cos\varphi_P + \frac{1}{2}\frac{\alpha}{a^3}\right\}\cos^2\Theta_B,$$

$$(f_\Theta)_{\text{av}} = \frac{3\alpha}{8\pi a^3} E_0^2 \left\{-\cos\varphi_P + \frac{\alpha}{a^3}\right\}\sin\Theta_E\cos\Theta_B,$$

that is to say, the nature and magnitude of the force which acts on the surface of the bunch in the electric field can vary over wide limits depending on the phase shift between the polarization of the bunch and the electric field associated with the wave. In particular, the radial component of the surface force can change sign in certain frequency regions. For example, in broad waveguides, using the expressions developed earlier for $\cos\varphi_p$ and α, we have

$$(f_r)_{\text{av}} = \frac{3}{8\pi}\omega_0^2 E_0^2 \frac{\frac{3}{2}\omega_0^2 - \omega^2}{(\omega_0^2-\omega^2) + \left(\frac{2}{3}\frac{e}{m}Q\frac{\omega^3}{c^3}\right)^2}\cos^2\Theta_E,$$

$$(f_\Theta)_{\text{av}} = \frac{3}{8\pi}\omega_0^2 E_0^2 \frac{\omega^2}{(\omega_0^2-\omega^2)^2 + \left(\frac{2}{3}\frac{e}{m}Q\frac{\omega^3}{c^3}\right)^2}\sin\Theta_E\cos\Theta_E.$$

In this case the radial component of the forces is directed inwards when $\omega > \sqrt{\frac{3}{2}}\omega_0$.

In addition to the forces which have been examined we must consider the forces due to the interaction between the surface currents and the magnetic field. In the case in which the total electromagnetic field does not penetrate to the inside of the bunch, the total interaction force at the surface of the bunch is

$$(f_r)_{\text{av}} = \frac{9}{16\pi}\left\{E_0^2\cos^2\Theta_E - \frac{1}{4}H_0^2\sin^2\Theta_E\right\},$$

where E_0 and H_0 are the amplitudes of the fields in the region in which the bunch is located while Θ_E and Θ_H are angles between the direction of the normal to the surface of a spherical bunch and the direction of the vector fields. If the electromagnetic field is such that in the region in which the bunch is located $E_0 << H_0$ (for example,, the bunch is located at the axis or close to the axis of a magnetic axially-symmetric wave), the magnetic compression predominates. In a plane wave the total pressure at the surface is

$$p = \frac{9}{16\pi}E_0^2\left\{\frac{1}{4}\sin^2\Theta_H - \cos^2\Theta_E\right\}.$$

In particular, in the direction of wave propagation and in the opposite direction $\left(\Theta_E = \Theta_H = \pm\frac{\pi}{2}\right)$ the bunch experiences a compression force (the pondermotive forces acting on a bunch in a plasma in the field associated with a plane wave have also been considered in Reference [6]).

We now consider a possible approach to the problem of maintaining small dimensions of moving bunches by means of external fields, which is directly related to the newly-proposed method of obtaining plasma bunches (cf. for example, Ref. [7]) and accelerating them; we analyze the localization of an accelerated plasma bunch which travels through a magnetic undulator along the axis of which a spatially distributed magnetic field changes in both magnitude and direction.

For simplicity it will be assumed that the plasma bunch moves at nonrelativistic velocities and is small (i. e., the external field is quasi-homogeneous within the dimensions of the bunch); we also assume that the external inhomogeneous field does not penetrate to the inside of the bunch (the shielding conditions are satisfied, thus certain well-known requirements are satisfied as to the plasma parameters and the magnetic field).

In an axially-symmetric undulator, using the longitudinal projection of the inhomogeneous magnetic field $H_z(z)$ it is easy to estimate the magnitude of the forces which act on a quasi-spherical bunch when it is displaced from the axis by a distance which exceeds the dimensions of the bunch. As a matter of fact, using the transverse field components in the "bunch" coordinate system the main force which acts is found to be $H_r = -\frac{r}{2} \cdot \frac{\partial}{\partial z} H_z$ so that at nonrelativistic velocities $E_\Theta = \frac{v}{c} H_r << H_r$. Hence, taking the time average of the radial forces which act on the bunch:

$$(F)_{av} = \nabla_r (\overline{M}\overline{H})_{av} = -\frac{a^3}{8} \left(\frac{\partial H_z}{\partial z} \right)^2_{av} \cdot r.$$

For example, with $H_z(z) \approx H_a \sin 2\pi \frac{z}{l}$

$$(F)_{av} = -\frac{a^3}{16} H_a^2 \left(\frac{2\pi}{l} \right)^2 \cdot r,$$

i. e., a nonrelativistic bunch in a shielding plasma is stable with respect to displacements from the axis of an axially-symmetric undulator. In this case the surface of a bunch which moves close to the axis of such an undulator experiences a nonuniform compression due to the magnetic pressure; the pressure depends on the angle between the field direction and the normal to the surface of the quasi-spherical bunch.

In many cases this nonuniform pressure is undesirable since it leads to deformation of the bunch (compression in the transverse direction and expansion in the axial direction). Hence it is of interest to find methods of realizing uniformly distributed surface pressures. For instance,one can build an "isotropic" undulator; in such an undulator the magnetic field seen by a bunch which moves along the axis is a "rotating" field, i. e., its direction in a fixed coordinate system alternates, thereby producing, on the average, a quasi-isotropic magnetic pressure at the surface of the shielding bunch.

By placing a system of appropriate coils along the trajectory of the bunch it is possible to excite radial volume oscillations and to obtain still higher short-term compression of the bunch. It is apparent that a process of this kind will be most effective in the case in which the modulation frequency of the average pressure at the surface of the bunch is close to the quasi-acoustical resonance frequency of the radial oscillations of the bunch; this frequency is of the order of magnitude of the ratio of the volume wave propagation velocity in the plasma to the dimensions of the bunch. Short-term compression of a plasma bunch is of interest for realizing effective action in pulsed acceleration, for studying short-term processes which occur when bunches move in strong localized fields, for extracting bunches through an aperture,etc. It is also possible to study the compression of a bunch under a sharp magnetic impulse.

Despite the simplicity of the model which has been used for such a short-lived structure as a plasma bunch, the results which have been obtained are useful for investigating the interaction between a quasi-neutral bunch and electromagnetic waves and fields and for developing methods of weakening the Coulomb repulsion between electron bunches used in generating coherent electromagnetic radiation. It is also interesting to consider the possibility of studying these effects on an astronomical scale in connection with the motion of cosmic plasma formations in cosmic magnetic fields.

In conclusion the author wishes to express his gratitude to Professor M. S. Rabinovich and Professor M. L. Levin for a number of valuable comments and their interest in the work.

Received September 26, 1957

LITERATURE CITED

[1] V. I. Veksler, CERN Symposium on High Energy Accelerators and Pion Physics, Proceedings 1, Geneva, 1956.

[2] V. I. Veksler, J. Atomic Energy 2, 427 (1957).*

[3] M. L. Levin, 1957 (unpublished).

[4] M. A. Divil'kovskii, J. Tech. Phys. (USSR) 9, 433 (1939).

[5] L. de Broglie, Electromagnetic Waves in Waveguides and Cavity Resonators, (IL Moscow, 1948), p. 32.

[6] M. S. Rabinovich and V. V. Iankov, 1955 (unpublished); V. V. Iankov, J. Exptl. Theoret. Phys. (USSR) 32, 926 (1957).

[7] W. Bostick, Phys. Rev. 104, 292 (1956).

---

* Original Russian pagination. See C. B. Translation.

** See English translation.

SIMILITUDE RELATIONS FOR CRITICAL HEAT LOADING IN FORCED LIQUID FLOW

B. A. Zenkevich

The presently available experimental data [2, 4, 5-9] indicated that the transition from nucleate boiling to film boiling in forced water flow occurs at some definite heat loading q_{cr}, the value of which is determined by the physical parameters and the water velocity.

In film boiling under conditions of forced liquid flow the existence of a vapor layer between the heated surface and the liquid which flows along the surface is possible only if the vapor layer is continuously replenished by vapor which is formed during the time the liquid evaporates from the surface of the interphase boundary as a consequence of heat transfer from the heated surface through the vapor layer. The vapor which is formed has a hydrodynamic effect on the liquid which flows along the heated surface (Fig. 1) *; this effect results from the reactive force which arises by virtue of the change in the amount of liquid flow produced by the phase transformation.

The common flow of the liquid and vapor phases in the zone of the transition has an effect on the velocity profile set up in each component by the normal and tangential viscous forces on the liquid side of the interphase boundary.

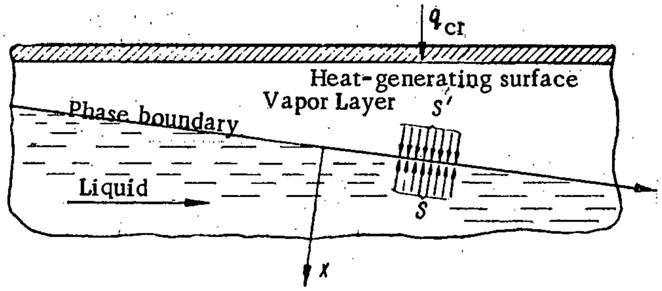

Fig. 1. Diagram for critical boiling load (the z-axis is perpendicular to the plane of the page). The S forces act on the phase boundary from the liquid side (surface tension and normal viscous forces); the S' forces are the reactive vapor forces.

For simplicity we shall neglect the normal forces on the vapor side; then, the following forces must be considered in examining the equilibrium of the mechanical forces normal to the boundary: the phase-transformation reaction, the surface tension, and the normal forces due to the viscosity of the liquid. In addition to the mechanical forces at the boundary we must consider the heat balance relation; this relation is characterized by the fact that the thermal flux from the heated surface through the vapor layer to the liquid induces that boiling rate for which the reactive forces required for equilibrium are obtained. When an underheated nucleus of the liquid is heated to the saturation temperature t_s, q_{cr} is increased, corresponding to the greater flow of heat through the liquid which flows through the phase boundary. At equilibrium the phase boundary is such that the amount by weight of liquid which flows to it is equal to the amount by weight of vapor which is produced.

In accordance with the foregoing the requirements on the mechanical, thermal, and mass reactions between the phases at the boundary may be written as follows [considering the projection along the x-axis of a rectangular coordinate system x, y, z in which the x-axis is normal to the surface of the phase boundary (Fig. 1)]:

---

* The general effect of the hydrodynamic nature of the transition in boiling has been suggested by Kutateladze [1].

1) Equation for mechanical equilibrium*

$$\frac{1}{\Delta\tau}\int\limits_{\Delta\tau} d\tau \int\limits_{F} \frac{W_x\gamma}{g}\left(W''_x-W_x\right)dF= =\frac{1}{\Delta\tau}\int\limits_{\Delta\tau} d\tau \int\limits_{F} \sigma\left(\frac{1}{R_1}+\frac{1}{R_2}\right)dF+ +\frac{1}{\Delta\tau}\int\limits_{\Delta\tau} d\tau \int\limits_{F} \mu\left(\frac{\partial W_x}{\partial x}+\frac{\partial W_x}{\partial y}+\frac{\partial W_x}{\partial z}\right)dF; \quad (1)$$

2) Heat-balance equation**

$$\int\limits_{\Delta\tau} d\tau \int\limits_{F} (q_{cr})_x\,dF=\int\limits_{\Delta\tau} d\tau \int\limits_{F} rW''_x\gamma''\,dF+ +\int\limits_{\Delta\tau} d\tau \int\limits_{F} C_p\,\Delta t_H W_x\gamma\,dF; \quad (2)$$

3) Mass-balance equation

$$\int\limits_{\Delta\tau} d\tau \int\limits_{F} W''_x\gamma''\,dF=\int\limits_{\Delta\tau} d\tau \int\limits_{F} W_x\gamma\,dF. \quad (3)$$

In these equations W_x is the projection along the x-axis of the instantaneous phase velocity, x is the acceleration of gravity, γ, μ and σ are respectively the specific gravity, viscosity and surface tension, r is the evaporation, C_p is the heat capacity, Δt_H is the amount by which the liquid is underheated with respect to t_S; R_1 and R_2 are the principle radii of curvature for the surface of the phase boundary at a given point; quantities denoted by two primes refer to the vapor phase.

The integral form of Eq. (1)-(3) means that the equilibrium boundary between the phases is taken as the mean statistical boundary during a time $\Delta\tau$ over an area F. The quantity $\Delta\tau$ is much larger than the period of the local fluctuations in the boundary which arise as a result of local underheating in the turbulent motion of the phase and F is much larger than the area of the local excitations of the boundary which arise as a consequence of these fluctuations.

Analyzing the system of equations in (1)-(3) by dimensional analysis, we obtain the following primary similitude criteria:

$$\left\{\frac{W''}{W};\ \frac{\gamma W\nu}{\sigma g};\ \frac{Wl}{\nu};\ \frac{q_{cr}}{W''\gamma''r};\ \frac{C_p\Delta t_H W\gamma}{W''\gamma''r};\ \frac{W''\gamma''}{W\gamma}\right\}, \quad (4)$$

where W and W" are the mean linear velocities for the liquid and vapor with respect to the heated surface, ν is the kinematic viscosity of the liquid and l is a defining dimension of the system.

Carrying out the appropriate transformations for the system given in (4) we arrive at the following criteria:

$$\left\{\frac{\gamma''}{\gamma};\ \frac{C_p\,\Delta t_H}{r};\ \frac{Wl}{\nu};\ \frac{q_{cr}}{r}\sqrt{\frac{\nu}{\sigma g W_g}};\ \frac{W''}{W};\ \frac{q_{cr}}{W''\gamma''r}\right\}, \quad (5)$$

where W_g is the velocity of liquid flow associated with gravity.

---

* The first term is a result of Eq. (3).

** The effects associated with heat conductivity in each of the phases are not considered. Eq. (2) should include one additional term to take into account the heat consumed in heating the boiling liquid. It is assumed, however, that this effect need not be taken into account.

The last three criteria in (5) determine q_{cr}. Neglecting $\frac{W''}{W}$ and $\frac{q_{cr}}{W''\gamma'' r}$, we can write the following expression:

$$\frac{q_{cr}}{r}\sqrt{\frac{\nu}{\sigma g W_g}}=f\left(\frac{\gamma''}{\gamma};\frac{C_p\Delta t_{H}}{r};\frac{Wl}{\nu}\right). \qquad (6)$$

The functional form of (6) was determined by examining the particular relations between the criteria being defined and each of the defining criteria, using the experimental data obtained earlier [2] on critical heat loading in forced water flow for an underheated nucleus heated to a temperature t_S; the results of special experiments carried out in the same way, but with wider limits of variation for the water parameters, were also used.

In analyzing the data approximately 870 experimental points were used in the pressure range 100-210 atm with underheating down to $t_S - \Delta t_H = 2 - 100$°C and water velocities of $W = 0.5-8$ meters/second.

In computing the similitude criteria for each of the experimental points the physical parameters for the water (kinematic viscosity $-\nu$, specific gravity $-\gamma_H$ and enthalpy $-i_H$) were taken at the mean temperature at exit from the working section [2].

Furthermore, since the results obtained in Ref. [2] and those obtained in the special experiments tend to verify the fact that q_{cr} is independent of the linear dimensions of the working section (tubes with internal diameters ranging from 4 to 12 mm and operating lengths ranging from 185 to 1600 mm) the defining dimension in the criterion $\frac{Wl}{\nu}$ was taken as $\sqrt{\frac{\sigma}{\gamma'-\gamma''}}$ [10], where γ' is the specific gravity of water at t_S.

In light of the last remarks, Eq. (6) assumes the form *

$$\frac{q_{cr}}{r}\sqrt{\frac{\nu}{\sigma g W_g}}=f\left(\frac{\gamma''}{\gamma_H};\frac{i_S-i_H}{r};\frac{W\sqrt{\frac{\sigma}{\gamma'-\gamma''}}}{\nu}\right), \qquad (7)$$

where i_S is the enthalpy of the water at temperature t_S.

Using the appropriate notation for the corresponding similitude criteria, we have

$$K=f(K_1;\ K_2;\ R). \qquad (7')$$

In analyzing the experimental data it was assumed that there are two regions of R (Reynold's number) for which the criterion K is "self-reproducing" with respect to R. This effect depends on the values of K_1 and K_2 and starts later with increasing R, the smaller these values. The effect of R on K in the non-self-reproducing regions is found to be an inverse function of the values of K_1 and K_2.

In other words, the effect of viscosity forces on the transition in boiling starts earlier as the water velocity is reduced, the lower the pressure and the closer the water temperature to t_S.

The following criterion equation is obtained from an analysis of all of the experimental data:

$$K=K_1^{0.65}(95+420K_2)\left[1+0.32\cdot10^{6}\cdot R^{-(1.1+2.6K_1+0.9K_2)}\right]10^{-5}. \qquad (8)$$

---

* The physical parameters for the water were taken from the table given by Vukalovich [12]. The surface tension was calculated using the Bachinskii formula [3]:

$$\sigma = 0.00714\left(\frac{\gamma'-\gamma''}{1000}\right)^4 \quad \text{kg/m}.$$

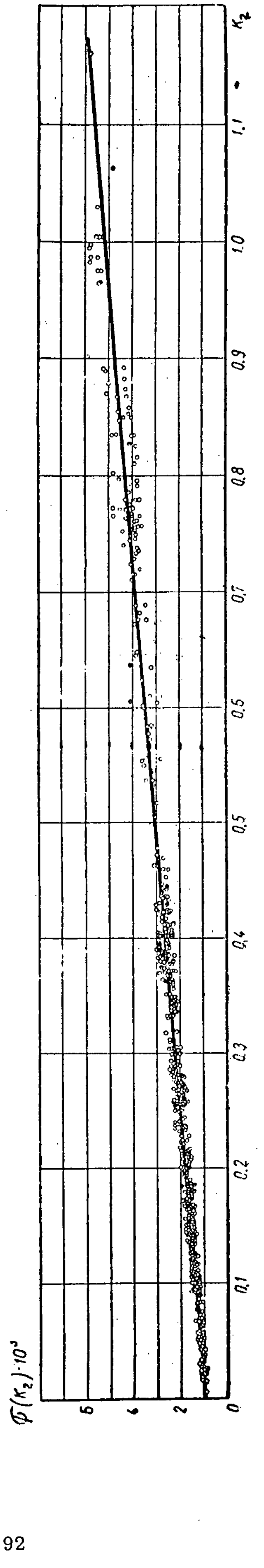

Fig. 2. The relation $\frac{K}{K_1^{0.65}[1+0.32\cdot10^6 R^{-(1.1+2.6K_1+0.9K_2)}]}=\psi(K_2)$. o) is for the upward motion of water, the dissolved air content is the ordinary value (30-130 N cm³/kg H_2O [2]); ●) the same but with a dissolved air content of 600-670 N cm³/kg H_2O; ⊙) the same but with a dissolved air content of 1450 N cm³/kg H_2O; ⊕) downward motion of water, with ordinary dissolved-air content.

This equation establishes a relation between q_{cr}, the velocity and the physical parameters of the water.

The dimensional form of Eq. (8) is

$$q_{cr}=r\sqrt{\frac{\sigma g W_g}{\nu}}\cdot K_1^{0.65}(95+420K_2)\times$$
$$\times[1+0.32\cdot10^6 R^{-(1.1+2.6K_1+0.9K_2)}]10^{-6}\frac{\text{kcal}}{\text{m}^2\,\text{hour}}. \quad (9)$$

In Fig. 2 is shown the graphical relation corresponding to Eq. (8).

Approximately 85% of the experimental points lie within a relative spread $\delta\leqslant10\%$; for the others we have $\pm10\%<\delta\leqslant\pm20\%$.

In Fig. 3 we show Eq. (8) and the experimental data obtained by Buchberg [4].* These data are in satisfactory agreement with Eq. (8).

The empirical formula suggested in Ref. [2] for computing q_{cr} in the pressure range 140-210 atm is in agreement with Eq. (9) when K is self-reproducing with respect to R within approximately ±10% over the entire pressure region 100-210 atm if $\Delta t_H \geq 10°C$.

The comparison shown in Fig. 4 indicates that the value of q_{cr} for small velocities and small underheating in the pressure region $120<P\leq210$ atm may be lower than the values of q_{cr} under conditions of free convection of the boiling water.

It should be noted that the Kutateladze formula gives most satisfactory agreement with the experimental results obtained by Kazakov using nichrome sheets for boiling large volumes of water at pressures up to 205 atm [1, 11].

SUMMARY

1) The concrete nature of the hydrodynamic effect of the transition in boiling loads has been taken into account in examining this phenomenon in forced liquid flow.

2) A system of criteria (6) is obtained from a mathematical analysis of this model.

3) Analyzing the experimental data on critical heat loading in forced water flow for a nucleus underheated to temperature t_s in the pressure range 100-210

---

* Since there are no tabulated data in Ref. [4] the values of q_{cr} and W_g are taken from the graph.

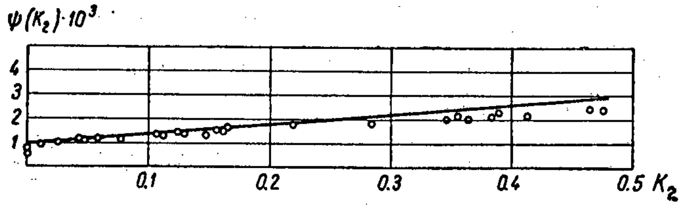

Fig. 3. Experimental data obtained by Buchberg [4] compared with the criterion equation (8).

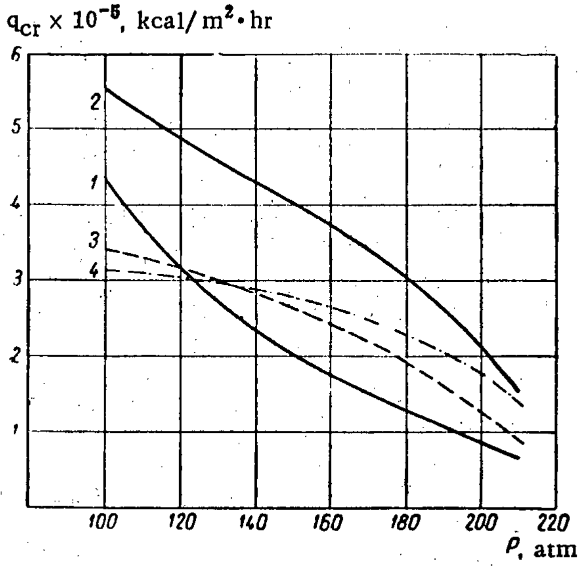

Fig. 4. Comparison of the calculated values of q_{cr} for forced water flow with the calculated values q_{cr} for free convection of boiling water. 1) $\Delta t_H = 5°C$, $Wg = 3 \cdot 10^6$ kcal/m^2·hour, 2) $\Delta t_H = 5°C$, $Wg = 18 \cdot 10^6$ kcal/m^2·hour, from Eq. (9); 3) using the S. S. Kutateladze formula taking $K_1 = 0, 14$ [1]; 4) using the G. N. Kruzhilin formula taking $B = 1.4 \cdot 10^4$ [3].

atm a criterion equation (8) is obtained; this equation is found to be in satisfactory agreement with the experimental data obtained by Buchberg.

4) An analysis of the above-mentioned experimental data has been used to investigate the possibility of using the criteria system given in (6) for establishing similitude relations in critical heat loading for forced liquid flow.

Engineers O. L. Peskov and N. D. Sergeev took part in the special experiments required in the present work. The calculational and graphical work was carried out by Engineers E. F. Deriugin and Technician N. A. Gushchin.

The author is indebted to Dr. of Physico-Mathematical Sciences A. K. Krasin for his constant interest in this work.

Received May 13, 1957

LITERATURE CITED

[1] S. S. Kutateladze, Heat Transfer in Condensation and Boiling, [in Russian] (Mashgiz, 1952).

[2] B. A. Zenkevich and V. I. Subbotin, J. Atomic Energy 3, 149 (1957).*

[3] M. A. Mikheev, Fundamentals of Heat Transfer,** (GEI ***, 1949).

[4] H. Buchberg et. al., Heat Transfer and Fluid Mechanics Inst. (June 1951, Stanford, California).

[5] W. H. Jens, Mech. Eng. 76, 981 (1954).

[6] F. C. Günther, Trans. ASME. 73, 115 (1951).

[7] W. H. McAdams et. al., Ind. Eng. Chem. 41, 1945 (1949).

[8] V. S. Chirkin and V. P. Iukin, J. Tech. Phys. 26, 1542 (1956).****

[9] M. A. Styrikovich, M. E. Shitsman and Z. L. Miropol'skii, Teploenergetika 12, 32 (1955).

[10] W. Fritz, Physik Z. 1935, No. 11.

[11] Problems of Heat Exchange in Change of Aggregate States of Materials, Coll.:** S. S. Kutateladze (editor) (GEI ***, 1953).

[12] M. P. Vukalovich, Thermodynamic Properties of Water and Water Vapor ** (Mashgiz, 1955).

---

*Original Russian pagination. See C. B. Translation.

**In Russian.

***State Power Engineering Publishing House.

****See English translation.

Sr^{90} AND Sr^{88} YIELDS IN Pu^{239} FISSION BY REACTOR NEUTRONS

L. M. Krizhanskii and A. N. Murin

The available data on light-fragment yields in Pu^{239} fission have been obtained by radiochemical methods and are relatively incomplete [1]. In particular, the literature contains no data on the yields of Sr^{88} and Sr^{90}. The yields of these nuclides in Pu^{239} fission, however, are of great interest in view of the fact that they can be used to determine the number of fission events which occur in a sample under prolonged exposure [2] and because of the biological significance of the Sr^{90} isotope.

We have carried out a mass-spectrometer determination of the Sr^{88} and Sr^{90} yields in a sample of Pu^{239} which was exposed to an integrated flux of slow neutrons of $2.7 \cdot 10^{20}$ neut/cm^2. The mass spectrometer determination of the strontium isotope yields was carried out without preliminary chemical separation of this nuclide from the mixture of exposed Pu^{239} and the fission fragments (the exposure conditions and methods employed in determining the yields are described in Reference [3]).

TABLE 1

Relative Yield of Strontium Isotopes in Pu^{239} Fission by Reactor Neutrons and Data on Isotopic Dilution.

Isotope	Mass spectrometer ratio	Relative fission yield	Mass spectrometer ratio after isotopic dilution				No. of atoms of Sr^{90} in ml of original solution of fission products	
			No. of atoms added to 1 ml original sol. of fission products	mass spectrometer ratio	No. of atoms added to 1ml of original sol. of fission products	mass spectrometer ratio		
			I dilution		II dilution		I	II
Sr^{90}	1	1*	—	1	—	1	$1.085 \cdot 10^{16}$	$1.075 \cdot 10^{16}$
Sr^{88}	0.687 ± 0.003	0.595**	$2.65 \cdot 10^{16}$	3.10	$1.574 \cdot 10^{16}$	2.16	—	—
Sr^{86}	0.0094 ± 0.0004	—	—	—	—	—	—	—
						Mean	$1.08 \cdot 10^{16}$	

---

*A correction is introduced for the decay of Sr^{90} ($T_{1/2}$ = 19.9 years [7]).

**A correction is introduced for the natural strontium content. The isotopic composition of natural strontium is: Sr^{88} – 82.56%; Sr^{86} – 9.86% [7].

The correction for the natural strontium content in the Pu^{239} was introduced in accordance with a measurement of the Sr^{86} content of the sample. This procedure is valid since virtually no Sr^{86} is formed in fission and the independent Sr^{86} yield is neglibibly small; moreover, the yield of the nuclide which precedes it, Rb^{86}, in all, is only $1.2 \cdot 10^{-4}$% [5] (Rb^{86} is a "shielded" nucleus, i. e., the nucleus which is a neighbor of a stable isobar). Using isotopic dilution the absolute number of Sr^{88} and Sr^{90} atoms in the irradiated Pu^{239} sample was determined;

TABLE 2

Absolute Yields of Sr^{88} and Sr^{90} for Pu^{239} Fission by Reactor Neutrons

Isotope	Absolute No. of atoms in 1 ml of solution	Absolute yield,%	Absolute yield computed from the smooth yield curve, %
Nd^{143}	$2.93\cdot10^{16}$*	5.98	—
Sr^{90}	$1.11\cdot10^{16}$**	2.28	2.2
Sr^{88}	$0.641\cdot10^{16}$	1.35	1.20

---

*Measured by the isotopic dilution method introducing corrections for the $Nd^{143}(n, \gamma)Nd^{144}$ reaction which has a cross section σ = 334 barns [6].

**A correction is introduced for the decay of Sr^{90} ($T_{1/2}$ = = 19.9 years).

for comparison purposes the absolute number of the nuclide Nd^{143}, the yield of which is 5.98 % [6], was also determined. From these the absolute yield of the strontium isotopes was determined (Tables 1 and 2).

The following remarks may be of interest. On the basis of the early radiochemical measurements of yields it has usually been assumed that the chief difference between the yield curves for fission fragments for two different fissile nuclei is that the difference in mass of these nuclei leads to a shift in the most probable yield in the light-fragment region whereas the position of the maximum of the yield curve in the heavy-fragment region remains fixed. A comparison of the recent mass-spectrometer data on fragment yields in Pu^{239} fission [3], [6] with the U^{235} data does not seem to be in agreement with this interpretation. The results of this comparison indicate that there is a definite shift in the "heavy" peak in the direction of higher mass. In comparing the mass spectrometer curves for U^{233} and U^{235}, Tomlinson [8], on the basis of the results obtained in Reference [9], indicates that both the "light" and "heavy" peaks exhibit shifts; in this case there is a shift by one unit in the direction of lower mass numbers.

It is impossible, on the basis of the strontium data obtained by us, to introduce any meaningful corrections for the position of the maximum of the light-fragment yield curve although these data indicate some displacement of the mass spectrometer curve in the direction of lower mass as compared with the radiochemical yield curve. Before a definite answer can be given to this question, further experimental work will be required to determine the yields of rubidium, molybdenum and zirconium.

We wish to express our gratitude to B. K. Preobrazhenskii and Ia. Malyi for assistance in setting up and carrying out these experiments.

Received August 27, 1957

LITERATURE CITED

[1] E. P. Steinberg and L. E. Glendenin, Proceedings of the International Conference on the Peaceful Uses of Atomic Energy 7 (UN, N. Y., 1956,) p. 3.

[2] M. P. Anikina and B. V. Ershler, J. Atomic Energy 2, 275 (1957).*

[3] L. M. Krizhanskii, Ia. Malyi, A. N. Murin and B. K. Preobrazhenskii, J. Atomic Energy 2, 276 (1957).*

[4] D. R. Wiles, B. W. Smith, R. Horseley and H. G. Thode, Can. J. Phys. 31, 419 (1953).

[5] A. C. Pappas, Proceedings of the International Conference on the Peaceful Uses of Atomic Energy 7, (UN, New York, 1956), p. 19.

[6] D. R. Wiles, J. Petruska and R. Tomlinson, Canad. J. Chem. 34, 227 (1956).

[7] G. T. Seaborg, I. Perlman and J. M. Hollander, Tables of Isotopes (IL, 1956).

[8] R. Tomlinson, Private communication .

[9] S. Katcoff, Handbook of Nuclear Engineering (Addison-Wesley, 1956).

---

*Original Russian pagination. See C. B. Translation.

THE (n, p) REACTION IN GALLIUM AND GERMANIUM AND THE (n, α) REACTION IN GERMANIUM AT NEUTRON ENERGIES OF 14 Mev

V. N. Levkovskii

A study has been made of the (n, p) and (n, α) reactions in gallium and germanium at neutron energies of 14 Mev; these reactions occur in the irradiation of radioactive isotopes of zinc and gallium. The reaction products were separated from the irradiated targets by radiochemical methods.

(n, p) Reaction in Gallium and the (n, α) Reaction in Germanium

Oxides of gallium and germanium (0.5-5 grams) were exposed for periods ranging from 1 to 30 minutes to 14-Mev neutrons from the high-voltage machine at the Institute for Chemical Physics, Academy of Sciences, USSR and separated by boiling in hydrochloric acid (under these conditions the germanium tetrachloride is distilled off); then the zinc, in the form of $ZnHg(CNS)_4$, was precipitated from the carrier solution. In the gallium experiments the zinc precipitation was preceded by the removal of copper in the form of CuCNS to eliminate the radioactive isotope Cu^{66} which is formed in the $Ga^{69}(n, \alpha)Cu^{66}$ reaction. The $ZnHg(CNS)_4$ precipitates were reprecipitated and dried and their activities measured with a standard aluminum Geiger counter having a wall thickness of 44 mg/cm^2.

The decay curves and the results of the graphical analysis indicate that in both cases there are four radioactive components with half-lives as follows: 13.9 hours, 52.5 minutes, 3.9 hours and 2.3 minutes. The first two half-lives are undoubtedly those of the well-known isomeric pair Zn^{69*} and Zn^{69}, formed in the $Ga^{69}(n, p)$ and $Ge^{72}(n, \alpha)$ reactions.

The 2.3-minute activity, apparently due to Zn^{71}, has been observed earlier only in the products of the Ge(n, α) and Zn(n, γ) reactions [1], [2].

The 3.9-hour activity is not mentioned in the literature. Inasmuch as this activity is observed in the products of both reactions, it may possibly be due to the isomer Zn^{71} which is formed in the $Ga^{71}(n, p)Zn^{71*}$ and $Ge^{74}(n, \alpha)Zn^{71*}$ reactions. An additional factor in favor of this interpretation is that fact that a similar period (3 hours) has been observed earlier (although without chemical identification) in products of the (n, γ) reaction in zinc enriched with the Zn^{70} isotope. The energy of the β-radiation from Zn^{71*} was measured by the absorption method and found to be 1.5 Mev, in good agreement with the data of Reference [2]. The half-life of this radiation was accurately followed several times for a period of 18-20 hours and found to be 3.92 ± 0.05 hours. To determine the relative yields of β-particles from the isomeric pairs, formed in the irradiation of gallium and germanium by neutrons, the measured results were corrected for the absorption of the β-radiation in the walls of the counter. In the case of the 52.5-minute, 13.9-hour and 3.9-hour activities these corrections were determined experimentally by absorption measurements. The accuracy of these corrections was checked by a measurement of the activity with an end-window counter with a thin window (approximately 1.5 mg/cm^2). In the case of the 2.3-minute activity the absorption correction was computed from the maximum energy of the β-spectrum [2] using the empirical relation $E = 2.12 \cdot 10^{-2} d + 0.17$, where d is the decay thickness in cm^2/mg [3]. The validity of this relation in the present geometry was checked in special experiments with sources giving β-particles with known energies, P^{32}, Pd^{109}, Pd^{111}, Ag^{111}, Ag^{112}, Y^{90} and Y^{91},etc.

Using the data on the relative yields of β-particles and the known contents of the Ga^{69}, Ga^{71}, Ge^{72} and Ge^{74} isotopes in the targets, the relative cross sections for the reactions in question were computed:

$$\sigma_{n,\alpha}Ge^{72} : \sigma_{n,\alpha}Ge^{74} = 1 : (0.47 \pm 0.02),$$
$$\sigma_{n,p}Ga^{69} : \sigma_{n,p}Ga^{71} = 1 : (0.50 \pm 0.05).$$

As the atomic weight increases by 2 units the cross sections for these reactions are reduced by approximately a factor of 2; this corroborates the characteristic reduction in the cross sections for the reactions in isotopes of the same element noted in Reference [4].

Calculations were also made of the relative yields of the isomeric pairs in the different reactions. It is of interest to note that in each case both pairs of isomers are formed with approximately the same ratios, differing, however, in absolute magnitude by approximately a factor of 2.

For the reaction Ge(n, α) $Zn^{69*}/Zn^{69} = 1.1$; $Zn^{71*}/Zn^{71} = 2.3$.

For the reaction Ga(n, p) $Zn^{69*}/Zn^{69} = 2.4$; $Zn^{71*}/Zn^{71} = 2.3$

The (n, p) Reaction in Germanium

The activity of the radioactive gallium isotopes was measured with an end counter with a thin mica window (approximately 1.5 mg/cm^2). An analysis of a number of decay curves for the gallium fraction indicates the existence of four β-components with the following half-lives: (20.5 ± 0.5) minutes, (4.5 ± 0.5) hours, (13.4 + 0.2) hours and (8 ± 1) minutes. Within the experimental spread the first two half-lives correspond to those of Ga^{70} and Ga^{73}. The 13.4-hour activity can only be assigned to Ga^{72}, for which, however, the literature gives a somewhat larger half-life (14.2 hours); in accordance with Reference [5] the last half-life (8 minutes) may be assigned to Ga^{74}, which has not been investigated.

Using the data on relative yields of β-particles, computations were made of the relative cross sections for the four reactions which were observed:

$$\sigma_{n,p}Ge^{70} : \sigma_{n,p}Ge^{72} : \sigma_{n,p}Ge^{73} : \sigma_{n,p}Ge^{74} =$$
$$= 1 : (0.39 \pm 0.02) : (0.24 \pm 0,02) : (0.13 \pm 0,03).$$

The obtained cross-section ratios differ from those computed from the statistical theory and those measured in the work of Paul and Clarke [6] and corroborate the characteristic reduction in $\sigma_{n,p}$ in isotopes of the same element noted in Reference [4].

The author wishes to express his gratitude to senior research worker N. S. Reshetov and senior engineer Iu. V. Lapitskii for their halp in this work.

Received July 4, 1957

LITERATURE CITED

[1] J. M. Hollander, J. Perlman and G. T. Seaborg, Rev. Mod. Phys. 25, 2, 469 (1953).

[2] J. M. LeBlanc, J. M. Cork and S. B. Burson, Phys. Rev. 97, 750 (1955).

[3] E. Broda, Contemporary Status of Radiochemistry* (State Chemistry Press, Moscow, 1953) p. 122.

---

* In Russian.

[4] V. N.Levkovskii,J. Exptl.-Theoret. Phys. (USSR) 31, 360 (1956).*

[5] H. Morinaga, Phys. Rev. 103, 504 (1956).

[6] E. B. Paul, R. L. Clarke, Can. J. Phys. 31, 267 (1953).

---

*See English translation.

ALPHA-DECAY OF RdAc ON THE COLLECTIVE MODEL AND THE SPIN OF THE AcX NUCLEUS

S. G. Ryzhanov

The most complete and exact energy level scheme for the AcX nucleus and the α-decay scheme for the RdAc nucleus to these levels is given in Reference [1]; the α-particle yields in percent are also given (cf. Figure). According to the Bohr-Mottelson collective model of the nucleus [2] the ground state and excited levels of AcX with energies of 59, 286 and 332 kev must be considered single-particle states because α-decay to these levels is most probable (cf. Figure). Apparently the levels at 110, 173 and 238 kev are rotational satellites of the second level, forming a developed rotational band. Actually, according to [2] the energy of rotational excitations for an even-odd nucleus (A_CX is Ra_{223}^{88}) is given by the expression

$$E_r = B[I(I + 1) - K(K + 1)], \tag{1}$$

where I is the rotational moment of the level while K is the moment for the single-particle level; B is the rotation constant $B = \frac{\hbar^2}{2J}$ (J is the effective moment of inertia). In even-odd nuclei we have I = K, K + 1, K + 2, etc. It is easy to show that the difference in energies between the levels 110 − 59; 173 − 59; 238 − 59 are in good agreement with Equation (1) for K equal to 5/2, 7/2 or 9/2 with a rotational constant of 6.97, 5.55 and 4.62 kev, respectively. The level at 79 kev is apparently of nonrotational nature.

The probability for α-decay to a given level of the daughter nucleus is given by the Ter-Martirosian formula [3]

$$W_I^K = C \sum_{l=|I-K|}^{I+K} |C_{I,K,l,0}^{K}|^2 (2l+1) e^{-\beta l(l+1)} \cdot e^{-\alpha E_r}, \tag{2}$$

where $C_{I,K,l,0}^{K,K}$ is the Clebsch-Gordan coefficient, l is the orbital moment of the α-particle, C is a constant for a given rotational band, α and β are semi-empirical constants the values of which are determined from empirical data. According to Equation (2) W_I^K always falls off monotonically with increasing excitation energy. However, in RdAc the relative yield of α-particles to the 173-kev level is twice as large as to the neighboring level. This departure may possibly be explained by assuming that single-particle levels of an odd nucleon in the field of a strongly-deformed nuclear core (cf. Ref. [4]) with spin K are not very different in energy from rotational levels with spins K + 2 and K + 3. Since the squares of the Clebsch-Gordan coefficients fall off rather sharply with increasing I the probability of α-decay to these rotational states becomes negligibly small and the observed yields of α-particles are actually determined only by the contributions from the single-particle levels with spin K. The factor C in front of the exponential is the same for all bands being considered; hence, the yield ratio for α-particles corresponding to the formation of levels with energies of 173 and 59 kev (4%: 21%) is determined only by the exponential factor $e^{-\alpha E_r}$ which is due to the reduction in the penetrability of the potential barrier caused by the reduction in the energy of the alpha particle owing to excitation of the daughter nucleus. The latter quantity is equal to the difference of energies of these levels. Thus, we find the factor $\alpha = 14.2$. The above also applies for the energy levels at 238 and 173 kev. Hence the yield ratio for α-particles corresponding to the formation of these levels (2%: 4%), should be equal to the ratio of the exponential factors indicated above, i. e., $e^{-\alpha \cdot 0.238}/e^{-\alpha \cdot 0.173}$ With $\alpha = 14.2$, this ratio is close to the empirical value, i. e., 1/2. To compute the constant β which appears in the exponential factor and which is determined by the height of the centrifugal barrier use can be made of the yield of α-particles corresponding to the formation of the level at 110 kev (the first rotational satellite of the band).

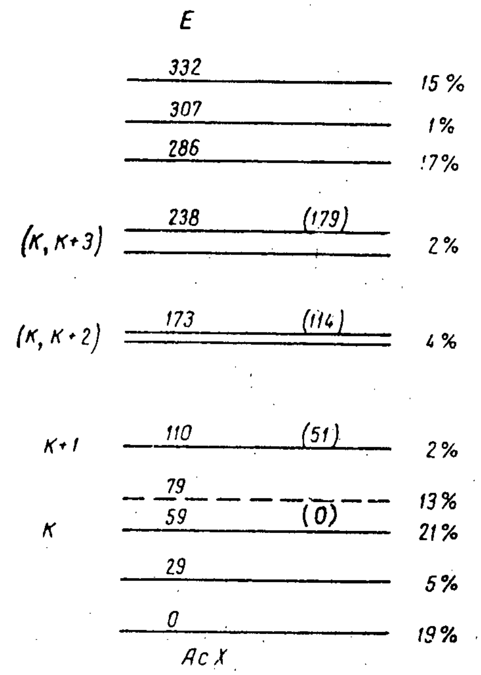

Level scheme for AcX. E is the energy of the level with respect to the ground state in kev; the figures in brackets are the energies of the rotational levels with respect to the level at 59 kev. The figures at the right indicate the α-particle yield (in percent) for α-decay of RdAc with formation of the corresponding AcX level.

We propose, that in accordance with conservation of parity, l can take on only even values of the natural series. The squares of the Clebsch-Gordan coefficients for K equal to 5/2, 7/2 and 9/2 and $l = 2$ are correspondingly 5/14, 56/165, 45/143 (the terms in Equation (2) with $l > 2$ can be neglected). The empirical ratio for the yields of α-particles corresponding to the formation of levels with energies of 110 and 59 kev is 2%: 21%, while the energy exponent for these levels is 0.487. From this it follows that $\beta = 0.365$. The value of α is close to that of the exponent $170/E^{3/2}_{\text{decay}}$ in the Bethe formula [5] and is also close to the corresponding exponent for Am^{241} [3]. The factor β is in exact agreement with that given for Am^{241} [3]. This means that the nuclides AcX and Am^{241} have the same elongation.* If it is also assumed that decay is accompanied by a change of parity (odd l) then β is found to be 0.166. This cannot be explained. Hence the authors of Reference [1] have apparently found it completely justifiable to assign the transition with an energy of 50.2 kev to the levels with the energies of 286 and 238 kev. However, the empirical multipolarity of the γ-lines found in Reference [1], do not find any direct reflection in the rotational scheme given in Reference [2].

Received May 31, 1957

LITERATURE CITED

[1] M. Frilley, S. Rosenblum, W. Waladares and G. Boussier, J. de Phys. et Rad. 15, 43 (1954); 16, 378 (1955).

[2] A. Bohr and B. R. Mottelson, Problemy Sovremennoi Fiziki No. 9, 78 (1955); A. Bohr, and B. R. Mottelson, Phys. Rev. 90, 717 (1953).

[3] L. L. Gol'din, L. K. Peker and G. I. Novikova, Usp. Fiz. Nauk 59, 3, 459 (1956).

[4] B. R. Mottelson and S. Nielsen, Problemy Sovremennoi Fiziki No. 1, 186 (1956).

[5] H. Bethe, Nuclear Physics (State Tech Press, 1948) Chapter 2, p. 179.**

---

*Hence the value K = 5/2 is to be preferred for the band being considered.

** Russian translation.

ELECTRONIC SPECTRUM OF Pu^{240}

P. S. Samoilov

INTRODUCTION

Pu^{240} is an α-radiator and decays in accordance with the scheme shown in Figure 1 [1], [5].

The daughter nucleus U^{236} has a number of excited levels which contribute to the rotational structure [2]. The internal conversion electrons of U^{236} and U^{235} have been investigated in References [3] and [4]. The transmission and resolving power of the spectrometers used by the authors of these papers did not allow resolution of all the conversion electron lines and thus the multipolarity of the γ-transitions in U^{236} have not been determined.

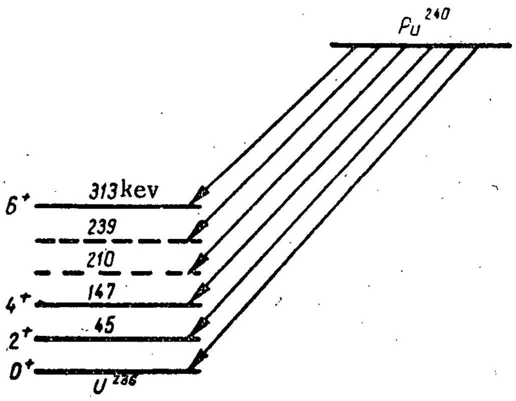

Fig. 1. α-decay scheme in Pu^{240} and levels in the U^{236} nucleus.

We have undertaken to measure the relative conversion coefficients for γ-transitions in the U^{236} nucleus to the L and M-subshells of the atom, thus making it possible to determine the multipolarity of the γ-radiation and thereby establish the nature of the levels in the nucleus.

EXPERIMENTAL RESULTS

The electronic spectrum of Pu^{240} was measured with a double-focussing β-spectrometer [6]. The sources were four samples of plutonium of different dimensions (from 1 to 20 cm^2) with surface densities ranging from 20 to 250 $\mu g/cm^2$ but having the same isotopic composition (Pu^{239} – 12%; Pu^{240} – 88%; Pu^{241} less than 0.2%).*

In the electronic spectrum of plutonium, which is shown in Figure 2,** the relatively small signal-to-noise ratio observed in the energy region between 0 and 21 kev is due to the superposition of Auger-electron lines and electrons emitted by the Pu^{239} and Pu^{241} isotopes present in the sample being studied [1], [2].

The intense lines denoted by 1, 2, 3, 4, and 5 are conversion electron lines from U^{236}. Further on in the spectrum (Fig. 3) lines 6, 7, 8 and 9 are found. The interpretation of the conversion electron lines is given in the table.

---

*According to the data of G. M. Kukavadze.

**These measurements were performed by Moscow State University Diplomate Students, V. A. Belov and V. A. Vasil'ev.

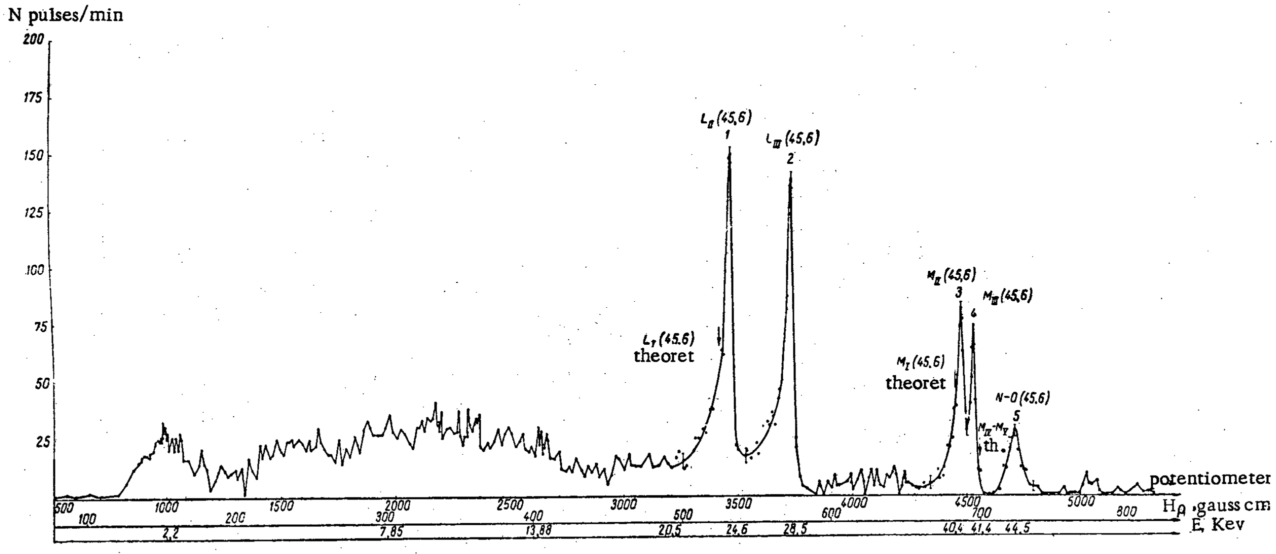

Fig. 2. Electronic spectrum for Pu^{240}.

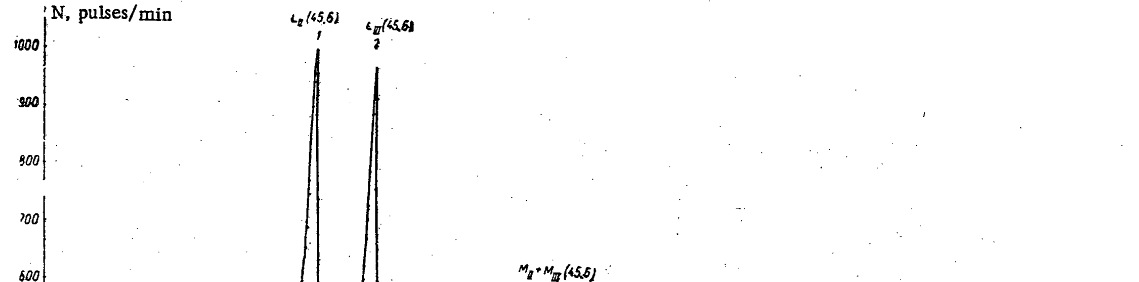

Fig. 3. Electronic spectrum in Pu^{240}. The lines marked 1, 2, 3, 4 and 5 were measured with a source having dimensions 11 x 35 mm^2 and a surface density of 20 $\mu g/cm^2$; lines 6, 7, 8 and 9 were measured with a source of dimensions 10 x 40 mm^2 having a surface density of 250 $\mu g/cm^2$.

The following relative conversion coefficients are found for the γ-transition with an energy of 45.6 kev by averaging over all measurements:

$$\frac{L_{II}}{L_{III}} = 1.05 \pm 0{,}05; \qquad \frac{M_{II}}{M_{III}} = 1.4 \pm 0{,}05;$$
$$\frac{L}{M} = 2.6 \pm 0.2.$$

To compare the experimental values of the conversion coefficients with the theoretical values for the coefficients in the L-subshells we have used the data reported by Dranitsyna [7] who has carried out an interpolation over energy and z of the appropriate data in the table given by Rose [8]. According to these data the relative conversion coefficients for the γ-transitions at 45.6 kev have the following values:

$$\left.\frac{L_{II}}{L_{III}}\right|_{E2} = 0.8; \qquad \left.\frac{L_{II}}{L_{III}}\right|_{E3} = 1.09;$$
$$\left.\frac{L_{II}}{L_{III}}\right|_{E1} = 0.888; \qquad \left.\frac{L_{II}}{L_{III}}\right|_{M1} = 181$$

The values closest to the experimental value for L_{II}/L_{III} are those theoretical values for E1, E2 and E3 transitions. The possibility of an E1 transition is excluded by the fact that the absolute values of the conversion coefficients for this transition are three orders of magnitude smaller than for the E2 and E3 transitions and the corresponding conversion electrons cannot be observed because of the small intensity. To make more exact interpretations of the nature of the 45.6 kev γ-transition it will be necessary to obtain experimental data on conversion to the M-subshell. According to Reference [9], with the E2 transition, M-conversion occurs mostly to the M_{II}- and M_{III}-subshells while for an E3-transition there is considerable conversion to the M_{IV}- and M_{V}-subshells.

Line No. in Figs. 2 and 3	Mean value of electron kinetic energy, kev	Subshell in the U^{236} atom	Binding energy of electron in subshell, kev	Transition energy, kev	Mean value of transition energy, kev	Transition energy given in [3]	Transition energy given in [1]
1	24.63	L_{II}	20.94	45.57	45.62±0.1	44.6	44.9
2	28.48	L_{III}	17.16	45.64			
3	40.45	M_{II}	5.18	45.68			
4	41.39	M_{III}	4.30	45.69			
5	44.2	N	1.44	45.64			
6	83.08	L_{II}	20.34	104.02	103.95±0.5	—	102.1±2
7	87.02	L_{III}	17.16	104.18			
8	98.87	M_{II}	5.18	104.05			
9	102.1	N	1.44	103.54			

From the experimental data (Fig. 2) it is apparent that the M-conversion of the 45.6 kev γ-transition occurs mainly to the M_{II}- and M_{III}-subshells. It follows that this transition in an E2-transition.

The 30 percent discrepancy between the experimental and theoretical data are apparently a consequence of the inadequate accuracy of the tabulated values for the conversion coefficients to the L-subshells, which have been obtained by interpolation of the corresponding coefficients in the Rose table. Moreover the conversion coefficients have been calculated by Rose without taking account of the finite dimensions of the nucleus.

From the spectrum in Figure 3 the following relative conversion coefficients are found for the 104-kev γ-transition:

$$\frac{L_{II}}{L_{III}} = 1.7 \pm 0.2; \quad \frac{L}{M} = 2.8 \pm 03.$$

The theoretical relative conversion coefficients [7] for this transition are as follows:

$$\left.\frac{L_{II}}{L_{III}}\right|_{E2} = 1.43; \quad \left.\frac{L_{II}}{L_{III}}\right|_{E3} = 2.2;$$
$$\left.\frac{L_{II}}{L_{III}}\right|_{E1} = 1.01; \quad \left.\frac{L_{II}}{L_{III}}\right|_{M1} = 20.$$

The theoretical values closest to the experimental value for L_{II}/L_{III}, are for the E2 and E3 transitions. The 104-kev transition must be considered an E2-transition on the basis of the same considerations which were used in analyzing the 45.6-kev transition.

Thus the existence of a second excited level in U^{236}, first reported in Reference [5] and investigated further in Reference [1] using the same method, has been verified by an independent method.

According to the present data the energy of the first excited level is 45.6 kev and the energy of the second level is 149.6 kev.

Starting from the nature and multipolarity of the γ-transitions with energies of 45.6 and 104 kev, it must be concluded that the excited levels in U^{236} have spins and parities in agreement with the values computed on the basis of rotational levels (cf. Fig. 1 and Refs. [1] and [2]).

The energy values for the first and second excited levels are in the ratio 1:3.29, which is in good agreement with the value 1:3.28 obtained in Reference [1] and the value 1:3.33 computed on the basis of the data reported in Reference [2].

In Reference [1] it is also reported that the energy for the third excited level (6^+ in Fig. 1) is in complete agreement with the theoretical data.

In the present work an attempt was made to find this level. For this purpose, in measuring the electronic spectrum in Pu^{240} samples were used having an area of 20 cm^2 (the solid angle of the spectrometer is 0.8 percent of 4π). The intensity of the conversion electron lines for the γ-transitions of energies of 104 and 45.6 kev increases by a factor of 15 in this case as compared with the intensity of these lines shown in Figure 3. However, no additional lines were found.

An estimate of the statistical errors indicates that the intensity of the γ-transitions from the third excited level to a lower-lying level in U^{236} is less than 2 percent as compared with the intensity of the γ-transition from an energy of 104 kev.

Received August 31, 1957

LITERATURE CITED

[1] L. N. Kondrat'ev, G. I. Novikova, Iu. P. Sobolev and L. L. Gold'din, J. Exptl.-Theoret. Phys. (USSR) 5, 11 (1956).*

[2] A. Bohr and B. R. Mottelson, Phys. Rev. 90, 717 (1953).

[3] K, N. Shliagin, J. Exptl.-Theoret. Phys. (USSR) 30, 5, 817 (1956).*

[4] M. S. Freedman, T. Wagner and D. W. Engelkemier, Phys. Rev. 88, 1155 (1952).

---

* See English translation.

[5] I. Perlman and F. Asaro, Ann. Rev. Nucl. Sci. 4, 157 (1954).

[6] P. S. Samoilov, Proceedings of the Seventh All-Union Conference on Nuclear Spectroscopy (Leningrad, 1957).*

[7] G. F. Dranitsyna, Internal Conversion Coefficients for the L_I-, L_{II}-, L_{III}-Subshells* (Izd. AN SSSR, Moscow-Leningrad, 1957).

[8] K. Seigbahn, Beta and Gamma Ray Spectroscopy, (Amsterdam, 1955,) p. 905.

[9] E. L. Church, and J. F. Monahan, Phys. Rev. 98, 718 (1955).

---

*In Russian.

ELIMINATION OF SCATTERED γ-RADIATION EFFECTS IN STANDARDIZING RADIOMETERS

A. S. Shilov

In recent years radiometer methods have been widely used to determine the uranium content of ores at deposits as well as ores loaded in carts and automatic machinery. These methods are based on measurements of the intensity of the γ-radiation [1], [2]. To obtain quantitative results in these measurements the radiometer is standardized by usual methods using standard radium point sources [1], [3]. The intensity of the γ-radiation is computed from the expression

$$I = \frac{8.4 \cdot 10^5 m}{l^2} \ \mu r/\text{hour},$$

where m is the amount of radium in the standard in grams, and l is the distance between the standard and the source in meters.

Generally, in addition to the direct γ-radiation from the standard, the counter is also subject to γ-radiation scattered by near-by objects; this situation leads to errors in the calibration.

To determine the errors due to the effect of scattered γ-radiation, we have carried out experimental measurements. A diagram of the scheme used for the measurements, and the results, are shown in Figures 1 and 2, respectively.

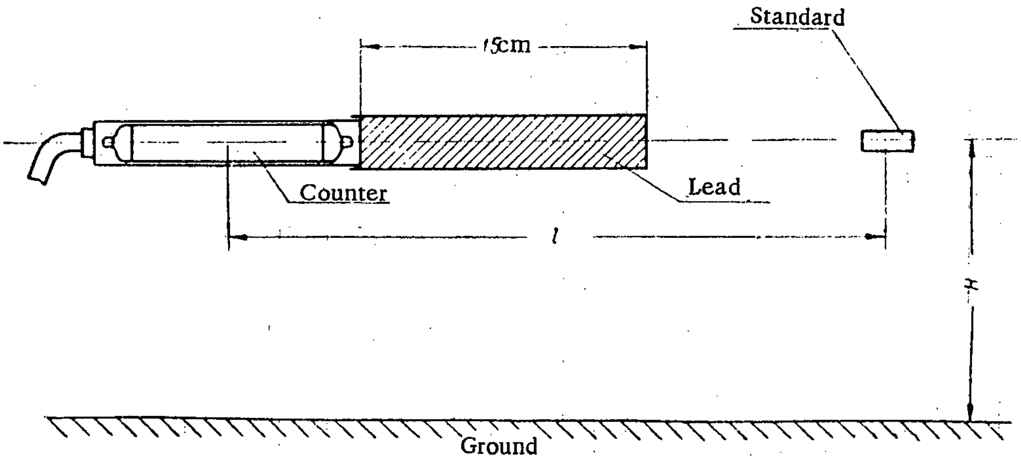

Fig. 1. Diagram of the arrangement used in measuring the intensity of scattered γ-radiation.

The intensity of the scattered γ-radiation and the relative error in the calibration increase as the Z number of the material used in the cathode of the counter is increased (Figs. 2 and 3). Consequently the energy of the scattered γ-radiation is generally about 0.7 Mev or less (in this energy region the counter sensitivity as a function of energy of the γ-photons is different for different cathode materials). The spectral composition of the γ-radiation can be qualitatively estimated from the ratio of intensities measured by counters with cathodes of metals having high and low values of Z.

l_M	0.5	0.5	0.5	1.0	1.0	1.0	2.5	2.5	2.5
H_M	0.5	1.4	2.75	0.5	1.4	2.75	0.5	1.4	2.75
I_{VS}/I_{MS}	8.4	5.3	3.9	6.8	5.1	3.9	6.5	5.3	5.0

Note: I_{VS} is the intensity measured with a VS-4 counter; I_{MS} is the intensity measured with a MS-4 counter.

From the table shown it follows that as H and l are reduced the energy of the scattered γ-radiation is likewise reduced (for γ-radiation from a radium standard $I_{VS}/I_{MS} \approx 1.8$).

A reduction of the distance between the standard and the counter or between these and the surface of the earth leads to an increase in I_{scat}. It is important to note that the dependence of the intensities of the scattered and direct radiation from the standard as a function of l may be significantly different for different H (Fig. 2). Because of this situation the relative error in calibration σ does not remain constant but increases as l is increased. The intensity of the γ-radiation detected in standardization is found to be larger than the calculated value. Hence the results of the γ-exposures, analyzed with the distorted calibration curve, will be too low; this effect will be larger the smaller the intensity of the radiation being measured.

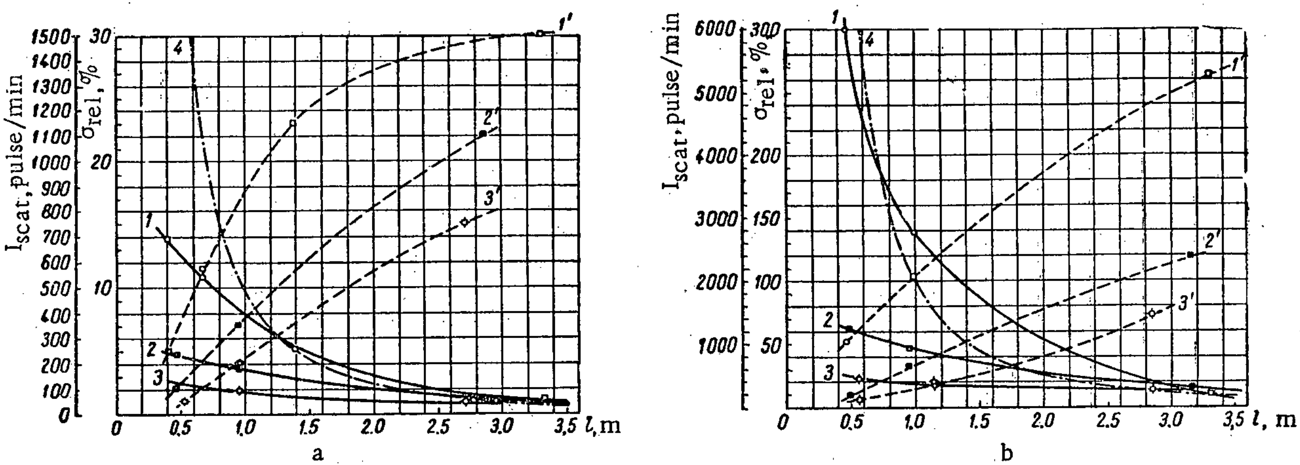

a b

Fig. 2. Intensity of scattered γ-radiation I_{scat} (solid lines) and relative calibration error σ (dotted lines) as a function of the distance between the standard and the counter l and the distance between these and the surface of the earth H. a) MS-4 counters; b) VS-4 counters; 1 and 1') with H = 0.5 m; 2 and 2') with H = 1.4 m; 3 and 3') with H = 2.75 m; 4) the function $I = f(1/l^2)$.

In quantitative interpretation of the results of the γ-exposures, because of uncertainties due to the errors in calibration, the proportionality between the concentration of γ-radiators and the intensity of the γ-radiation is disturbed: this proportionality exists with all other conditions being equal. Thus, with a change of the uranium content in the rock from 0.03 to 0.3 % the proportionality is affected by 25 and 50%, respectively, in measurements with the type MS or VS counter (standardized in the room). The measurements with different types of counters, carried out under the same conditions and expressed in percent of equivalent radium, give different results.

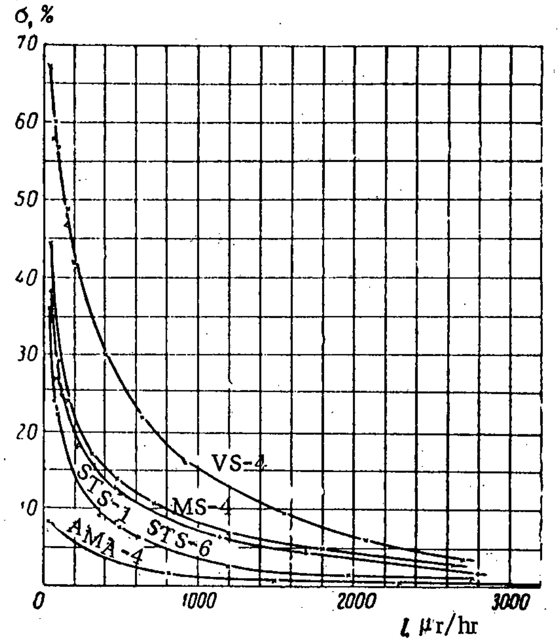

Fig. 3. Calibration error as a function of γ-radiation intensity. The measurements were carried out with different types of counters in the chamber (length 5.5 m, width 3.5 m and height 3 m) with a radium standard m = 1 mg I of the standard with l = 1 m is 840 μr/hour, H = 1.7 m.

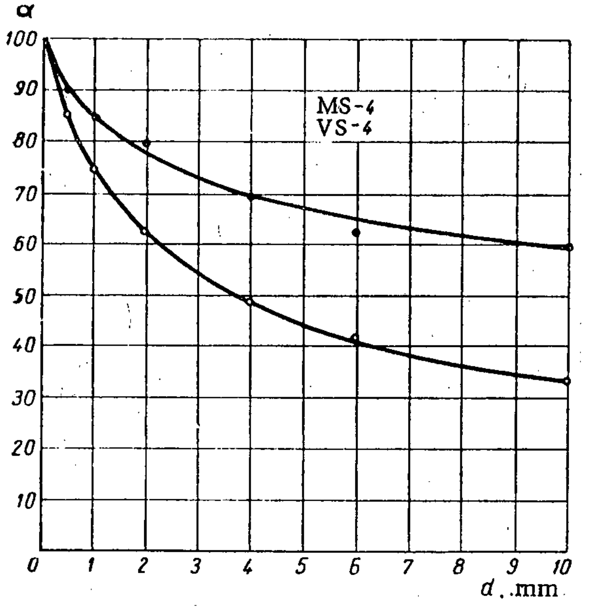

Fig. 4. The attenuation coefficient for γ-radiation from the radium standard as a function of the thickness of the lead cylindrical filter α placed on an aluminum case 1 mm thick in which the counter is located.

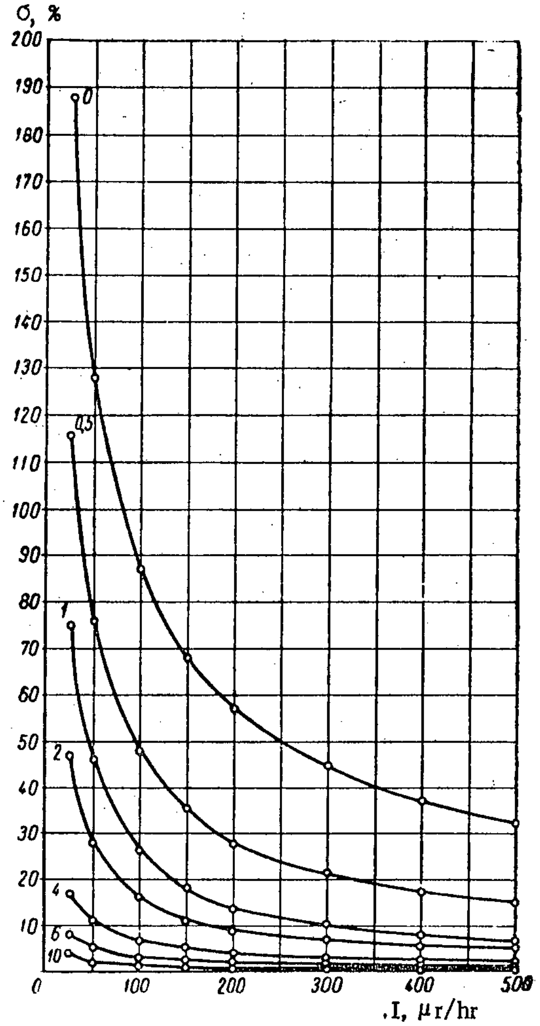

Fig. 5. Calibration errors as a function of γ-radiation intensity and thickness of the lead cylindrical filter. The calibration was carried out in a chamber with a VS-4 counter. I of the standard with l = 1 m is 840 μr/hour, H = 1.7 m (the thickness of the filter is shown on the curve in mm).

In prospecting and searching for deposits the standardization of the radiometers is generally carried out at the site. The errors produced under these conditions exceed the allowable uncertainties in the measurements. Several methods may be used to take account of or eliminate the scattered γ-radiation to eliminate errors in calibration:

1) The "lead wedge" method proposed earlier makes it possible to exclude the scattered radiation

($I_{scat.}$) from the sum ($I = I_{stand.} + I_{scat.}$). The total radiation and the scattered radiation are measured with different distances between the standard and the counter. The magnitude of $I_{scat.}$ is determined with total absorption of the direct radiation from the standard by a lead filter placed between the standard and the counter (cf. Fig. 1). To plot the calibration curve the difference $I - I_{scat.} = I_{stand}$ is used.

This method gives good results when calibration is carried out in the open. However, when there are changes in position the value of I_{scat} will be lowered (because of absorption in the lead of part of the scattered radiation and the absence of uniformly scattered γ-photons in sections in which direct radiation from the standard does not strike the lead), leading to a considerable distortion of the calibration curve.

2) The lead filter method, in which virtually all the scattered γ-radiation is absorbed. The calibration is carried out according to the usual method but the intensity of the γ-radiation of the standard is increased, taking account of its degradation by the lead filter, using the expression

$$I = \alpha \frac{8.4 \cdot 10^5 m}{l^2} \mu r/\text{hour}.$$

The attenuation coefficient for the γ-radiation, α, is determined experimentally under conditions of minimum γ-radiation scattering. The results of determination of α with $l = 30$ cm are shown in Figure 4.

The thickness of the cylindrical lead filter is determined as a function of the maximum allowable error in the calibration for a given region of measurement of γ-radiation intensity using the curve given in Figure 5. Such curves can be used for any calibration conditions as follows. At the counting device (for example type B) the intensity of the radiation from the standard is measured (for detection conditions in which there are no errors) at various filter thicknesses and various values of l. Then the values of $I_i l_i^2$ are determined for which detection of the direct radiation from the standard is uniform for any value of l (larger than three times the length of the cathode of the counter). Then, using the ratio of $I_i l_i^2$ to the value of this product for $l = 30$ cm the errors in the calibration σ are determined and the curve showing the dependence of σ on l with various filter thicknesses is plotted. From this curve, the standardization errors are determined as a function of the quantity l ($l = \sqrt{\alpha \cdot 8.4 \cdot 10^5 m/I}$) corresponding to a given radiation intensity I. If a standard of fixed intensity is used it is more convenient to use the curve showing the dependence of σ on I with different filter thicknesses (Fig. 5).

3) When calibration is carried out using the total ($I_{stand} + I_{scat}$) γ-radiation, the scattered radiation is considered as a supplementary γ-radiation source. At given distances between the standard and the counter the intensity of the γ-radiation is determined at the counting device in pulses/min. Using well-known methods [4], [5] the "dead time" of the counter is determined and a correction is introduced to take account of the lost pulses in the counter. After excluding the natural background the intensities measured in pulses/min are converted into μr/hour using the conversion coefficient

$$k_{conv} = \frac{I}{8.4 \cdot 10^5 m/l^2}$$

computed for $l \approx 30$ cm (under these conditions the error σ, as shown experimentally, is less than 1-2 percent). The results of the measurements are used to plot a curve showing the total γ-radiation ($I_{stand} + I_{scat}$) as a function of distance l. Using this curve the γ-radiation intensities are determined (rather than the computed values) for a given l and the calibration curve is plotted. If the geometry and type of counter are kept fixed the measurements at the counter need be carried out just once.

Using this method of calibration the proximity of the standard to the counter at a given distance does not lead to an error. Consequently it is possible to use standardization of radiometers having pick-up units with several parallel connected counters (for example, a type RKS radiometer).

When the recommended methods are used the results of the quantitative interpretation of the data of field γ-exposures have been found completely satisfactory in practice.

Received August 28, 1957

LITERATURE CITED

[1] V. L. Shashkin, J. Atomic Energy 2, 48 (1957).*

[2] L. N. Posik and I. M. Tenenbaum, J. Atomic Energy 3, 28 (1957).*

[3] V. I. Baranov, Radiometry,** (Izd. AN SSSR, 1956).

[4] V. Bochkarov, I. Keirim-Markus, M. L'vova, and Ia. Prusalin, Measurements of the Activity of γ-adiation Sources** (Izd. AN SSSR, 1953).

[5] V. Veksler, L. Groshev and B. Isaev, Ionization Methods in Radiation Research,** (Gostekhizdat, 1949).

---

*Original Russian pagination. See C. B. Translation.

**In Russian.

MEASUREMENT OF THE CROSS SECTION FOR THE U^{238} (n, 2n) U^{237} REACTION

L. E. Sherman

The cross section for the U^{238} (n, 2n) U^{237} reaction has been determined by measurements with a 4π-counter [1] of the absolute number of β-decay events in the U^{237} nucleus which is formed.

Samples of natural uranium (in the form of lower oxides) were irradiated at the center of the core of a fast neutron reactor [2]. During the exposure the neutron flux at the irradiation site was $10^{12} - 10^{11}$ neut/cm^2·sec.

From the measured number of U^{237} decay events it is possible to find the number of radiators formed as a result of the (n, γ) reaction and U^{238} fission. The precipitation of the fission products was carried out by ether extraction. To separate out Np and to carry out additional purification the uranium was precipitated out of the fission fragments in a reducing medium with 8-hydroxyquinoline in presence of trilon B.

The half-life of the extracted U^{237} was found to be 6.5 days.

To measure the absolute number of β-decay events, using a micropipette, 0.2 mg/cm^2 of U^{237} was deposited on a thin film of cellulose nitrate (rainbow film). The specific β-activity was 3900 pulses/min · 0.1 mg. The measured cross section for the U^{238} (n, 2n) U^{237} reaction was found to be 11.24 ± 1.7 mbarns.

Starting from the known difference of the neutron spectrum at the exposure site as compared with the fission spectrum the cross section for the above reaction was estimated in the fission neutron spectrum; this quantity was found to be 17 ± 3 mbarns.

The chemical work in the present research was carried out by B. S. Kir'ianov. In conclusion the author wishes to express his gratitude to I. I. Bondarenko for his interest in the work and a number of valuable comments.

Received August 28, 1957

LITERATURE CITED

[1] Cohen, Annales de Phys. 7, 3-4, 185 (1952).

[2] A. I. Leipunskii et al., J. Atomic Energy 2, 6, 497 (1957).*

---

*Original Russian pagination. See C. B. Translation.

CONTROL OF THE MOTION OF SINKING AND EXTRACTION MACHINES BY MEANS OF RADIOACTIVE INDICATORS

V.G. Segalin and A.A. Rudanovskii

One of the important problems encountered in automation of coal-mining operations is the automatic control of the motion of sinking and extraction machines in accordance with a given program and the hypsometry of the stratum. This problem is of equal importance for sinking and extraction machines. For instance, the absence of continuous control over the direction of motion has a noticeable effect on the rate and quality of a sinking operation. In extracting operations, when the machine departs from the required direction of motion the cutter digs into earth or into the covering strata, aggravating the operator's task, producing loading peaks on the engine, accelerating cutter wear, contaminating the extracted coal, and leading to loss of the coal that remains in the ground.

To bring about automatic control of the motion of sinking and extraction machines, the following design problems must be solved: 1) coordinate sensors for control of rectilinear motion of the machines in plan or elevation, for control of the slope of motion, for sensing the coal-dirt line, and for control of radius of curvature and parallelism of tunnels; 2) sinking and extraction machines that lend themselves to control through sensors and have the required controllability.

Currently a scientific research program aimed at development of automatic sensors which can detect departures from a course determined by stratum hypsometry is being pursued in the Laboratory of Radioactive Aids to Automation, VUGI (All-Union Scientific Research Institute of the Coal Industry). These sensors generate signals for the guidance of sinking or extraction machines along the contours of coal strata.

The authors suggested using the characteristics of nuclear radiation interactions with matter, which allow qualitative determination of the composition of solid bodies but do not require direct contact with them or complicated physicochemical means of research.

Control along an exposed demarcation line of coal-dirt strata. In this case (Figure 1) coordinate sensors control the motion of a sinking combine along an exposed line of demarcation between coal strata and dirt. The control parameter here is the distance from the mine level to the upper or lower stratum boundary, h, which must be maintained to the required degree of accuracy $\pm \Delta h$ (amplitude value). A sensor of vertical departure from the coal-dirt line must be used in this case, and the principles of operation may be based on: 1) the effect of induced radioactivity, or 2) the effect of Compton scattering of gamma rays in matter.

The basis of the first method is the dependence of the induced gamma activity intensity, at equilibrium, on the nature of the exposed shaft surface. The induced radioactivity is effected by a wide beam of thermal neutrons emitted from a source and fixed firmly to the frame of the sinking combine. The secondary radiation intensity is measured by means of a receiving device (e.g., the VUGI developed gamma-electron relay working from a scintillation counter) fixed to the same frame and separated from the neutron source by a fixed distance.

Since the induced gamma activity emanating from the irradiated area will be approximately proportional to the ratio of dirt area to the entire area, then, as the portion of irradiated area covered with coal increases, the intensity of secondary radiation will decrease. Conversely, as the dirt area increases, the induced gamma activity will also increase.

Operation of the gamma-electron relay must be correlated with the distribution of neutron irradiated area

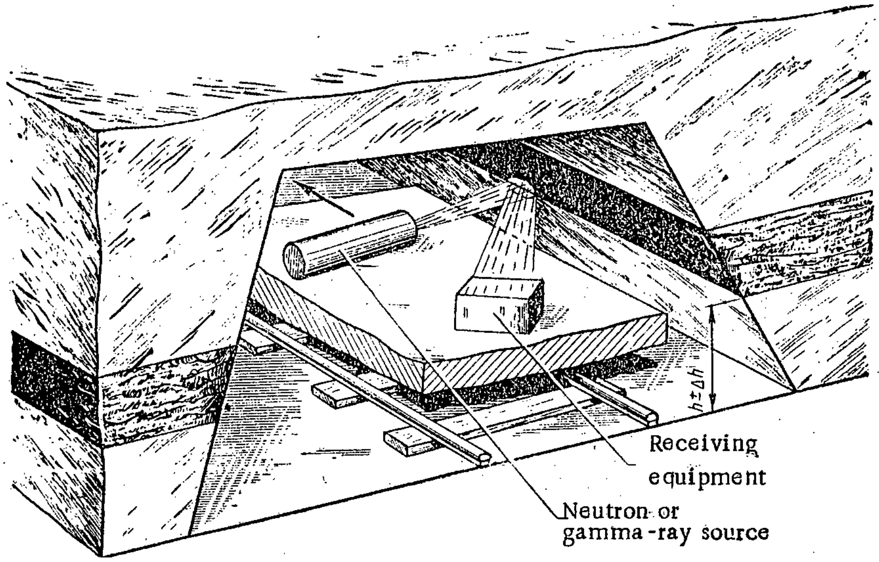

Fig. 1. Control of direction of motion along an exposed line of demarcation.

over the dirt-coal line so that actuation of the relay corresponds to a shift of area distribution toward increased dirt area while its inactive state corresponds to increased coal area, or vice versa. Linking the relay contacts with a steering servomechanism connected to the steering gear of the combine may be done in a conventional manner.

The basis of the second method is the dependence of the reflected gamma ray intensity on the density of the reflecting medium, i.e., again on the ratio of dirt to coal in the area irradiated. In this case, the effect utilized is the variation of intensity of reflected gamma radiation, which depends on the value of the linear absorption coefficient of the material. The mechanism of this effect is the loss of energy by gamma quanta after experiencing a Compton scattering collision, this loss of energy being proportional to the linear absorption coefficient of the material, thus leading to a difference of absorption in coal and in soil. Thus, the integrated scattered radiation intensity detected by the gamma-sensitive element in the equipment must depend on the proportion of the radiation scattered by coal, and will increase as the ray is displaced in the direction of the coal layer. The receiving element here is also a gamma-electron relay working with a scintillation counter of the VUGI laboratory.

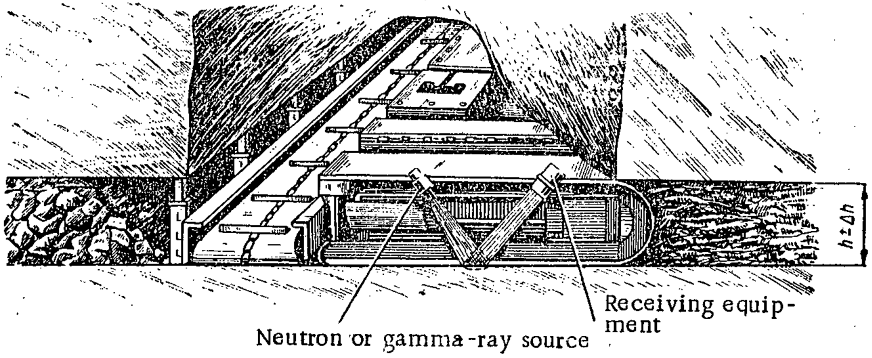

Fig. 2. Control of direction of motion along an exposed plane of demarcation of strata.

Control along an exposed plane of demarcation of coal-dirt strata. The task of the coordinate sensors in this case (Figure 2) is to control the motion of an extracting combine so that its cutting tool moves constantly along a plane of demarcation of coal-dirt strata without digging into the soil or leaving large amounts of lost coal.

Here the methods discussed above are also expedient. In this case, however, the area of irradiation will be located either on a dirt surface or on a coal surface. Therefore, the variations in intensity detected by the receiving gamma-electron relay and scintillation counter will be greater than in the first case, and this will make the operation of the apparatus more precise.

Control along a concealed demarcation of coal-dirt strata. The function of the coordinate sensors, in this case, is control of the motion of the combine in such a way that a constant thickness of coal is maintained over the shaft (Figure 3). Because in some cases a considerable thickness of coal may be required, it was decided to use penetrating radiations, or, more accurately, to use the back-scattering effect of the Compton scattering of gamma rays. In principle this is close to the system discussed in the first case. In this case, however, it is important to exclude any detection of multiply-scattered quanta, which can be done by thoroughly collimating both the incident and reflected rays.

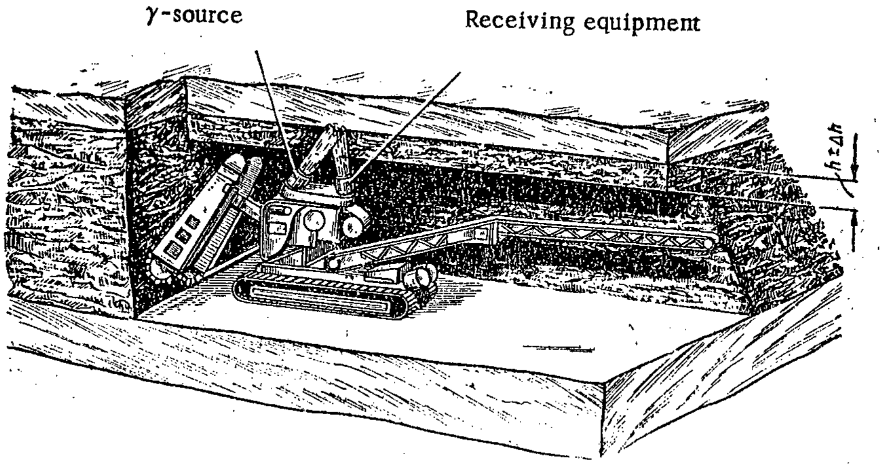

Fig. 3. Control of direction of motion along a concealed line of demarcation of strata.

At present, research is being conducted at the VUGI Laboratory on the utilization of the gamma scattering effect for control of combines. In principle, it is possible to produce sensors which will automatically give signals that may be used for actuation of the steering gear of a combine. This has been done on laboratory mock-ups of the equipment.

In all the above cases the following was achieved with various automatic sensors:

1. The case of exposed line of demarcation of strata – in the proportional phase it was possible to detect motion of the detector in relation to the demarcation line with an accuracy of ± 0.5 cm, and in the relay phase (the operation of the entire system with dependable actuation of the final relays) it was possible to detect motion of the detector from the median position to 5 cm into the dirt strata, and 3 cm into the coal strata.

2. The case of concealed line of demarcation – it was possible to achieve operation of the proportional phase of the system through motion of the detector at a distance of from 0 to 200 mm from the concealed demarcation line, and to achieve an accuracy of ± 2 mm.

3. The case of exposed plane of demarcation of strata – it was possible to operate through the relay phase of the system, with an accuracy of ± 10 mm in passing from a plane of coal to a plane of dirt.

The experiments carried out so far also established that control of motion along a plane of demarcation (for extracting combines) may be effected with an accuracy of ± 10 mm when a nominal ground cover of coal amounting to 15 mm is allowed to be left in the shaft.

It should be noted that the mock-up made in the laboratory does not incorporate the best possible performance; it is thought that much better sensitivity will be achieved in the more perfected mock-up now under construction.

Received June 6, 1957

NOMOGRAM FOR FINDING DIFFERENCES OF EXPONENTIAL FUNCTIONS

E. M. Tsenter

In problems concerned with the accumulation of radioactive material it is frequently necessary to find functions of the form

$$\left(1-e^{-\ln 2\frac{t_1}{T}}\right)e^{-\ln 2\frac{t_2}{T}};\ e^{-\ln 2\frac{t}{T_1}}-e^{-\ln 2\frac{t}{T_2}}.$$

These problems can be reduced to finding the difference $e^{-\ln 2\, n_1} - e^{-\ln 2\, n_2}$, where n_1 and n_2 are the times expressed in half-lifes.

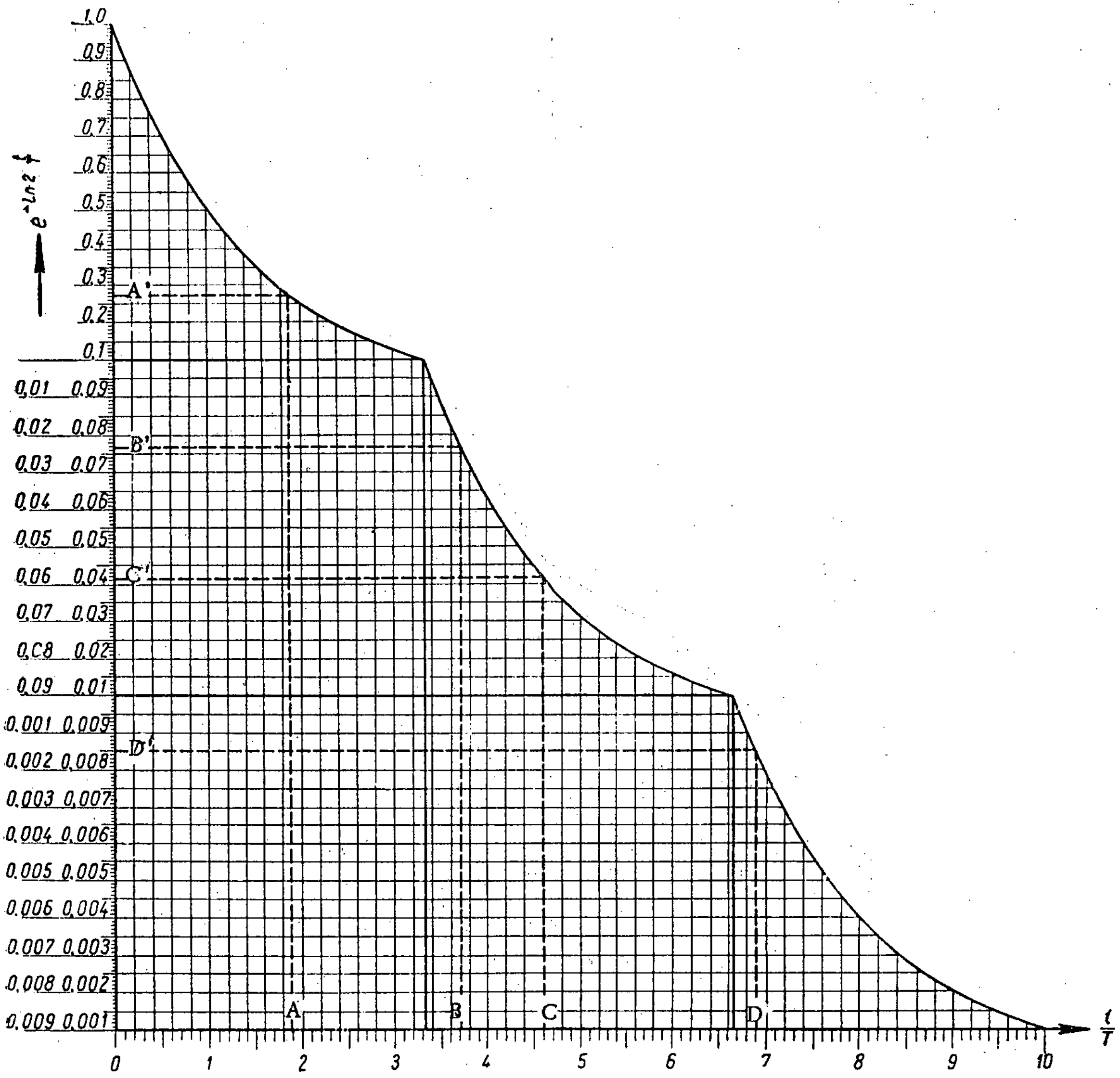

Similar problems are encountered in calculating the accumulation of charges and leakage in systems with a given RC constant. Such exponential functions and the differences between them can be found from exponential curves. However, at large values of n_1 and n_2 such a determination becomes inaccurate because of the relative reduction of the scale. The nomogram being presented here avoids this difficulty. In plotting this nomogram use is made of the fact that 10 half-lives correspond to a value of $\frac{1}{1024} \approx \frac{1}{1000}$ for the exponential. Consequently each $3^1/_3$ half-lives correspond to a reduction by a factor of 10.

The nomogram is plotted for 10 half-lives and the ordinate scale for half-lives from $3\,^1/_3$ to $6\,^2/_3$ is increased by a factor of 10; for half-lives from $6\,^2/_3$ to 10 the scale is increased by a factor of 100. Thus, using this nomogram it is easy to find both the values of the exponentials as well as their difference. If the number of half-lives is greater than 10, it is possible to choose a number of half-lives, which is a multiple of 10, multiplying the result by 10^{-3l}, where l is 1/10 the number of chosen half-lives.

Example 1. Find $\left(1-e^{-\ln 2\frac{t_1}{T}}\right)e^{-\ln 2\frac{t_2}{T}}$, if $\frac{t_1}{T}=2.7$, $\frac{t_2}{T}=1.9$.

On the abscissa axis we mark the point 1.9 (A) and on the ordinate axis we find the corresponding point A'. From point A along the abscissa axis we mark off 2.7 units to B and on the ordinate axis find the corresponding point B'. The quantity being sought is obtained as a difference between points A' and B'. In the present case its value is 0.229 or approximately 0.23. For convenience in reading the difference on the ordinate scale an inverse scale is plotted alongside the direct scale.

Example 2. Find $e^{-\ln 2\frac{t}{T_1}}-e^{-\ln 2\frac{t}{T_2}}$, if $\frac{t}{T_1}=3.7$, $\frac{t}{T_2}=6.9$.

Along the abscissa axis we find points C and D (3.7 and 6.9) and along the ordinate axis we find the corresponding points C' and D' and the difference between them, which is 0.0685.

Received July 11, 1957

SCIENTIFIC AND TECHNICAL NEWS

THE USE OF RADIOACTIVE ISOTOPES IN SCIENTIFIC INVESTIGATIONS

The International Conference on the Use of Radioactive Isotopes in Scientific Investigations, sponsored by UNESCO, took place in Paris from the 9th to the 20th of September,1957.

More than a thousand people from 60 nations and 25 international organizations participated in the work of the conference.

The conference began with a plenary meeting at which welcoming speeches were made by the Director of the UNESCO Department of Exact and Natural Sciences, Auger, the Director-General of UNESCO, Evans, the head of the United Kingdom Atomic Energy Authorigy, J. Cockroft, et al.

In all there were 39 meetings, at which 206 reports were read and discussed and of these 49 were from the USSR, 38 from France, 31 from the USA and 29 from England.

The work of the conference proceeded simultaneously in a physical sciences section and a biological sciences section.

In the physical sciences section reports were read on the production of isotopes, dosimetry, the preparation and use of strong γ-sources and the use of isotopes in metallophysics, metallography, metallurgy, chemical investigations, geophysics etc.

Kohman, Rightmire et al., (USA) reported the preparation of a long-lived Al^{26} isotope (half-life ~ 10^6 years) by the reactions $Mg^{25}(d, n)Al^{26}$ using 15 Mev deuterons and $Mg^{26}(p, n)Al^{26}$ using 21 Mev protons. Al^{26} may be used in the preparation of standard β- and γ-radiation sources and also as a radioactive indicator.

M. S. Petrova, K. G. Shvebel'blit, D. M. Ziv et al., (USSR) reported original methods of preparing α-, β- and γ-sources using the high sorption capacity of an oxide film on aluminum and introducing radioisotopes (Sr,etc.) into enamel and then depositing them on a sample. These methods make it possible to prepare sources of various forms which are reliable in operation and have minimal self-absorption losses.

In their report, Stang, Tucker et al. (USA) described methods of preparing new short-lived isotopes (Mg^{28}, I^{132}, I^{133}, F^{18}).

The reports by Saddington (England) and V. I. Spitsyn (USSR) were devoted to the extraction of Cs^{137} from fission product solutions. The accepted method of separating Cs^{137} in England is by precipitating it with phosphotungstic acid in the form of the sulfate. In the USSR cesium is concentrated in the form of the chloride by the ferrocyanide method. Using this method a Cs^{137} source has already been prepared with an activity of 1000 curies.

Wolf's report (USA) was devoted to the problem of using the recoil energy of a C^{14} atom, as a new method of synthesizing labelled organic compounds. The recoil energy of C^{14}, formed by thermal neutron radiation of nitrogen-containing organic compounds, is sufficient for breaking its previous bonds and substituting other atoms in the molecule. This leads to the formation of a new labelled organic compound.

Smith's report (England) described an electromagnetic method of separating radioactive isotopes. A description of an apparatus for the separation of α-, β- and γ-active isotopes was given.

The report of the Soviet investigators (A. Kh. Breger, V. L. Karpov, V. A. Belynskii,et al.) on the construction in the USSR of a unique and powerful γ-apparatus containing Co^{60} with an activity of 21,000 g-equiv of radium was received with great interest. The apparatus is intended for radiation chemistry investigations and has a chamber with a volume of 1 m^3. The dose strength may reach 1000 r/sec. The apparatus described is the most powerful one known .

The USSR delegation presented the largest number of reports on the use of isotopes in metallophysics, metallurgy, metallography, thermophysics and in the study of the mechanism and kinetics of chemical reactions and the metabolism in plants.

The use of radioactive isotopes for solving some problems in the theory of diffusion in metals made it possible to establish a series of general rules, for example to measure the thermodynamic and diffusion characteristics of solid solutions, to study the self-diffusion coefficient of dissolved silver with positive and negative deviations from Raoult's law, as well as to investigate diffusion in heterogeneous systems (A. A. Zhukhovitskii M. E. Ianitskaia, A. D. Sotskov — USSR).

A study of the mobility of carbon atoms and the interatomic reaction in alloys using radioactive indicators made it possible to explain a series of facts on physical and chemical properties of iron and nickel alloys. Thus, for example, it was shown that the structural factor does not affect carbon diffusion in an iron-nickel alloy (P. L. Gruzin et al., — USSR).

Investigations on the effect of compositions and structure of a metal on diffusion of the components along grain boundaries, using an autoradiographic method, established that small additions of various elements can substantially change the diffusion rate of components along grain boundaries; the rate of intercrystal diffusion increases with an increase in the grain size; a relation exists between the recrystallization process and the local character of diffusion, etc. (S. Z. Bokshtein, S. T. Kishkin, L. M. Moroz — USSR).

A paper on an investigation of electrotransference in solid solutions using radioactive isotopes C^{14}, Fe^{59}, Cr^{51}, Mo^{99}, W^{185} received merited approval. The method developed allows the determination of rate and direction of transfer of separate components of binary alloys under the effect of a direct current, at various temperatures. New facts on interatomic reaction in alloys were established (I. N. Frantsevich — USSR).

A paper on the use of Cr^{51} for studying inert films on metals was interesting. In contrast to methods used previously (chemical analysis or electron diffraction), the autoradiographic method gives exhaustive information on the quantity and distribution of substances on the surface (Brasher, De, Kingsbury, Mercer — Great Britain).

A paper on the investigation of the solubility of involatile substances in high pressure steam has great practical and scientific value. The use of radioisotopes made it possible to detect extremely small concentrations of dissolved substances (up to 10^{-5} mg/kg). The investigation was carried out over a wide range of temperatures and pressures (M. A. Stryrikovich — USSR).

A report on an investigation of the effect of modifying agents in flotation using the isotopes S^{35}, C^{14}, P^{32}, Cu^{64}, Fe^{59}, Zn^{65}, Ca^{45}, caused great interest and a lively discussion. It was established that the nature of the reaction between flotation reagents and minerals is varied and that effective mineral flotation requires only partial (20-40% of monolayer) activation of the surface (O. S. Bogdanov, V. I. Khainman, N. A. Ianis, A. K. Podpek — USSR).

A paper on the measurement of the gap between the rotor and the stator of high pressure steam turbines using Ir^{192} was of practical interest. The accuracy of measurement of a 2 mm gap was ± 5%. The use of Ir^{192} made rapid adjustment and control of the size of the gap possible during operation (Favereau, Laverlochere — France).

Two reports devoted to the effect of nuclear radiation on semiconductors were highly appreciated. In one of them the structural defects in germanium monocrystals, caused by the action of β-particles and fast neutrons, were investigated. (V. S. Vavilov, L. S. Smirnov, A. V. Spitsyn, V. M. Patskevich, M. V. Chukichev — USSR), in the other — the action of β-particles on germanium and silicon crystals (V. S. Vavilov, L. S. Smirnov, V. M. Patskevich — USSR).

A paper on an investigation of the rate of corrosion processes in solid bodies at high temperatures was interesting both from the point of view of the experimental results and the method used. Using radioisotopes, important data were obtained on Cu_2O, NiO, ZnO, MgO and Al_2O_3 which make it possible to evaluate the enthalpy and entropy of defect formation. It was established that high-temperature gaseous corrosion of metals is directly dependent on the diffusion coefficient, which, in its turn, is dependent on the components of the protective film on the metal surface (Moore — USA).

In another paper the effect of chlorine on the semi-conducting layer of aluminum oxide was studied by autoradiographic method and it was shown that corrosion of chlorine-anodized aluminum occured only in the presence of impurities in the metal (Verkerk — Holland).

Papers on the measurement of the relative lability of cations in mixtures of molten oxides (V. I. Malkin, L. A. Shvartsman — USSR) and the investigation of the thermodynamics of metallurgical reactions (L. A. Shvartsman USSR) are important from the practical point of view, as is an investigation of the migration of ions of the material and impurities in crystals of silver alkali and alkali earth metal salts (A. N. Murin — USSR).

Papers on the investigation of the movement of charge materials in blast furnaces were of practical interest. In contrast to the method used in the USSR, the authors "labelled" the ore by wetting it with aqueous radioisotope solutions (Kohn, et al. — France).

The results of investigations of phase conversion and movement of moisture inside capillary-porous and colloidal bodies may be of great importance in selecting the conditions for drying various materials (A. I. Veinik — USSR).

A paper on the investigation of the sequence of formation of intermediate products in the oxidation of hydrocarbons is of great theoretical and practical importance (A. V. Nalbandian, M. B. Neiman, N. M. Emanuel — USSR), as is that on the study of isotopic sulfur exchange and the mechanism of reactions of sulfur-containing compounds (A. I. Brodskii, G. P. Miklukhin — USSR).

Of the eight reports on analytical chemistry, the following attracted attention.

A method was reported for the quantitative isolation of alkali and alkali earth elements by deposition on cellulose and rare earths — by chromatography on ion exchange resins (Fouarge and Fuger — Belgium).

Tellez-Plasencia (France) reported results, which are important from the practical point of view, on the use of radioisotopes in determining the content and distribution of photolytic silver in irradiated photoemulsions.

A paper on the use of radioactive isotopes in spectral analysis is interesting (E. E. Vainshtein, L. I. Pavlenko, Iu. I. Beliaev — USSR).

A report on the application of organic reagents — coprecipitants — for removing very small amounts of impurities aroused great interest. This is of great importance in developing methods for controlling the purity of semi-conductors, alloys and other materials. The proposed method makes it possible to determine the amount of a substance down to a ten billionth of a gram per liter of solution (V. I. Kuznetsov — USSR).

Peirson and Iredale (England) reported an application of γ-spectrometry for the identification of radioisotopes without chemical separation of isotope mixtures. The authors' proposal to record the impulses of the γ-spectrum of radioisotopes on a magnetic tape is interesting.

Three meetings were devoted to problems on the application of radioisotopes in physical chemistry.

The results of using a kinetic isotopic method for studying the mechanism of the catalytic dehydrogenation of butane into divinyl were given in a report by A. A. Balandin, et al. (USSR).

S. Z. Roginskii's report (USSR) was devoted to catalysis problems and in it he gave the results of investigating the mechanism of catalytic processes. The data obtained explain these processes from a new point of view and indicate that it is necessary to reexamine the established ideas on the mechanism of a series of catalytic processes. He also gives the results of using isotopes for studying the surface structure of solid catalysts.

A report on the equilibrium between ions of rare earth elements and the complex-former — triton B is interesting. The results obtained could be used for quantitative calculation of the process of chromatographic separation of rare earth elements (P. Betts, et al. — Canada).

New data was given in a report on the application of isotopic methods to the investigation of the structure and properties of heteropolycompounds (V. I. Spitsyn — USSR).

The study of solvent diffusion in crystalline high polymers using Cl^{36} made it possible to detect an essential difference in the rates of transverse diffusion through a sample with parallel chains and through spherolytic polyethylene, in whose crystals the chains are arranged radially (Point — Belgium).

The use of Pt^{197} and Pt^{193} radioisotopes made it possible to study the sublimation of platinum during the catalytic oxidation of methane at high temperature (Bussiere, Domanski — France).

Sulfuration of metallic surfaces was studied with the help of S^{35}. The activation energy of the process and the relation of the reaction rate to temperature was determined (Lopis, Gamboa, Arizmendi — Spain).

An original method of investigating the properties of a glass surface and various films on it by measuring the depth of permeation of radioactive gas atoms (radon, xenon) ionized by a high frequency discharge, was proposed by Jech (Czechoslovakia). By using this method the thickness, nature and physicochemical properties of surface films on glass can be established. In particular, this method may be used to study the surface of catalysts.

There were two very interesting reports on dosimetry of ionizing radiations.

The property of glass to change color under the effect of radiation was used for a rapid check on the total γ-radiation dose. The dose was evaluated by comparing the optical density with a standard (Bálestic, Bonnaud, Le Clerc — France).

Investigation of functioning electronic spectra and the spectral sensitivity of ionization chambers, counter tubes and light sensitive films made it possible to establish a rational method for calibrating equipment for measuring β- and γ-radiation (K. K. Aglintsev, V. P. Kasatkin, V. V. Smirnov — USSR).

The paper on chemical dosimetry of γ-rays and fast neutrons using a phenol solution of trichloroethylene and tetrachloroethylene was interesting. The former was equally sensitive to γ-rays and neutrons, the latter was insensitive to neutrons. Therefore, the simultaneous use of both in mixed (n, γ) fields made it possible to separate the doses, obtained from various types of radiation. The high light and heat stability of such types of dosimeters was noted (Taplin — USA).

There were papers on different subjects in the field of geophysics.

A report on the isotopic composition and the ratio of S^{32}/S^{34} of meteorites and the earth was found interesting and induced a profitable discussion. Magmatic and volcanic soils as well as rock and iron meteorites were the subjects of the investigation. It was established that there is a noticeable difference in the isotopic ratios of these objects which would indicate differences in their origin (A. P. Vinogradov — USSR).

A study of the radioactivity of meteorites and tektites, caused by cosmic radiation, gave valuable information on the history of meteorites, before and after falling to earth and on the intensity of cosmic rays in the past. Apparently, the average value of cosmic ray intensity has not changed appreciably over the past several million years (Kohman and Ehmann — USA).

Interesting data on the determination of the rate of accumulation of deposits were obtained by the radiochemical analysis of deep sea deposits (V. I. Baranov, L. A. Kuz'mina — USSR).

At a joint meeting of both sections reports were read on methods of using isotopes and techniques of measuring activity.

The greatest interest was roused by a report on particularly fine-grained emulsions for nuclear investigations. If the emulsion usually used had grain sizes of $\sim 0.28\ \mu$, when treated again it had microcrystals of 0.04 to 0.08 μ and the possibilities of an experiment were greatly increased (N. A. Perfilov, N. R. Novikova, E. I. Prokof'eva* — USSR).

A report on the use of liquid scintillators for measuring soft β-radiation on a paper filter, saturated with the scintillating solution, was interesting from the point of view of method (Roucayrol —Saar).

Another method for measuring soft β-emitters (C^{14}, H^3) employed a bulb for liquid samples, with a capacity of less than 1 ml, which was prepared from a scintillating plastic and placed between two photomultipliers, connected to a coincidence system (Schram, Lombaert — Belgium).

---

* See p. 45 [Russian] of this issue [translation, page 47].

Reports on the use of isotopes in medicine, agriculture and biology were read in the section on biological sciences. The extensive factual material reported at the conference and the original investigation procedures indicate the great progress made in many fields of the biological sciences.

A lot of interest was aroused by the work of the Soviet biochemists A. V. Palladin, E. M. Kreps, M. N. Prokhorova, G. E. Vladimirov, who used isotopes to follow the metabolism of proteins, nucleic acids, glycogen and other compounds at various functional states of the brain. It was shown that the higher the organism in the evolutionary respect, the faster the metabolism occured.

A special meeting was devoted to one of the most important problems of modern biochemistry — the study of the metabolism of nucleic acids. It was noted that the processes of new growth and transformation of nucleic acids occur with the participation of vitamin B_{12} — one of the important factors in blood production (Schweigert — USA).

The Belgian scientists (Brachet et al.) performed very delicate experiments using methods of measuring the activity of isolated cells and autoradiography to determine quantitatively the process of the penetration of enzymes into living cells from the surrounding medium and to establish a close relation between the physiological activity of a cell and the intensity of penetration of an enzyme.

Zakrzewski et al. (Poland), studying the biochemistry of leucocytes and the biochemical changes arising from phagocytosis, observed that during the process of phagocytosis the amount of ribonucleic acid in the cytoplasm increased more than 10 times.

In a report by Rumanian investogators (Parhon, Potop, Nicolescou-Zinca) data were presented showing that in the growth of tumors in the liver and other organs, the accumulation of P^{32} in them increased. On introducing the lyzate of thymus the fixation of phosphorus in the liver and other organs increased and decreased in the tumor. The authors drew conclusions on the effect of the thymus on the growth of tumors from the effect on phosphorus exchange.

The English specialists demonstrated an apparatus which made it possible to introduce radioactive substances into the hypophysis with great accuracy. Such an apparatus can find use not only in treatment of tumors of the hypophysis, but also in treatment of cancer of the mammary glands and in experimental work.

In the meetings on physiology and biochemistry of plants as a results of a general discussion, the scientists agreed with the basic premises of A. L. Kursanov that, besides the circulation of organic substances in plants, a continuous circulation of phosphorus occurs and in this circulation there is 20-30 % of the total reserve of phosphorus and 20-50% of the photosynthesis products. The rate of transfer of organic substances in plants is on the average 80-100 cm/hours.

Biologists were very interested in Chain's (Italy) apparatus for automatic scanning of chromatograms of labelled compounds. The apparatus executes work with high accuracy, which would require a long time under normal conditions.

A lively discussion was provoked by the report of Z. N. Zhurbitskii and D. V. Shtrausberg (USSR) on the effect of temperature conditions of the ground and the air on the intake by plants of various fertilizers labelled with P^{32}, S^{35} and Ca^{45}. The results of these investigations make it possible to select most advantageously the conditions of feeding plants in relation to climatic conditions.

In the USA, Japan and other countries P^{32} and C^{14} have been used for studying the process of phosphorylation, connected with photosynthesis, which revealed the similar mechanisms of "collecting" light energy in chemical bonds. The same problem was considered in the report of A. A. Nichiporovich (USSR).

Iu. I. Sorokin (USSR) carried out original work using C^{14} to determine the primary efficiency of reservoirs for photosynthesis and chemosynthesis and to study the feeding processes of water invertebrates which act as food for fish.

The meeting devoted to the behavior of fission products in soil, plants and animals was interesting.

V. M. Klechkovskii and I. V. Guliakin (USSR) presented a voluminous report in which, in particular, a new phenomenon was described — a different distribution of yttrium in plants when it enters from without and when it is formed inside the plant as a result of the decay of Sr^{90}.

Bauer (Sweden) reported a method of observing strontium and calcium metabolism in man using the short-lived isotopes Sr^{85} and Ca^{47}. The method made it possible to follow regenerative processes in bone fractures and to detect bone tumors.

Due to the important role of milk, with which radiostrontium is introduced into the child's organism, there was interest in a report by Middleton et al. (England), devoted to the study of the metabolism of strontium, iodine and tellurium in dairy cows. The authors mentioned that 90% of the radioactivity of milk from atomic explosions was accounted for by radioactive strontium and iodine.

Ward (Ghana) reported the results of the first experiments performed on the toxicity of Sr^{90} to monkeys. It was found that monkeys, expecially young ones, had a very high sensitivity to the effect of Sr^{90} radiation: a dose of Sr^{90} in the bones of monkeys, exceeding the "permissible" level (1000 $\mu\mu$C of Sr^{90}/1 g Ca) in all of 18 cases, was sufficient to produce a lethal effect over 3 years.

The conference was officially closed on September 17th.

On September 19th the Soviet delegation held a press conference at which information was given on the situation and prospects for the application of isotopes in the USSR. The head of the Soviet delegation gave information on the construction of large scale undertakings in the USSR for the production of isotopes.

During the conference, scientists of the Soviet delegation had many meetings and conversations with scientists of foreign countries, during which, in particular, there were discussions on ways of establishing closer contacts between Soviet scientists and scientists of the USA, England, France and other countries.

During the working period of the conference, 12 public lectures were given. Various examples were given in the popularized lectures on the use of isotopes in industry, agriculture, medical diagnosis and treatment and scientific investigations. Data were given (Libby — USA) on the expected economic effect of the use of isotopes. In particular, it was pointed out that the USA had saved 3-5 billion dollars in the last 4-5 years as a result of the use of isotopes.

Soviet scientists gave two lectures: A. P. Vinogradov on the theme: "Isotopic composition of the earth and meteorites" and A. A. Nichiporovich — "The method of labelled molecules and the problem of photosynthesis," which were received with great interest by the listeners.

During the conference, the members of the Soviet delegation visited more than 20 scientific and industrial French organizations and thus established a closer contact with the scientific and business spheres of France and became acquainted with the organization of scientific research and the equipment and planning of laboratories.

The overall result of the conference was to reaffirm that radioactive isotopes are being used all the more widely for solving problems in scientific research as well as in industry. The rational application of radioisotopes nowadays allows the solution of problems, which not too long ago would have seemed fantastic.

The conference demonstrated the enormous value of establishing scientific contacts and the live exchange of opinions between scientists of various countries in the general inclination towards the peaceful use of atomic energy — the greatest conquest of human thought.

P. Savitskii, E. Finkel', V. Serenko, N. Bulatova

INTERACTION OF NEUTRONS WITH NUCLEI

An international conference on the interaction of neutrons with nuclei was held at Columbia University (New York, USA) from September 9-13, 1957. More than 200 physicists participated in the conference. The delegates from the Soviet Union were V. V. Vladimirskii, N. A. Vlasov, L. V. Groshev, V. I. Mostovoi and M. I. Pevzner.

About 70 lectures and short reports were given at the sessions. The subjects may be divided into the following basic categories: 1) Slow-neutron spectroscopy. 2) Interaction of neutrons with fissionable nuclei and fission physics. 3) Interaction of fast neutrons (up to 20 Mev) with nuclei. 4) Gamma rays accompanying neutron capture in nuclei.

The first session was devoted to review papers by Bethe (Cornell University, USA), Hughes (Brookhaven, USA) and Taschek (Los Alamos, USA). Bethe surveyed the present status of the theory of nucleon interactions with nuclei and analyzed the successes and shortcomings of the optical model of the nucleus in which a complex potential is employed.

This model does not take into account single-particle inelastic collisions of nucleons; this fact explains the observed discrepancy between theory and experiment. In particular, the experiment indicates that the imaginary part of the potential is a function of nucleon energy, a finding which is surprising at first glance. In this connection Bethe emphasized the great value of the analysis given by Bruchner which is based on a consideration of direct nucleon-nucleon collisions with the Pauli principle taken into account. This analysis should be improved by taking account of the surface effect, i. e., the fact that the nucleon density at the surface is smaller, and consequently that the limitations imposed by the Pauli principle are weaker. In the optical model this means an increase in the imaginary part of the potential close to the surface as compared with the value inside the nucleus. From this point of view the experimentally observed reduction in the imaginary part of the potential in heavy nuclei can be understood in terms of the reduction in the ratio of surface to volume.

Hughes analyzed the results of work in slow-neutron spectroscopy (Hughes's paper is published in the present issue of this journal).

Taschek summarized the basic trends of work being carried out chiefly at Los Alamos. The first problem is an exact measurement of neutron fluxes over the entire available energy region. In this connection he pointed out the necessity for exact measurements of the cross sections for the $B^{10}(n, \alpha)$, $Li^6(n, \alpha)$ and $He^3(n, p)$ reactions which are used in neutron detection. In particular, it is of great interest to examine the behavior of the cross section close to threshold where a nonmonotonic increase with energy is observed; this effect is related to the new reaction channels which become available. A theoretical implication of this effect was given in a paper by Wheeler. The third basic problem is the investigation of spectra and angular distributions for fast neutron scattering. In this region Cranberg has observed a dependence in the temperature of the nucleus on the energy of the primary neutron; this observation has been verified and refined in later investigations. The angular distribution of inelastically scattered neutrons exhibits anisotropic components, characteristic of a direct interaction. Taschek emphasized the importance of studying the γ-rays which accompany inelastic neutron scattering and the (n, 2n), (n, p), (n, α) and other reactions. Studies of this type will require accelerators with beam intensities about one order of magnitude higher than those which are presently available.

The next four sessions were devoted to slow-neutron work.

A report given by Rainwater (USA) described a neutron spectrometer which uses the Columbia University synchrocyclotron as a pulsed neutron source. The 1,000-channel time analyzer makes use of a "fast" electrostatic memory system and a "slow" memory in which a magnetic drum is employed. With this system a resolving power of 0.01 μsec/m can be achieved with a flight distance of 35 m. Cross sections for silver, tantalum and U^{238} were shown as an example of the results obtained with this spectrometer.

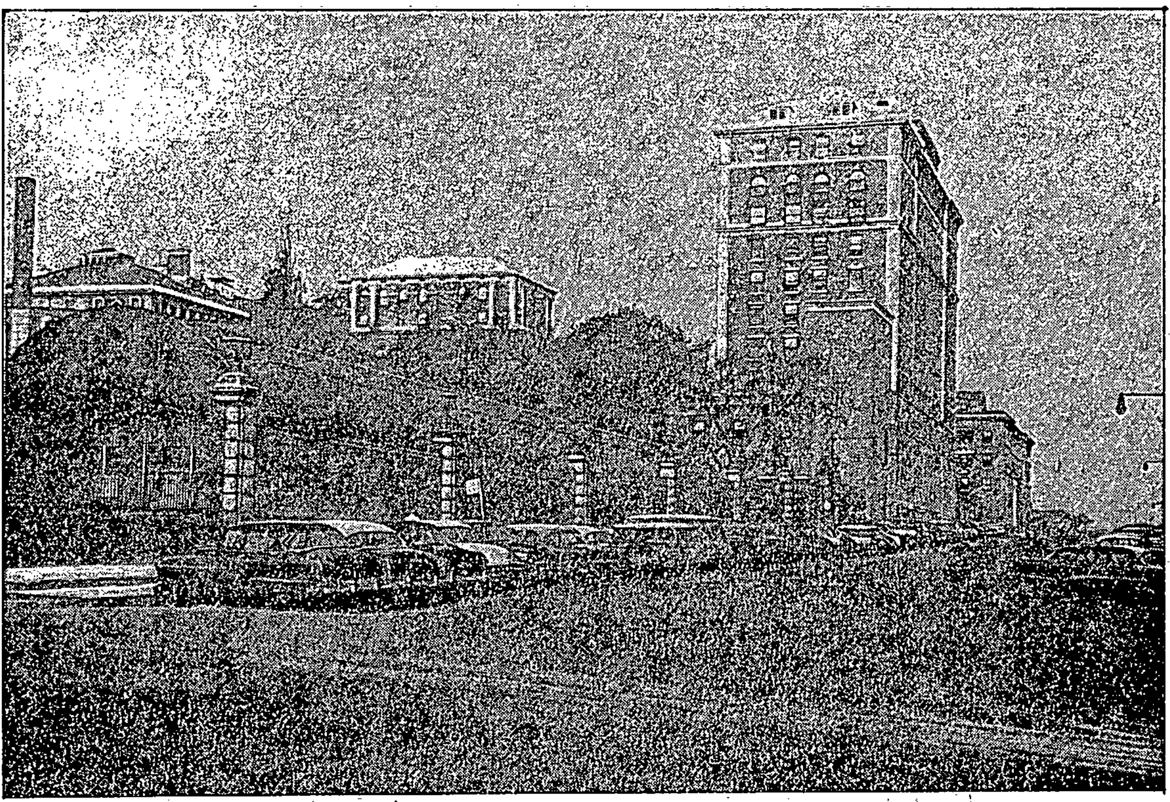

Physics building, Columbia University — site of the conference.
(Photo by N. Vlasov)

A rather sophisticated mechanical neutron selector has been built at Argonne National Laboratory (report given by Bollinger, Cote, Kennett and Thomas, USA). The neutron detectors are a liquid scintillation counter and a gas scintillation fission chamber. A resolving power of 0.01-0.015 μsec/m is achieved with a flight distance of 100 m.

A report by Hubert (Saclay, France) described a mechanical velocity selector used for eliminating higher order reflections in work with a crystal spectrometer. Using this device work has been done on the cross sections of neodymium, iridium and thorium in which the cross section for Nd^{143} indicates the existence of a negative level with $E_0 = -1.5 \pm 0.5$ ev and $\sigma_0 \Gamma^2 = 415$ barn · ev^2.

A paper by Melkonian (Columbia University, USA) was devoted to the use of electronic computing machines in analyzing data obtained with multichannel analyzers.

A group of reports presented new data on level parameters and other nuclear characteristics important for the optical model of the nucleus. A paper by Cote (Argonne, USA) presented the results of a measurement of the strength function $\overline{\Gamma_n^0}/D$ for nuclei with atomic weight ~ 50. The existence of a maximum in the strength function in this region, predicted by the optical model, was verified; however, the quantitative agreement cannot be considered too good. New results on strength functions were reported by Zimmerman (Brookhaven, USA) and

Fluharty (Phillips Petroleum Company, USA). The most interesting conclusion to be drawn from this data is the double-humped nature of the maximum in the strength function in the region A = 150. This result is qualitatively explained by the optical model when the nonsphericity of the nucleus is taken into account. The appropriate calculations have been carried out by Vladimirskii, (TTL, USSR) and by Margolis and Troubetzkoy (Columbia University, USA). These calculations were reported at the conference.

In a paper by Seth (Brookhaven, USA) the results were given for the determination of the cross section for potential scattering in 18 elements as obtained by two different methods. In accordance with the predictions of the optical model the cross sections which were found exhibit a nonmonotonic dependence on A.

Reports given by Landon (Brookhaven, USA) summarized the results of recent measurements of radiation widths, carried out with a crystal spectrometer. The accuracy of these measurements at the present time is such that in a number of cases a comparison can be made with the calculations by Blatt and Weisskopf. A group of reports (Porter, Lane, Cameron and Dressner, USA) were devoted to studies of the fluctuations in the mean cross sections, due to the distributions in magnitude of the level parameters such as neutron widths, level spacing and so on.

Participants at the conference.

(Photo by N. Vlasov)

A description and analysis of the experimental results obtained in studies of the interaction of slow monochromatic neutrons with fissionable nuclei was given in reports by Bollinger on Pu^{239} (Argonne, USA), Evans on U^{233} (Phillips Petroleum Company, USA) and Shore on U^{235} (Brookhaven, USA).

An analysis of the experimental results has been carried out using an analysis of fission based on the collective model of the nucleus. The basic conclusions of this theory (the number of channels by which fission can be realized, the distribution of fission widths, asymmetry in fission, etc.) are verified by the experimental data which has been obtained. The fission widths have a Porter-Thomas distribution with one or two degrees of freedom. This result indicates that the number of fission channels is not greater than two. In a small number of channels there is also an indication of level interference in the behavior of the fission cross section. The measured fission cross section is found to be in good agreement with a multi-term interference formula under the assumption of one fission channel. Additional evidence for the interference of levels in fission and the absence of interference in radiative capture (large number of radiated channels) is the change in η close to resonances.

Analysis of the Pu^{239} data indicates that both spin states appear in fission and the mean value of the fission widths for these states is of the same order of magnitude.

The papers given by Bollinger and Evans reported the first results of measurements of yields for fragments of different masses in neutron-induced fission in U^{233} (E_n = 1.8 ev) and U^{235} (E_n > 2 ev). These measurements indicate that in fission of the compound nucleus in different spin states the mass distribution of the fragments is different.

In a paper by Auclair (Saclay, France) which was presented by Vendryes, using a crystal spectrometer measurements were made of the probability for triple fission of U^{235} by monochromatic neutrons. Within the limits of the experimental errors (10-15 percent) no energy dependence of the probability for triple fission was found in the range 0.02-0.2 ev.

In the energy region above 0.2 ev, the probability for triple fission by neutrons which pass through cadmium and boron absorbers is the same to within the limits of experimental error.

Terrell (Los Alamos, USA) indicated that the distribution of the number of neutrons emitted in a fission event should be Gaussian and can be determined by two parameters: $\bar{\nu}$, the mean number of neutrons emitted in fission and σ, the width of the distribution for the total excitation energy of the fragments.

All experimental data on secondary fission neutrons are in good agreement with the universal formula with $\sigma = 1.08\ E_0$, where E_0 is the mean change in excitation energy for one emitted neutron. The sole exception is Cf^{252}, in which $\sigma = (1.21 \pm 0.01)\ E_0$. The width of the distribution of total excitation energy of the fragments computed with $\sigma = 1.08\ E_0$ and $E_0 = 6.7 \pm 0.7$ Mev is in good agreement with the experimental data. The change in $\bar{\nu}$ with energy of the incident neutron $\left(\frac{d\nu}{dE_n} \approx \frac{1}{E_0}\right)$ also yields a reasonable value for E_0.

Cohen (Oak Ridge, USA), reported on the design of a high-resolution magnetic spectrometer for measurements of fission-fragment energy. Measurements have been made of the energy distribution for fragments with mass 97 and 91 formed in neutron-induced fission of U^{235}. The most probable kinetic energy for these fragments is 174 and 164 Mev, respectively, while the half-width of the distribution is (11.4 ± 0.8)%. Using the spectrometer as a mass analyzer, the authors measured the width of the charge distribution (2.3 ± 0.5 charge units) for a given fragment mass chain. The magnetic spectrometer was also used to measure the probability of triple fission and the energy distribution of long-range α-particles.

Coté (Argonne, USA) presented the results of measurements for the cross sections in Pu^{240}, Pu^{242} and Am^{243} carried out with a mechanical selector.

In Pu^{240}, levels at energies of 20.4 and 38.2 ev were found in addition to the well-known level at 1.056 ev and their parameters investigated. The total cross section for Pu^{242} was measured up to E_n = 1 kev and only two levels were found (2.65 and 53.6 ev). The Am^{243} cross section was measured up to E_n = 20 ev.

The results of measurements of total cross sections for certain product nuclei of fission, carried out with the mechanical selector using samples of very small area (up to 1 mm^2) were presented by Harvey (Oak Ridge, USA). Using the measured transmission curves the level parameters for Sm^{147}, Sm^{149}, Sm^{151} and Pm^{147} were obtained. Special attention is merited by Sm^{151}, which has a level density which is several times larger and a value of Γ_n^0/D which is noticeably smaller than the other nuclei.

No resonances were found for I^{129} and Zr^{93} in the neutron energy region 1-100 ev.

Papers by Bigham and Tunnicliffe (AE, Canada) were devoted to measurements of the fission cross section for a Maxwellian neutron spectrum at temperature of 20°C.

Bigham reported the following results for the relative measurements:

$$\frac{\sigma_f(U^{233})}{\sigma_f(U^{235})} = 0.9323 \pm 0.0013,$$

$$\frac{\sigma_f(Pu^{239})}{\sigma_f(U^{235})} = 1.4056 \pm 0.009,$$

$$\frac{\sigma_f(Pu^{239})}{\sigma_f(U^{233})} = 1.5048 \pm 0.009,$$

$$\frac{\sigma_f(Pu^{241})}{\sigma_f(Pu^{239})} = 1.351 \pm 0.006.$$

The ratio of the U^{233} and U^{235} cross sections is in good agreement with the international values for these cross sections which have been adopted at the present time. The ratios of the fission cross section in Pu^{239} to the cross sections in U^{233} and U^{235} are high by 3% as compared with the corresponding ratios computed on the basis of the international cross sections.

Tunnicliffe reported on results of a measurement of the ratio of the fission cross section in U^{233} to the capture cross section in gold. From this ratio and the gold activation cross sections, $\sigma_{2200\,m/sec} = 98.8 \pm 0.3$ barns and the half life U^{233} $T_{1/2} = (1.611 \pm 0.008) \cdot 10^5$ years, the absolute value of the fission cross section in U^{233} is obtained: $\sigma_{f\,2200\,m/sec} = 524 \pm 4$ barns.

Papers by Westcott (AE, Canada), Dayton and Pettus (Babcock and Wilcox Company, USA) were concerned with measurements of resonance intervals.

Westcott presented a method and results of the measurements of the ratio of the resonance interval to the thermal integral in Pu^{240} by a determination of the cadmium ratio for Pu^{240} and gold in a neutron beam by counting the capture γ-rays.

The measured ratio

$$\frac{\int \sigma_c \frac{dE}{E}}{\sigma_{c\,2200\,m/sec}} = 25.5 \pm 5\%$$

is used for determining the level width at 1.056 ev ($\Gamma = 39 \pm 2$ Mev) and the thermal neutron capture cross section in Pu^{240} ($\sigma_c = 335$ barns). In the latter case the resonance integral in Pu^{240} is taken as 8700 barns.

Dayton reported on the results of measurements of the effective resonance integral for thorium and thorium oxide carried out with cylindrical and flat slabs of different diameter and thickness. The resonance integral was determined by using boron and the "danger coefficient" technique.

The obtained experimental results are consistent with the following:
for Th

$$\sigma_{a\,\mathrm{eff}} = 2.9 + 24.1\sqrt{\frac{S}{M}},\quad 0.1 \leqslant \frac{S}{M} \leqslant 1.3;$$

for ThO_2,

$$\bar{\sigma}_{a\,\mathrm{eff}} = -0.1 + 35.2\sqrt{\frac{S}{M}},\quad 0.2 \leqslant \frac{S}{M} \leqslant 1.3,$$

where S is the area of the slab and M is the mass of the slab.

The effect on the cross section of the 1/v law was not taken into account in these data.

Keepin (Los Alamos, USA)* presented an interpretation of the observed regularities in yield and half life of delayed neutrons, on the basis of the liquid drop model of the nucleus taking shell structure into account. On

---

*The paper by Keepin will be published in this journal.

the basis of this model, for each group of delayed neutrons a prediction has been made of the most probable precursors. Using this choice of the most probable precursors and the Glendenin-Pappas postulate of equal charge displacement, the author has computed the yield of delayed neutrons for six investigated materials (U^{233}, U^{235}, U^{238}, Pu^{239}, Pu^{240} and Th^{232}). The results of the calculation are found to be in agreement with the experimental data and furnish a reasonable explanation for the increase in the total yield of delayed neutrons in going from Pu^{239} to Th^{232}.

Northrop (Los Alamos, USA) presented the results of an investigation of fission which accompanies deuterum stripping (d, pf). The process is similar to fission in neutron capture, but in contrast with the (n, f) reaction, the neutron which is captured as a result of deuteron stripping can have either positive or negative energy. For example, it is possible to determine the "threshold" for fission in nuclei such as U^{235}. A second peculiarity is the fact that a neutron with small or even negative energy can introduce an orbital moment different from zero into the nucleus. The report contained the measured cross sections for the (d, p) and (d, pf) reactions in U^{235} and U^{238} for a deuteron energy of 14 Mev. In U^{238} the dependence of the cross section for the (d, pf) reaction is similar to the dependence for the cross section for the (n, f) reaction. In U^{235} the exponential reduction in the fission cross section extends into the region of negative neutron energy, exhibiting a wide (approximately 700 kev) maximum in the region of zero energy. A determination was made (taking into account the neutron binding energy) of the difference in the excitation energy for U^{236} and U^{239} corresponding to the fission threshold (in U^{236} the barrier is 0.6 Mev lower). The report also contained results on measurements of the angular distribution for protons which accompany fission. These results indicate the capture of neutrons with orbital moments of 2, 3 and even 4.

Three of the sessions were devoted to fast neutron interactions. The first papers in this section were concerned with the results of studies of individual resonance levels, their distribution, and determination of the strength function in the region 2-400 kev. It was concluded that the strength function is independent of the angular momentum of the captured neutron (Newson, Duke University, USA) and the surprisingly small value of the strength frunction in Y^{89} was noted (Good, Oak Ridge, USA) in the region 2-40 kev.

Data on total neutron cross sections for a large number of nuclei, obtained by time-of-flight methods in the energy range 7-14 Mev were reported by Peterson (Livermore, USA).

The results of measurements of the differential cross sections for elastic scattering of 14-Mev neutrons were presented by Nakada (Livermore, USA), Berko (Virginia, USA), and Rayburn (Argonne, USA). An analysis of these data indicates the need for introducing a different radial dependence for the real and imaginary parts into the expression for the complex potential of the "cloudy" nucleus. In addition, the intensity of scattering at higher angles requires the introduction of the spin-orbit interaction. Measurements of the differential cross section for elastic scattering on light nuclei at an energy of 1 Mev were reported by Fowler (Oak Ridge, USA) and for an energy of 1.9-3.5 Mev on Ne^{22} (from the recoil nuclei spectrum in an ionization chamber) by Sikkema (University of Groningen, Holland). These results were used to determine the characteristics of individual levels in light nuclei.

Barschall (Wisconsin, USA) reported on results of measurements of neutron polarization at 380 and 980 kev in scattering on a large number of elements with atomic weights from 50 up to 240. Neutrons with 30 percent polarization were obtained from the Li^7(p, n) reaction at an angle of 50°. In the case of 380 Mev neutrons a smooth dependence on atomic weight of the scatterer was found at angles of 55 and 90°. The maximum polarization (approximately 15 percent) was achieved at $A \approx 100$. These results were compared with the predictions of the optical model. If we take potentials in the optical model which are in good agreement with the total neutron cross sections the data on polarization is in sharp disagreement with the optical model for any reasonable assumptions as to the spin-orbit interaction.

Inelastic scattering of fast neutrons was considered in reports by Cranberg (Los Alamos, USA), Naggiar (Saclay, France), Nakada (Livermore, USA) and Glasoe (Brookhaven, USA).

Cranberg reported results of studies on inelastic neutron scattering at 0.55, 1 and 2 Mev on U^{238}, U^{235} and Pu^{239}. At Saclay a resonance has been found in the inelastic scattering cross section for Fe^{56} and I^{127} at approximately 1.5 Mev. The angular distribution of inelastically scattered neutrons is predominantly isotropic, but for certain components of the sepctra, an anisotropic distribution, indicating the existence of a direct interaction, was found. The γ-rays characteristic of inelastic neutron scattering were discussed in a report by Freeman

(Harwell, England). The γ-ray spectrum and the yield of various γ-lines as a function of neutron energy were investigated. The parameters of several levels in F^{19} and Na^{23} were determined.

Bonner (Rice Institute, USA), in his report, discussed cross sections for radiative capture in fluorine in the energy range 20-1700 kev. Fifteen resonances were found (from 2 to 15 ev) and the widths Γ_γ were determined. The capture cross section varies from 620 mbarns at 27 kev to 0.15 mbarns at 1.640 kev.

The work on (n, p) and (n, α) reactions was reported by Allan (Harwell, England), Colli (Milan, Italy), Crimeland (Norway), Shapiro (USSR — the report was read by Pevzner) and March (Glasgow, England). A "giant" resonance, known from other work on the neutron interactions was reported (Colli, Italy). In the work reported by Shapiro (and a group of co-workers) a deviation from the 1/v law was found for the He^3 (n, p) reaction in the energy region 0-20 kev, indicating the existence of an excited state of He^4, corresponding to a negative energy for the neutron.

Measurements of the cross section for the (n, 2n) reaction at E_n = 14 Mev for several elements from deuterium to bismuth measured with a liquid scintillator volume of 900 liters was reported by Taylor (Livermore, USA).

An investigation of the neutron spectra for the (p, n) and (d, n) reaction in light nuclei was given in two reports by Vlasov (USSR). In the first the Be^6 nucleus was found and the energy of its ground state was determined. The existence of an excited state for He^4 at 22 Mev was verified; this was found earlier from the behavior of the cross section fot the T(p, n) reaction.

The neutron spectrum for D(p, n) (3.5-3.9 Mev) and a comparison with the calculations of Frank and Hammel were discussed in a report by Ferguson (Harwell, England).

Cranberg discussed the energy dependence of the cross section for neutron induced fission in U^{238} close to threshold. The results obtained at Oak Ridge indicate a sharply nonmonotonic increase in the cross section beyond threshold, apparently connected with the appearance of new fission channels and inelastic scattering as the neutron energy is increased. In a report by Diven (Los Alamos, USA) results were presented of measurements of the ratio of the cross section for radiative capture of the fast neutron to the fission cross section in U^{235}.

The last day of the conference was devoted to γ-rays which are produced in neutron capture in nuclei. A survey paper on this subject was read by Bartholomew (Chalk River, Canada) who discussed methods being applied for investigation of neutron capture γ-rays and analyzed the nature of the γ-spectra for elements in different atomic-weight regions. The problem of relative intensities for E1-, M1- and E2-γ-transitions was considered in some detail. Reports were given on the results of new measurements carried out at Chalk River with a new improved spectrometer (resolution of 0.8-1 percent) for the high energy region and with a crystal diffraction spectrometer for low energies (resolution of 0.3 percent at 1 Mev). Results were presented for weakly absorbing elements (lithium, boron and nitrogen) as well as for titanium and tantalum; the latter were measured with greatest resolution with both types of instruments.

In the next two papers, Groshev (USSR) reported on certain results of studies of capture γ-rays carried out with a magnetic spectrometer using electron recoil. As is known, in these investigations considerably more data on the capture γ-ray spectrum are obtained than in work carried out at other laboratories since the investigations covered a wider γ-ray energy range: from 0.3 to 10-12 Mev.

The first of the reports was devoted to γ-rays associated with radiative capture of thermal neutrons in even-even nuclei with rotational levels. In these elements the γ-ray spectra exhibit a sharply-defined feature, the existence of a group of intense line with energies of the order of 1 Mev; these lines are not present in other types of nuclei.

The second report considered the features of γ-transitions in light odd nuclei which are formed in thermal neutron capture.

The material in these reports is given in greater detail in articles published in the "Journal of Atomic Energy" by Groshev and Demidov (No. 8, 1957)* and Groshev, Demidov, Lutsenko and Pelekhov (cf. this issue).

Work reported by Schultz (Yale University, USA) which was carried out with a scintillation spectrometer, was devoted to measurements of the capture γ-ray spectra produced during the time of flight of monochromatic neutrons with energies corresponding to the production of various resonance levels. γ-spectra were obtained

---

* See C. B. Translation.

for neutrons with energies of 0.096, 0.86 and 4.9 ev (Sm^{149}); 3.4 ev (Sm^{147}); 8.2 ev (Sm^{152}); 0.46, 0.58, 6.1 and 9.6 ev (erbium) as well as spectra corresponding to a number of resonances in indium and hafnium. The gamma spectra for Sm^{149} are identical and differ from the γ-spectra for Sm^{147} and Sm^{152}.

An interesting report was read by Trumpy (Norway) concerning measurements of the degree of angular polarization of γ-rays produced in capture of polarized neutrons by nuclei. These measurements make it possible to draw conclusions as to the spins of certain nuclei. The results given in the report are contained almost completely in a paper in "Nuclear Physics" (2, 664 (1957)).

The last report at the conference was that of Sargent (Massachusetts Institute of Technology, USA). This report described the use of a time-of-flight method to measure the spectra of photoneutrons produced in bismuth, gold and tantalum by the bremsstrahlung generated by 17 Mev neutrons from a pulsed linear accelerator. In the region below 3 Mev the neutron spectra for the three indicated elements are given by the exponential relations of the form $e^{-E/T}$ where T assumes the values 0.8, 0.58 and 0.45 Mev, respectively, for bismuth, gold and tantalum. The fast neutron fraction is about 2-8 % of the total number. These are approximately in the ratio Bi : Au : Ta = 4 : 2 : 1.

One of the basic conclusions reached at the conference is that the crystal-ball model of the nucleus furnishes a reasonably good description of the interaction of neutrons with the nucleus.

However, there are a whole series of discrepancies in the details of the theoretical predictions as compared with the experimental data. These discrepancies point to both nonuniform "cloudiness" in the nucleus and the need for taking into account various effects such as nonsphericity, spin-orbit coupling, excitation of rotational levels or even variation of the basic parameters of the complex potential in going from a given nucleus to its neighbor.

N. Vlasov, L. Groshev, V. Mostovoi and M. Pevzner.

AERORADIOMETRIC TECHNIQUES USED IN PROSPECTING FOR VARIOUS VALUABLE ORES

(Based on material from the foreign literature)

From the very first application of aeroradiometric techniques in prospecting for radioactive ore, much of the aerogeophysical work was carried on with the simultaneous use of radiometric and magnetometric apparatus. This made it possible to gather additional data, without incurring any great increase in expense, on the geology of a given area and the radioactivity of its rock constituents, and also facilitated prospecting for deposits of not only radioactive, but also magnetic, minerals,

Airplanes equipped for simultaneous magnetic, electromagnetic, aeroradiometric and aerophotosurvey operations are given the name "flying geophysical laboratories" [1, 2].

The work organized by a Texas company showed that registering weak radioactivity variations in alluvia made it possible to carry out a reliable mapping operation, in a number of cases, of the rocks and structures subjacent to the alluvia.

It was established that the presence of alluvia of even considerable width does not preclude the possibility of carrying out geological mapping.

Similar results were reported in Australia and Canada where, with the aid of aeroradiometric photography, discrete rock complexes were mapped, contact areas were followed up and faults were localized [3].

Systematic studies of radioactivity distribution and geological correlation of the data obtained broaden the range of useful ores which can be detected in aeroradiometric prospecting operations.

An aeroradiometric photosurvey makes it possible to locate pegmatite veins containing valuable minerals, and deposits of rare and nonferrous metals labeled by radioactive anomalies associated with the presence of trace amounts of uranium and thorium in the deposits .

In Canada, in the British West Indies, Africa and other countries, the technique of prospecting gas and oil deposits with the aid of aeroradiometric surveying has gained wide popularity [4-6]. During 1950-1952, Canadian geophysicists undertook experimental research which demonstrated that the radioactivity of rocks overlying oil and gas deposits is sharply diminished, while the radioactivity response picks up sharply as the periphery of the deposit site is approached. This phenomenon may be explained by the vertical diffusion of dissolved radioactive substances in peripheral segments of the deposit, while the deposit itself is impermeable to diffusion flux. The technique of radiometric oil prospecting boils down to constructing a series of profiles on which gamma-radiation intensity curves are plotted. The flights are carried out at an altitude range of 60-160 m [5]. Despite a whole series of factors which act to complicate the interpretation of the data so obtained, the method is accepted as effective in oil prospecting.

The aeroradiometric surveying method has recently come into use for purposes of diamond prospecting in South Africa. Aeroradiometric measurements serve for the pinpointing of kimberlite tube-like veins characterized by a local dropoff in radioactivity on a high background due to interfering granitic rock species. Tree-grazing flights are at an altitute of 60-80 m. Radiometric prospecting of the yields of kimberlite tube-like veins is carried out with the simultaneous use of findings from magnetometric surveying [7].

The USA Atomic Energy Commission has published a communication on the priority of utilization of aeroradiometric data, in which it is noted that aerogeophysical work will be carried out only in combination with geological research and will be of use not so much for locating anomalies as for localizing prospective areas with the object of setting up more detailed helicopter and ground-based research.

Ia. G. Ter-Oganesov,
T. I. Gvaita, Iu. V. Roshchin

LITERATURE CITED

[1] Aviation Week 64, No. 2, 74 (1956).

[2] Canad. Chem. Process 37, No. 13, 66 (1953).

[3] W. C. Kellog, Mines Mag. 46, No. 7, 31 (1956).

[4] H. Lundberg, World Petrol. 23, No. 5, 109 (1952).

[5] Mining J. 243, No. 6226, 708 (1954).

[6] Engng and Mining J. 1954, No. 7, 266 (1953).

[7] Photogramm. Engng. 20, No. 4 (1954).

CONFERENCE OF YUGOSLAV PHYSICISTS

The Second Conference of Yugoslav Physicists convened during the summer of 1957. The conference was organized along the line of a "summer school", such as have been in progress for many years in France, Italy and other countries.

The first Conference in Yugoslavia took place in 1956, based on the topic "The Structure of the Atom." The 1957 Conference was devoted to nuclear reactions. The small resort town of Cikat, located on Losinj island, in the Northern Adriatic near the Triestian peninsula, was selected as the site for the conference.

In contrast to the 1956 Conference, where the audience was composed solely of Yugoslav physicists, about 30 physicists from various countries attended the second conference. The largest representations were from France and Italy. Physicsts from both parts of Germany, from Denmark, Sweden, the USA, the USSR, Israel, Mexico and Finland also attended.

Lectures were devoted to the following topics: "Coulombic Excitation of Levels and the Collective Model of the Nucleus" B. Mottelson (Denmark); "Optical Model of the Nucleus" C. Porter (USA); "Deuteron Stripping Reactions" A. Messiah (France); "Photonuclear Reactions" K. Wildermuth (West Germany); "High Energy Nucleon Scattering" Ia. Smorodinskii (USSR).

The lectures embodied both a review of theoretical papers and an account of the trends taken by current research. For instance, the lecture delivered by C. Porter took up the problem of the distribution function of level widths. B. Mottelson told of his recent papers on the tie-up of the collective model of the nucleus with the shell model (calculation of interaction of points in the shell model),etc.

The evening seminars also stimulated great interest. One of the seminars was addressed to the question of the contemporary state of the theory of β-decay. As is known, after the first successes of the two-component ("longitudinal") neutrino model, results of new experiments were published which refuted that model. The seminar heard discussion of the possible consequences ensuing from the new experiments and, in particular, of the symmetry existing between electron and positron decay. One of the seminars was devoted to a discussion of the papers on the theory of superconductivity, which have recently been advanced by Cooper, Bardeen and Schrieffer.

The Italian physicists Facchini and Colli gave an account of their work with neutrons of 14 Mev energy. Conjot (France) told of her research on inelastic neutron scattering by iron and iodine nuclei.

Cindro (Yugoslavia) gave an account of attempts at observation of photon scattering by a Coulomb field (Delbruck scattering).

The results of theoretical researches were treated in papers presented by Alag (Yugoslavia) "On Pseudoscalar Coupling in β-Decay Reactions" and Sawicky (Poland) "On the Polarization of Nucleons in Deuteron Photodisintegration."

The problem of the technique of neutron cross section measurements was taken up in a report delivered by Kazachkovskii (USSR).

At the last seminar, Zupancic (Yugoslavia) told of experiments directed at investigating the structure of "giant" resonance in photonuclear reaction in oxygen, started in the betatron at Ljubljana.

After the conference, the Soviet delegates had the opportunity of becoming acquainted with physics institutes in Belgrade, Zagreb and Ljubljana. These are three moderately sized institutes, organized after the war. They have only recently begun their activities.

In Belgrade, a reactor is under construction at the Boris Kidric Institute; at Zagreb, a cyclotron (16 Mev deuterons) is being built at the Ruder Boskovic Institute; and at the Jozef Stefan Institute in Ljubljana, a betatron is in operation and a Van de Graaff generator is under construction. In all three institutions, there are chemical and biological sections which are conducting interesting work.

Aside from the work reported at the Conference, noteworthy work is under way, on spectroscopy at the laboratory of M. Mladjinovic, on nucleon polarization in the stripping reaction at the laboratory of M. Juric at Belgrade, and work by a theoretical group headed by V. Glazer in Zagreb.

The physicists of Yugoslavia maintain active contact with physicists in many countries; the conference at Losinj is an example of such ties. This acts as a substantial aid in speeding up the process of development of physics in their own country. Coming together in "summer schools" provides good chances for discussion. My feeling is that the organization of such a "school" among us in the USSR would render a valuable contribution.

Ia. A. Smorodinskii

DEVELOPMENT OF ATOMIC ENERGY IN INDIA

The inadequacy of oil and coal resources in India is compensated for by the presence of extensive reserves of atomic raw material. These reserves are equivalent to 600 billion tons of coal, which is 15 times greater than the known coal reserves in India. In particular, uranium reserves are assessed at 12-14 thousand tons, thorium at 150-180 thousand tons [1].

Of the total uranium reserves, approximately 7000 tons are contributed by monazite sands in the states of Travancore-Cochin (now Kerala) and Madras. The uranium content in the monazite amounts to from 0.2% to 0.4%. Up to 4000 tons are assigned to the Singhbum site and up to 3000 tons of uranium are concentrated in deposits at Aravalli, Khetra, Dariba and Khandeli. The uranium content in these ores is evaluated at 0.03-0.1%.

In addition to uranium, monazite sands contain sizable amounts of thorium. India's thorium reserves are based for the most part on the Travancore monazite sands. In the same state, a variety of monazite is mined — sheralite — which contains up to 29% thorium oxide and up to 4% uranium oxide.

In pegmatite mica deposits in Bihar, there have been found several new sites yielding niobium, tantalum, beryllium and some uranium-containing minerals. Large beryllium deposits exist in the state of Rajastan and in the north of the state of Bihar, whose yields have reached several hundred tons annually. Appreciable reserves of zirconium are available in ilmenite sands found in the state of Travancore-Cochin [2]. A deposit of a rare mineral — brannerite — containing uranium and titanium, has been discovered in the country [3].

The following basic enterprises are working on the processing of the raw material in India.

A plant in Allepey (State of Travancore-Cochin), built in 1952, processes metallic thorium. The original productivity of the plant (1.5 thousand tons of monazite annually) has been doubled at the present time.

A factory at Trombay (State of Bombay), built in 1955, processes crude thorium and uranium-rich concentrates. The original plant output (roughly 200 tons of thorium nitrate annually [4]) has since been increased by almost 5 times [5].

A factory located at Ghatsila (State of Bihar) undertakes the extraction of uranium from the waste products of copper ore processing. A pilot plant in operation there is scheduled to process 200 tons of copper ore screenings daily.

The construction of a series of other industrial enterprises for the mining and processing of atomic raw material is scheduled for the immediate future. In particular, planning has been completed and installation orders issued for the first uranium concentrating mill producing metallic uranium from uranium concentrates. The factory will start operating about the middle of 1958 [6]. The construction of processing mills for beryllium and zirconium production is on the drawing boards. A decision has been made to build a plant for heavy water production with a productivity of 10-12 tons annually [7]. It has been suggested that the plant should be in operation by 1960. According to the suggestion of the Committee on Atomic Energy (founded in 1948, chairman Homi J. Bhabha), heavy water production should be put into shape to meet the needs of all newly arising chemical fertilizer businesses.

August 1956 saw the starting up of India's first nuclear pile (swimming-pool reactor, 1000 kw power). The pile was built for the most part by the efforts of Indian engineers and most of the installation and instrumentation was also of Indian manufacture.

The following two piles are still in the stages of planning and construction:

1. A Canadian-Indian reactor, an accord for the building of which was signed between Canada and India on April 28, 1956. A reactor with 40 thousand kw thermal power (Canadian Chalk River NRX model) will be built at Trombay. The total construction costs should surpass 5 million pounds sterling [8]. This pile will operate on natural uranium fuel with heavy water as moderator. It is intended for the preparation of radionuclides and for the study of the properties of various materials when subjected to bombardment. The startup of the pile is scheduled for March,1958.

2. Planning and preparation for installation stages of the heavy water reactor "Zerlina" should be completed by the end of 1957. This zero-power reactor will be used for carrying out scientific research work (especially in the field of biology) and for the training of engineers and technicians. The reactor will be heavy-water moderated with combined uranium-thorium fuel. The startup should take place toward the end of 1958.

It has been suggested that the new Indian reactors be fueled with natural or weakly enriched uranium, using graphite or beryllium oxide as moderator, and a gas coolant system.

In India's atomic energy development program, the construction of atomic-fuel electric power stations takes priority. In an address at the startup of India's first pile, Dr. H. J. Bhabha stated that India has need of the construction of small-sized atomic power plants of 20-50 thousand kw power.

The Atomic Energy Department (founded in 1954, seat located at Bombay) projects the construction of several atomic electric power plants in the coming five years. According to estimates by specialists, 50,000 kw atomic electric power stations would provide electric power at a cost of 0.5 anna per 1 kw-hour. (In 1955, the cost of power for industrial purposes reached 0.754 per 1 kw-hour, and power costs for other needs, especially in cities remote from power stations, ran as high as 1.2 anna per 1 kw-hour.)

India has already joined in a project with the French Commission de l'Energie Atomique for building atomic electric power stations, scheduled for several years hence. The basic installation equipment for these stations will be imported, but a considerable portion of the instrumentation and materials used, including the graphite and uranium, will originate in India.

It has been announced that the construction of the first atomic-fuel electric power plant will probably take place in the Ahmedabad area [9], since that area is far from the coal mining areas of Bengal and Bihar, and since the only coal-consuming electric power station supplying electric power to Ahmedabad burns up a thousand tons of coal daily. Dr. Bhabha spoke on the necessity of building an atomic electric power station in the Delhi region, which is without water power or a fuel base [10]. Word was also given of the possibility of building an atomic electric power station in Rajastan.

The principal center in India for scientific research work in the field of nuclear physics is the Institute of Atomic Energy at Trombay. Over 300 scientific workers are employed, and their number will have swelled to some 900 by 1959. The Institute boasts three departments: physics, chemical research and engineering. There is also a health physics service.

Among the leading scientific research nuclear physics institutes of India must also be counted the Tata Institute of Basic Research in Bombay, founded in 1945 (director of the Institute: Dr. H. J. Bhabha), the Calcutta Institute of Nuclear Physics (the laboratory of the Institute owns a 32-inch cyclotron); the Indian Agricultural Research Institute at New Delhi, where research is carried out on the uses of tracer isotopes in agriculture, and a number of others. In December 1956, construction was started on a nuclear physics laboratory at Andhra University.

The Indian government has approved a broad program encompassing the training of specialists for atomic industry. A special school has been instituted at the Department of Atomic Energy, where, beginning with July 1957, an annual training course will accomodate 250 college and university graduates.

S. Baranov

LITERATURE CITED

[1] H. J. Bhabha, The need for power in India during the next years and the possibilities of the economic use of atomic power (Report No. 868, Presented by India at the International Conference on the Peaceful Uses of Atomic Energy, Geneva, 1955).

[2] Indian Commerce and Industry, 12, 18 (1956).

[3] The Times of India, 29, IX (1956).

[4] Ind. Min. Stand., 109, No. 2767 (1954).

[5] Atom. Industry, January 1957, p. 3.

[6] The Hindu, 22, XII (1956).

[7] The Statesman, 19, V (1956).

[8] Nuclear Engng. 1, 3 (1956).

[9] The Times of India, 23, I (1957).

[10] The Eastern Economist XXVIII, 4, 131 (1957).

ANNIVERSARY CELEBRATION OF THE CZECH ADVANCED TECHNICAL SCHOOL

1957 marked the 250th year since founding of the Czech Advanced Technical School in Prague. It is the oldest educational institution of its kind in Europe.

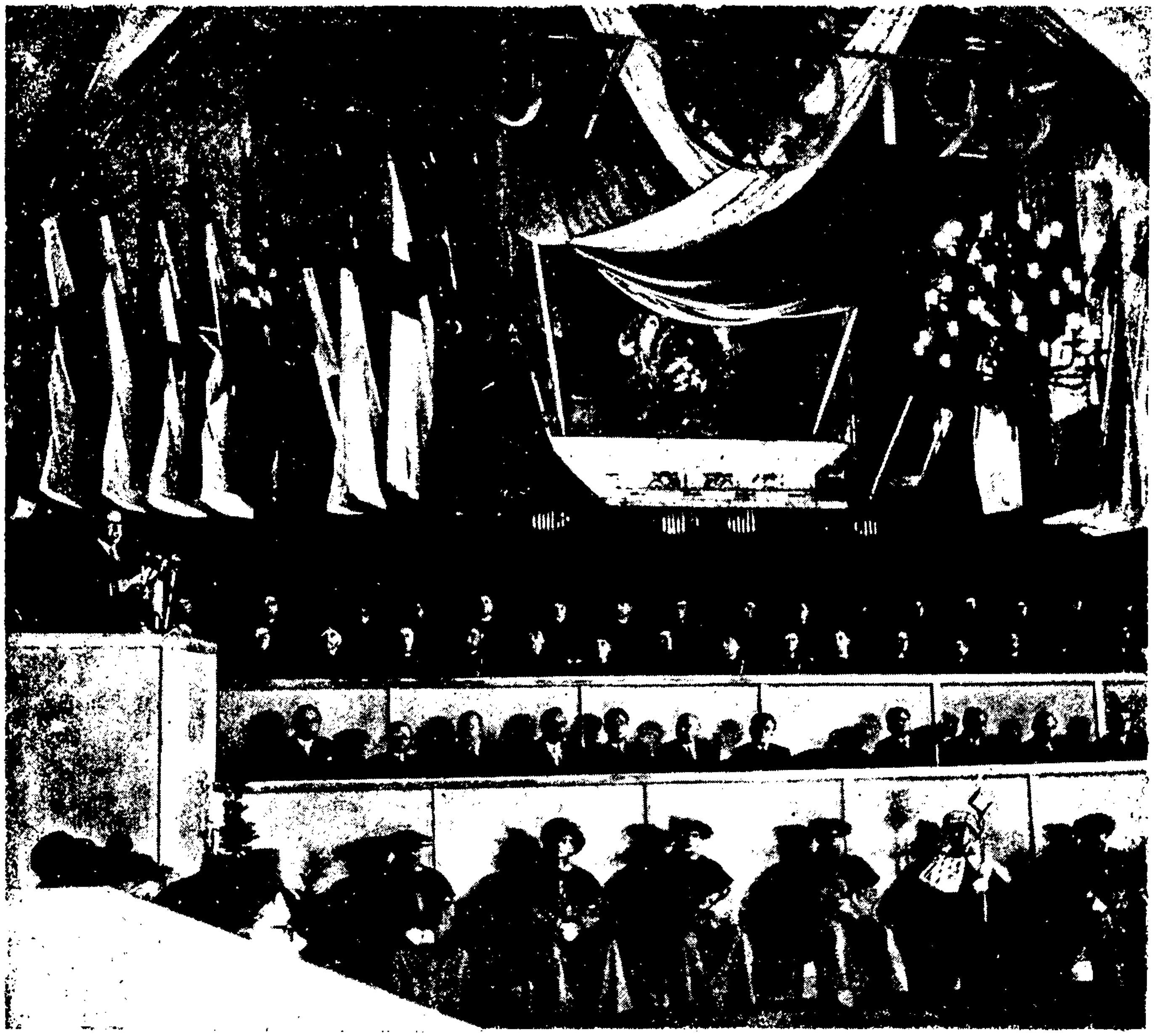

The inaguration of ceremonies dedicating the 250th anniversary of the founding of the Advanced Technical School (Vyssi Technicka Skola) in Czechoslovakia. Mounted on the tribune of Vladislav Hall in Prazsky Hrad is the President of the Czechoslovak Republic, Antonin Zapotocky.

photo by Jiri Rublic.

150 scientists from 23 nations were in attendance at the solemnities in Prague marking the anniversary jubilee.

Soviet science was represented by a sizable contingent of scientists. Among them were Academicians M. P. Kostenko (Leningrad), N. S. Streletskii (Moscow), Director of the Consolidated Institute for Nuclear Research Professor D. I. Blokhintsev, Director of the Leningrad Polytechnical Institute Professor V. S. Smirnov, Professor T. A. Nikolaev (Moscow) and others.

Participating in the anniversary ceremonies were the leaders of the Czechoslovak Communist Party and of the national government: A. Zapotocky, A. Novotny, V. Siroky, V. Konecky, and others.

Solemn act of awarding degree of "Honorary Doctor of Technical Sciences of Czechoslovakia" to the Director of the Consolidated Institute for Nuclear Research at Dubno, D. I. Blokhintsev.

photo by Jiri Rublic.

On the day initiating the ceremonies at Charles University, the degree of "Honorary Doctor of Technical Sciences of Czechoslovakia" was conferred on Professors D. I. Blokhintsev (USSR) and M. Roschke (Switzerland). This ceremonial was consummated in the ancient Karolinum assembly hall and was maintained in the spirit of time-honored traditions.

On the second day, D. I. Blokhintsev delivered a lecture, "On the Physical Basis of Atomic Energy" and M. Roschke delivered a lecture entitled "On the Principles Underlying Materials Endurance Analysis." Panel sessions were then convened, where Czechoslovak scientists and their guests read a large number of scientific reports on various branches of technical advances.

The guests visited a number of institutes and industrial enterprises in Czechoslovakia. The Director of the Nuclear Physics Institute Professor C. Simane acquainted the guests in detail with the work of the Institute. Theoretical and experimental work carried on by scientists at the Institute is correlated with the lines of investigation pursued at the Consolidated Institute for Nuclear Research at Dubno and several other Soviet scientific institutions. The work of the Institute has been even more expedited by setting into operation a number of additional new pieces of equipment: a physics research reactor, an accelerator and new laboratories – one for radiochemistry and one for physics research. Czechoslovak scientists entertain a favorable perspective for the development of all the more vital aspects of present-day atomic science: high-energy physics, neutron physics, applied physics (atomic electric power stations, reactor construction engineering, etc).

The anniversary jubilee of the Czech Advanced Technical School in Prague was an important contribution to the cause of strengthening international collaboration among scientists. It was a demonstration of the unity of ideas and interests of scientists from many nations.

M. Lebedenko

USES OF ATOMIC POWER IN SWEDEN

From September 2 to September 14, 1957, a seminar was held at Lund University (Sweden) on the theme "Man and Machine," organized by the Student Union together with other organizations. Sixty-five representatives from 38 different countries, including a delegation from the Soviet Union, took part in the work of the seminar. Eleven lectures were delivered and several general discussions held.

Lund University.
photo by author.

Much interest was stimulated by a lecture delivered by the Swedish engineer Gustav Soderval, entitled "Atomic Energy as a Substitute for Conventional Raw Materials Resources," in which he discussed applications of atomic power in Sweden.

The conventional fuel resources of the country are sufficient to meet only one-fourth of the requirements. Reserves of uranium ore are available in the country, but the ore is low grade. The utilization of atomic energy in Sweden is proposed, in the first instance, for generating heat rather than electric power, since most areas of Sweden require residential heating for 8 months out of the year. The construction of large-scale atomic-powered heating plants is proposed. One of these plants is already under construction in Stockholm and will become operative in 1960. An average of one heat power plant per year is expected to go into operation over the next decade. It is expected that heat obtained from these power plants, under the conditions prevailing in Sweden, will prove to be more economical. The building of atom-fueled heat power plants will improve Sweden's economic position, as imports of oil and coal will be reduced. On the basis of atomic-powered heat power plants, an extension of scientific research undertakings to the area of atomic energy is proposed. By 1960, the Swedes consider it necessary to have one or two powerful atomic electric power stations in shape. The first pile working on Swedish fuel was started up in 1954.

A. Petrovskii

UZHOROD SCIENTISTS AT WORK

A conversation with the Director of the "Structure of Matter" department of the physics-mathematics faculty of the Uzhorod State University, Candidate of physical-methematical sciences, Assistant Professor V. A. Shkoda-Ulianov.

The work of Uzhorod scientists occupied with research on the atomic nucleus takes on two directions: experimental and theoretical.

In the realm of the experimental, preparatory work is being carried on jointly with Kharkov Physics and Technical Institute on the arrangement of experiments to determine the excitation functions of (γ, n) reactions. The experiments will be performed using the linear electron accelerator at the Kharkov Physics and Technical Institute. During these experiments, our collaborators will strive to verify the new technique for determining the excitation functions of (γ, n) reactions, based on the utilization of the equilibrium spectrum of photons (avalanche theory).

In addition, theoretical analyses are underway in our department, utilizing the avalanche theory. These analyses, if they yield positive results, will be of assistance to geologist scouts engaged in oil prospecting. In the process, we are examining the medium of infinite thickness with the expectation that it will be possible to use the neutron yield from oil bombarded by high-energy electrons to determine and obtain the necessary data. The difficulty presented by the problem lies in the segregation of the water from the oil on the basis of the amount of neutron yield. The water contains oxygen, which can liberate neutrons in response to bombardment by high-energy electrons and photons. The oil contains carbon, which can also eject neutrons under the same conditions. In carbon, there is one threshold for photonuclear reactions; in oxygen, another. We shall clear up the question of in just which energy region the photoneutron yield from water and from oil is different to the extent that it would become perceptible, i. e., clear up whether the difference is sufficiently great to enable its being registered. But, for the time being, this is only purely theoretical work.

A number of projects are already completed or underway in the "Structure of Matter" department. For example, the collaborators working with the department are in the process of investigating the radioactivity of mineral-water sources in the Zakarpatie [Carpatho-Russia, Tatra mountain area of USSR continguous to Hungary and Slovakia]. We have before us the task of finding out the balneological value of each [mineral-water] source, i. e., whether or not it meets medical standards. Up to that point, no detailed systematic investigations had been carried out in the Zakarpatie. There were some investigations undertaken by Czech scientists, and their findings were reported in Czech publications. We are at present in the process of arranging scientific ties with them. However, as far as we know, this line of work only deals with the radium content in the mineral wells. There are some scanty bits of information available from other literature sources.

We investigated about 20 wells for their radon content, and there still remain about 200 wells, counting only those which are officially registered. We were successful in finding out that the biggest wells which we investigated possessed weak radioactivity. They are 2-3 times weaker than the Tskhaltubo * waters, but have a high rate of flow. The work will be kept up in the future.

---

* Hot springs resort in the Georgian SSR.

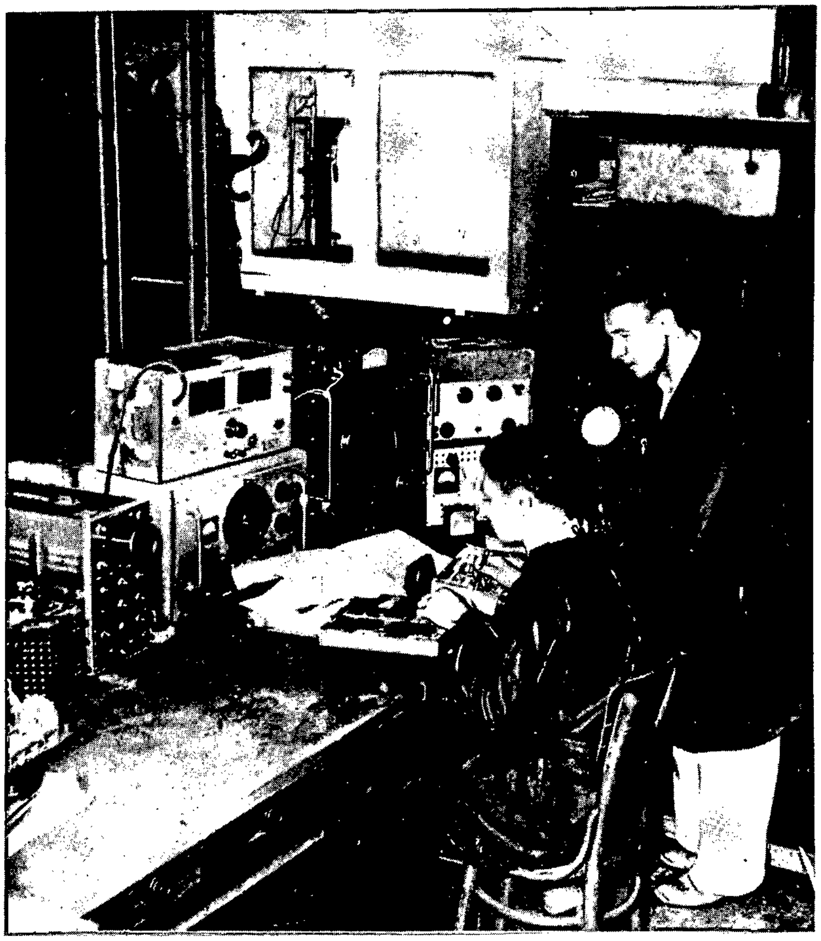

In the atomic physics laboratory of Uzhorod University. Picture shows tuning of measuring devices used for research in the field of nuclear physics.

photo by V. Parkhit'ko.

There is another group of theoretical physicists at the department working in the area of quantum electrodynamics and meson dynamics. They are engaged in work linked with the problem of overcoming the principal difficulties inherent in the present-day quantum theory. They recently computed the cross sections for several problems in theory where these difficulties are met (annihilation of antinucleons, antinucleon scattering by nucleons, meson scattering by protons, etc).

After our department organized a laboratory for the study of the physics of radioactive isotopes, we were in a position to assist scientists attached to other faculties in arranging research on the application of tracer atoms for scientific purposes. At the present time, scientists on the medical faculty are carrying on research on the effect of ionizing radiations on the sex organs and intrauterine development of animal embryos and they are studying the distribution of microbes in the animal organism and the assimilation of radioelements by bacteria.

Other topics to be investigated in thenear future at our university are those connected with the utilization of radioisotopes for the solution of scientific and practical problems.

V. P.

FRENCH SCIENTISTS VISITING THE USSR

The Soviet Union was host, in November 1957, to a delegation of the French Comissariat de l'Energie Atomique headed by Supreme Commissaire Professor Francis Perrin. During his conversation with members of the editorial staff, Professor Perrin pointed out that the French delegation intended to become familar, during its stay in the USSR, with the work of Soviet scientists and organizations whose efforts are directed toward the utilization of atomic energy for peaceful purposes. This trip was made at the invitation of the Academy of Sciences of the USSR and by the Main Control Agency on the utilization of atomic energy attached to the Soviet of Ministers of the USSR.

He spoke of the construction of the first French atomic-powered electric power station, delivering a power of 70 thousand kw, which should be ready for operation in 1958. A second station, which is still only in the planning stages, will supply 80 thousand kw power, and completion of its construction is scheduled for the end of 1959 or beginning of 1960.

In the USSR, the delegation visited an atomic electric power plant, inspected reactors of various types and became acquainted with several projects. The delegation was most impressed by an experimental prototype of a nuclear reactor slated for installation in a future high-power electric power plant, a heavy water reactor, and also the research reactor of the Academy of Sciences of the USSR. At Moscow University, the delegation became acquainted with the organizational setup of the educational system and inspected the nuclear physics laboratory. The delegation visited the V. I. Vernadskii Institute of Geochemistry and familiarized itself with some of the work accomplished at the Institute. At the Consolidated Institute for Nuclear Research, the delegation was particularly interested in the 10 Bev synchrocyclotron and proton synchrotron.

Professor Perrin stated that he first became familar with the accomplishments of the Soviet Union in the area of the utilization of the energy of the atomic nucleus at the 1955 Geneva conference on the peaceful uses of atomic energy, and that everything he had seen in the USSR during the present visit attested to the remarkable progress and to still broader horizons. F. Perrin noted the creation of various types of nuclear reactors in the USSR, making possible a selection of the most economical from among them. In the view of F. Perrin, atomic-fuel electric power stations delivering a net power of up to 2.5 million kw, such as those earmarked for construction, will assume a key place in the development of atomic power.

Professor Perrin expressed his conviction that the good relations existing between scientists and specialists of the USSR and France will be maintained in the future. The French government has already extended an invitation to a group of Soviet specialists working in the field of the utilization of atomic energy to visit France.

V. P.

THE INTERNATIONAL ATOMIC ENERGY AGENCY

In October 1957, the first session of the General Conference of the International Atomic Energy Agency, summoned to contribute to broad collaboration among the nations and to render aid to underdeveloped countries in the area of the utilization of atomic energy for peaceful purposes, convened in Vienna. Delegates from 67 countries, UN representatives and observers from the Consolidated Institute for Nuclear Research participated in the work of the Conference.

Supplementing the 13 members of the Council of Directors (Australia, Brazil, India, Canada, Portugal, Great Britain, USA, USSR, France, Czechoslovakia, Sweden, Union of South Africa and Japan), designated in accordance with Article VI of the Statutes (cf. Atomnaia Energiia I, No. 4, 166 (1956)* as a preparations committee, 10 additional members were also chosen as members of the Council of Directors (Argentina, Guatemala, Egypt, Indonesia, Italy, Korean Republic, Pakistan, Peru, Romania, Turkey). The program adopted by the Conference considered as the first stage of the Agency's work assistance to member nations in the scientific and technical training of personnel, the organization of the exchange of scientific and technical information, the realization of exchange of scientists and experts, the establishment of dosimetric standards and of safety and health rules and the coordination of work in this field on an international scale, the carrying out of reactor construction programs, etc.

In consonance with the Statutes, each particular country should be given assistance only on its request. The activity of the Agency should be closely linked with the immediate needs of its members, agreements on aid should be reached directly between the governments of the member-nations and the Agency.

The Conference also affirmed a budget and set up a revolving fund for the initiation of the Agency's activity. Cole (USA) was designated as Director of the Agency. His assistants are: Jolles (Switzerland) on administrative matters, de Laboulaye (France) on technical and operational matters, Migulin (USSR) on the training of personnel and technical information, Seligman (England) on research work and isotopes. The General Conference selected Vienna as its permanent seat. It was decided that the second session of the General Conference of the Agency be set for September 1958.

V. Chernyshev

---

*Original Russian pagination. See C. B. Translation.

BRIEF COMMUNICATIONS

USSR. A jubilee scientific session of the Institute of Physics of the Academy of Sciences of the USSR met, dedicated to the 40th Anniversary of the Great October Socialist Revolution.

Eleven review papers were heard at the session, covering the work of scientists of the Institute, including an account by V. I. Mamasakhlisov on reactions of light nuclei, a report by G. R. Khutsishvili on some interesting phenomena of β-disintegration and a report by a group of young scientific workers on investigations of the properties of heavy unstable particles.

USSR. In the vicinity of Alma-Ata, construction will begin on the Institute of Nuclear Physics of the Academy of Sciences of the Kazakh SSR. Plans call for the building of a nuclear pile and a cyclotron. Fifteen laboratories will be housed in the Institute.

USSR. The All-Union Scientific Research Institute for the Canned Food Industry is carrying on successful experiments on radiation sterilization and pasteurization of food products. The radiation of food products is accomplished using high-speed electrons and γ-rays. For example, raw meat, sterilized by irradiation, has already been preserved for a year without jeopardizing its taste qualities.

USSR. At the Research Institute for Hydrological and Meteorological Instrumentation, a device has been developed for the determination of water supplies in snow drifts. A leaden container with a source of Co^{60} γ-rays is placed in the bottom part of a metallic tube, which is allowed to sink down into a snow mantle such that the source reaches ground level. At a distance of 2.5-4 m above the earth's surface, a γ-radiation detector is attached. The time required for measuring the weight of the snow is about a minute. The device appreciably facilitates the work of meteorologists and hydrologists.

England. At Harwell, the "Neptune" atomic reactor has been set into operation. Experiments conducted with the new reactor will make possible constructive analyses valuable in the planning of a land-based prototype of the reactor for submarines, work on which is already underway. The "Neptune" reactor will employ enriched uranium as fuel and light water as moderator. No special coolant system is required for this reactor, since it produces a thermal power of only a few watts. The reactor design makes it possible to assemble and interchange cores of the most varied types. Heat-producing elements, in the form of plates, are placed inside an aluminum tank, containing the moderator — light water. The water level in the tank may be changed, which is one of the methods for control of the reactor, together with cadmium control rods. The water used in the pile is not pressurized. It may be heated to about 90° C with the aim of studying the behavior of neutrons as the temperatures of the moderator and of the heat-producing elements are raised.

England. At Winfrith Heath (Dorset), an experimental gas-cooled reactor will be built. The reactor will have a thorium cycle of fuel utilization; the fuel temperature will reach 760° C. The heat-producing elements will be ceramic. The reactor will be installed for the study of the problems of utilizing gas turbines and turbines calculated for super-high steam parameters in nuclear energy projects.

England. At the end of November 1957, a pile for materials testing, PLUTO, was started up at Harwell. The reactor thermal power is 10 Mw , maximum neutron flux 10^{14} neutrons/$cm^2 \cdot sec$. This reactor is similar in design to the DIDO reactor and is intended for the assembling of experimental loops.

England. At Harwell, an injector has been built (proton energy: 500 kev, pulsating beam current: almost 20 ma) for a linear accelerator of 50 Mev energy.

Brazil. The chairman of the National Commission for the utilization of atomic energy, Otasilio Cunha, stated that the official inauguration of the atomic reactor at Sao Paulo University will take place on January 25, 1958, and that Brazil has plans for the construction of two mills for reprocessing uranium ores.

Hungary. The Soviet exhibit "Atomic Energy in the Service of Peace" was on display in Budapest during November and December 1957. It was visited by over 50,000 persons in the 30-day period.

India. The chairman of the Commission on Atomic Energy, H. Bhabha, stated that, in most cases, the utilization of atomic energy in India will be an economical business. One of the factors which result in the application of atomic energy being economical is the inadequacy of power supplies in industrial areas. The government of India is considering several suggestions at the present time with a view to reorganizing the Department of Atomic Energy. This reorganization is due to significant and rapid successes achieved in scientific research on the atomic nucleus, successes registered in the application of atomic energy to peaceful purposes and a broad program for the future.

Poland. The council on affairs of peaceful utilization of atomic energy awarded prizes to a large group of Polish scientists for successes achieved in the area of research and utilization of atomic energy. First prize, for work in the field of cosmic ray research, was awarded to Professor M. Mensowicz. Second prizes went to E. Gerulja, J. Werle, J. Janik, W. Kolos, J. Kampbell and D. Sugar. Third and fourth prizes were received by a large group of Polish scientists.

Philippines. The construction of a large atomic research center is suggested for Manila. The key role in the creation of the center will be assumed by the USA, which suggests building a research reactor at the center.

USA. On the second of December, 1957, at Shippingport (Pennsylvania), the reactor of the first large-scale American atomic electric power station went critical (60 thousand kw power). The reactor core contains 14 tons of natural uranium and 74.6 kg of heavily enriched uranium. Reactor control is brought about using 32 hafnium control rods. Over 110 million dollars were spent on the installation of the power station (twice as much as was estimated at the beginning of the project). On December 23, the station was brought up to design power. The power requirements of the station proper amount to 8 thousand kw.

USA. An experimental reactor using an organic coolant-moderator (terphenyl), the OMRE, was built at the reactor-testing station in the state of Idaho and went critical on September 17, 1957. The maximum thermal power of the pile is 16 megawatts.

USA. In September 1957, at the National Reactor Testing Station, Arco, Idaho, an ETR reactor, slated for engineering research, was started up.

The average neutron flux of the reactor is very high, amounting to $1.9 \cdot 10^{15}$ neutrons/$\text{cm}^2 \cdot$sec. The reactor core has a channel whose dimensions are $23 \times 24 \times 90$ cm^3, which is intended for the study of the behavior of various reactor materials under the action of intense bombardment.

The power of the reactor is 175 megawatt, core size $75 \times 75 \times 90$ cm^3. It is moderated and cooled by light water. The reactor cost 14 million dollars.

USA. Launching and commencement of operations of the third atomic submarine, the "Skate," took place at Groton (Connecticut). This vessel is looked upon as a mass-production prototype of American atomic-powered submarines.

USA. An Oregon factory has installed a 24 Mev betatron, intended for the detection of internal defects in large castings. There are seven similar installations in the USA.

USA. At the World Metallurgic Congress, which met in Chicago November 2-8, 1957, about 100 reports (almost 25% of the total number) dealt with questions connected with atomic energy production: the metallurgy of plutonium, nuclear metals and their metallography, uranium metallurgy, cyclic heat treatment and uranium welding, and also nondestructive testing of nuclear reactor components. The congress was concluded with the solemn inauguration of a memorial bas-relief dedicated to the 15th anniversary of the first chain reaction, the ceremony taking place at the Enrico Fermi Institute of the University of Chicago.

USA. For the first half year, the reprocessing of uranium ores at concentrating mills was in excess of 9 thousand tons daily output. During this time, 1694 thousand tons of ore (average U_3O_8 content: 0.28%) were reprocessed, giving a yield of 4.141 tons of U_3O_8.

USA. General Electric Company has developed and tested insulating materials showing good resistance to intense neutron and γ-ray irradiation (felt made from aluminum oxide and silicon dioxide, and pure silicon dioxide cotton).

Southwest Africa. A uranium bonanza has been uncovered in the Namib desert. The length of the ore-bearing area is 25-30 km, its width, roughly 0.8 km.

Japan. The chairman of the Japanese Atomic Energy Commision, Koiichi Uda, announced that the purchase of a Calder Hall-type nuclear power reactor would be more practical than the purchase of an American PWR-type power reactor. The Calder-type reactor could be set into operation 4 years from the time the order was sent out. The PWR-type reactor could become operative at an earlier time, but it would be more economical, from Japan's standpoint, to import a power reactor of the English type, for which Britain stands ready to supply a sizable amount of natural uranium fuel.

NEW LITERATURE

Books and Compendia

Rare Earth Metals. Symposium of articles, edited by L. N. Komissarova and V. E. Pliushchev. Published by Foreign Literature Press, 1957, 419 pp, 24 rubles, 95 kopeks.

The symposium gives the translations of 57 articles published in the foreign literature in recent years: on the chemistry of rare earth metals (mostly dealing with the chemistry of complex compounds), separation of rare earth elements by fractional crystallization and fractional precipitation, separation of rare earth elements by the ion exchange method, separation of rare earth elements by extraction methods, electrochemical method of separating and producing rare earth metals, the metallurgy of rare earth metals, determination of rare earth elements in mixtures and minerals, applications of rare earth metals and their compounds.

Photonuclear Reactions. Problems of contemporary physics, No. 6 (1957). Symposium of translations and reviews of the foreign periodical literature. Published by Foreign literature Press, 206 pp., 10 rubles, 50 kopeks.

Includes the most interesting experimental and theoretical papers on photonuclear reactions published during 1953-1956. At the beginning of the symposium, a review is given of photonuclear reactions, embracing a series of papers not appearing in the symposium. The symposium is divided into four sections: deuteron photodisintegration, photonuclear reactions at "giant" resonance energy levels, photonuclear reactions at energy levels above "giant" resonance, photofission of heavy nuclei. In addition, an appendix gives an article by Alvarez et al. on "Catalysis of μ-meson Nuclear reactions."

Questions of Nuclear Power Engineering. Symposium of translations and reviews from the foreign periodical literature, No. 4, 1957. Published by Foreign Literature Press, 78 pp., 7 rubles.

In the section "Stations and Schemata," translations of the following articles are presented: "Liquid-metal-fuel Reactor Problems" from Nuclear Engineering 1, 8, 334 (1956); "Comparative Data on Water-Moderated and Water-Cooled Reactors and on Graphite-Moderated and Sodium-Cooled Reactors" from Engineering, 182, 4735, 727 (1956); "Calder-Hall" from Engineer 202, 5264, 841 (1956); "The Enrico Fermi Atomic Power Station Reactor" from Nuclear Engineering 2, 12, 112 (1957).

In the section "Construction and Materials" we find an article, translated, "Contemporary Achievements in Production Technology of Ceramic Materials Used in Nuclear Power Engineering" from J. Franklin Inst. 260, 6, 455 (1955).

In the section "Fuel and Fuel Elements," a translation of the article "Fuel Elements for Atomic Reactors" from Combustion 27, 8, 41 (1956).

In the section "Heat Exchange and Coolants," a translation of the article "Uses of Sodium and Sodium-Calcium Alloy as Coolants" from Atomics 7, 5, 167; 6, 189 (1956).

In the section "Shielding," a translation of the article "Nuclear Reactor Shielding" from J. Brit. Nucl. Energy Conf. 2, 1, 54 (1957).

In the section "Nuclear Power Engineering News," translations of the articles "Heat and Corrosion Shielding" from Nucl. Engineering 2, 12, 111 (1957); "Nuclear Fuel" from Engineering 183, 4739, 29 (1957); "The Shippingport Reactor" from Engineering 182, 4736, 761 (1956).

K. V. Astakhov. Atomic Energy and the Pathways of its Practical Utilization. Voenizdat [Military Press], 1957, 280 pp., 4 rubles, 25 kopeks.

The book gives a systematic approach, in popular form, to the structure of the atom and the fundamentals of atomic power utilization.

F. Münziger. Atomic Energy. Translation from the German, edited by P. A. Petrov, State Power Press, 1957, 112 pp., 3 rubles, 10 kopeks.

A review of materials published in the English and American literature (prior to the 1955 Geneva conference) on nuclear power reactors. A classification and short description of the reactors dealt with is given. The future prospects of these types of reactors, from the viewpoint of electric power production and the feasibility of competition with electric power plants operating on conventional fuel, are considered. Also considered are questions of heat transfer in reactors and heat exchangers, and the economic features of steam turbines operating on saturated steam.

The book is written for students taking power engineering curricula in advanced educational institutes and technical schools.

Articles from Professional Journals

V. T. Aleksanian, Absorption Spectra of Some Tetravalent Uranium Compounds at Liquid Oxygen Temperature, Proc. Acad. Sci. USSR 115, 2 (1957). *

I. P. Alimarin, Radiochemical Methods of Analysis in the USSR. Zavodskaia Laboratoriia No. 10 (1957).

B. V. Bobykin and K. M. Movik., Identification of the Internal Conversion Spectrum of the Long-lived Isotopes Eu^{152} and Eu^{154}. Proc. Acad. Sci. USSR 115, 2 (1957). **

S. I. Braginskii, Transition Phenomena in Completely Ionized Two-temperature Plasma. J. Exptl.-Theoret. Phys. 33, 8 (1957). **

S. S. Bugorkov et al., Ionization Chambers for Alpha-particle Counts. Pribory i Tekhnika Eksperimenta, No. 4 (1957).

A. E. Buzynov and I. G. Fakidov, Gamma-exposure Meter for Betatron Gamma-Defectoscopy. Pribory i Tekhnika Eksperimenta No. 4 (1957).

V. P. Vasil'ev et al., Research on Metal-Metal Diffusion Processes by the Technique of Labeled Atoms (applied to oxide-coated cathode technology). Transactions of Central Asia University, No. 91, Physical and Mathematical Sciences, book 15, 1957.

A. I. Veinik and A. S. Shubin, Application of Labeled Atom Method to the Study of Phase Transformation of Moisture in the Drying Process. Transactions of Moscow Technological Institute for the Food Industry, No. 8 (1957).

A. N. Gamaleia et al., Alterations in the Circulatory System Induced by Acute Radiation Damage. Vestnik Rentgenol. i Radiol. No. 4 (1957).

N. P. Glazkov, A He^3-chamber for Neutron Spectrometry. Pribory i Tekhnika Eksperimenta No. 4 (1957).

V. M. Gorbachev and M. I. Kazarinova, Registration of Fission Fragments and of Heavy Charged Particles by Thin Scintillation Films. Pribory i Takhnika Eksperimenta, No. 4 (1957).

A. I. Grigor'ev et al, On the Interaction of Beryllium Oxyacetate and Alcohols. Zhur. Neoganicheskoi Ximii 2, 9 (1957).

---

* See C. B. Translation.

** See English translation.

Kh. E. Gunne and M. V. Surgucheva, Radioactive Liquid Level Indicator, Priborostroenie, No. 9 (1957).

G. P. Jamais, Uses of Radioisotopes in Medical Practice. (Report by a French scientist at the III International Seminar of Medical Students.) Vestnik Rentgenol. i Radiol. No. 4 (1957).

G. G. Iordan, Basic Questions of Theory and Analysis of Self-compensating Radioactive Level Sensing Devices. Priborostroenie, No. 9 (1957).

E. A. Kaner, Cyclotron Resonance in Plasma (letter to the editors), J. Exptl.-Theoret. Phys. 33, 8 (1957).*

E. G. Kardash, A Radioactive Wall Thickness Meter. Bezopasnost Truda v Promyshlennosti [Safety on the Job in Industry], No. 9 (1957).

R. M. Kogan and N. K. Pereiaslova, A Photographic Film-Scintillating Crystal System Used for Gamma-Radiation Registration. Pribory i Tekhnika Eksperimenta, No. 4 (1957).

B. Cork et al, Antineutrons Obtained by Overcharging of Antiprotons (articles by American scientists). Uspekhi fizicheskikh Nauk 62, 4 (1957).

V. I. Korogodin and G. G. Polikarpov, Primary Processes in Radiation Injury. Uspekhi Sovremennoi Biol. 44,4 (1957).

A. A. Kravchenko, Effect of Ionizing Radiation on Bone Regeneration. Ortoped., Travmatol. i Protez. No. 4 (1957).

Iu. N. Kriukov, Formation of Post-Operative Hernia in Response to Acute Radiation Injury, Experimentally Induced Khirurgiia, No. 8 (1957).

V. V. Larionov, Effect of Absorbing Properties of Collectors on the Determination of Their Porosity by Neutron Gamma-techniques. Geologiia Nefti [Petroleum Geology] No. 9 (1957).

E. G. Lomovskaia and E. I. Vorob'eva, Some Trends in the Development of Progeny of Females Exposed to Gamma-Rays During Pregnancy. Biofizika, 2, 4 (1957).

N. V. Luchnik, On the Distribution of Mortality with Respect to Time in Irradiated Animals. Biofizika, 2, 4 (1957).

E. M. Moroz, On New Possibilities of Enhancing the Effectiveness of Charged-particle Accelerators. Proc. Acad. Sci. USSR 115, 1 (1957). *

P. K. Oshchepkov, Light-Particle Accelerators in Science and in the National Economy. Vestnik Akad. Nauk SSSR, No. 9 (1957).

R. V. Petrov, Endogenic Infection in the Irradiated Organism, Uspekhi Sovremmenoi Biol., Vol. 44, 4 (1957).

A. A. Peredel'skii et al, Radioecological Significance of Insects. Theses of report to III Conference of All-Union Entomological Society, Tbilisi, October 4-9, 1957, No. 1 (Acad. Sci. USSR).**

K. D. Sinel'nikov et al, Isotope Separation in the Passing of an Atomic Beam through an Ionization Space. Proc. Acad. Sci. USSR 115, No. 1 (1957).*

L. B. Slepian, Electrons, Photons and Radio-frequency Radiation. Radiotekhnika 12, 8 (1957).

V. S. Sokolov, Safety Problems in Gamma-ray Fluoroscopy of Metals. Bezopasnost' Truda v Promyshlennosti, No. 9 (1957).

V. G. Sochevanov et al, Study of Conditions for Precipitation of Uranyl Ferrocyanide from Aqueous Solutions. Zhur. Neorganicheskoi Khimii 2, 9 (1957).

I. E. Starik and E. V. Sobotovich, Lead in its Natural Forms and its Isotope Abundance. Izvest. Akad. Nauk SSSR, Ser. Geol. No. 9 (1957).

Iu. A. Surkov and A. P. Moskaleva, Physical Apparatus and Measuring Techniques in Radiochemical Research. Zavodskaia Laboratoriia, No. 9 (1957).

---

*See English translation.

**In Russian.

I. A. Terskov and I. I. Gitel'zon, Contribution to the Question of the Dynamics of Changes Occurring in Red Blood Cells in Response to Acute Radiation Injury. Biofizika, 2, 4 (1957).

V. S. Tongur et al, Effect of Small Doses of Ionizing Radiation on Deoxyribonucleoproteins, Biofizika, Vol. 2, 4 (1957).

N. V. Ushakov, Photographic Effect Produced by the Radiation Emissions of Some Radioactive Isotopes. Zavodskaia Laboratoriia, No. 9 (1957).

I. M. Khanin et al, Application of Radioactive Isotopes to Gas Flow Studies in Coke Ovens. Koks i Khimiia, No. 10 (1957).

SOVIET JOURNAL OF ATOMIC ENERGY VOLUME 4, NUMBER 1, 1958

CONTENTS

Letters to the Editor

Scientific and Technical News

(continued)

CONTENTS (continued)

SIGNIFICANCE OF ABBREVIATIONS MOST FREQUENTLY ENCOUNTERED IN SOVIET PHYSICS PERIODICALS

AN SSSR	*Academy of Sciences, USSR*
FIAN	*Physics Institute, Academy of Sciences USSR*
GITI	*State Scientific and Technical Press*
GITTL	*State Press for Technical and Theoretical Literature*
GOI	*State Optical Institute*
GONTI	*State United Scientific and Technical Press*
Gosenergoizdat	*State Power Press*
Gosfizkhimizdat	*State Physical Chemistry Press*
Gozkhimizdat	*State Chemistry Press*
GOST	*All-Union State Standard*
Goztekhizdat	*State Technical Press*
GTTI	*State Technical and Theoretical Press*
GUPIAE	*State Office for Utilization of Atomic Energy*
IF KhI	*Institute of Physical Chemistry Research*
IFP	*Institute of Physical Problems*
IL	*Foreign Literature Press*
IPF	*Institute of Applied Physics*
IPM	*Institute of Applied Mathematics*
IREA	*Institute of Chemical Reagents*
ISN (Izd. Sov. Nauk)	*Soviet Science Press*
I YaP	*Institute of Nuclear Studies*
Izd	*Press (publishing house)*
KISO	*Solar Research Commission*
LETI	*Leningrad Electrotechnical Institute*
LFTI	*Leningrad Institute of Physics and Technology*
LIM	*Leningrad Institute of Metals*
LITMiO	*Leningrad Institute of Precision Instruments and Optics*
Mashgiz	*State Scientific-Technical Press for Machine Construction Literature*
MATI	*Moscow Aviation Technology Institute*
MGU	*Moscow State University*
Metallurgizdat	*Metallurgy Press*
MOPI	*Moscow Regional Institute of Physics*
NIAFIZ	*Scientific Research Association for Physics*
NIFI	*Scientific Research Institute of Physics*
NIIMM	*Scientific Research Institute of Mathematics and Mechanics*
NII ZVUKSZAPIOI	*Scientific Research Institute of Sound Recording*
NIKFI	*Scientific Institute of Motion Picture Photography*
OIYaI	*Joint Institute of Nuclear Studies*
ONTI	*United Scientific and Technical Press*
OTI	*Division of Technical Information*
OTN	*Division of Technical Science*
RIAN	*Radium Institute, Academy of Sciences of the USSR*
SPB	*All-Union Special Planning Office*
Stroiizdat	*Construction Press*
URALFTI	*Ural Institute of Physics and Technology*

NOTE: Abbreviations not on this list and not explained in the translation have been transliterated, no further information about their significance being available to us.—*Publisher.*

ELEMENTARY PARTICLE ACCELERATORS

IN ENGLISH TRANSLATION

Supplement 4, 1957 Soviet Journal of Atomic Energy

Eight papers by 20 leading Soviet physicists, presented at the Session on Elementary Particle Accelerators at the All Union Conference on the Physics of High-Energy Particles, Moscow, May 1956. Of great value in work with cyclic or linear elementary particle accelerators. Contents: Physical Design Principles of the 10-Bev Proton Synchrotron; Magnetic Characteristics of the 10-Bev Protron Synchrotron at the Joint Inst. for Nuclear Research; Certain Features of High-Energy Cyclic Electron Accelerators; The Sector Cyclotron; Incoherent Electron Radiation in the Synchrotron and Its Applications in Studying Accelerator Operation; Features of the 280-Mev Synchrotron at the Inst. of Physics, Acad. Sciences, USSR; Experimental Basis for the Theory of Particle Capture in Betatron Acceleration; Concerning the Theory of Particle-Beam Focusing in a Linear Accelerator by a System of Transverse Lenses.

English translation, 75 pages, **$15.00***

Special price to subscribers to our translation of the 1957 Soviet Journal of Atomic Energy: only $10.00

Now available: 1957 Issues 1–9, Soviet Journal of Atomic Energy

THE PHYSICS OF FISSION—Supplement No. 1. Published Oct. 1957. 12 papers, comprising 209 pp, presented at this Conference, Jan. 1956, at the Inst. of Atomic Energy, Acad. Sciences, USSR. Reviews most important theoretical and experimental problems. English translation, **$30.00**

(For subscribers to J.A.E.: $20.00)

THE THEORY OF THERMAL-NEUTRON NUCLEAR REACTORS—Supplement No. 2–3. Published Jan. 1958. Textbook and handbook for design and operation of reactors, both power and experimental types.

English translation, 339 pp, 16 pg appendix, 2 parts, **$60.00**

(For subscribers to J.A.E.: $40.00)

Consultants Bureau's translations by *bilingual physicists*. Books staple bound in durable paper covers; text, which includes all integral diagrammatic and tabular material, is clearly reproduced by multilith process from IBM "cold type." **For free catalogs describing C.B.'s current Russian translation-publishing program, write to Dept. S.**

CONSULTANTS BUREAU, INC.
227 W. 17th St., NEW YORK 11, N. Y.